

ELECTROCHEMICAL STUDIES RELATED TO THE DESIGN
OF NEW INORGANIC OXIDANTS

Thesis by
Stephen Lloyd Gipson

In Partial Fulfillment of the Requirements
for the Degree of
Doctor of Philosophy

California Institute of Technology
Pasadena, California

1986

(Submitted June 18, 1985)

ACKNOWLEDGMENTS

First, it cannot be stressed enough that the work reported in this thesis is part of a joint project with the members of the Collins group. Without their considerable synthetic and inorganic skills and knowledge this work could not have been done. I am particularly indebted to Terry Krafft, who performed all of the synthesis and characterization work associated with the oxidative ligand degradation and catalyst projects. Likewise, John Keech synthesized and characterized all of the osmium CHBA-DCB complexes and provided a lot of valuable input on the ligand isomerization project. The osmium HBA-B complexes were synthesized by Geoffrey Peake and the cobalt complexes were synthesized by Thomas Richmond. Judy Christie (now Judy Audett) supplied me with my first osmium compounds, and Brian Treco and Claudia Barner have given me many interesting compounds, most of which are not reported in this work. I have enjoyed my interaction with all of the Collins group immensely and have learned a great deal from them.

I wish especially to thank my advisor, Fred Anson, for the enormous freedom he has given me to pursue this project. Very few professors would be as willing as he was to allow me to work on whatever the Collins group came up with and pursue any paths that seemed interesting. I am also appreciative of the insightful advice and comments from Fred over the years.

The success of this work has been due in large part to Terry Collins. He designed the ligands which were the source of the rich synthetic chemistry of his group, and he never failed to come up with an explanation for the many puzzling reactions we observed. His imagination, insight and

perseverance have been an inspiration to me. My interactions with Terry have broadened my horizons both inside chemistry and out.

I want also to thank all of the members of the Anson group, past and present, for their interaction and instruction in the ways of electrochemistry. I am grateful to Professor Allen Bard and Dr. John Gaudiello for teaching me the details of working with liquid sulfur dioxide as an electrochemical solvent.

Financial support for my work was provided by the National Science Foundation through a grant to Fred Anson. I am very grateful for the exceedingly generous financial support provided to me by the NSF, the IBM Corporation, the chemistry department and Caltech.

Finally, I would like to thank my parents, Harold and Bernita Gipson, for the many years of loving support they have given me. I could never have completed twenty years of schooling without their support and encouragement.

ABSTRACT

The electrochemistry of complexes designed to address important questions in the field of oxidation chemistry has been examined. There is a need for new ligands capable of forming stable complexes with high oxidation state metal centers for the development of new oxidants with enhanced selectivity and reactivity for the oxidation of organic substrates. The electrochemistry of complexes of a family of potentially tetradentate tetraanionic ligands was examined to probe their reactivity, stability to oxidation and ability to stabilize high-valent metal centers.

An osmium(IV) complex of the ligand 1,2-bis(3,5-dichloro-2-hydroxybenzamido)ethane (CHBA-Et) was found to undergo degradation of the ligand upon oxidation to Os(V) in CH_2Cl_2 . In the presence of alcohols or water this oxidative degradation proceeded in a selective and stepwise fashion through a number of intermediate complexes which were isolated and characterized. The identification of the intermediates allowed a detailed mechanism for the degradation, accounting for both the products and their diastereomeric distribution, to be proposed. The final products of the oxidative degradation and subsequent hydrolysis reactions were found to contain bidentate dianionic 3,5-dichloro-2-hydroxybenzamido ligands (CHBA) and to be catalysts for the electrochemical oxidation of alcohols. These catalysts, and analogs prepared chemically, catalyzed the selective electrochemical oxidation of alcohols to aldehydes and ketones, but had limited lifetimes. During the catalytic oxidation reactions the catalysts decomposed to unknown, inactive products. The maximum catalyst lifetime observed corresponded to the oxidation of approximately 150 moles of benzyl alcohol to benzaldehyde per mole of catalyst.

The oxidative degradation of the CHBA-Et ligand was eliminated by replacement of the ethylene bridge with a dichlorobenzene bridge. Osmium (IV) complexes of the new ligand, 1,2-bis(3,5-dichloro-2-hydroxy-benzamido)-4,5-dichlorobenzene (CHBA-DCB) displayed reversible oxidations to Os(V) in CH_2Cl_2 . Complexes of the non-chlorinated analog of this ligand, HBA-B, also displayed reversible oxidations to Os(V). There is some question about the oxidation state assignment in these complexes since oxidized forms of the ligands could contribute to the structure of the complexes and so reduce the formal oxidation state assignment of the metal. It is believed that at least the CHBA-DCB ligand forms true Os(V) complexes.

Controlled potential oxidation of complexes such as $\text{Os}(\text{CHBA-DCB})(\text{pyridine})_2$ led to partial isomerization from the trans to the cis-alpha isomer. This isomerization is believed to be triggered by the decrease in electron density at the metal center upon oxidation. Because of restriction of amide resonance in the nonplanar form of the ligand, it is a better electron donor in the cis-alpha isomer and so isomerization helps offset the loss of electron density caused by oxidation. A similar decrease in electron density and isomerization to the cis-alpha isomer is observed upon coordination of electron-withdrawing ligands to the Os(IV) complexes. Reduction of some of these cis-alpha Os(IV) complexes can cause isomerization to the more planar cis-beta isomer. An approximate correlation between the electron donating ability of the monodentate ligands and the equilibrium constant for the trans/cis-alpha isomerization at Os(V) was demonstrated. This observation indicates that the isomerization is primarily, but not exclusively, under electronic control.

Because of the limited anodic range of the CH_2Cl_2 used as a solvent for the electrochemical studies of the CHBA-DCB complexes, no anodic activity past the Os(V/IV) couples could be observed. Therefore, the electrochemistry of some of these complexes was examined in liquid SO_2 which has an anodic range to about +4 V vs. SCE. The complexes displayed additional reversible oxidations in SO_2 , but these oxidations are believed to be ligand-localized. The complex $\text{Os}(\text{CHBA-Et})(\text{pyridine})_2$ and its degradation products were also examined in SO_2 and were found to display additional reversible oxidations not observable in CH_2Cl_2 .

Complexes of the tetradentate tetraanionic ligands with cobalt(III) were also studied. These complexes could be oxidized to stable Co(IV) compounds. A second oxidation observed in acetonitrile and CH_2Cl_2 did not produce a stable Co(V) complex. In liquid SO_2 the cobalt complexes displayed four reversible oxidations.

Chemically modified electrodes were prepared from some of the complexes studied. The most stable electrodes were prepared by reductive electropolymerization of the complex $\text{K}[\text{Os}(\text{CHBA-Et})(4\text{-vinylpyridine})_2]$. These electrodes showed stable electrochemical responses in acetonitrile, CH_2Cl_2 and aqueous media, but were not stable in nonaqueous acidic media or upon oxidation to Os(V). Because of the sensitivity to acid, these polymer modified electrodes could not be converted to the catalyst compounds.

TABLE OF CONTENTS

	Page
ACKNOWLEDGMENTS	ii
ABSTRACT	iv
LIST OF FIGURES	ix
LIST OF TABLES	xiii
LIST OF SCHEMES	xv
ABBREVIATIONS	xvi
CHAPTER I. Introduction	1
References and Notes	10
CHAPTER II. The Selective Oxidative Degradation of Os(CHBA-Et)(Py) ₂ Leading to a Catalyst for the Electrochemical ² Oxidation of Alcohols	12
Introduction	13
Results and Discussion	15
Conclusions	53
Experimental	56
References and Notes	63
CHAPTER III. The Catalytic Electrooxidation of Alcohols by Osmium Compounds Containing 3,5-Dichloro-2-hydroxybenzamide Ligands	65
Introduction	66
Results and Discussion	68
Conclusions	92
Experimental	95
References and Notes	100
CHAPTER IV. The Electrochemical Production of Stable Os(V) Compounds and the Interconversion of their Stereoisomers Induced by Modification of Electron Density at the Metal Center	101
Introduction	102
Results and Discussion	105
Conclusions	141
Experimental	143
References and Notes	146

TABLE OF CONTENTS (Continued)

CHAPTER V.	Investigation of the Electrochemistry of Osmium Complexes Containing Multianionic Chelating Ligands in Liquid Sulfur Dioxide	148
	Introduction	149
	Results and Discussion	152
	Conclusions	165
	Experimental	167
	References and Notes	175
CHAPTER VI.	The Electrochemistry of Cobalt Complexes Containing Multianionic Chelating Ligands	177
	Introduction	178
	Results and Discussion	180
	Conclusions	189
	Experimental	190
	References and Notes	192
CHAPTER VII.	Chemical Modification of Electrodes with Osmium Complexes of Multianionic Chelating Ligands . . .	193
	Introduction	194
	Results and Discussion	196
	Conclusions	204
	Experimental	205
	References and Notes	207

LIST OF FIGURES

Figure		Page
1.1	Potential high-valent chelate complexes with schematic tetradentate tetraanionic ligands	5
1.2	Two potentially tetradentate tetraanionic ligands for coordination to high oxidation state transition metals . .	7
2.1	Structure of Os(CHBA-Et)(Py) ₂	15
2.2	Cyclic voltammogram of 1 mM <u>5</u> in CH ₂ Cl ₂ , 0.1 M TBAP at 0.17 cm ² BPG electrode	16
2.3	Cyclic voltammogram of 1 mM <u>5</u> + 1 M benzyl alcohol in CH ₂ Cl ₂ , 0.1 M TBAP at 0.17 cm ² BPG electrode	18
2.4	Cyclic voltammogram of the product from oxidation of 1 mM <u>5</u> + 0.5 M benzyl alcohol in CH ₂ Cl ₂ , 0.1 M TBAP at 0.17 cm ² BPG electrode	20
2.5	Cyclic voltammograms of 1 mM <u>5</u> + 0.5 M methanol in CH ₂ Cl ₂ , 0.1 M TBAP at 0.17 cm ² BPG electrode during controlled potential electrolysis at +0.87 V	22
2.6	Cyclic voltammogram of 1 mM <u>7</u> in CH ₂ Cl ₂ , 0.1 M TBAP at 0.17 cm ² BPG electrode	26
2.7	Two resonance forms of <u>7</u>	27
2.8	Cyclic voltammogram of 0.5 mM Me- <u>8</u> in CH ₂ Cl ₂ , 0.1 M TBAP at 0.17 cm ² BPG electrode	30
2.9	Structures of <u>9</u> and <u>9'</u>	32
2.10	Isomer nomenclature for octahedral complexes of tetradentate ligands	32
2.11	Cyclic voltammogram of 1 mM <u>9</u> in CH ₂ Cl ₂ , 0.1 M TBAP at 0.17 cm ² BPG electrode	34
2.12	Proposed structure of protonated <u>11</u>	36
2.13	Cyclic voltammograms of 1 mM <u>11</u> in CH ₂ Cl ₂ , 0.1 M TBAP at 0.17 cm ² BPG electrode, upon addition of HTFMS	37
2.14	Visible spectra of <u>trans</u> -Os(CHBA) ₂ (<u>t</u> -Bupy)(Ph ₃ P=O), <u>13</u> , in CH ₂ Cl ₂ during gradual addition of 9 equivalents of HBF ₄ ·H ₂ O in THF	39
2.15	Cyclic voltammograms of 1.4 mM Me- <u>8</u> + <u>t</u> -butanol in CH ₂ Cl ₂ , 0.1 M TBAP at 0.17 cm ² BPG electrode	49

Figure		Page
3.1	Structures of <u>11</u> and <u>11'</u>	68
3.2	Proposed structure of protonated <u>11</u>	69
3.3	Cyclic voltammogram of 1 mM $H_2-\underline{11}^{2+}$ + 1 M benzyl alcohol in CH_2Cl_2 , 0.1 M TBAP at 0.17 cm ² BPG electrode	70
3.4	Cyclic voltammogram of 1 mM <u>11</u> + 1 M benzyl alcohol in CH_2Cl_2 , 0.1 M TBAP at 0.17 cm ² BPG electrode	71
3.5	Cyclic voltammogram of 1 mM $H_2-\underline{11}^{2+}$ + 0.5 M <u>n</u> -butanol in CH_2Cl_2 , 0.1 M TBAP at 0.17 cm ² BPG electrode	73
3.6	A possible dimeric structure for <u>15</u>	75
3.7	UV-visible spectra taken during controlled potential electrolysis of 60 μM $H_2-\underline{11}^{2+}$ + 0.5 M benzyl alcohol in CH_2Cl_2 , 0.1 M TBAP at +0.97 V	77
3.8	Plot of Absorbance vs. Charge with data taken from Figure 3.7 for electrolysis of 60 μM $H_2-\underline{11}^{2+}$ + 0.5 M benzyl alcohol	78
3.9	Cyclic voltammogram of 1 mM <u>11</u> in CH_2Cl_2 , 0.1 M TBAP at 0.17 cm ² BPG electrode	89
4.1	Structure of $H_4CHBA-DCB$	105
4.2	Cyclic voltammogram of 1 mM $Os(CHBA-DCB)(\underline{t}\text{-Bupy})_2$ in CH_2Cl_2 , 0.1 M TBAP at 0.17 cm ² BPG electrode	106
4.3	Isomer nomenclature for octahedral complexes of tetradentate ligands	108
4.4	Cyclic voltammogram of 1.2 mM $Os(HBA-B)(Ph_3P)(\underline{t}\text{-Bupy})$ in CH_2Cl_2 , 0.1 M TBAP at 0.17 cm ² BPG electrode	110
4.5	Structure of $Os(H-HBA-B)(phen)$	112
4.6	Alternate electronic structures of the CHBA-DCB ligand	113
4.7	Cyclic voltammograms of 4.1 mM $Os(CHBA-DCB)(\underline{t}\text{-Bupy})_2$ in CH_2Cl_2 , 0.1 M TBAP at 0.03 cm ² Pt electrode, before and after oxidation to $Os(V)$	115
4.8	Normal pulse voltammogram of 1 mM $Os^V(CHBA-DCB)(\underline{t}\text{-Bupy})_2^+$ in CH_2Cl_2 , 0.1 M TBAP at 0.03 cm ² Pt electrode	119
4.9	Measurement of K_V from NPV of 1 mM $Os^V(CHBA-DCB)(\underline{t}\text{-Bupy})_2^+$ in CH_2Cl_2 , 0.1 M TBAP at 0.03 cm ² Pt electrode	120

Figure		Page
4.10	Hammett plot of K_V data for $\text{Os}(\text{CHBA-DCB})(\text{X-Py})_2$ complexes	127
4.11	Amide delocalization in CHBA-DCB complexes	129
4.12	X-ray crystal structure of $\text{Os}(\text{CHBA-DCB})(\text{Ph}_3\text{P})(\text{t-BuNC})$. .	130
4.13	Cyclic voltammograms of 1.2 mM $\text{Os}(\text{CHBA-DCB})(\text{t-BuNC})_2$ in CH_2Cl_2 , 0.1 M TBAP at 0.03 cm ² Pt electrode, before and after reduction to $\text{Os}(\text{II})$	133
4.14	Proposed molecular orbital diagrams for $\text{Os}(\text{CHBA-DCB})(\text{Py})_2$	139
5.1	Cyclic voltammogram of 1 mM $\text{Os}(\text{CHBA-DCB})(\text{Ph}_3\text{P})_2$ in SO_2 , 0.1 M TBABF ₄ at -60 °C at 0.03 cm ² Pt electrode	153
5.2	Cyclic voltammograms of 2 mM $\text{Os}(\text{CHBA-DCB})(\text{Py})_2$ in SO_2 , 0.1 M TBABF ₄ at +22 °C at 0.32 cm ² glassy carbon electrode	157
5.3	Cyclic voltammogram of 3 mM $\text{Os}(\text{CHBA-Et})(\text{Py})_2$ in SO_2 , 0.1 M TBABF ₄ at -60 °C at 0.32 cm ² glassy carbon electrode . .	160
5.4	Cyclic voltammogram of 2.4 mM $\text{Os}(\text{CHBA-Ethylene})(\text{Py})_2$, <u>7</u> , in SO_2 , 0.1 M TBABF ₄ at -40 °C at 0.32 cm ² glassy carbon electrode	161
5.5	Cyclic voltammogram of 4.4 mM <u>cis-alpha</u> - $\text{Os}(\text{F}_9\text{-CHBA})_2(\text{Py})_2$, <u>9</u> , in SO_2 , 0.1 M TBABF ₄ at -40 °C at 0.32 cm ² glassy carbon electrode	163
5.6	Three-compartment electrochemical cell for work in SO_2 .	169
5.7	Vacuum line for SO_2 electrochemistry	172
6.1	Structure of $\text{Na}[\text{trans-Co}(\text{CHBA-DCB})(\text{t-Bupy})_2]$	180
6.2	Cyclic voltammogram of 3.7 mM $\text{Na}[\text{trans-Co}(\text{CHBA-DCB})(\text{t-Bupy})_2]$ in acetonitrile, 0.1 M TBAP at 0.17 cm ² BPG electrode	181
6.3	Alternate electronic structures of the CHBA-DCB ligand . .	185
6.4	Cyclic voltammogram of 1 mM $\text{Na}[\text{trans-Co}(\text{CHBA-DCB})(\text{t-Bupy})_2]$ in SO_2 , 0.1 M TBABF ₄ at -40 °C at 0.32 cm ² glassy carbon electrode	187
7.1	Cyclic voltammograms of 1.1 mM $\text{K}[\text{Os}(\text{CHBA-Et})(\text{vpy})_2]$ in acetonitrile, 0.1 M TBAP at 0.17 cm ² BPG electrode after 0, 7, 20, 40, 60, 90, 120 and 180 minutes of continuous cycling	199

Figure		Page
7.2	Cyclic voltammogram of Os(CHBA-Et)(vpy) ₂ polymer modified electrode in acetonitrile, 0.1 M TBAP	200
7.3	Cyclic voltammogram of Os(CHBA-Et)(vpy) ₂ polymer modified electrode in 0.1 M aqueous NaClO ₄	201
7.4	Cyclic voltammograms of Os(CHBA-Et)(vpy) ₂ polymer modified electrode in 0.1 M aqueous HClO ₄	203

LIST OF TABLES

Table		Page
1.1	Known high-valent manganese compounds	3
2.1	TLC R_f 's of compounds observed in the oxidative degradation of $\text{Os}(\text{CHBA-Et})(\text{Py})_2$	23
2.2	Isomer distribution in electrolyses of <u>8</u> and <u>8*</u> in the presence of ethanol and <u>t</u> -butanol	46
2.3	Effects of alcohol, alcohol concentration and water on isomer distribution in electrolyses of <u>8</u> and <u>5</u>	47
2.4	Formal potentials of <u>5</u> and its oxidation products	55
3.1	Catalysts for the electrochemical oxidation of alcohols .	74
3.2	Electrochemical data for catalyst compounds	75
3.3	Effects of reaction conditions on the oxidation of benzyl alcohol with <u>11</u>	80
3.4	Oxidation of benzyl alcohol with different catalyst compounds	83
3.5	Oxidation of other alcohols with <u>11</u>	85
4.1	Formal potentials of some osmium complexes containing the CHBA-DCB ligand	107
4.2	Comparison of formal potentials of $\text{Os}(\text{CHBA-DCB})(\text{Ph}_3\text{P})_2$ with complexes containing more common ligands	108
4.3	Formal potentials of osmium complexes containing the HBA-B ligand	111
4.4	Formal potentials of $\text{Os}(\text{CHBA-DCB})(\text{X-Py})_2$ compounds . . .	124
4.5	Equilibrium constants for $\text{Os}(\text{CHBA-DCB})(\text{X-Py})_2$ compounds .	125
4.6	Changes in formal potential upon isomerization from trans to cis-alpha	129
4.7	Formal potentials of CHBA-DCB complexes displaying cis-beta isomers	136
4.8	Formal potential differences between isomeric osmium complexes containing the CHBA-DCB ligand	137
5.1	Formal potentials of osmium CHBA-DCB complexes in SO_2 . .	154

Table		Page
5.2	Formal potentials of $\text{Os}(\text{CHBA-Et})(\text{Py})_2$ and its derivatives in SO_2	164
6.1	Formal potentials of cobalt complexes in acetonitrile . .	184

LIST OF SCHEMES

Scheme		Page
2.1	Controlled potential oxidation of $\text{Os}(\text{CHBA-Et})(\text{Py})_2$, <u>5</u> , in the presence of ROH in CH_2Cl_2 at +0.87 V	25
2.2	Synthesis of <u>7</u> from <u>5</u>	27
2.3	Synthesis of <u>8</u> and <u>8*</u> from <u>7</u>	31
2.4	Hydrolysis of <u>9</u> and <u>9'</u> to <u>11</u> and <u>11'</u>	35
2.5	Mechanism of electrochemical oxidation of <u>5</u> to <u>8</u>	41
2.6	Mechanism of electrochemical oxidation of <u>8</u> to <u>9'</u>	43
3.1	Electrochemical oxidation of alcohols by <u>11</u>	88
4.1	Thermodynamic ladder used to calculate equilibrium constants for trans/cis alpha isomerization of $\text{Os}(\text{CHBA-DCB})(\text{t-Bupy})_2$ at Os(IV), Os(III) and Os(II) . . .	121

ABBREVIATIONS

Ac	acetyl
BPG	basal plane pyrolytic graphite
bipy	2,2'-bipyridine
Bz	benzyl
CV	cyclic voltammogram
DDQ	2,3-dichloro-5,6-dicyano-1,4-benzoquinone
diphos	1,2-bis-(diphenylphosphino)-ethane
E_f	formal potential
E_p	peak potential
Et	ethyl
$Et_3P=O$	triethylphosphine oxide
F	Faraday, 96485 coul/mol
Fc	ferrocene
HPLC	high performance liquid chromatography
HTFMS	trifluoromethanesulfonic acid
I	current
<u>i</u>	<u>iso</u>
IR	infrared spectroscopy
L	ligand, usually neutral, monodentate
MAC	multianionic chelating ligand
Me	methyl
MeO	methoxy
<u>n</u>	<u>normal</u>
NMR	nuclear magnetic resonance spectroscopy
NPV	normal pulse voltammogram
Oct	<u>n</u> -octyl

ABBREVIATIONS (continued)

Py	pyridine
phen	1,10-phenanthroline
Ph ₃ P	triphenylphosphine
Ph ₃ P=O	triphenylphosphine oxide
Pr	propyl
Q	charge
R	alkyl group
ROH	alcohol or water
SCE	saturated calomel reference electrode
SSCE	saturated sodium chloride calomel reference electrode
<u>t</u>	<u>tert</u>
TBABF ₄	tetrabutylammonium tetrafluoroborate
TBAP	tetrabutylammonium perchlorate
<u>t</u> -Bu	<u>tert</u> -butyl
<u>t</u> -Bupy	4- <u>tert</u> -butylpyridine
THF	tetrahydrofuran
TLC	thin layer chromatography
vpy	4-vinylpyridine

CHAPTER I

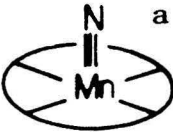
Introduction

This thesis reports the results of a joint project, the goal of which was to examine the electrochemistry of complexes specifically designed to address some of the important problems in the field of oxidation chemistry. Although most of the details of the synthetic and inorganic chemistry will not be dealt with here, this chemistry is inextricably connected with the electrochemistry. Therefore, it seems appropriate to include here an introduction to the ideas and chemistry, originated in Professor Terrence Collins' group, that formed the basis for much of the work to be described in this thesis. More detailed accounts can be found in the appropriate references [1-5].

The need for progress in the field of oxidation chemistry was clearly outlined at a recent workshop on activation of dioxygen species and homogeneous catalytic oxidations [6]. Most industrial oxidation reactions suffer from inefficiency and lack of selectivity. The key to progress in improving the efficiency and selectivity of these reactions lies in increased mechanistic understanding. Three specific areas which deserve serious investigation are: (i) new ways of activating molecular oxygen for selective oxidations, (ii) applying new instrumental methods to the understanding of reaction mechanisms and (iii) the development of new ligands for providing selectivity (chemo-, regio-, diastereo-, enantio- or shape-selectivity) and for the synthesis and study of new high oxidation state metal complexes. The Collins group has been working in the third area. Through the design of new ligands capable of forming stable complexes with high oxidation state transition metals, they intend to develop new oxidants capable of the selective stoichiometric or catalytic oxidation of organic substrates.

Efforts to develop new inorganic oxidants with higher selectivity have in the past been hampered by the limited number of ligands capable of forming stable complexes with high-valent transition metals. Because of oxidative instability, generally only simple, highly electronegative groups such as oxo, peroxo, chloro, fluoro and nitrido are found coordinated to high-valent metal centers. This lack of stable ligands limits the number of complexes available and so limits attempts to modify reactivity. For example, there are only a handful of well-characterized Mn(V), (VI) and (VII) complexes in existence (Table 1.1) [7-10]. In contrast, there are literally thousands of known compounds of manganese in lower oxidation states [7], providing a wide range of reactivity and structural variation.

Table 1.1. Known high-valent manganese compounds [7-10].

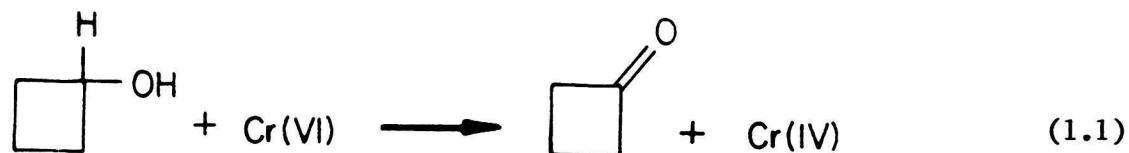
Mn(V)	Mn(VI)	Mn(VII)
MnO_4^{3-}	MnO_4^{2-}	MnO_4^-
MnOCl_3	MnO_2Cl_2	MnO_3Cl
		MnO_3F
(TpMPP)MnN		Mn_2O_7

^aSee Reference 10. TpMPP = tetrakis(p-methoxyphenyl)porphyrinato dianion.

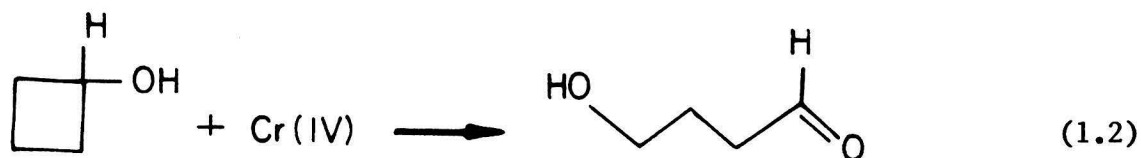
Those high oxidation state complexes which are available, such as Cr(VI) and Mn(VII) oxo species, frequently exhibit poor selectivity for the oxidation of organic substrates. It seems likely that in many instances this poor selectivity is due not to the inherent strength of the

oxidant, but rather to the fact that intermediate inorganic species which react with different selectivities are formed during oxidations with these reagents. For example, the oxidation of isopropanol by permanganate does not cleanly produce the two-electron oxidation product, acetone [11]. Instead, a mixture of products including acetone, formate and carbon dioxide is produced. Since the oxidation of isopropanol to acetone is a two-electron process, while the permanganate undergoes a five-electron change to Mn(II), it is obvious that intermediate inorganic oxidants must be formed in this reaction. These intermediates could be responsible for the poor selectivity of the overall reaction.

Loss of selectivity caused by the production of intermediate inorganic oxidants has been clearly demonstrated in the oxidation of cyclobutanol by Cr(VI) [12]. As shown in equation 1.1, the initial reaction of Cr(VI) with cyclobutanol selectively produces cyclobutanone.



However, the inorganic product is a Cr(IV) species which is still a potent oxidant. The Cr(IV) reacts with more cyclobutanol by a one-electron radical pathway and eventually leads to the ring-opened product (eq. 1.2).



Thus, even though the initial reaction of Cr(VI) with cyclobutanol is quite selective, the production of an intermediate inorganic oxidant destroys the overall selectivity of the reaction.

The approach of the Collins group has been to develop new multi-anionic chelating ligands capable of forming stable complexes with high-valent transition metals. These ligands will allow the synthesis of novel high-valent complexes which should display new modes of reactivity. Some of the structural types which serve as synthetic goals are shown in Figure 1.1.

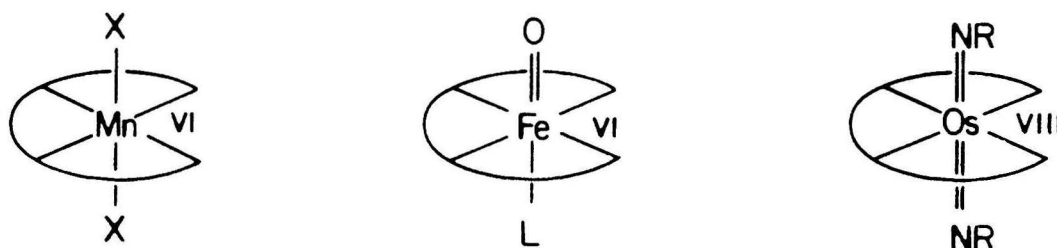
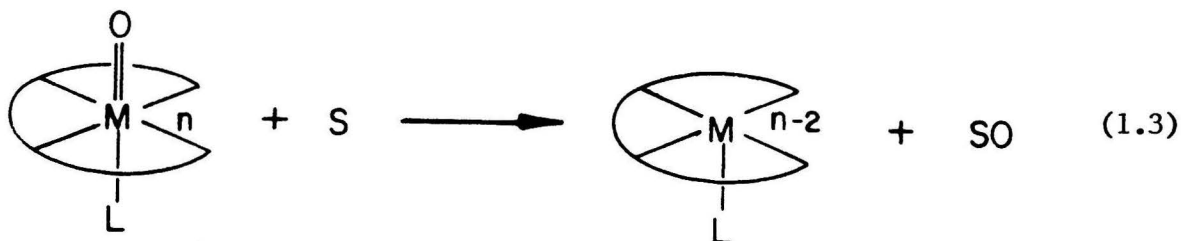


Figure 1.1. Potential high valent chelate complexes with schematic tetradentate tetraanionic ligands.

One example of the type of reactivity sought is oxo-transfer as shown in equation 1.3.



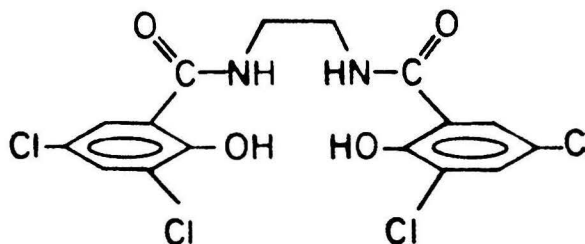
Another key goal of this work is control of redox changes at the metal center. The oxo-transfer reaction would be of little value if the inorganic product reacted with the oxygenated product or with more

substrate and so destroyed the selectivity of the reaction. It is expected that the multianionic chelating ligands will be capable of stabilizing intermediate oxidation states so that these selectivity-destroying side reactions will be eliminated.

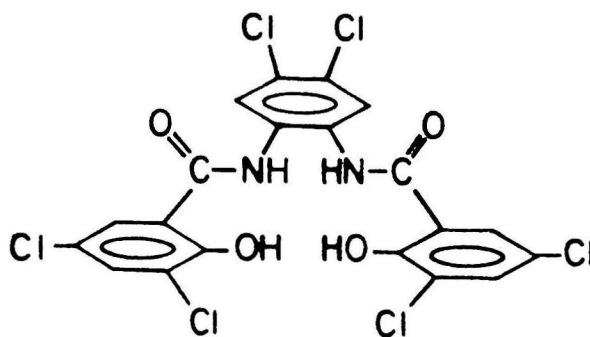
Structural features which were considered necessary for the new ligands include: (i) resistance to oxidation, (ii) the formation of five- and six-membered metallacycles upon coordination, (iii) negative charge sufficient to counter the positive charge of the metal center, (iv) chemically innocent binding sites that are resistant to hydrolysis and other displacement reactions, (v) ease of derivatization to vary the oxidizing power of the complex and to incorporate steric bulk or chiral centers to achieve regio-, enantio- and stereoselective transformations and (vi) convenient syntheses [1]. Two ligands which incorporate some or all of these features are $H_4CHBA-Et$, 1, and $H_4CHBA-DCB$, 2, shown in Figure 1.2.

These ligands can, and in most instances do, coordinate as tetradentate tetraanions. They incorporate phenoxy [13] and amido [14] groups which are known to be strong sigma donors. The deprotonated, N-coordinated amido group has been shown to shift formal potentials of metal complexes to lower potentials, demonstrating its ability to stabilize the higher oxidation state [15,16]. It was anticipated that the ethane bridge of ligand 1 might be oxidatively sensitive, but because of its ease of synthesis it was used for the initial work. The ethane bridge did indeed turn out to be oxidatively sensitive, so in other work the ligand 2 was used.

Chapter II of this thesis will discuss the oxidative degradation of 1 coordinated to osmium. Similar degradations have been observed [17] but



1,2-bis(3,5-dichloro-2-hydroxybenzamido)ethane, $H_4CHBA-Et$



1,2-bis(3,5-dichloro-2-hydroxybenzamido)-4,5-dichlorobenzene, $H_4CHBA-DCB$

Figure 1.2. Two potentially tetradentate tetraanionic ligands for coordination to high oxidation state transition metals.

in this case many of the intermediates in the degradation have been isolated, synthesized independently and characterized, allowing an unprecedented level of understanding of the reaction. The study of this degradation provided valuable information about the oxidative sensitivity of the groups encountered and so impacted future ligand designs.

The ligand degradation ended at a compound which was found to be a catalyst for the electrochemical oxidation of alcohols to aldehydes and ketones. The results of studies of the activity of this catalyst will be reported in Chapter III. Although in its present form the catalyst has a very limited lifetime, its discovery provides the basis for future studies of the effects of changes in the coordination sphere on the activity and lifetime of the catalyst. Once a long-lived catalyst is developed, mechanistic studies can be done. Also, further modification of the ligands may lead to asymmetric induction and resolution of racemic alcohols through selective oxidation of one enantiomer.

In order to avoid the oxidative degradation experienced with ligand 1, osmium complexes of ligand 2 and its nonchlorinated analog were synthesized. Electrochemical studies showed that these compounds formed stable osmium(V) species. These compounds did not display any catalytic activity, but another interesting reaction was discovered. It was found that upon oxidation to Os(V), $\text{Os}(\text{CHBA-DCB})(\text{t-BuPy})_2$ underwent partial isomerization from the trans to the cis- α isomer. It was concluded that the isomerization is triggered by changes in the electron density on the metal center which drive the ligand to adopt a more or less electron donating configuration, whichever is appropriate. This discovery may also impact future ligand designs such that the flexibility to adopt different conformations may be included or eliminated depending upon the degree of stabilization desired. Chapter IV discusses the details of this study of the interconversion of stereoisomers induced by changes in electron density at the metal center for a number of different osmium complexes.

One of the limitations encountered in the work with complexes containing 2 was an insufficient anodic potential range in the common

electrochemical solvents such as methylene chloride and acetonitrile. In order to be able to examine the behavior of the complexes at very high potentials, liquid sulfur dioxide was employed as a solvent. The low temperature and high purity of SO_2 also allowed investigation of compounds, such as the Os(V) form of 5, which are very unstable at room temperature in normal solvents. These results are reported in Chapter V.

Some work was done on the electrochemistry of complexes of ligands 1, 2 and others with transition metals other than osmium. In particular, the formation of a stable cobalt(IV) species further demonstrated the ability of the multianionic chelating ligands to stabilize high oxidation states. This work will be discussed in Chapter VI.

It was anticipated that if any good catalysts were developed in these studies they might be useful for localization at the electrode surface. The binding of electrocatalytic species to electrode surfaces, either chemically or electrostatically in polyelectrolyte films, is advantageous for a number of reasons. Among these are the limited amounts of catalyst required and the absence of the catalyst from the bulk solution. The literature contains many examples of modified electrodes and their uses [18-20]. Chapter VII will discuss some results of modification of electrodes with complexes of 1 and 2.

References and Notes

1. F.C. Anson, J.A. Christie, T.J. Collins, R.J. Coots, T.T. Furutani, S.L. Gipson, J.T. Keech, T.E. Krafft, B.D. Santarsiero and G.H. Spies, J. Am. Chem. Soc., **106**, 4460-4472 (1984).
2. T.E. Krafft, Ph.D. Thesis, California Institute of Technology, February, 1985.
3. F.C. Anson, T.J. Collins, R.J. Coots, S.L. Gipson and T.G. Richmond, J. Am. Chem. Soc., **106**, 5037 (1984).
4. F.C. Anson, T.J. Collins, R.J. Coots, S.L. Gipson, J.T. Keech, T.E. Krafft, B.D. Santarsiero and G.H. Spies, manuscript in preparation.
5. F.C. Anson, T.J. Collins, R.J. Coots, T.T. Furutani, S.L. Gipson, J.T. Keech, T. Lai, S.C. Lee, G.T. Peake and T.G. Richmond, manuscript in preparation.
6. T.J. Collins, ed., Report of the International Workshop on Activation of Dioxygen Species and Homogeneous Catalytic Oxidations; Galzignano (Padova), Italy, June 28-29, 1984.
7. F.A. Cotton and G. Wilkinson; Advanced Inorganic Chemistry, Fourth Ed.; John Wiley and Sons: New York, 1980, pp. 736-749.
8. W. Levason and C.A. McAuliffe, Coord. Chem. Rev., **7**, 353 (1972)
9. T.S. Briggs, J. Inorg. Nucl. Chem., **30**, 2866 (1968).
10. C.L. Hill and F.J. Hollander, J. Am. Chem. Soc., **104**, 7318 (1982).
11. R. Stewart, in Oxidation in Organic Chemistry, Part A; K. Wiberg, ed.; Academic Press, Inc.: New York, 1965, pp. 1-68.
12. J. Rocek and A.E. Radkowsky, J. Am. Chem. Soc., **90**, 2986 (1968).
13. R.D. Jones, D.A. Summerville and F. Basolo, Chem. Rev., **79**, 139 (1979).
14. H. Sigel and R.B. Martin, Chem. Rev., **82**, 385 (1982).
15. L. Fabbrizzi, A. Perotti and A. Poggi, Inorg. Chem., **22**, 1411-1412 (1983).
16. F.P. Bossu and D.W. Margerum, Inorg. Chem., **16**, 1210 (1977).
17. J.S. Rybka and D.W. Margerum, Inorg. Chem., **20**, 1453 (1981).
18. R.W. Murray, Electroanal. Chem., **13**, 191-369 (1984).
19. W.J. Albery and A.R. Hillman, Annual Report, C., R. Soc. Chem. London, **1981**, 377-437.

20. L.R. Faulkner, Chem. Eng. News, 62, No. 9, 28-45 (1984).

CHAPTER II

The Selective Oxidative Degradation of $\text{Os}(\text{CHBA-Et})(\text{Py})_2$

Leading to a Catalyst for the Electrochemical

Oxidation of Alcohols

Introduction

The first complexes containing multianionic chelating ligands to be studied electrochemically in this project contained the CHBA-Et ligand. It was suspected that this ligand might be oxidatively sensitive, but because of its ease of synthesis it was used for preliminary studies. Initial electrochemical results showed that $\text{Os}(\text{CHBA-Et})(\text{Py})_2$, 5, could be reduced reversibly to the Os(III) and Os(II) species but that its oxidation was completely irreversible.

It was found that the cyclic voltammetric peak current for the oxidation of 5 increased substantially in the presence of alcohols. Since it was anticipated that the complexes under investigation might serve as catalysts for the electrochemical oxidation of organic substrates, experiments were performed to determine whether this anodic activity were due to alcohol oxidation. No alcohol oxidation was found, but it was observed that the osmium complex in solution underwent a series of changes. It was these reactions occurring with the osmium complex rather than alcohol oxidation that were responsible for the increased anodic current. Furthermore, it was found that the final product of this degradation reaction was a catalyst for the oxidation of alcohols to aldehydes and ketones.

The discovery of the catalyst prompted a detailed study of the oxidative degradation of 5 to determine the mechanism of the degradation and the nature of the catalyst. Through chemical and electrochemical syntheses a number of the intermediates on the pathway from 5 to the catalyst were prepared, isolated and characterized. Knowledge of the nature of these intermediates allowed the proposal of a detailed mechanism for the oxidative degradation. This work also provided input into future

ligand designs by identifying the location of the oxidative sensitivity of the CHBA-Et ligand and its derivatives.

Results and Discussion

Electrochemistry of Os(CHBA-Et)(Py)₂

The first of the Collins group's compounds to show promising electrochemistry was Os(CHBA-Et)(Py)₂, 5 (Figure 2.1) [1-3].

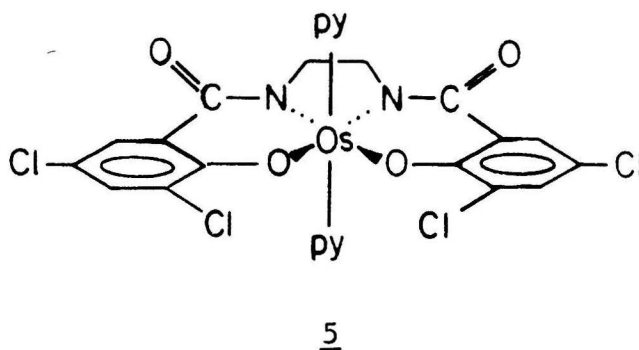


Figure 2.1. Structure of Os(CHBA-Et)(Py)₂.

The cyclic voltammogram (CV) of 5 in methylene chloride is shown in Figure 2.2. The compound undergoes two reversible, diffusion-controlled one-electron reductions at $E_f = -0.65$ and -1.88 V vs Fc^+/Fc [4]. However, the oxidation at $E_p = +0.70$ V is completely irreversible at scan rates below 5 V/sec.

Controlled potential electrolysis experiments confirmed that the reductions were completely reversible. Reduction of 5 at -0.9 V in methylene chloride consumed 1.0 F/mol and produced an orange solution of the Os(III) complex, 4 [5]. Reoxidation restored the blue color and the CV of the original Os(IV) complex. Similarly, reduction at -2.2 V in acetonitrile consumed 2.0 F/mol and produced a dark purple solution of the highly air sensitive Os(II) complex. Controlled potential oxidation of 5 consumed a variable amount of charge, always more than one F/mol, and produced at least four major products as determined by TLC.

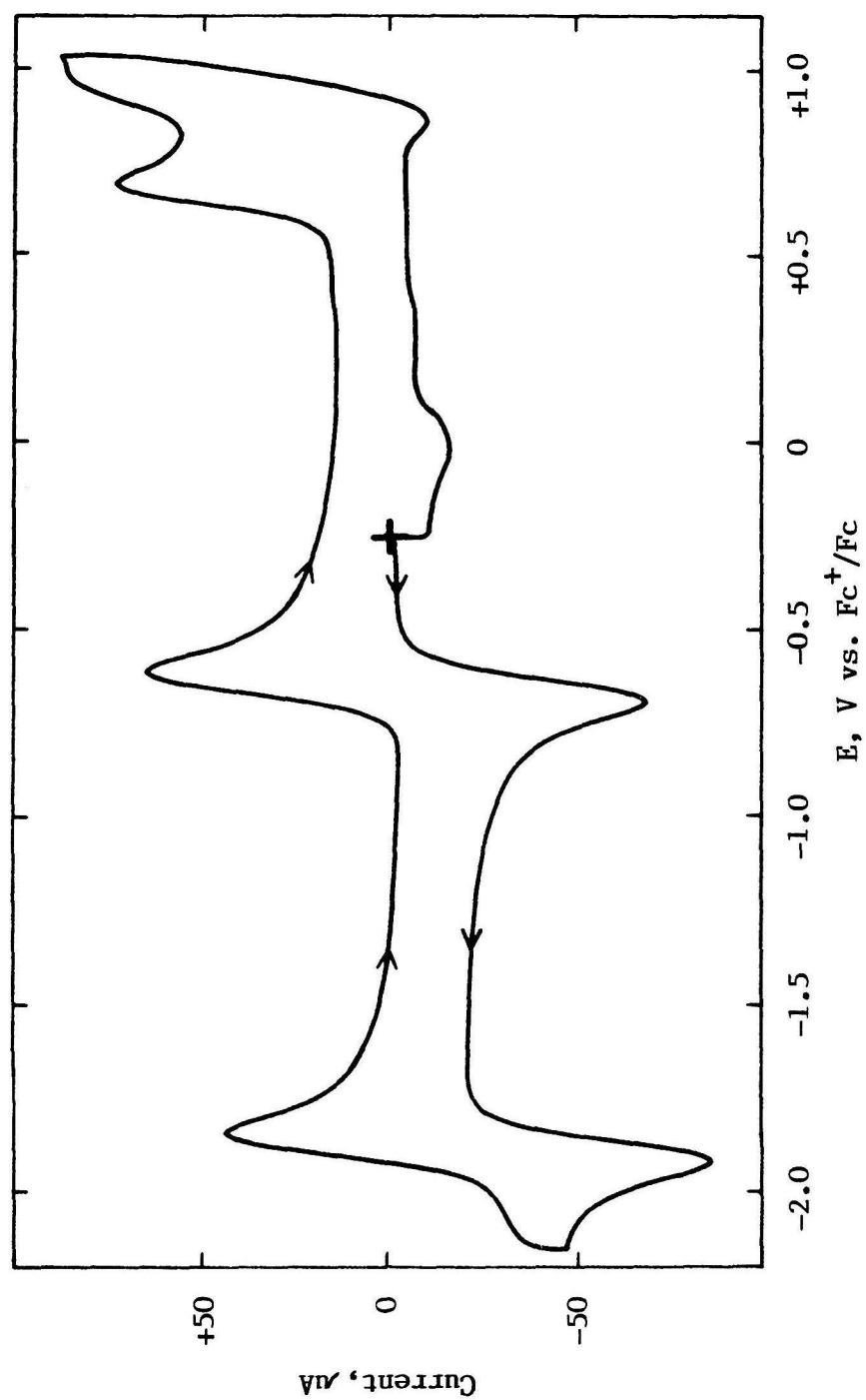


Figure 2.2. Cyclic voltammogram of 1 mM 5 in CH_2Cl_2 , 0.1 M TBAP at 0.17 cm^2 BPG electrode.
Scan rate = 200 mV/sec.

Oxidation of Os(CHBA-Et)(Py)₂ in the Presence of Alcohols

The irreversibility of the oxidation of 5 was not unexpected, but was nevertheless disappointing. Not only was the Os(V) oxidation state not stable, but it seemed unlikely that such an unstable species could function as a catalyst for the oxidation of organic substrates. However, it was possible that if the Os(V) species reacted with a substrate much faster than it underwent decomposition, then a catalytic oxidation might be observed. Alcohols seemed likely substrates for such an oxidation, so various alcohols were added to solutions of 5 to see if there were any effect on its CV which might indicate oxidation of the alcohol were taking place. Figure 2.3 shows the results of such an experiment.

The addition of a number of alcohols including benzyl alcohol, isopropanol and t-butanol caused a substantial increase in the anodic current for the oxidation of 5. Benzaldehyde and acetone had no effect. This led to the initial suggestion that the new anodic activity might result from selective oxidation of the alcohols to aldehydes and ketones, although the reaction with t-butanol was surprising. In order to test this assumption, controlled potential electrolyses of isopropanol and benzyl alcohol in the presence of 5 were conducted. The electrolyses consumed between 6 and 27 F/mol of Os before the current reached a steady, low background value. The product solutions were analyzed for carbonyl products by derivatization with 2,4-dinitrophenylhydrazine. In no case was any significant amount of carbonyl product detected.

As part of an investigation of the effect of the concentrations of alcohol and 5 on the charge consumed in the electrolyses, several experiments were performed with 0.5 M benzyl alcohol and 1 mM 5. This allowed observation of changes in the CV of the solutions after the

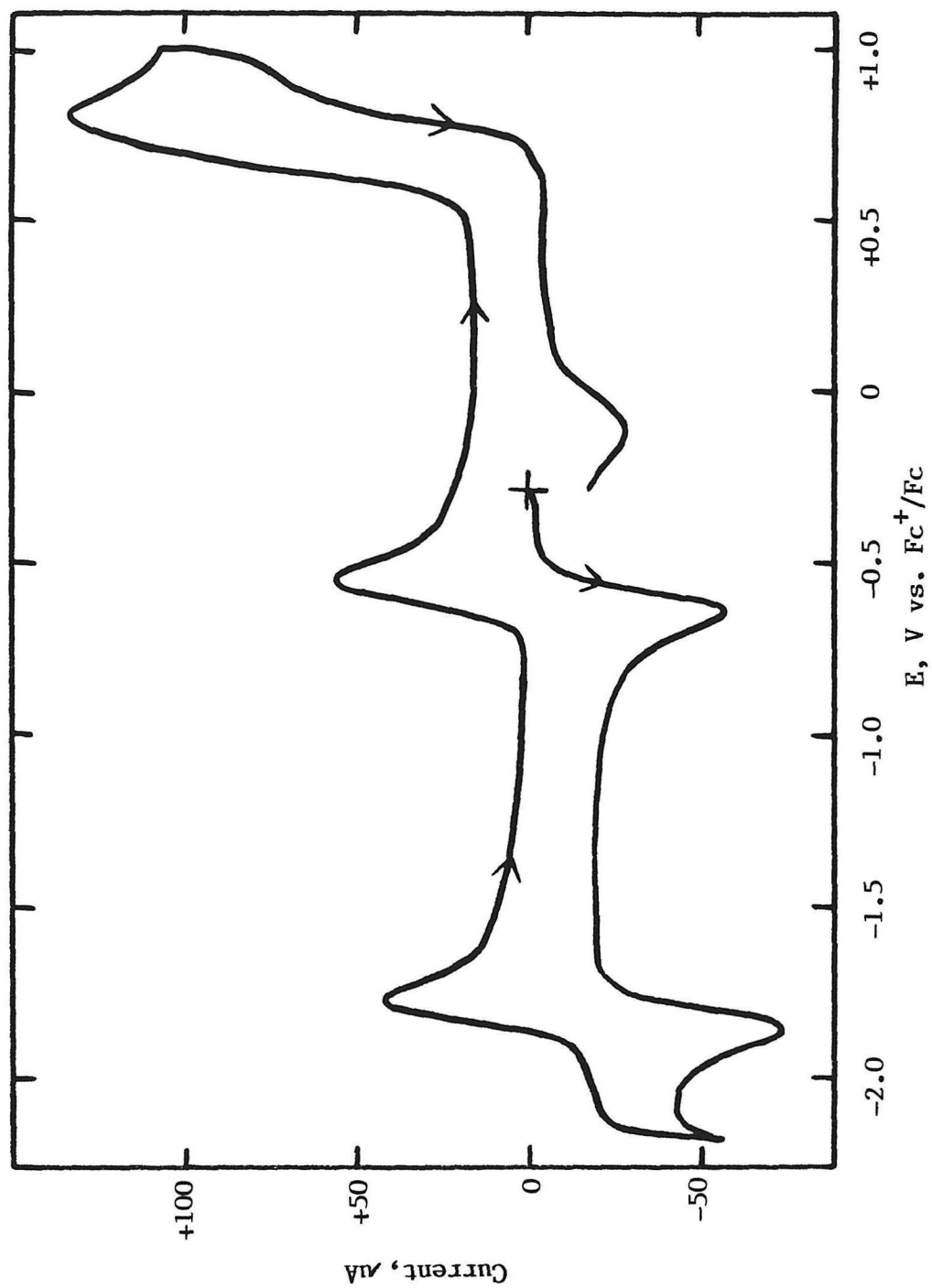


Figure 2.3. Cyclic voltammogram of 1 mM 5 + 1 M benzyl alcohol in CH_2Cl_2 , 0.1 M TBAP at 0.17 cm^2 BPG electrode. Scan rate = 200 mV/sec.

electrolyses. It was observed that after an electrolysis all of the anodic activity, including the irreversible oxidation of 5, was gone. In addition, the Os(IV/III) couple of 5 at -0.65 V had been replaced with a broad reversible reduction at -0.25 V. By chance, the CV of one such solution was observed to undergo changes as it sat at room temperature for several days. When the experiment was repeated and the CV monitored more closely it was found that over a period of several weeks at room temperature the reversible reduction at -0.25 V was replaced sequentially by two new reductions at about -0.1 and $+0.1$ V. During that time TLC also indicated that different species were being formed.

In addition to the changes in the cathodic activity of these solutions, the anodic background at potentials above about $+0.8$ V was seen to rise substantially. The CV in Figure 2.4 was performed when the conversion to the final product was almost complete. Both reductions and the large anodic currents can be seen. It seemed possible that this anodic activity might be due to catalytic oxidation of the benzyl alcohol in solution by the new osmium species. Controlled potential electrolyses at potentials where the anodic activity was observed, about $+1.0$ V, confirmed that benzaldehyde was being produced with high current efficiency (see Chapter III). This observation prompted a detailed study of the oxidative degradation of 5 to ascertain the identity and mechanism of formation of the catalytic species.

Since CV's and TLC had indicated the changes taking place after electrolyses, it was decided to use them to examine changes taking place during the electrolyses. It was found that the reaction proceeded most cleanly in the presence of primary and secondary alcohols, so electrolyses of 1 mM 5 in the presence of 0.5 M of a number of alcohols were performed.

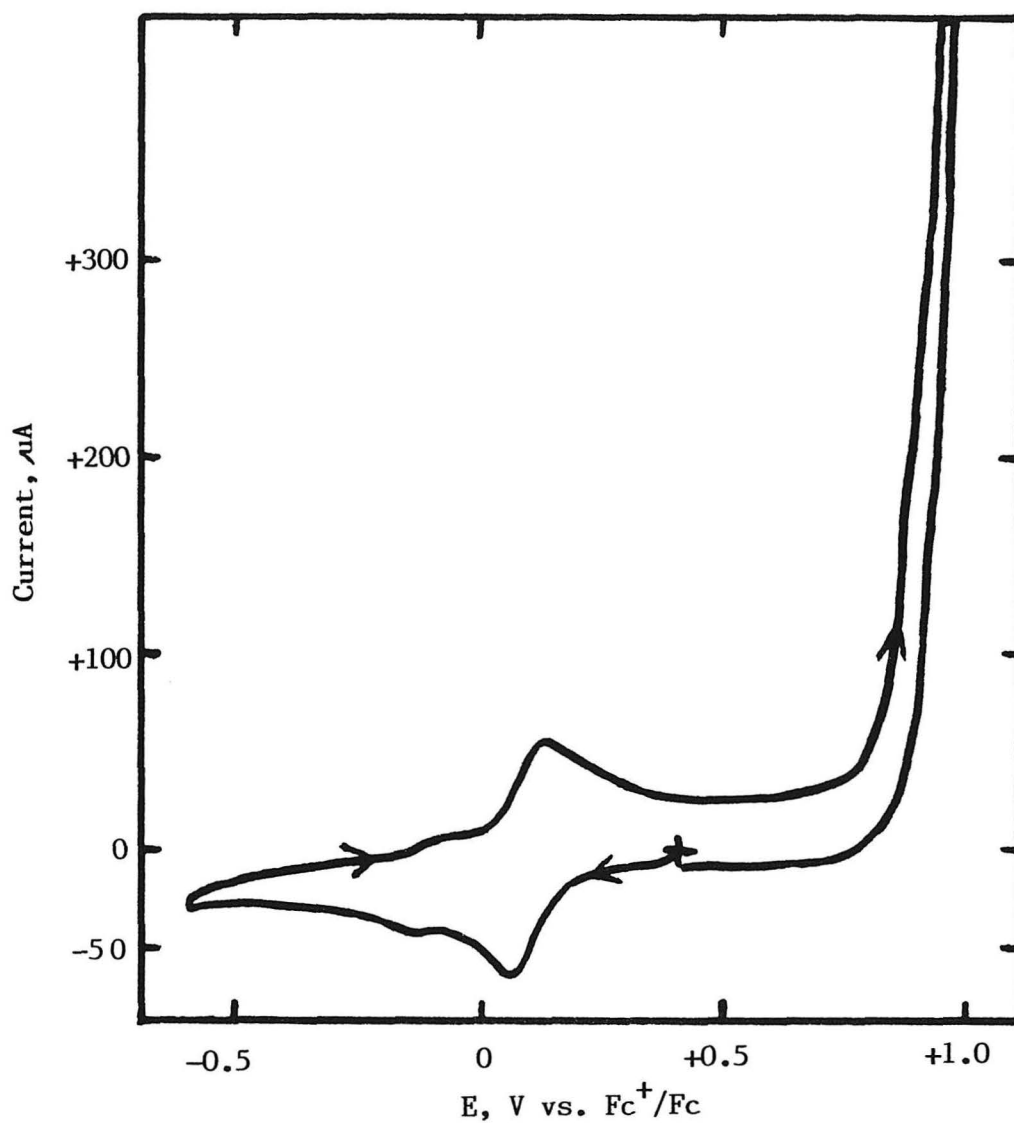


Figure 2.4. Cyclic voltammogram of the product solution from oxidation of 1 mM 5 + 0.5 M benzyl alcohol in CH_2Cl_2 , 0.1 M TBAP at 0.17 cm^2 BPG electrode. Scan rate = 200 mV/sec.

Very similar results were seen with each alcohol, including formation of the same final product.

Figure 2.5 depicts the changes in the CV of a solution of 1 mM 5 and 0.5 M methanol during an electrolysis at +0.9 V. Initially the anodic scan showed a large irreversible oxidation. As the electrolysis progressed, this anodic peak became smaller and more reversible. A small irreversible oxidation and a pair of reversible reductions also appeared during the early stages of the electrolysis. After approximately 3 F/mol Os had been passed only one reversible reduction and one apparently reversible oxidation remained. During the next 3 F/mol Os the reversible oxidation was seen to decrease in size while the reduction remained unchanged.

The TLC of this solution was also monitored during the electrolysis. After 1 F/mol Os the TLC showed four spots, one for 5 and three others labelled compounds 6, 7 and 8. All of the spots were a deep blue color except for 7 which was bright yellow. After 2 F/mol Os the spot for 6 was no longer visible. By 3 F/mol Os only the spot for 8 could be seen. During the last half of the electrolysis, as the reversible oxidation seen in the CV decreased in size, the TLC spot for 8 also decreased in size and a new spot for compound 9 grew in. At the conclusion of the electrolysis only the spot for 9 was left. The conversion of 9 to the catalyst, which originally took place at room temperature over several weeks, was hastened by refluxing the product solution containing 9. In this way complete conversion to the catalyst was obtained in about 24 hours. During the reflux, TLC showed that 9 was converted through another compound, 10, into the catalyst, 11. This is in agreement with the initial CV observation

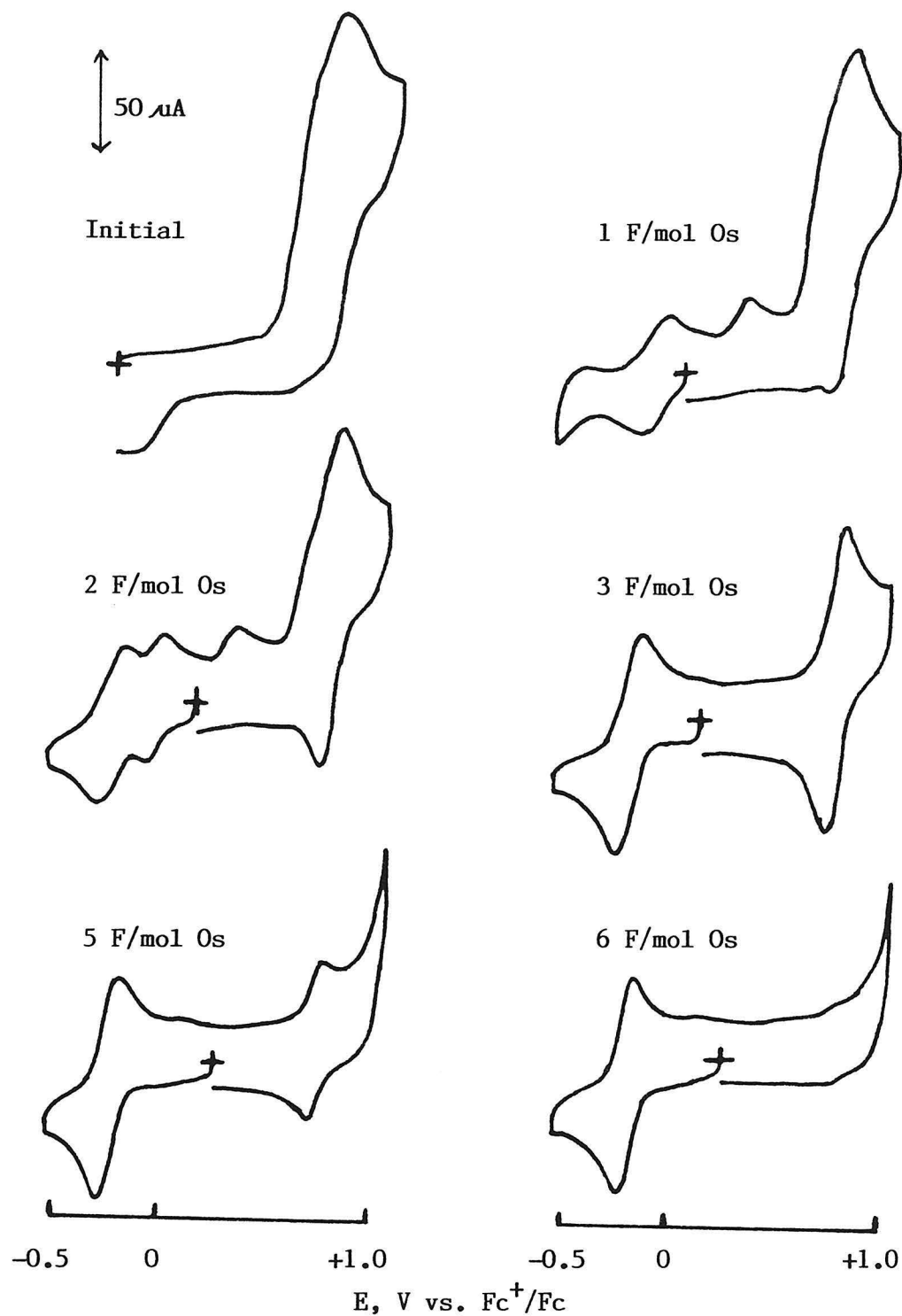


Figure 2.5. Cyclic voltammograms of 1 mM 5 + 0.5 M methanol in CH_2Cl_2 , 0.1 M TBAP at 0.17 cm^2 BPG electrode during controlled potential electrolysis at +0.87 V. Scan rate = 200 mV/sec.

that the reduction of 9 is replaced sequentially by two new reductions to give the catalyst.

This electrolysis experiment was repeated with a number of different primary and secondary alcohols. In each case almost identical CV results were obtained. The TLC results were qualitatively the same but some variation was observed. During the electrolyses the same number of TLC spots was observed and they appeared and disappeared at the same points in the electrolyses, but the R_f 's of some of the spots varied while others remained constant. The results of these experiments are shown in Table 2.1.

Table 2.1. TLC R_f 's of Compounds Observed in the Oxidative Degradation of $\text{Os}(\text{CHBA-Et})(\text{Py})_2^a$

Compound	MeOH	EtOH	<u>n</u> -PrOH	<u>n</u> -BuOH	BzOH	<u>i</u> -PrOH
<u>5</u>	0.07	0.09	b	0.06	b	0.04
<u>6</u>	0.21	0.40	b	0.54	b	0.42
<u>7</u>	0.73	0.75	b	0.73	0.76	0.71
<u>8</u>	0.56	0.73	0.79	0.82	0.87	0.80
<u>9</u>	0.69	0.69	0.69	0.69	0.71	0.69
<u>10</u>	b	b	b	0.61	0.56	b
<u>11</u>	0.49	b	b	0.52	b	0.50

^aSilica gel GF plates, solvent = 9:1 $\text{CH}_2\text{Cl}_2/\text{THF}$. ^bNot measured.

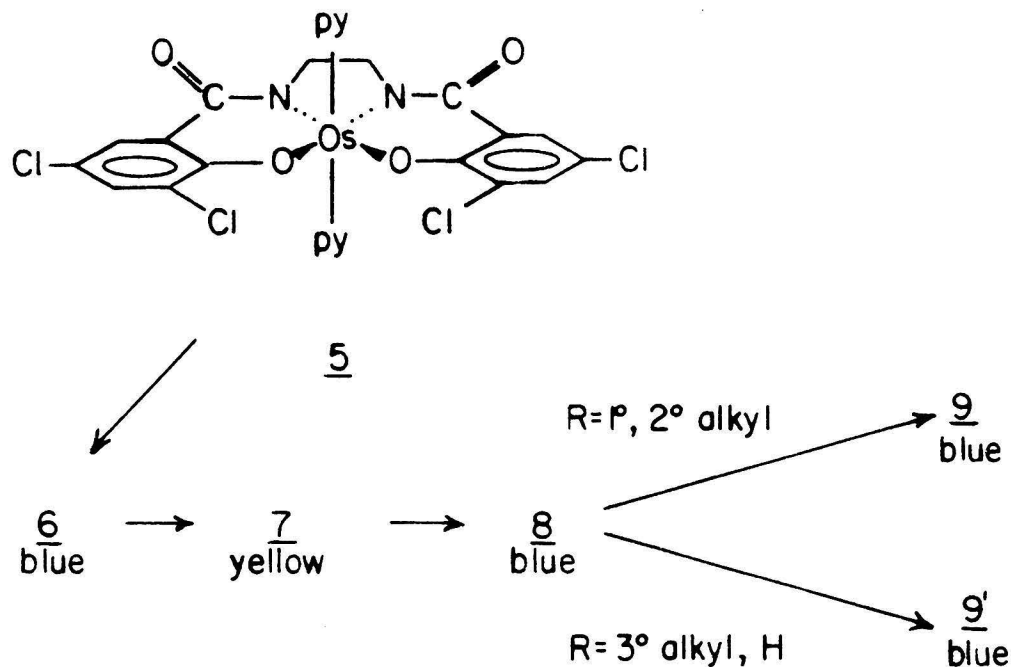
The R_f 's of compounds 5, 7, 9, 10 and 11 were constant with different alcohols. The R_f 's of compounds 6 and 8, however, varied in a regular manner with size of the alcohol in solution. This result indicated that

the alcohols were somehow associated with compounds 6 and 8 but not the others.

At this point it should be noted that this oxidative degradation can be performed in the presence of tertiary alcohols or water. TLC indicated that additional intermediates were formed during the oxidation, but a single major product is formed. This product, 9', has been found to be an isomer of 9 (*vide infra*), and the only other product of the reaction was a small amount of 9. Approximately equal amounts of 9 and 9' are formed if the electrolysis is conducted in the presence of both isopropanol and water. The compound 9' also underwent chemical reactions, though more slowly than 9, to give 10' and 11', which is also a catalyst for alcohol oxidation.

Based on the electrochemical and TLC results, a qualitative scheme for the oxidative degradation of $\text{Os}(\text{CHBA-Et})(\text{Py})_2$ to give the catalyst species could be proposed (Scheme 2.1). However, neither the electrochemical nor the TLC results provided any definitive structural data other than the association of the alcohol with compounds 6 and 8. The only way to approach the problem at this point was isolation and characterization of the individual compounds. Since it would have been very difficult to isolate the transient species from the electrochemical medium, because of low concentrations and a large excess of supporting electrolyte, it seemed necessary to develop chemical syntheses for at least some of the compounds. This became feasible when Terry Krafft of the Collins group discovered that a yellow impurity resembling 7 was recovered when 5 was purified by column chromatography on silica gel. The next section describes the results of the cooperative effort between Terry Krafft and myself aimed at identifying the compounds involved in the

Scheme 2.1. Controlled potential oxidation of $\text{Os}(\text{CHBA-Et})(\text{Py})_2$, 5, in the presence of ROH in CH_2Cl_2 at +0.87 V.



oxidative degradation of 5. All chemical syntheses and structural characterizations were performed by Terry Krafft [6].

Synthesis and Characterization of Oxidation Intermediates

$\text{Os}(\text{CHBA-Ethylene})(\text{Py})_2$, 7 [7]. A sample of the minor yellow impurity collected from silica gel purification of 5 was examined by TLC and CV. The TLC R_f and color matched exactly those of 7. The CV of the compound is shown in Figure 2.6. Two reversible reductions are observed at -0.62 and -1.76 V. One reversible oxidation is seen at +0.37 V followed by an irreversible oxidation at $E_p = +0.92$ V. The anodic peak potential of the reversible oxidation corresponds very closely to that of the small irreversible oxidation observed during electrolyses of 5 between 1 and 3 F/mol Os when TLC indicates that 7 is present. The reversible oxidation of the possible 7 was also made irreversible by the addition of large concentrations of alcohols as are present during the electrolyses. The

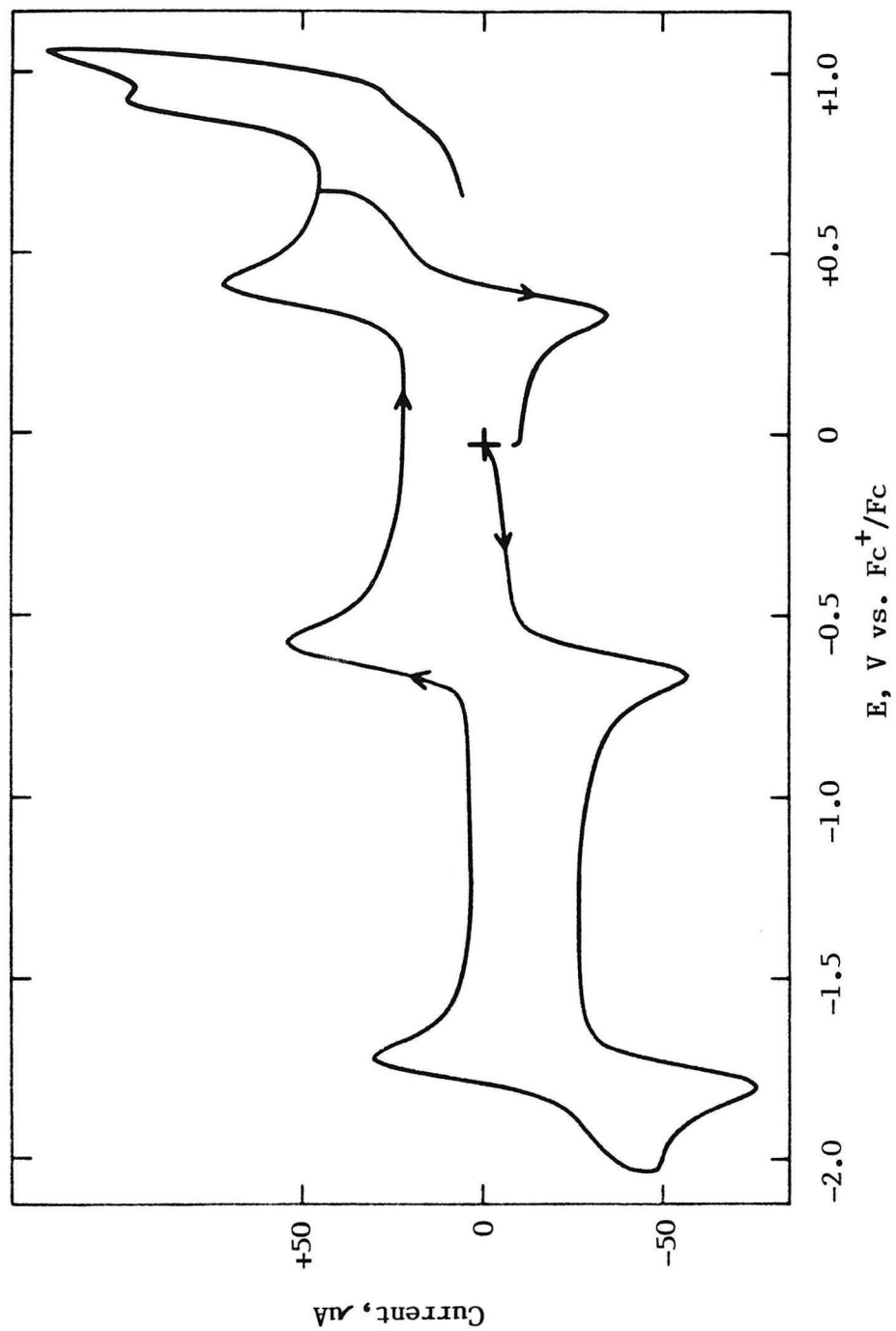
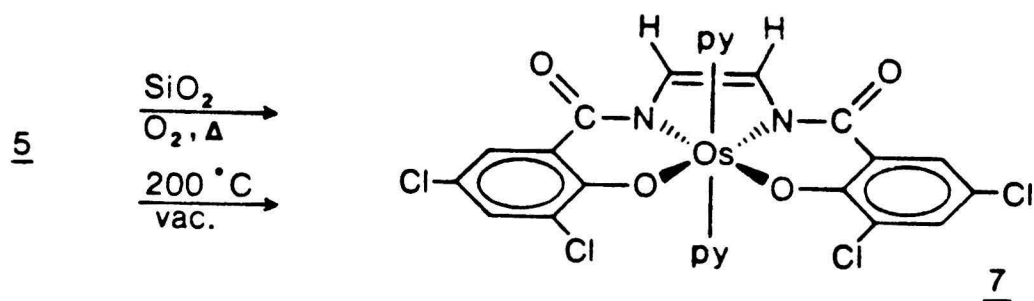


Figure 2.6. Cyclic voltammogram of 1 mM 7 in CH_2Cl_2 , 0.1 M TBAP at 0.17 cm^2 BPG electrode.
Scan rate = 200 mV/sec.

reversible reduction of the possible 7 at -0.62 V could have been observed during the electrolyses but was not. This is probably because the acid formed during the oxidation of 5 has shifted its formal potential positive to the area where reversible reductions are observed during the electrolyses (*vide infra*). Controlled potential oxidation of the possible 7 in the presence of alcohol produced compounds 8 and 9 as would be expected. Therefore, it was concluded that the yellow impurity was compound 7.

An effort was then made to synthesize significant quantities of 7 chemically. It was discovered that adsorption of 5 onto silica gel, followed by heating in air, produced a substantial quantity of 7 (Scheme 2.2) [5,6]. Removal of 7 from the silica left a mixture of $[\text{Os}(\text{CHBA-Et})(\text{Py})_2]^-$, 4, and the starting material, 5. By cycling the silica gel several times, more than 90% of 5 could be converted to 7. Characterization of 7 by IR, NMR, elemental analysis and an x-ray crystal structure of the 4-t-butylpyridine analog [8] confirmed the structure as shown in Scheme 2.2.

Scheme 2.2. Synthesis of 7 from 5.



The structure drawn for 7 in Scheme 2.2 is actually one of two resonance forms as shown in Figure 2.7.

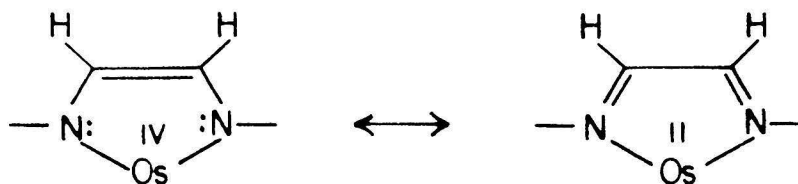


Figure 2.7. Two resonance forms of 7.

In the ethylene-bridged form on the left the osmium has a formal oxidation state of IV. In the diimine form on the right the oxidation state of the osmium is II. Since the two reductions of 7 occur at formal potentials very close to the Os(IV/III) and Os(III/II) couples of 5, it seems likely that at Os(IV) and lower oxidation states the diimine resonance form makes little contribution. However, the formal potential for the reversible oxidation of 7 is over 300 mV lower than the peak potential for the irreversible oxidation of 5 to Os(V). This suggests that the oxidized form of 7 may experience significant resonance stabilization from the diimine form which lowers the oxidation state of the osmium from V to III. Bond length data from the x-ray crystal structure of 7 indicate little contribution from the diimine form in the neutral species [6].

Os(CHBA-t-1,2-di-RO-Et)(Py)₂, 8 [7]. TLC results indicated that 8 was formed by oxidation of 7 in the presence of alcohols and that the alcohol was in some manner associated with 8. Therefore, the chemical synthesis of 8 was attempted by the oxidation of 7 in the presence of alcohols or water. It was found that blue compounds with variable TLC R_f 's could be produced by oxidation of 7 with dichlorodicyanobenzoquinone (DDQ) [5,6]. Samples of the product of the oxidation of 7 with DDQ in the presence of ethanol and methanol were examined by CV and TLC. The TLC R_f 's matched exactly those of 8 produced electrochemically from 5.

However, the CV, shown in Figure 2.8 for the compound prepared from methanol, did not match that seen during the electrolysis experiments when TLC indicated that only 8 was present (see Fig. 2.5). Instead of a reversible reduction at about -0.2 V and a reversible oxidation at +0.8 V, two reversible reductions at -0.64 and -1.95 V and a partially reversible oxidation at +0.8 V were seen. However, the addition of trifluoroacetic acid shifted the potential of the first reduction positive to about -0.2 V [8] and the addition of methanol made the oxidation completely reversible on the CV time scale (*vide infra*). These observations, combined with the fact that electrochemical oxidation of 8 produces 9, led to the conclusion that the chemically synthesized compounds were identical to the electrochemically produced 8.

Characterization of 8, made with a number of different alcohols, by NMR, IR and elemental analysis indicated that the five-membered metallacycle in 8 was substituted symmetrically by trans-alkoxide groups as shown in Scheme 2.3 [6]. In the presence of alcohol and small amounts of water the major product of the chemical oxidation was the unsymmetrically substituted complex 8*, which bears trans-alkoxide and hydroxide groups. An x-ray crystal structure of 8* containing methoxy and hydroxy groups has been performed, confirming the trans orientation of the methoxy and hydroxy groups and of the two pyridine ligands.

Os(Fo-CHBA)₂(t-Bupy)₂, 9 and 9' [7]. The next compounds encountered in the oxidative degradation of 5 are 9 and 9', obtained by electrochemical oxidation of 8. Because of the high formal potential of the Os(V/IV) couple of 8, no clean chemical route from 8 to 9 or 9' could be found. It was found that on a small scale 5 could be relatively cleanly converted to 9' by reaction with tetrabutylammonium

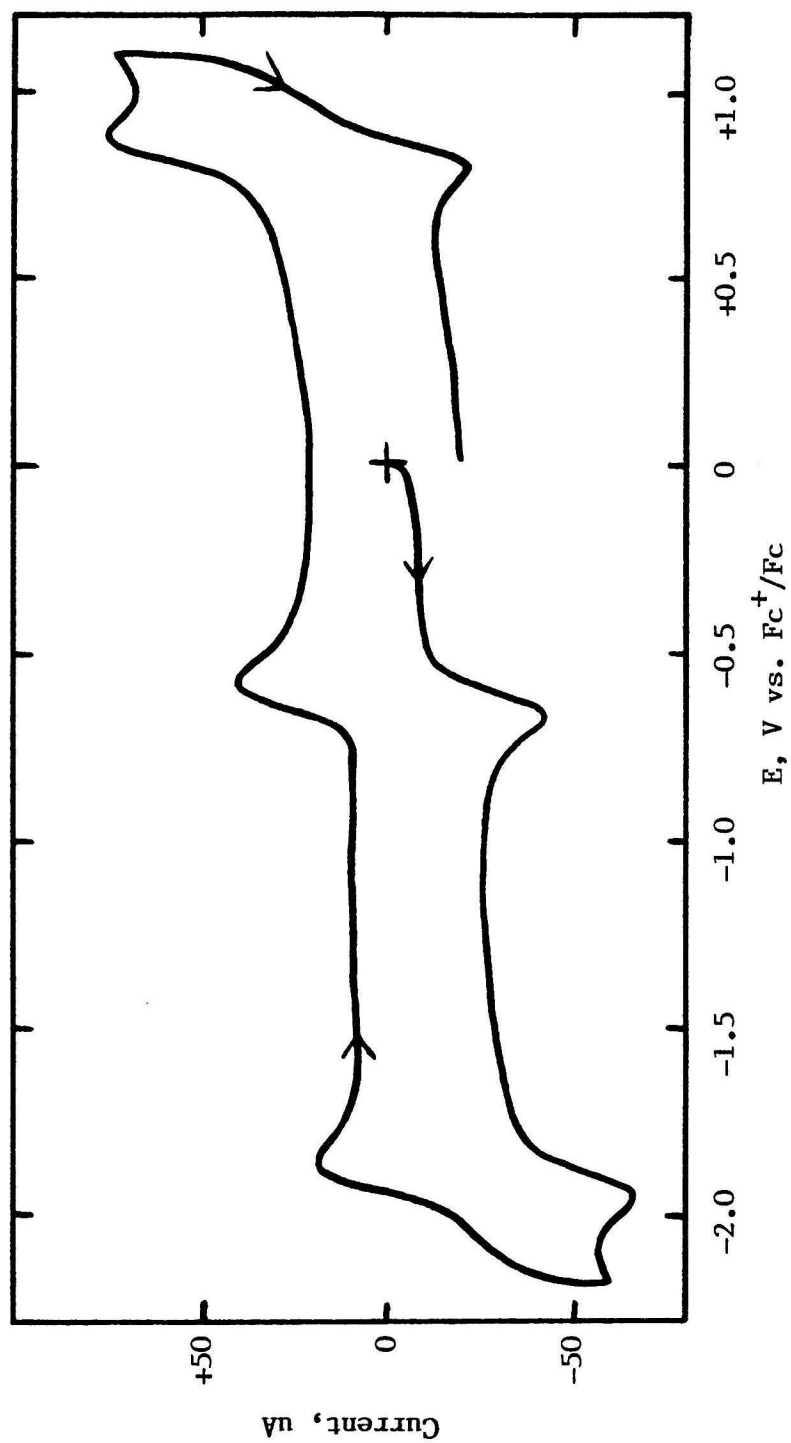
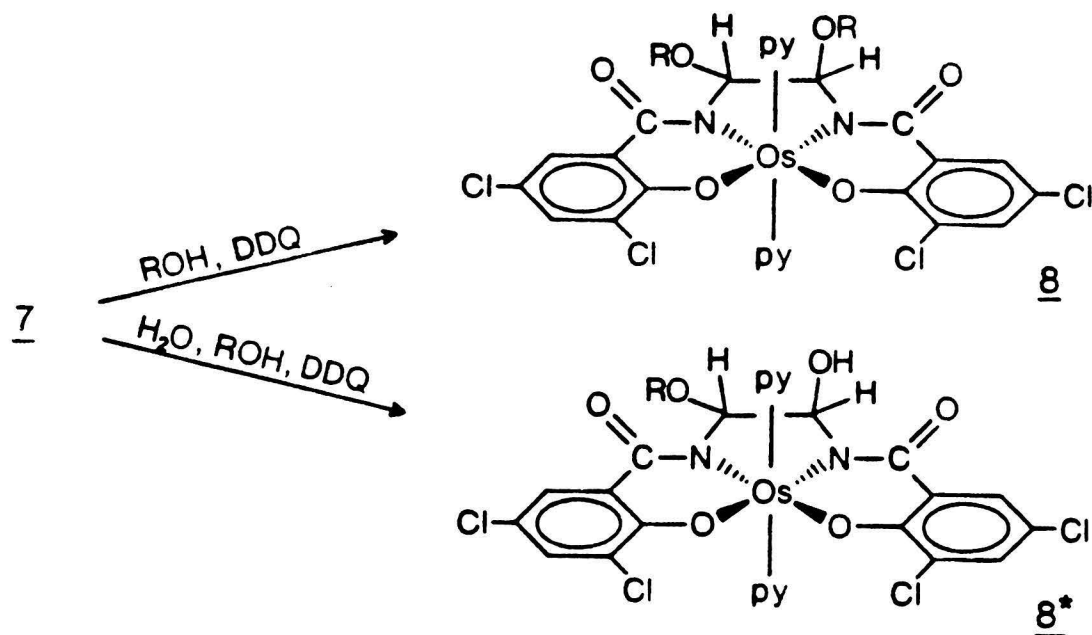


Figure 2.8. Cyclic voltammogram of 0.5 mM Me-8 in CH_2Cl_2 , 0.1 M TBAP at 0.17 cm^2 BPG electrode.
Scan rate = 200 mV/sec.

Scheme 2.3. Synthesis of 8 and 8* from 7.

periodate in the presence of trifluoroacetic acid. However, since no chemical route to 9 could be found and since the electrochemical synthesis selectively produced 9 or 9' in high yields, it was decided to use this route for their preparation. After the electrolysis it was only necessary to remove the large excess of TBAP supporting electrolyte and the solvents to obtain pure samples of 9 and 9'. This was done by recrystallizing the crude product first from CH₂Cl₂/ether and then acetone/water. When the synthesis of 9 was performed with Os(CHBA-Et)(t-Bupy)₂ rather than Os(CHBA-Et)(Py)₂, significant amounts of 9' were also formed and the two compounds were separated by preparative thin layer chromatography.

The isolated compounds were structurally characterized by IR, NMR, elemental analysis and x-ray crystal structures of the t-butylpyridine analogs. Their structures are shown in Figure 2.9.

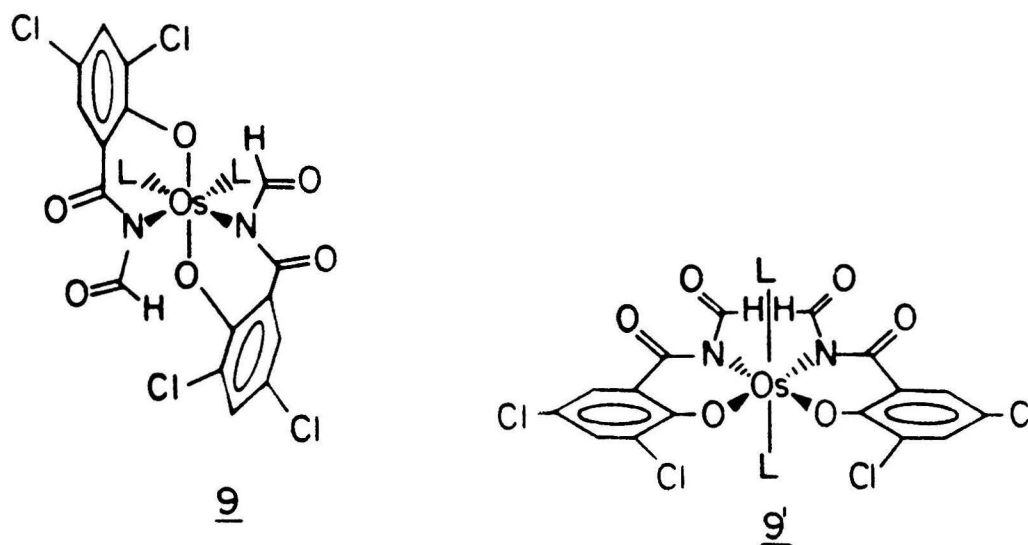


Figure 2.9. Structures of 9 and 9'.

As can be seen, the carbon-carbon bond of the ethane bridge has been broken. The alkoxy groups of 8 have been lost as the alcohol, which for the n-octyl-8 compound was detected in ca. 85% yield by gas chromatography. This leaves two bidentate dianionic ligands coordinated to Os(IV). The pyridines retain the trans relationship of the starting compound 5 in 9' but have isomerized to cis in 9. Compound 9 is referred to as the cis- α isomer using nomenclature previously developed for complexes containing similar ligand complements (Figure 2.10) [9].

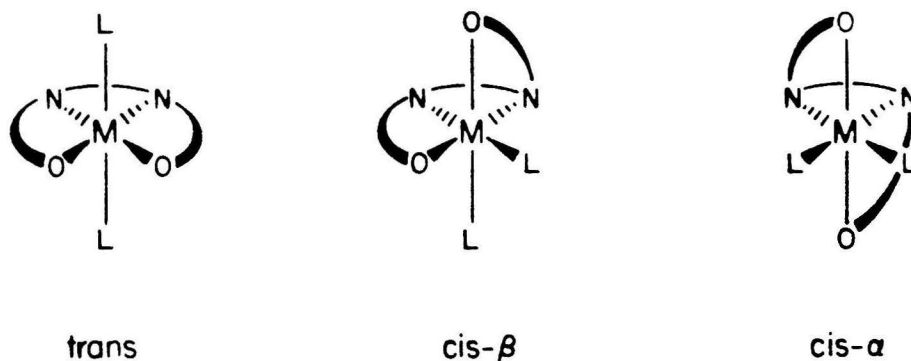


Figure 2.10. Isomer nomenclature for octahedral complexes of tetradentate ligands.

The CV of 9 is shown in Figure 2.11. Two reversible reductions can be seen at -0.46 and -1.88 V, but no anodic activity is observed at potentials below +1.1 V. Compound 9' displays very similar electrochemistry with reductions at -0.39 and -1.88 V. Compared to 5, the Os(IV/III) couple of 9' is 260 mV higher, and since the oxidation to Os(V) is not seen, its potential must be more than 400 mV higher. This is not surprising since the imido groups of 9 and 9' would be expected to be poorer electron donors than the amido groups of 5. The absence of anodic activity for 9 and 9' explains why the electrolyses stop at this point and give clean conversions to 9 and/or 9'.

Os(Fo-CHBA)(CHBA)(Py)₂, 10, and Os(CHBA)₂(Py)₂, 11 [7]. Two subsequent chemical reactions convert 9 and 9' through 10 and 10' to 11 and 11'. Experiments with isolated 9 showed that both alcohol and acid must be added to the CH₂Cl₂ to bring about the conversion of 9 to 11. Starting with 5, the alcohol is already added to ensure clean conversion to 9 or 9', while the necessary acid is formed during the electrolysis by the various degradation reactions. Compounds 11 and 11' were isolated and characterized by IR, NMR, elemental analysis and an x-ray crystal structure of 11'. Their structures are shown in Scheme 2.4. The compounds 10 and 10' were never isolated and characterized, but the fact that their TLC and electrochemical behaviors are intermediate between those of 9 and 9' and 11 and 11' strongly suggests the structures shown in the scheme. Thus the conversion of 9 and 9' to 11 and 11' simply involves two acid-catalyzed hydrolyses of the carbonyl groups from the two imido groups of 9 and 9'. This explains the necessity of the acid. Nucleophiles, such as alcohols, are also known to promote this type of reaction [10].

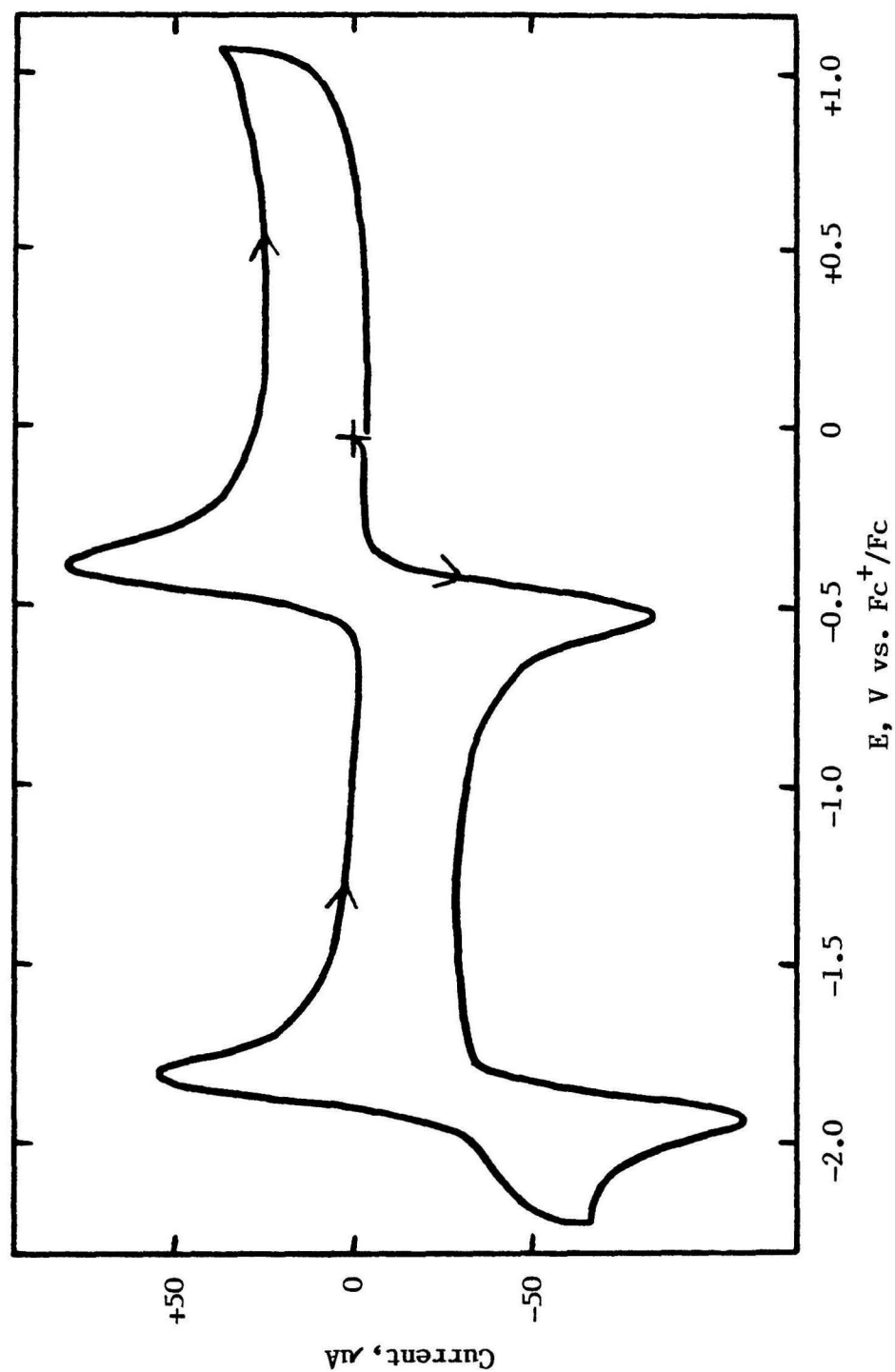
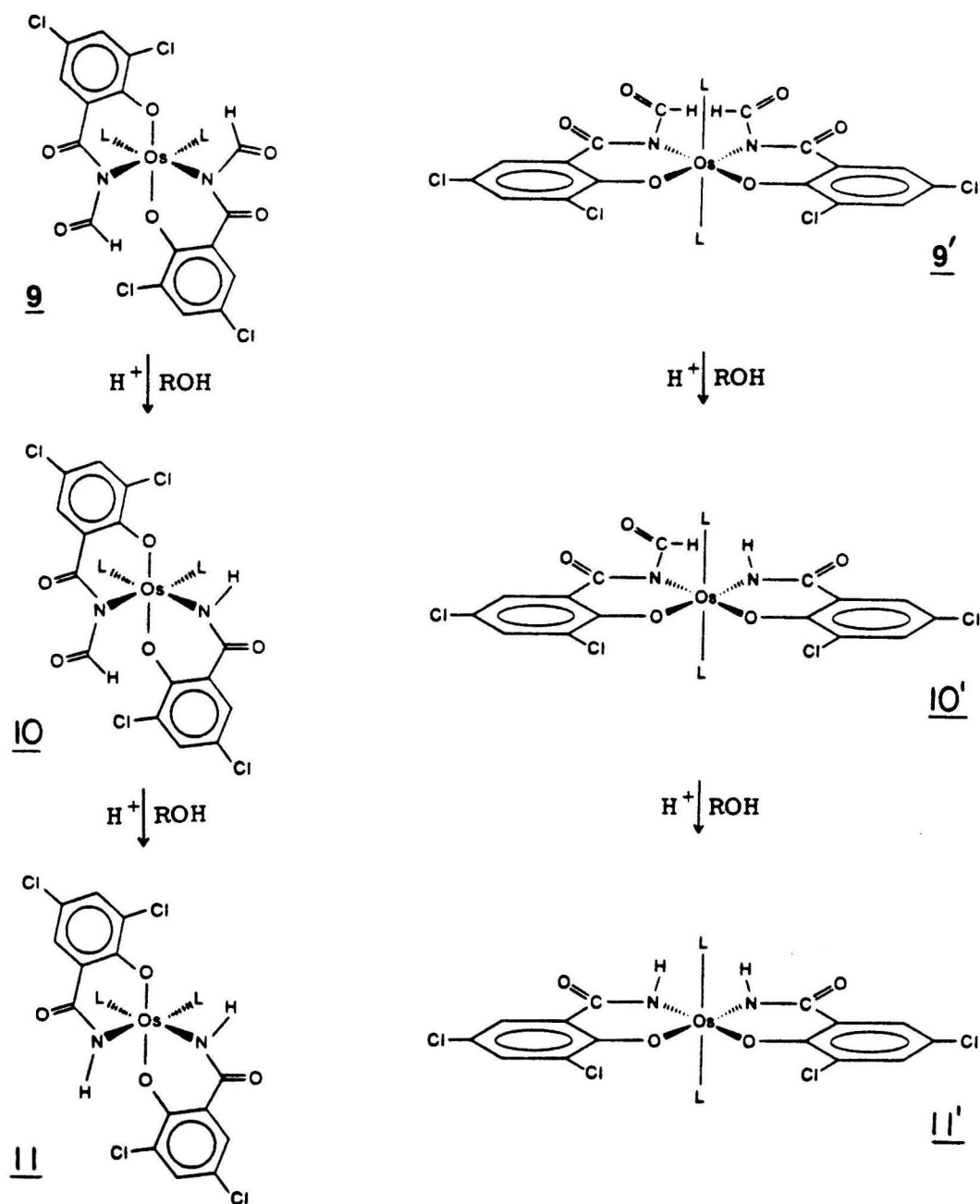


Figure 2.11. Cyclic voltammogram of 1 mM 9 in CH_2Cl_2 , 0.1 M TBAP at 0.17 cm^2 BPG electrode.
Scan rate = 200 mV/sec.

Scheme 2.4 . Hydrolysis of 9 and 9' to 11 and 11'.



The species actually produced in the syntheses of 11 and 11' are not those shown in Scheme 2.4. It is believed that under the acidic conditions of their syntheses, 11 and 11' are doubly protonated. The usual isolation procedure involved neutralization and/or column chromatography and so gave nonprotonated products, but careful recrystallization with the exclusion of water and other bases allowed the isolation of the protonated species. An elemental analysis consistent with the di-perchlorate salt of 11 has been obtained [6]. The proposed structure for this compound is shown in Figure 2.12. In addition to the elemental analysis there is electrochemical and spectroscopic evidence for the protonation of 11 and 11'. Figure 2.13 shows a series of CV's obtained by addition of trifluoromethanesulfonic acid (HTFMS) to a solution of the non-protonated form of 11. The initial CV shows the reversible Os(IV/III) couple of 11. After addition of 0.5 equivalent of HTFMS this couple had decreased in size and two new couples appeared at

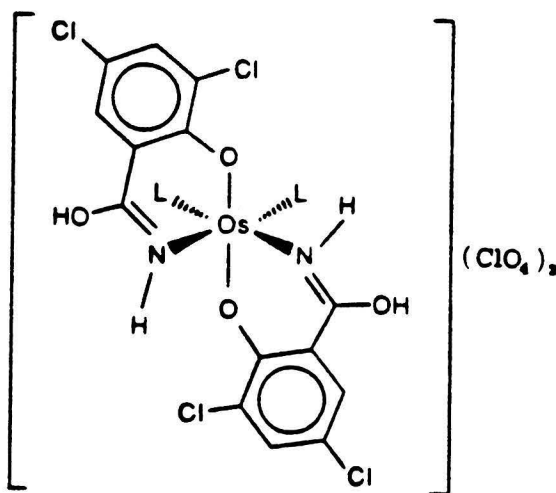


Figure 2.12. Proposed structure of protonated 11.

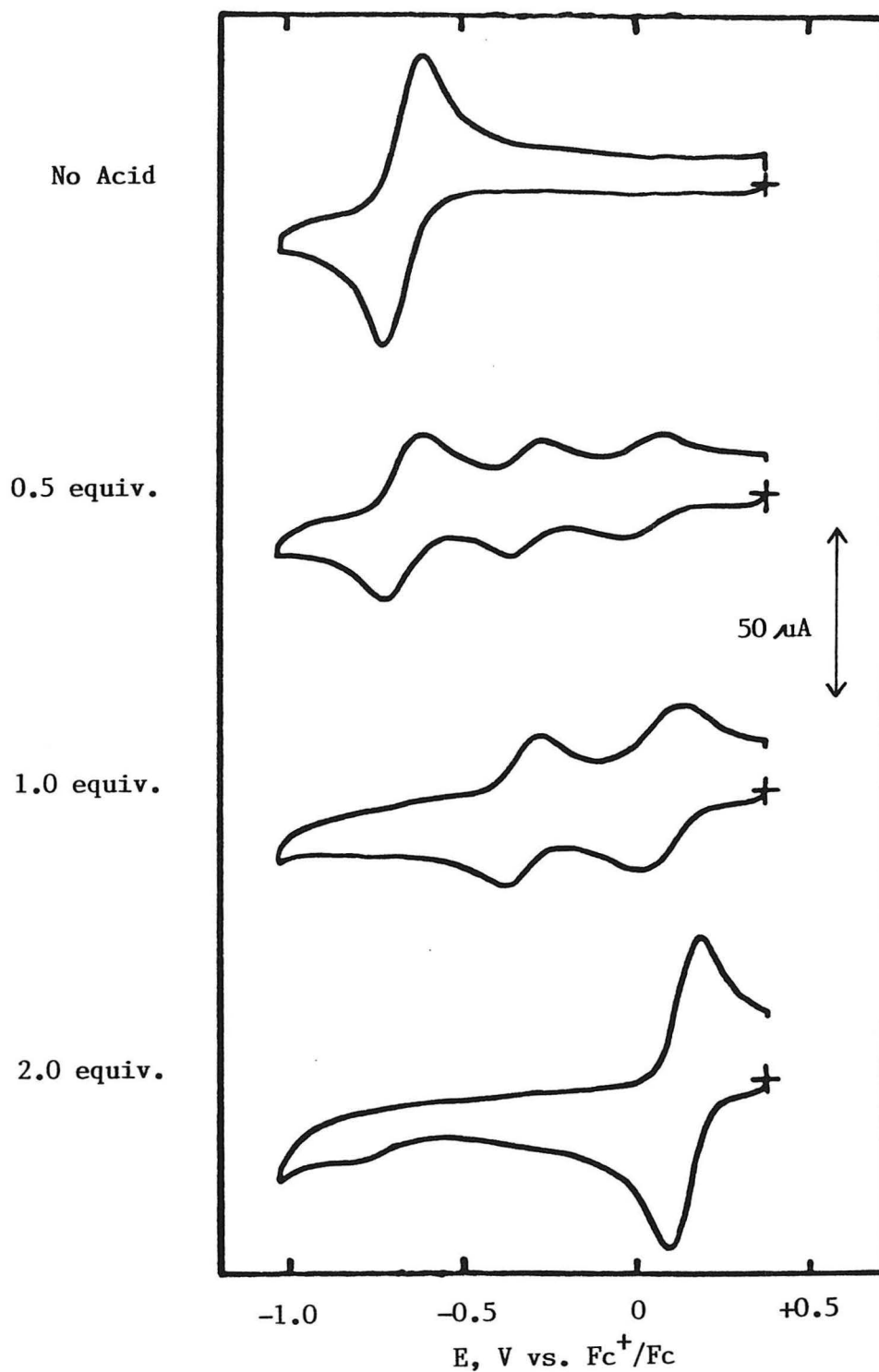


Figure 2.13. Cyclic voltammograms of 1 mM 11 in CH_2Cl_2 , 0.1 M TBAP at 0.17 cm^2 BPG electrode, upon addition of HTFMS. Scan rate = 200 mV/sec.

higher potentials. After addition of 2.0 equivalents of HTFMS only the couple at +0.1 V could be seen. This is the same potential observed for the catalyst species immediately after preparation and before isolation (see Figure 2.4). The addition of more than 2 equivalents of HTFMS to the solution caused no further changes in the Os(IV/III) couple, but a new irreversible reduction appeared at -0.9 V which blank experiments showed to be due to free acid. The potential of the Os(IV/III) couple shifted positive on protonation as would be expected, but a shift in two discrete steps was unexpected. This must mean that proton exchange in the nonaqueous solvent is very slow. Additional support for a two-step protonation was obtained by monitoring the visible spectrum of a related compound, Os(CHBA)₂(t-Bupy)(Ph₃P=O) (see Chapter III), during the addition of HBF₄ (Figure 2.14). Two isosbestic points were observed, indicating conversion among three different species. More details of the electrochemistry of 11 and 11' will be given in chapter III.

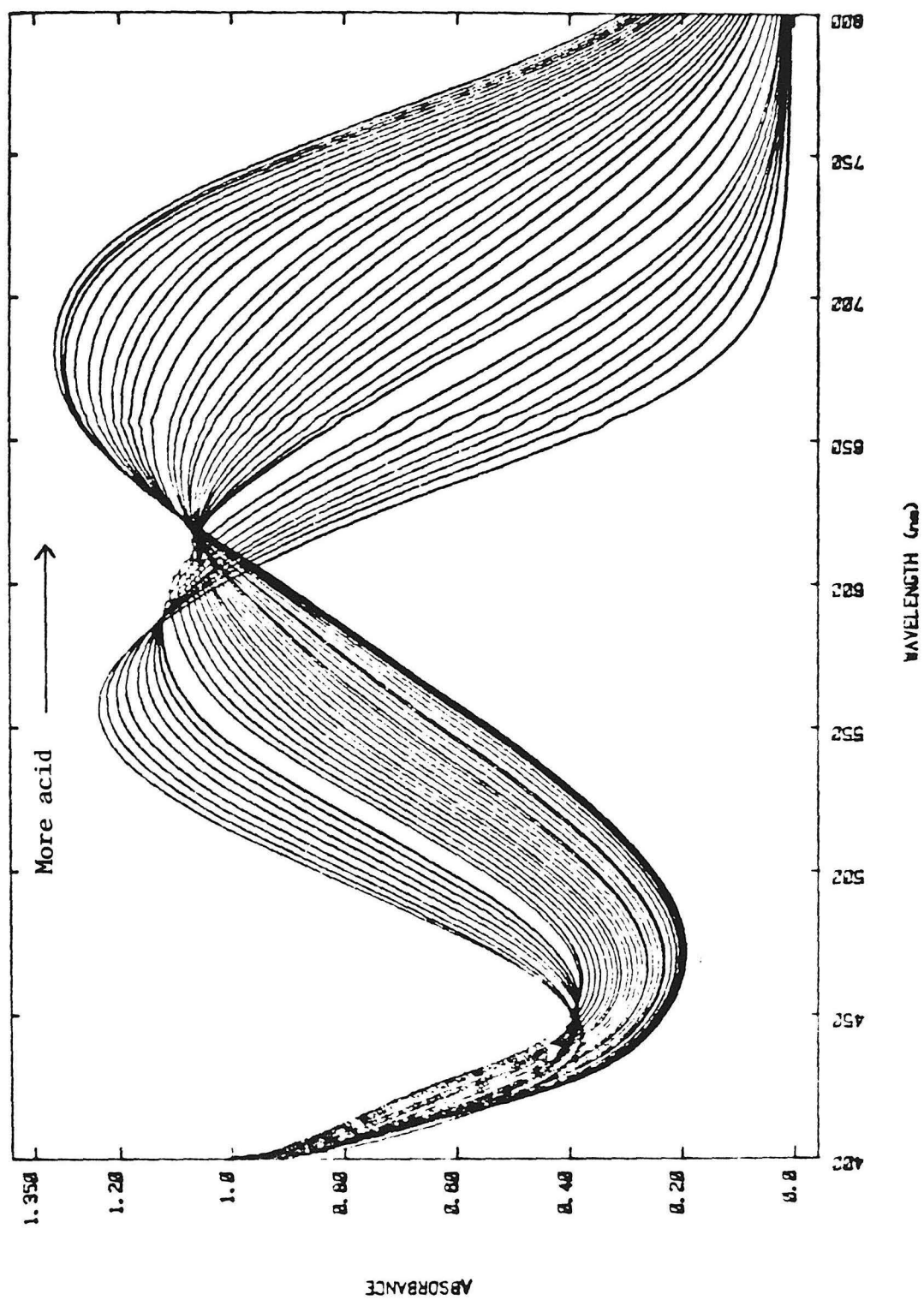


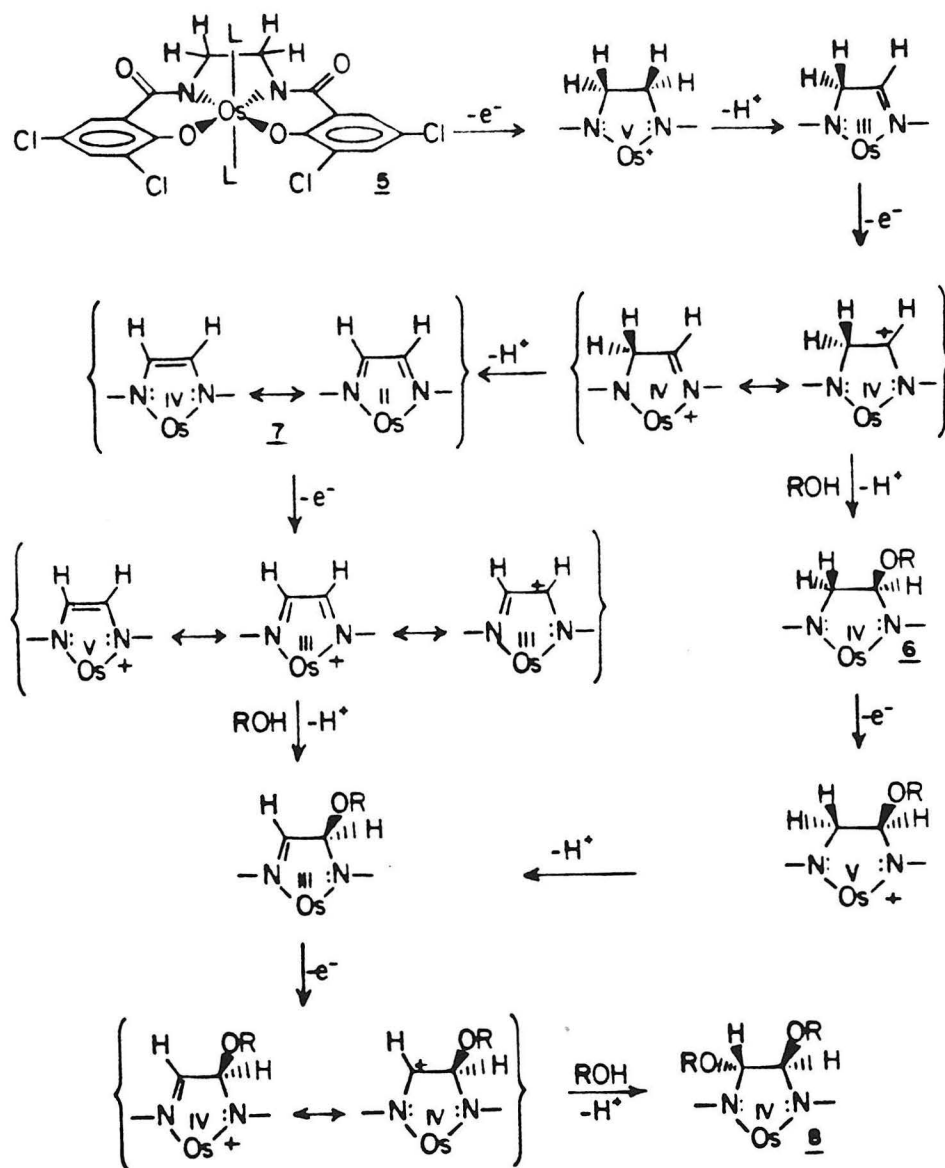
Figure 2.14. Visible spectra of trans- $\text{Os}(\text{CHBA})_2(\text{t-Bupy})(\text{Ph}_3\text{P}=\text{O})$, 13, in CH_2Cl_2 during gradual addition of 9 equivalents of $\text{HBF}_4 \cdot \text{H}_2\text{O}$ in THF.

Mechanistic Considerations for CHBA-Et Oxidation

Once the identity of the compounds formed during the oxidative degradation of $\text{Os}(\text{CHBA-Et})(\text{Py})_2$ had been established, it became possible to propose a mechanism to account for their formation. Scheme 2.5 shows a mechanism for the electrochemical conversion of 5 to 8 which we believe is consistent with all of the data. One-electron oxidation of 5 would produce a cationic Os(V) complex. This complex could then undergo reductive deprotonation to give an Os(III) monoimine species, which at the potential of the electrolysis would be rapidly oxidized. The resulting Os(IV) cation could undergo a second reductive deprotonation to yield 7. One-electron oxidation of 7 would produce a compound which possesses carbonium ion character at the carbon atoms of the bridge. Nucleophilic attack by the alcohol in solution followed by proton loss would lead to another Os(III) monoimine complex. Upon oxidation this species would be attacked by a second alcohol molecule to yield 8. Note that the oxidative conversion of 7 to 8 is 100% stereoselective, yielding only the trans substituted compounds 8 or 8*. Oxidative ligand dehydrogenations similar to that producing 7 have been previously reported [11-13].

Compound 6 was never isolated or identified. It was observed only very early in the electrolyses and in amounts much smaller than the other compounds. The TLC results indicate that 6 is neutral and contains the alcohol group. Its blue color suggests that it is an Os(IV) species. Since 6 was observed in oxidations of 5 but not 7 and led to the production of 8, it is assumed that it lies on a parallel pathway from 5 to 8. The pathway proposed in Scheme 2.5 is consistent with the known information.

Scheme 2.5. Mechanism of electrochemical oxidation of 5 to 8.

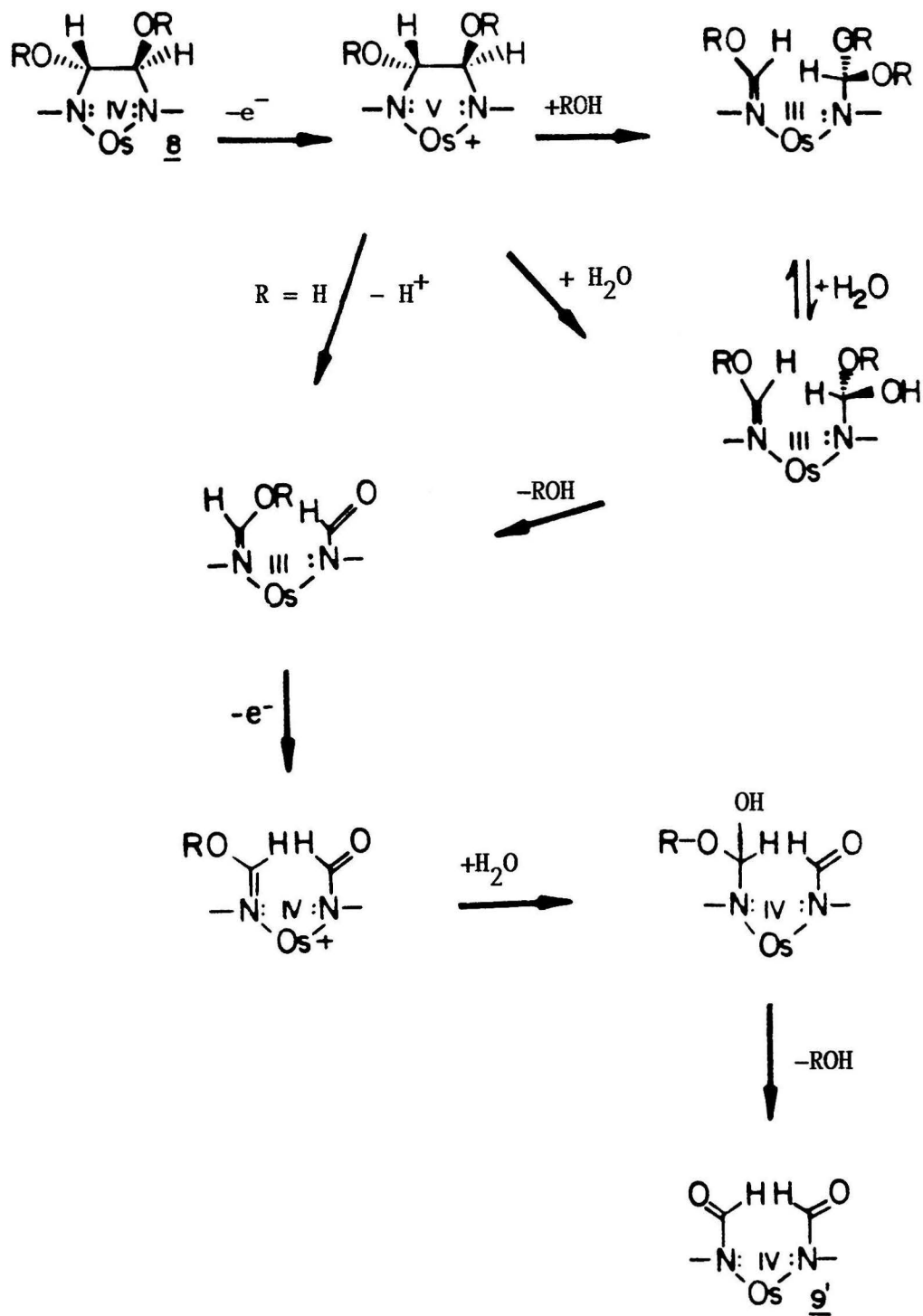


The conversion of 8 and/or 8* to 9 and/or 9' is a much more complex and less well-understood reaction. Starting with 5 the stereochemistry of the final product is determined primarily by the alcohol present during the electrolysis. Primary and secondary alcohols (methyl, ethyl, n-propyl, n-butyl, benzyl and isopropyl) consistently gave quantitative conversion to 9, the cis-alpha isomer. Tertiary alcohols (t-butyl and t-amyl) or water led to the production of high yields of the trans isomer, 9', with some 9 as determined by TLC. The identity of the monodentate ligands of 5 also had a small effect. The oxidation of $\text{Os}(\text{CHBA-Et})(\text{Py})_2$ in the presence of 0.5 M isopropanol produced only 9, while $\text{Os}(\text{CHBA-Et})(\text{t-Bupy})_2$ yielded a mixture of 9 and 9' in a ratio of about 7:3. It seems likely that the factors which determine the stereochemistry of the product are the relative rates of isomerization and another reaction, probably cleavage of the carbon-carbon bond of the bridge.

Scheme 2.6 depicts the mechanism believed to be most consistent with all of the available data. Oxidation of 8 by one electron produces an $\text{Os}(\text{V})$ species which can either isomerize or undergo a degradation reaction which breaks the carbon-carbon bond of the bridge. It has been shown that this type of $\text{Os}(\text{V})$ species can spontaneously isomerize from trans to cis-alpha in an effort to stabilize the electron deficient metal center (see Chapter IV). The relative rates of the isomerization and degradation reactions determine the stereochemistry of the product, but the same reactions are believed to lead from either cis-alpha- or trans-8⁺ to 9 or 9'.

Attack by either water (added deliberately or present as an impurity in the alcohol or methylene chloride) or alcohol at a bridge carbon of 8⁺ cleaves the carbon-carbon bond and forms an enol-ether group at one carbon

Scheme 2.6. Mechanism of electrochemical oxidation of 8 to 9'.



and either a hemi-acetal or an acetal at the other. Attack by alcohol gives the acetal which can be hydrolyzed to the hemi-acetal. Attack by water gives the hemi-acetal directly, and loss of alcohol from this group forms the N-formyl derivative of the CHBA ligand. If the original compound is 8* rather than 8, then the monoformyl intermediate can be formed directly by carbon-carbon bond cleavage and loss of the proton from the hydroxyl substituent. One-electron oxidation of the monoformyl intermediate to an Os(IV) cationic species is followed by a similar sequence of reactions to produce the second formyl group, completing the synthesis of 9 and/or 9'.

I would now like to outline the experimental evidence which supports this mechanism. The proposed mechanism for the conversion of 5 to 8 involves four one-electron oxidations. The mechanism just described for conversion of 8 to 9 and/or 9' involves another two one-electron oxidations for a total of six one-electron oxidations between 5 and 9 and/or 9'. The experimental charge consumed is variable but is always greater than or equal to 6.0 F/mol Os.

It was initially reported [5] that the alkyl groups of 8 were lost as carbonium ions and reacted with alcohol in solution to form an ether. This report was based on the detection of between one and three equivalents of benzyl ether after oxidation of 5 in the presence of benzyl alcohol. However, this observation has now been found to be erroneous. Blank experiments showed that the benzyl ether was formed by dehydration of the benzyl alcohol catalyzed by the acid formed during the electrolysis. It is now known that the alkyl groups of 8 are lost as the corresponding alcohol. Gas chromatographic analysis of the product solution from the oxidation of n-octyl-8 in the presence of t-butanol

confirmed that little or no t-butyl-n-octyl ether was formed. Instead, about 85% of the octyl groups were accounted for as the alcohol. The formation of the alcohol requires the participation of an oxygen source in the reaction. This source is almost certainly water.

It seems very likely that the isomerization from trans to cis- α occurs at the Os(V) form of 8. As will be discussed in Chapter IV, the tetradentate tetraanionic ligands produced by the Collins group are better electron donors in the non-planar conformations. Thus when the electron density on the metal center is decreased by oxidation, the ligand responds by adopting a non-planar conformation. For the complex Os(CHBA-DCB)(Py)₂ this results in an isomerization from trans to cis- α at Os(V). In contrast, there is very little driving force for isomerization once the carbon-carbon bond of the bridge has been broken, as evidenced by the very similar formal potentials of 9 and 9'. As will also be discussed in Chapter IV, the equilibrium constant for isomerization at Os(V) of Os(CHBA-DCB)(Py)₂ favors the cis- α form while that of Os(CHBA-DCB)(t-Bupy)₂ slightly favors the trans isomer. This difference arises from the added electron donating ability of t-butylpyridine. The same effect is probably responsible for the increased yield of 9' from Os(CHBA-Et)(t-Bupy)₂. Since this is a secondary effect, further discussion of the mechanism of degradation of 5 will be limited to the pyridine compound with the understanding that similar arguments can be made for the 4-t-butylpyridine compound.

It is not obvious from Scheme 2.6 why the stereochemistry of the product varies with the alcohol present during the electrolysis. One immediate question which arises is whether the alcohol in solution or the alkoxy groups on the bridge of 8 determine the stereochemistry of the

product. During the usual electrochemical syntheses of 9 and 9', all of the alkoxy groups are necessarily the same. However, the chemical synthesis of 8 allowed the two types of alkoxy group to be varied independently. Compounds containing a variety of different alkoxy groups (methyl, n-octyl, benzyl, isopropyl and t-butyl) were synthesized. Two asymmetric compounds, 8*, containing hydroxy and t-butyl or methyl groups were also prepared. Controlled potential electrolyses of these compounds in the presence of several alcohols and/or water were performed and the distribution of 9 and 9' in the product solution was determined by HPLC. The results of these experiments are shown in Tables 2.2 and 2.3.

Table 2.2. Isomer distribution in electrolyses of 8 and 8* in the presence of ethanol and t-butanol.^a

Compound	Concentration, mM	<u>9/9'</u> ^b	
		0.5M EtOH	0.5M <u>t</u> -BuOH
Me- <u>8</u>	0.1	100/0	63/37
Oct- <u>8</u>	0.1	100/0	69/31
Oct- <u>8</u>	1.0		21/79
Bz- <u>8</u>	0.1	100/0	61/39
<u>i</u> -Pr- <u>8</u>	0.1	100/0	79/21
<u>t</u> -Bu- <u>8</u>	0.1	100/0	79/21
Me- <u>8*</u>	0.1	100/0	37/63
<u>t</u> -Bu- <u>8*</u>	0.1	91/9	41/59
<u>5</u>	0.1		31/69

^aControlled potential oxidation in CH₂Cl₂ at +0.87 V in the presence of 0.5 M ROH. ^bRatio determined by HPLC with detection limit of ca. 5%.

Table 2.3. Effects of alcohol, alcohol concentration and water on isomer distribution in electrolyses of 8 and 5.^a

Compound	ROH in solution	<u>9</u> / <u>9'</u> ^b
Me- <u>8</u>	0.5M EtOH	100/0
Me- <u>8</u>	0.1M EtOH	98/2
Me- <u>8</u>	0.02M EtOH	76/24
Me- <u>8</u>	0.1M <u>i</u> -PrOH	87/13
<u>i</u> -Pr- <u>8</u>	0.5M EtOH	100/0
<u>i</u> -Pr- <u>8</u> ^c	0.5M EtOH + <0.2M H ₂ O [14]	80/20 ^d
<u>i</u> -Pr- <u>8</u>	<0.2M H ₂ O	30/70
<u>5</u> ^e	0.5M <u>i</u> -PrOH + <0.2M H ₂ O [14]	50/50 ^d
<u>5</u> ^e	0.5M <u>i</u> -PrOH	100/0 ^d

^aControlled potential oxidation of 0.1 mM 8 or 5 in CH₂Cl₂ at +0.87 V in the presence of ROH. ^bRatio determined by HPLC with detection limit of ca. 5%. ^c0.5mM 8. ^dRatio estimated from TLC. ^e1mM 5.

These results clearly show that the isomer distribution is determined principally by the alcohol, or water, in solution. With 0.1mM 8 and 0.5 M ethanol in solution, compound 8 produced only 9, the cis- α isomer, no matter what the alkoxy groups on the bridge were. However, with 0.5 M t-butanol in solution, significant amounts of 9', the trans isomer, were produced with all alkoxy groups. The presence of a hydroxyl group on the bridge does affect the distribution, increasing the yield of 9'. This increase agrees with the proposal in Scheme 2.6 that such compounds, 8*, can decompose by a unimolecular route. This unimolecular decomposition should be faster than the bimolecular attack by water and so should increase the yield of the unisomerized product, 9'. The oxidation of 5 in the presence of t-butanol produced an isomer distribution very close to

that of the 8* compounds, not like that of t-butyl-8. This is not surprising since TLC during the preparation of 9' from 5 and tertiary alcohols indicated the formation of very little 8. A number of other compounds, probably including 8*, were formed instead. The apparently higher yields of 9' (ca. 95%) from preparative scale electrolyses may stem from the concentration difference. On increasing the concentration of n-octyl-8 from 0.1 mM to 1.0 mM, the yield of 9' from oxidation in the presence of t-butanol increased from 31% to 79%. The reasons for this increase are unknown.

The production of 8* rather than 8 during the electrolysis of 5 with tertiary alcohols explains in part the resulting product distribution, but another factor must be involved since even the 8 compounds give significant yields of 9' in the presence of t-butanol. This factor seems to be a stabilization of the Os(V) form of 8, 8⁺, by the alcohol in solution. As noted previously, the addition of methanol to a solution of methyl-8 increased the reversibility of its oxidation. This effect can be seen in Figure 2.15 for the addition of t-butanol to a solution of methyl-8. At 50 mV/sec scan rate in the absence of added alcohol the oxidation of methyl-8 is totally irreversible. Upon addition of 20 mM t-butanol a small return wave can be seen, and with 100 mM t-butanol the oxidation appears very reversible. The same effect is seen with ethanol but at lower concentrations. With just 20 mM ethanol the oxidation appeared reversible at 50 mV/sec and almost so at 20 mV/sec. Surprisingly, water had an effect similar to t-butanol. The stabilization of 8⁺ which increases its lifetime and allows its reduction to be observed by CV, would also give it more time to isomerize to cis- α . Since ethanol stabilizes 8⁺ better than t-butanol or water, oxidations in the

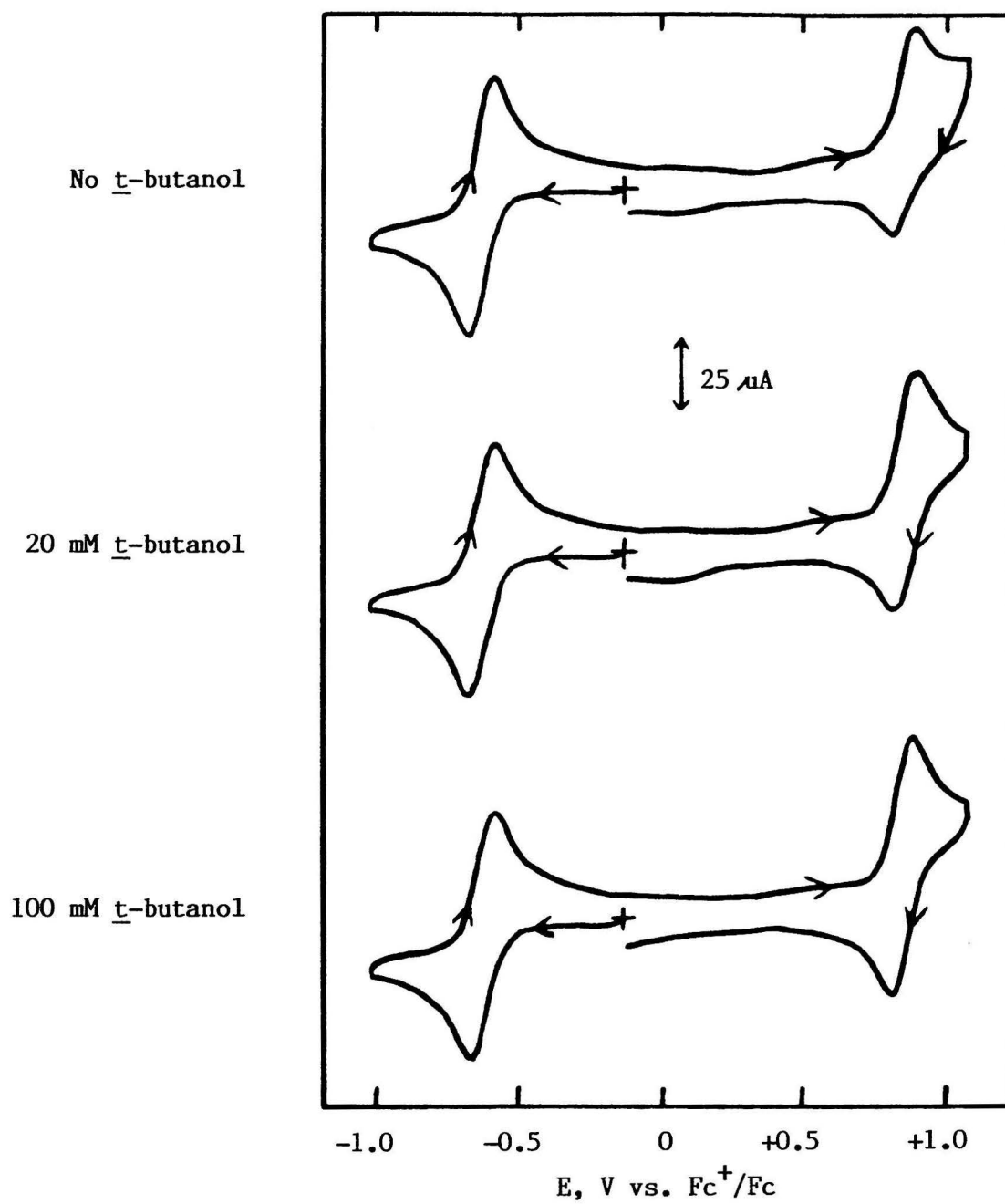


Figure 2.15. Cyclic voltammograms of 1.4 mM Me-8 + t-butanol in CH_2Cl_2 , 0.1 M TBAP at 0.17 cm^2 BPG electrode. Scan rate = 200 mV/sec.

presence of ethanol would be expected to yield more 9 and less 9', as is observed. This stabilization presumably involves solvation of the cationic Os(V) species by the alcohol or water. If this solvation involved coordination to the Os, then because of steric effects the stabilization should decrease from primary to secondary to tertiary alcohols. Water might be better than any of the alcohols for solvation because of its small size and high polarity, but its direct involvement in the decomposition of 8⁺ would certainly decrease its effectiveness for stabilizing 8⁺.

The results in Table 2.3 support these arguments. Decreasing the concentration of ethanol from 0.5 M to 0.02 M increased the amount of 9' formed from methyl-8 from none to 24%. Changing from 0.1 M ethanol to 0.1 M isopropanol, which is more sterically hindered, increased the yield of 9' from 2% to 13%. The oxidation of isopropyl-8 in the presence of 0.5 M ethanol gave only 9 as expected. In the presence of ethanol which stabilizes 8⁺ strongly and water which decomposes it, about 20% 9' was formed. With only water present, the yield of 9' increased to 70%.

It might be argued that the only reason that oxidations of 5 in the presence of tertiary alcohols produced 9' as the major product was that these alcohols contained more water than the others and so produced more 8* which led to 9'. However, as seen in Table 2.3, saturation with water of a solution containing 5 and 0.5 M isopropanol only increased the yield of 9' to 50%. During that reaction TLC indicated the formation of significant quantities of both 8 and 8*, whereas during the oxidations of 5 in the presence of tertiary alcohols very little 8 was formed. This result seems to indicate that yet another factor is involved in determining the isomeric distribution of the products of the oxidation of

5 in the presence of tertiary alcohols. Probably because of steric reasons, it is very difficult to form 8 from tertiary alcohols. Little 8 is observed in the electrolyses and for the chemical syntheses the solvents must be scrupulously dried to obtain significant yields of 8, a precaution which is not as important with primary and secondary alcohols [6]. Thus the difficulty of forming 8 from tertiary alcohols allows the formation of 8* and other unidentified compounds detected by TLC which lead preferentially to 9'.

In summary, the isomeric distribution of products from the oxidation of 5 in the presence of alcohols is determined by a very complex array of interconnected factors. For primary and secondary alcohols the process is relatively straightforward. The oxidation of 5 in the presence of primary and secondary alcohols initially results in total conversion to 8. Oxidation of 8 gives a cationic Os(V) species which is stabilized through solvation by the alcohol in solution. Before trace amounts of water initiate the series of reactions leading to 9, the 8⁺ isomerizes from trans to cis-alpha. Eventually attack by water cleaves the carbon-carbon bond of the bridge and leads to the formation of 9.

In the presence of tertiary alcohols, very little 8 is formed. Instead, 8* and other compounds, such as the di-hydroxy species, are formed. The compound 8* has been shown to give increased yields of 9', probably because of a shorter lifetime of the Os(V) form caused by the availability of a unimolecular decomposition pathway. The greater ease of decomposition of 8* is assisted by the fact that tertiary alcohols stabilize the Os(V) cation less strongly than primary and secondary alcohols. These factors combine to give high yields of 9' from the oxidation of 5 in the presence of tertiary alcohols.

Water is certainly involved in the synthesis of both 9 and 9'. The recovery of the alkoxy groups of 8 as the alcohol necessitates the presence of water to provide the extra oxygen atom. Water is also necessary for the formation of 8* in the presence of tertiary alcohols. Water has been shown to stabilize 8⁺ to some extent, but the fact that it is also involved in the ligand decomposition causes increased yields of 9' from the oxidation of 8 in the presence of both alcohol and water.

Conclusions

The electrochemistry of the complex $\text{Os}(\text{CHBA-Et})(\text{Py})_2$, 5, was examined in methylene chloride by cyclic voltammetry and controlled potential electrolysis. The complex was found to undergo two reversible, diffusion-controlled one-electron reductions to the orange $\text{Os}(\text{III})$ and purple $\text{Os}(\text{II})$ species. The oxidation to $\text{Os}(\text{V})$, however, was irreversible because of oxidative degradation of the CHBA-Et ligand. In the presence of alcohols or water this oxidative ligand degradation proceeds through a series of well-defined intermediates detected by CV and TLC. The reaction was studied by structural characterization of a number of the intermediates synthesized chemically and/or electrochemically.

The first compound characterized was 7, which is formed by oxidative dehydrogenation of the ethane bridge of 5. This complex, which was yellow rather than blue as were the other $\text{Os}(\text{IV})$ complexes studied, has two resonance forms. In one form the osmium is formally $\text{Os}(\text{IV})$ while in the other it is $\text{Os}(\text{II})$. This resonance may provide significant stabilization of the one-electron oxidized species. The chemical synthesis of 7 was accomplished by air oxidation of 5 adsorbed on silica gel.

Electrochemical or chemical oxidation of 7 in the presence of alcohols yielded 8. In this compound the unsaturated bridge of 7 has been selectively oxidized to a trans-1,2-diether. In the presence of alcohol and water the related trans-1-hydroxy-2-alkoxy complex, 8*, is formed. Further electrochemical oxidation of 8 and 8* results in cleavage of the carbon-carbon bond of the ligand bridge and loss of the alkoxy groups as the alcohol. The products, 9 and 9', contain two bidentate ligands in which each amide nitrogen bears a formyl group. The two products have been identified as different diastereomers, 9 being the cis-alpha isomer

and 9' the trans isomer. The diastereomeric distribution is determined primarily by the alcohol in solution. The two products of the electrolysis undergo selective hydrolyses of the formyl groups to give complexes containing bidentate primary amide ligands. These complexes catalyze the electrochemical oxidation of alcohols to aldehydes and ketones.

A mechanism for the oxidative degradation of 5 has been proposed which accounts for all of the observed intermediates and the diastereomeric distribution of the products. The mechanism involves six one-electron oxidations, each followed by one or more chemical reactions. The isomerization which leads to 9 is believed to occur at the Os(V) form of 8. If the rate of the following chemical reaction which breaks the carbon-carbon bond of the bridge is slower than the isomerization, then 9 is formed. If the chemical reaction is faster than isomerization then 9' is the major product. For a number of reasons tertiary alcohols increase the rate of the carbon-carbon bond cleavage and give 9' as the major product.

In addition to following the oxidative degradation of the CHBA-Et ligand in considerable detail and uncovering some interesting mechanistic steps, this study has provided valuable information about the requirements of ligands coordinated to highly oxidizing metal centers. Clearly the ethane bridge and its derivatives of CHBA-Et are not suitable components of desirable ligands. As detailed in chapter IV, replacement of the ethane bridge with a dichlorobenzene group prevents the oxidative degradation of the ligand. A summary of the formal potentials of the osmium complexes encountered in this study can be found in Table 2.4.

Table 2.4. Formal potentials of 5 and its oxidation products.

Compound	Formal Potential, V ^a		
	Os(III/II)	Os(IV/III)	Os(V/IV) ^b
<u>5</u>	-1.88	-0.65	(+0.70)
<u>5</u> -(t-Bupy)	-1.96	-0.70	(+0.66)
<u>7</u>	-1.76	-0.62	+0.37 ^c
Me- <u>8</u>	-1.95	-0.64	(+0.90)
<u>9</u>	-1.88	-0.46	d
<u>9'</u>	-1.88	-0.39	d
<u>11</u>	-1.90	-0.67	(+0.7)
<u>11</u> -(t-Bupy)	-1.99	-0.70	(+0.7)
<u>11'</u> -(t-Bupy)	-1.97	-0.70	(+0.6)

^aE_f measured in 0.1 M TBAP/CH₂Cl₂ and referenced to Fc⁺/Fc internal standard. ^bPotentials in parentheses are anodic peak potentials of irreversible oxidations. ^cCompound 7 also displays an irreversible oxidation at a peak potential of +0.92 V. ^dNo anodic activity seen below +1.1 V.

Experimental

Materials

Reagent grade methylene chloride (MCB or Mallinckrodt) was further purified by passing it over a short column of activated alumina (Woelm N. Akt. I). Acetonitrile (Burdick and Jackson, distilled in glass grade) was dried over 3A molecular sieves. All other solvents were reagent grade (Aldrich, Baker, Mallinckrodt, MCB or USI) and were used as received. Tetra-n-butylammonium perchlorate supporting electrolyte (Southwestern Analytical Chemicals) was dried, recrystallized twice from acetone/ether, and then dried under vacuum. Alcohols were reagent or spectrophotometric grade and were used as received, except for t-butanol (MCB) which was distilled once. Tetra-n-butylammonium periodate was prepared by reaction of periodic acid (Baker) with tetra-n-butylammonium hydroxide (25% in methanol, MCB) in ethanol, followed by precipitation with ether. t-Butyl-n-octyl ether was prepared by reaction of potassium t-butoxide (MCB) with 1-bromooctane (Aldrich) in t-butanol in the presence of a small amount of sodium iodide. Trifluoromethanesulfonic acid (3M) was distilled and stored at -10 °C. Trifluoroacetic acid (MCB), 2,4-dinitrophenylhydrazine (Kodak) and ferrocene (Aldrich) were used as received. Silica gel was 60-200 mesh (Davidson). Analytical and preparatory thin layer chromatography plates, 250 and 1000 micron, respectively, were silica gel GF (Analtech).

All samples of compounds 5, 7, 8 and 8* were supplied by Terry Krafft and details of their preparation can be found in the appropriate references (5,6). The characterization of all compounds was performed by Terry Krafft with details in the same references.

Osmium Complex Syntheses

Cis-alpha-Os(Fo-CHBA)₂(Py)₂, 9. Os(CHBA-Et)(Py)₂, 5, (40 mg, 0.051 mmol), was dissolved in CH₂Cl₂ (25 ml) containing 0.1 M TBAP and 1 M of a 1° or 2° alcohol (usually methanol or isopropanol). The solution was electrolyzed at a BPG anode at +0.87 V (+1.40 V vs. an aqueous Ag/AgCl reference electrode) until the current had decayed to <5% of its initial value and TLC indicated that the reaction was complete. The anolyte was transferred to a beaker and ether (65 ml) was slowly added. The precipitated TBAP was removed by filtration and the solvents were evaporated from the filtrate. The resulting oil was dissolved in acetone (25 ml) and the product was precipitated by addition of H₂O (50 ml). The dark blue product was redissolved in CH₂Cl₂, dried over MgSO₄ and precipitated with hexane: yield 30 mg (72%). Analysis calculated for C₂₆H₁₆Cl₄N₄O₆Os: C, 38.44; H, 1.99; N, 6.90. Found: C, 38.41; H, 2.06; N, 6.88.

Cis-alpha-Os(Fo-CHBA)₂(t-Bupy)₂, 9-(t-Bupy). Os(CHBA-Et)(t-Bupy)₂, 5-(t-Bupy), (50 mg, 0.050 mmol), was oxidized in the presence of methanol or isopropanol in the same manner used for the pyridine adduct of 9. The product, which was isolated as before, contained significant amounts of the trans isomer, 9'-(t-Bupy). The two compounds were separated on a preparative TLC plate (1000 micron, silica gel) by elution with CH₂Cl₂/THF (30:1). The product, 9-(t-Bupy) (32 mg, 62%), was isolated as a dark blue powder from CH₂Cl₂/hexane. Analysis calculated for C₃₄H₃₂Cl₄N₄O₆Os: C, 44.15; H, 3.49; N, 6.06. Found: C, 44.07; H, 3.68; N, 5.76.

Trans-Os(Fo-CHBA)₂(Py)₂, 9'. Method A. Os(CHBA-Et)(Py)₂, 5, was oxidized by the same method used in the synthesis of 9 except that the CH₂Cl₂ contained 1 M t-butanol or t-amyl alcohol, or was saturated with

water. TLC indicated that the product was formed in high yield but difficulty in purification and isolation produced a low yield (<30%) of the dark blue product. Analysis calculated for $C_{26}H_{16}Cl_4N_4O_6Os$: C, 38.4; H, 1.99; N, 6.90. Found: C, 38.63; H, 2.16; N, 6.79.

Method B. $Os(CHBA-Et)(Py)_2$, 5, (8 mg, 0.01 mmol) was dissolved in CH_2Cl_2 (10 ml) containing 0.5 M methanol and 2 M trifluoroacetic acid. To this solution was added a CH_2Cl_2 solution of tetrabutylammonium periodate (0.1 M). TLC indicated that 9' was produced in high yield.

Trans- $Os(Fo-CHBA)_2(t-Bupy)_2$, $9'-(t-Bupy)$. Method A. $Os(CHBA-Et)(t-Bupy)_2$, 5-(t-Bupy), (25 mg) was oxidized in the presence of 0.5 M t-butanol using the same procedure as for the pyridine adducts of 9 and 9'. TLC showed that the reaction was clean and that the product was formed in high yield. The high solubility of the dark blue compound led to a much lower yield of isolated material after recrystallization from boiling cyclohexane (15 mg, 58%). Analysis calculated for $C_{34}H_{32}Cl_4N_4O_6Os$: C, 44.15; H, 3.49; N, 6.06. Found: C, 44.02; H, 3.53; N, 5.93.

Method B. Compound 9'-(t-Bupy) was formed as a minor product in the above synthesis of 9-(t-Bupy). Ten milligrams (19%) of 9'-(t-Bupy) were recovered from the TLC separation of the two isomers.

Cis- α - $Os(CHBA)_2(Py)_2$, 11. $Os(CHBA-Et)(Py)_2$, 5, was electrolyzed in the presence of a primary or secondary alcohol to produce 9 as outlined above. Instead of isolating the 9, the anolyte solution was transferred to a 100 ml flask and refluxed until TLC indicated that the reaction was complete, about 24 hours. Pyridine (100 microliters) was then added to neutralize the acid and the solution was rotovapped dry at 60 °C. The solid was dissolved in ethyl acetate (20 ml) and then reprecipitated with

diethyl ether (20 ml). The light purple precipitate containing 11 and TBAP was collected on a frit and then the TBAP was dissolved away from the 11 with hot ethyl acetate (15 ml). A minimum amount of pyridine (25 ml) was used to dissolve the 11 off the frit, and the resulting solution was rotovapped dry at 60 °C. Xylenes (50 ml) were added and the mixture was again rotovapped dry at 60 °C. After drying under vacuum for 10 minutes, the 11 was dissolved in acetone (10 ml) and precipitated with water (20 ml). The solid was collected on a frit, dissolved in pyridine, rotovapped to low volume, xylenes added (50 ml), rotovapped to low volume, and finally precipitated with hexane (10 ml). Yield of 11 was about 75%.

[Cis-alpha-Os(HCHBA)₂(Py)₂](ClO₄)₂, Protonated 11. The protonated compound 11 was generated by the electrolysis and hydrolysis described above, except that the supporting electrolyte was 0.1 M tetra-n-hexylammonium perchlorate, THAP. The reaction mixture was evaporated to dryness and the residue, containing the protonated product (ca. 80 mg) and THAP (ca. 2.3 g), was then stirred with benzene (250 ml) for 15 minutes. The mixture, which contained the product as a blue oil, was allowed to stand for 2 hours and then decanted. The oily blue solid was washed with a second aliquot of benzene which was decanted after the mixture stood for 3 hours. The blue solid was collected by filtration, dissolved in CH₂Cl₂/acetone and precipitated with hexane. The crystalline product was dried under vacuum for 16 hours at 80 °C (60 mg). Analysis calculated for C₂₄H₁₈Cl₆N₄O₁₂Os: C, 30.11; H, 1.90; N, 5.85; Cl, 22.22. Found: C, 30.57; H, 2.21; N, 5.88; Cl, 22.09.

Cis-alpha-Os(CHBA)₂(t-Bupy)₂, 11-(t-Bupy). Method A. Compound 9-(t-Bupy) was prepared from 5-(t-Bupy) as described above with methanol as the alcohol, with which very little 9'-(t-Bupy) was formed. The

isolated 9-(t-Bupy) was dissolved in CH_2Cl_2 + 0.5 M methanol (50 ml), 24 microliters of 60% aqueous HClO_4 was added and the solution was refluxed for 17 hours. The solution was then rotovapped dry at 45 °C. The solid was dissolved in CH_2Cl_2 (10 ml), filtered and reprecipitated with pentane (100 ml). The solid was collected and dried under vacuum. Yield was about 50%.

Method B. Compound 11-(t-Bupy) can also be prepared without isolation of 9-(t-Bupy) as described for 11 above. Purification on two successive silica gel columns by elution with CH_2Cl_2 /acetone followed by recrystallization from CH_2Cl_2 /hexane yielded very pure 11-(t-Bupy). Analysis calculated for $\text{C}_{32}\text{H}_{32}\text{Cl}_4\text{N}_4\text{O}_4\text{Os}$: C, 44.25; H, 3.71; N, 6.45. Found: C, 43.94; H, 3.66; N, 6.33.

Trans-Os(CHBA)₂(Py)₂, 11'. Os(CHBA-Et)(Py)₂, 5, was electrolyzed in the presence of 0.5 M t-butanol to produce 9'. Conversion to 11' and isolation were performed as for 11. Yield was about 50%.

Trans-Os(CHBA)₂(t-Bupy)₂, 11'-(t-Bupy). Os(CHBA-Et)(t-Bupy)₂, 5-(t-Bupy), was electrolyzed in the presence of 0.5 M t-butanol to produce 9'-(t-Bupy). Conversion to 11'-(t-Bupy) and isolation were performed as described for 11-(t-Bupy), Method A. Yield was about 70%.

Apparatus and Procedures

Cyclic voltammetry was performed with a Princeton Applied Research (PAR) Model 173 potentiostat driven by a PAR Model 175 universal programmer using positive feedback IR-compensation. Current-voltage curves were recorded on a Houston Instruments Model 2000 X-Y recorder. Standard two-compartment electrochemical cells were used. When necessary, solutions were purged with argon to remove oxygen. The working electrode was a 0.17 cm^2 basal plane pyrolytic graphite (BPG, Union Carbide Co.)

disc mounted in a glass tube with heat-shrinkable tubing. The counter electrode was a platinum wire. Various reference electrodes were used, including SCE, SSCE, Ag/AgCl and a silver wire quasi-reference electrode. For each compound studied at least one experiment was performed in the presence of ferrocene as an internal potential standard. The formal potentials of all of the couples of the osmium compounds were then referenced to that of the ferrocene, which was consistently measured as +0.48 V vs. aqueous SCE. Formal potentials of reversible couples were taken as the average of the anodic and cathodic peak potentials. The supporting electrolyte was 0.1 M TBAP.

Controlled potential electrolysis experiments were performed with the PAR Model 173 potentiostat equipped with a Model 179 digital coulometer using positive feedback IR-compensation. Electrolyses in CH_2Cl_2 were performed in a standard three-compartment H-cell with a platinum gauze counter electrode in one compartment and the reference electrode and a 1.7 x 4.5 x 0.07 cm BPG working electrode in the third compartment. The liquid junction of the reference electrode was placed near the working electrode to minimize IR-compensation needed. Electrolyses in acetonitrile were conducted at a platinum gauze working electrode with a silver wire quasi-reference electrode isolated in another compartment. The experiments in acetonitrile were performed in a helium atmosphere dry box (Vacuum/Atmospheres Co.). All experiments were performed at room temperature, $22 \pm 2^\circ\text{C}$.

Analyses for aldehydes and ketones as products of the oxidation of alcohols in the presence of 5 and 11 were performed spectrophotometrically on a Hewlett Packard Model 8450A spectrometer. Samples were reacted with 2,4-dinitrophenylhydrazine and trifluoroacetic acid and then

chromatographed on silica gel to isolate the hydrazone. The absorbance of the hydrazone band at about 370 nm was compared to that of a standard solution to estimate the amount of aldehyde or ketone produced.

Gas chromatography was performed on a Hewlett Packard Model 5830A gas chromatograph equipped with a six-foot OV-101 column and a thermal conductivity detector. Analyses for 1-octanol and t-butyl-n-octyl ether were performed at 175 °C. Since CH₂Cl₂ was not compatible with the detector, samples were prepared by adding 10 ml of the test solution to 9 ml of 1-propanol in a 100 ml flask. The CH₂Cl₂ was then distilled off and the residual 1-propanol solution was diluted to 10 ml and analyzed for the alcohol and ether by comparison with authentic sample solutions.

HPLC analyses for 9 and 9' were performed on an IBM LC 9533 Ternary Gradient LC equipped with a phenyl column, an LC 9522 254 nm UV detector and a Hewlett Packard 3390A Integrator. The eluting solvent was 99.5% CH₂Cl₂ + 0.5% methanol. The ratio of concentrations of 9 and 9' was taken as equal to the ratio of the integrated areas of the HPLC peaks.

References and Notes

1. The numbering of the compounds was chosen so as to correspond most closely with those in the literature.
2. All potentially tetradentate tetraanionic ligands are coordinated as such in the compounds discussed in this thesis. Except where specifically stated, the ligands are coordinated in a planar manner with pyridines or other monodentate ligands occupying axial sites in a pseudo-octahedral coordination sphere.
3. The compound $\text{Os}(\text{CHBA-Et})(\text{O})_2^{2-}$ was examined first but showed no reversible electrochemistry in water, acetonitrile or methylene chloride.
4. Formal potentials are calculated as the average of the anodic and cathodic peak potentials determined by cyclic voltammetry. All potentials are referenced to the formal potential of a ferrocene internal standard, the potential of which in $\text{CH}_2\text{Cl}_2/0.1 \text{ M TBAP}$ has been consistently measured as +0.48 V vs aqueous SCE.
5. F.C. Anson, J.A. Christie, T.J. Collins, R.J. Coots, T.T. Furutani, S.L. Gipson, J.T. Keech, T.E. Krafft, B.D. Santarsiero and G.H. Spies J. Am. Chem. Soc., **106**, 4460-4472 (1984).
6. T.E. Krafft, Ph.D. Thesis, California Institute of Technology, February, 1985.
7. Ligand names are: 1,2-bis(3,5-dichloro-2-hydroxybenzamido)ethane, $\text{H}_4\text{CHBA-Et}$; 1,2-bis(3,5-dichloro-2-hydroxybenzamido)ethylene, $\text{H}_4\text{CHBA-Ethylene}$; 1,2-bis(3,5-dichloro-2-hydroxybenzamido)-trans-1,2-dialkoxyethane, $\text{H}_4\text{CHBA-t-1,2-diRO-Et}$; 1,2-bis(3,5-dichloro-2-hydroxybenzamido)-trans-1-hydroxy-2-alkoxyethane, $\text{H}_4\text{CHBA-t-1-OH-2-RO-Et}$; N-formyl-3,5-dichloro-2-hydroxybenzamide, $\text{H}_2\text{Fo-CHBA}$; 3,5-dichloro-2-hydroxybenzamide, CHBA; 1,2-bis(3,5-dichloro-2-hydroxybenzamido)-4,5-dichlorobenzene, $\text{H}_4\text{CHBA-DCB}$.
8. Much of the characterization work was done with compounds containing 4-t-butylpyridine instead of pyridine because of their much higher solubility.
9. A.M. Sargeson and G.H. Searle, Inorg. Chem., **4**, 45-52 (1965).
10. J. March, Advanced Organic Chemistry, Second Ed.; McGraw-Hill Book Co.: New York, 1977, pp. 310-311.
11. For example, see: (a) P.A. Lay, A.M. Sargeson, B.W. Skelton and A.H. White, J. Am. Chem. Soc., **104**, 6161-64 (1982). (b) M.J. Ridd and F.R. Keene, Ibid., **103**, 5733-5740 (1981). (c) M.S. Thompson and T.J. Meyer, Ibid., **103**, 5577-5579 (1981). (d) B.M. Brown, T.R. Weaver, F.R. Keene and T.J. Meyer, J. Inorg. Chem., **15**, 190-196 (1976).

12. For a recent review of alpha,alpha-diimine complexes including ligand oxidations see: G. Van Koten and K. Vrieze, Adv. Organomet. Chem., 21, 151-239 (1982).
13. Oxidation of methylene units in polypeptide systems has been reported. (a) J.S. Rybka and D.W. Margerum, Inorg. Chem., 20, 1453-1458 (1981). (b) L.J. Kirschenbaum and J.D. Rush, J. Am. Chem. Soc., 106, 1003-1010 (1984).
14. Saturated with water. Solubility of water in CH_2Cl_2 is 0.24% or about 0.18 M. See: Solvent Guide, Burdick and Jackson Laboratories Inc.: Muskegon, MI, 1980.

CHAPTER III

The Catalytic Electrooxidation of Alcohols by Osmium Compounds
Containing 3,5-Dichloro-2-hydroxybenzamide Ligands

Introduction

In Chapter II of this thesis it was reported that the oxidative degradation of $\text{Os}(\text{CHBA-Et})(\text{Py})_2$, 5, led to the production of the cis-alpha and trans isomers of $\text{Os}(\text{CHBA})_2(\text{Py})_2$, 11 and 11', and that these compounds are catalysts for the electrochemical oxidation of alcohols to aldehydes and ketones [1]. Chemical syntheses of 11' and several other Os(IV) compounds containing CHBA ligands have been developed by Terry Krafft [2,3]. The electrooxidation of a number of alcohols using these catalysts has been studied in an effort to gain information about the products and mechanism of the alcohol oxidation and the lifetime and mechanism of degradation of the catalysts.

The literature contains numerous examples of electrochemical oxidations of alcohols, both with [4-6] and without catalysts [7]. Usually there is no problem in oxidizing secondary alcohols to ketones, but the selective oxidation of primary alcohols to aldehydes is much more difficult. Frequently the oxidation of primary alcohols will produce aldehydes as the initial product, but then the aldehydes are further oxidized to carboxylic acids or esters. For example, the system $(\text{trpy})(\text{bpy})\text{RuO}^{2+}/(\text{trpy})(\text{bpy})\text{Ru}(\text{OH}_2)^{2+}$ oxidizes primary alcohols to aldehydes, but then readily takes the aldehydes on to carboxylic acids [4]. Iodonium catalyzes the oxidation of primary and secondary alcohols but produces only the ester from primary alcohols [5]. Primary alcohols can be selectively electrooxidized to aldehydes in the presence of 2,2,6,6-tetramethylpiperidine nitroxyl, but only low turnover numbers, 3 to 20 moles of alcohol per mole of catalyst, have been reported [6]. The electrooxidation of alcohols in the absence of catalysts generally

requires high potentials and proceeds with low selectivity and/or current efficiency [7].

The catalysts developed in the present work seem to have no tendency to oxidize aldehydes. No activity is detected by cyclic voltammetry or controlled potential electrolysis with aldehydes, and the aldehydes are obtained in high yields upon oxidation of primary alcohols. This feature makes these catalysts very attractive objects for study.

Unfortunately, though the catalysts appear to be selective, they all have very limited lifetimes. Compound 11 displays a maximum turnover number of about 300 in the presence of 1 M benzyl alcohol, corresponding to the production of 150 moles of benzaldehyde per mole of 11 before complete decomposition of the catalyst occurs. Other catalysts have even shorter lifetimes. Saturated and allylic alcohols are much poorer substrates and lead to much lower turnover numbers. The mechanism of catalyst decomposition is uncertain but may involve loss of ligands from the catalyst. Future modifications in the catalyst coordination sphere may lead to longer-lived catalysts. At that time more detailed mechanistic studies will become accessible and more exciting uses for the catalysts, such as resolution of racemic alcohols, could become possible.

Results and Discussion

Cyclic voltammetry of catalysts in the presence of alcohols

As reported in Chapter II of this thesis, the oxidative degradation of trans-Os(CHBA-Et)(Py)₂, 5, leads to two compounds containing bidentate CHBA ligands [1]. These compounds, cis-alpha-Os(CHBA)₂(Py)₂, 11, and trans-Os(CHBA)₂(Py)₂, 11', were found to be catalysts for the electrochemical oxidation of alcohols to aldehydes and ketones. Chemical syntheses have been developed by Terry Krafft for 11' and several other Os(IV) compounds containing CHBA ligands [2,3]. This group of compounds is referred to collectively as the catalysts and the structures of the prototype compounds, 11 and 11', are shown in Figure 3.1.

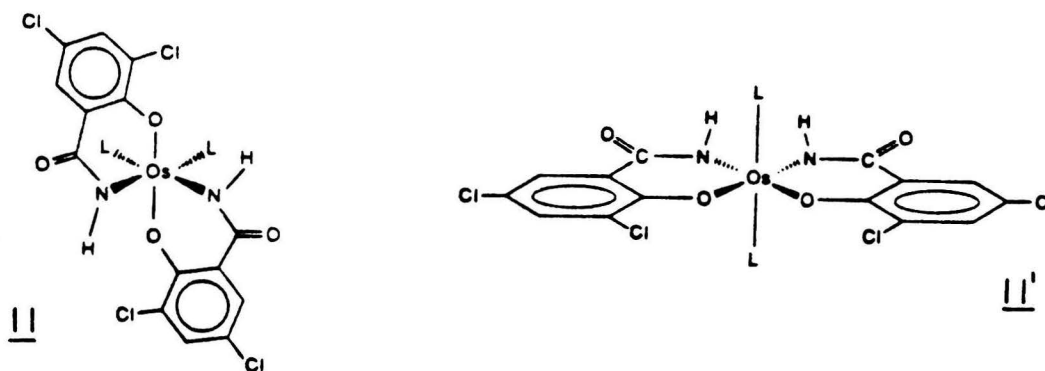


Figure 3.1. Structures of 11 and 11'.

Because acid is generated during the electrochemical syntheses of 11 and 11', the species initially formed are the dicationic diprotonated forms. The proposed structure of $H_2\text{-}\underline{11}^{2+}$ is shown in Figure 3.2. The cyclic voltammetric and spectroscopic evidence for the protonation of the catalyst compounds is discussed in Chapter II.

The cyclic voltammogram (CV) of $H_2\text{-}\underline{11}^{2+}$ in CH_2Cl_2 shows only a reversible Os(IV/III) couple at approximately +0.1 V vs. Fc^+/Fc [8].

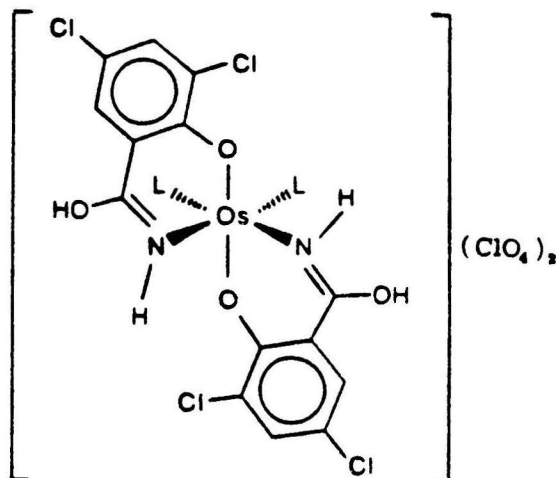


Figure 3.2. Proposed structure of protonated 11.

In the absence of added alcohol no anodic activity is seen below +1.1 V, but, as seen in Figure 3.3, the addition of 1 M benzyl alcohol gives rise to very large anodic currents at potentials above about +0.8 V. High concentrations of alcohol, greater than about 0.1 M, are necessary to observe this anodic activity with the catalysts. No anodic activity was seen with the alcohol in the absence of $\text{H}_2\text{-}\underline{11}^{2+}$. Controlled potential electrolyses have confirmed that this anodic activity is due to the catalytic oxidation of the benzyl alcohol to benzaldehyde (vide infra).

The catalyst compounds are most easily isolated in the nonprotonated neutral form. Figure 3.4 shows a CV of 11 in the presence of 1 M benzyl alcohol. The initial cathodic scan shows the Os(IV/III) couple of the deprotonated form of 11 at $E_f = -0.67$ V. The first anodic scan shows a shoulder corresponding to the irreversible oxidation to Os(V) and then the very large anodic currents as were seen with $\text{H}_2\text{-}\underline{11}^{2+}$. The acid formed by the alcohol oxidation protonates the catalyst in the vicinity of the electrode surface, so on the second scan the Os(IV/III) couple of $\text{H}_2\text{-}\underline{11}^{2+}$

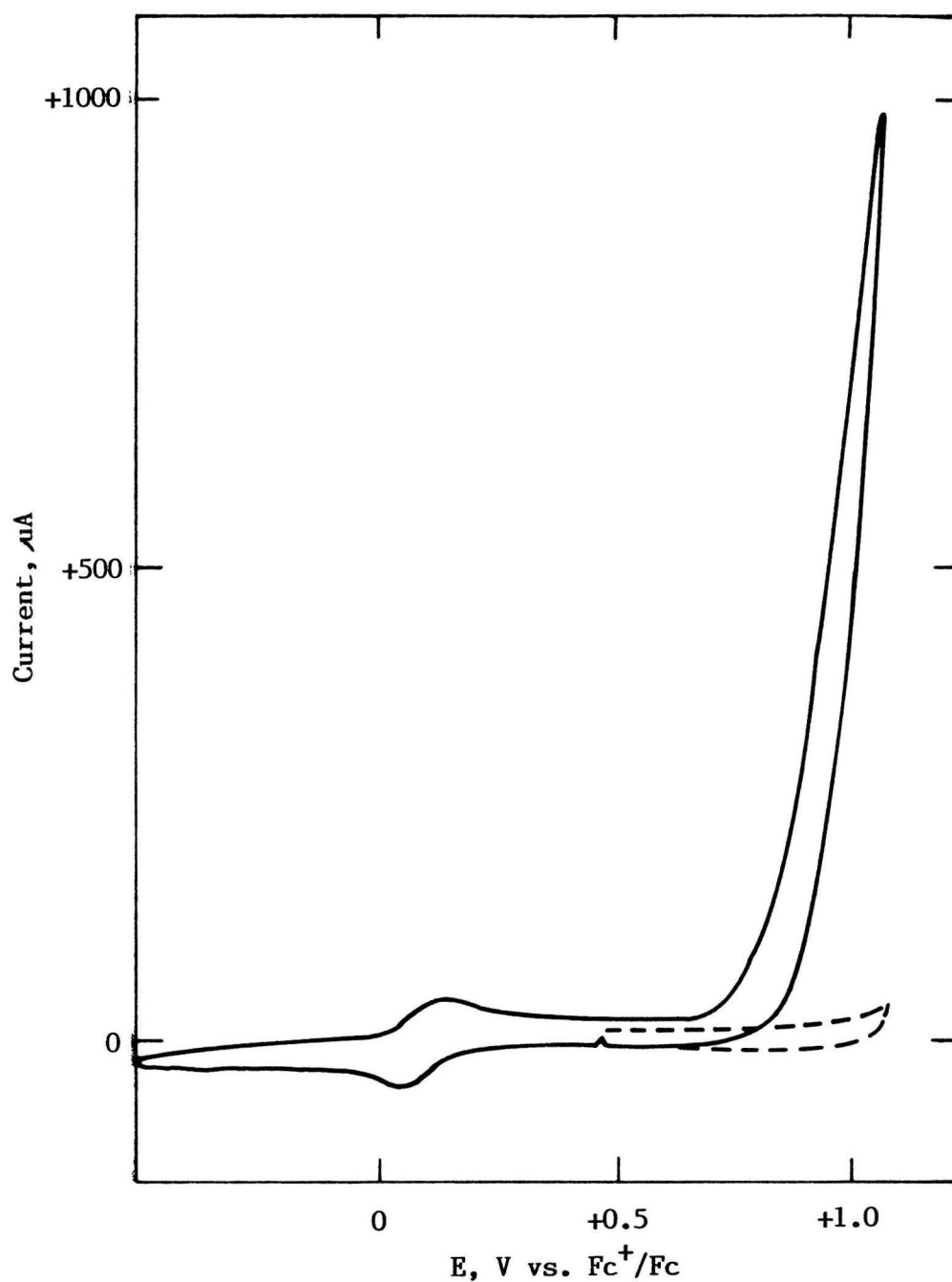


Figure 3.3. Cyclic voltammogram of 1 mM $\text{H}_2\text{-11}^{2+}$ + 1 M benzyl alcohol in CH_2Cl_2 , 0.1 M TBAP at 0.17 cm^2 BPG electrode. Scan rate = 200 mV/sec. Dotted line represents response with alcohol or catalyst alone.

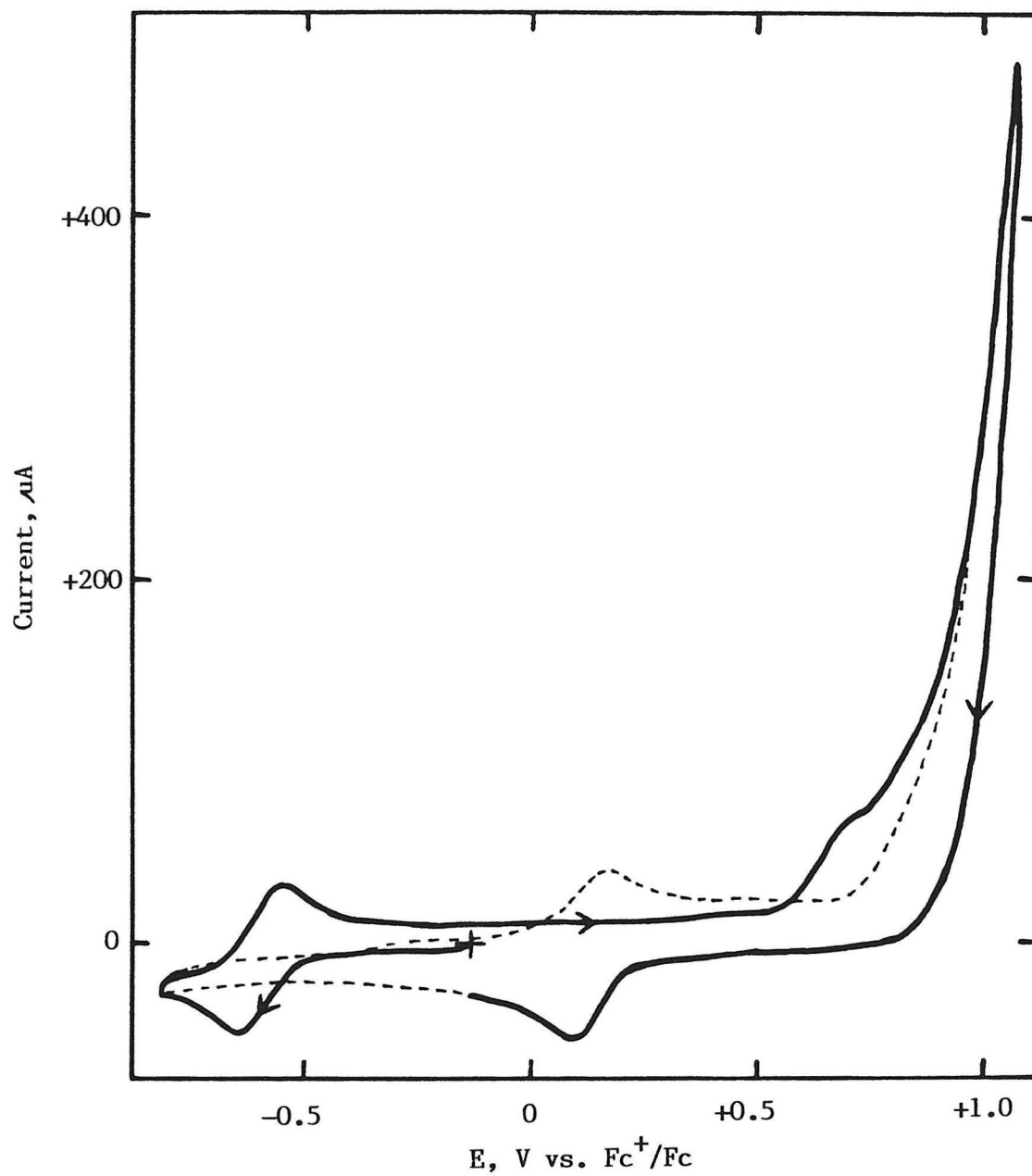


Figure 3.4. Cyclic voltammogram of 1 mM $\frac{11}{2}$ + 1 M benzyl alcohol in CH_2Cl_2 , 0.1 M TBAP at 0.17 cm^2 BPG electrode. Scan rate = 200 mV/sec. Dotted line is second scan.

at +0.1 V is seen. The shoulder for the oxidation of 11 is also gone on the second and succeeding scans, but the alcohol oxidation seems unaffected by the change from 11 to $\text{H}_2\text{-}\underline{11}^{2+}$.

Similar CV's were observed with other alcohols. Other benzylic alcohols gave rise to the same type of continuously rising anodic currents as observed with benzyl alcohol, but with lower currents. The CV's of 11 in the presence of saturated and allylic alcohols displayed peaks or waves at high potentials, as exemplified by n-butanol in Figure 3.5. In each case blank experiments run in the absence of 11 showed no anodic currents for direct oxidation of the alcohols at BPG. Very interesting results were obtained when CV's of $\text{H}_2\text{-}\underline{11}^{2+}$ were examined in the presence of both benzyl and n-butyl or ethyl alcohols. When both alcohols were present the anodic currents observed were greater than the sum of the currents observed with the alcohols in separate experiments. For example, one solution of 11 displayed a CV current at +1.07 V of 530 μA with 0.5 M benzyl alcohol and 200 μA with 0.2 M ethanol. In the presence of both 0.5 M benzyl alcohol and 0.2 M ethanol the current at +1.07 V was 1560 μA . This current is also much larger than would have been obtained with 0.7 M benzyl alcohol. The addition of benzaldehyde or acetone had no effect on the CV of $\text{H}_2\text{-}\underline{11}^{2+}$, indicating that the catalysts are not reactive toward aldehydes and ketones.

CV results obtained with the other catalyst compounds studied showed behavior qualitatively similar to 11. Some quantitative differences were observed depending upon the isomer and monodentate ligands of the catalysts. The compounds containing triphenylphosphine oxide, 13 and 14, were oxidized at lower potentials than the bis-pyridine compounds and so displayed alcohol oxidation at lower potentials. Studies with varying

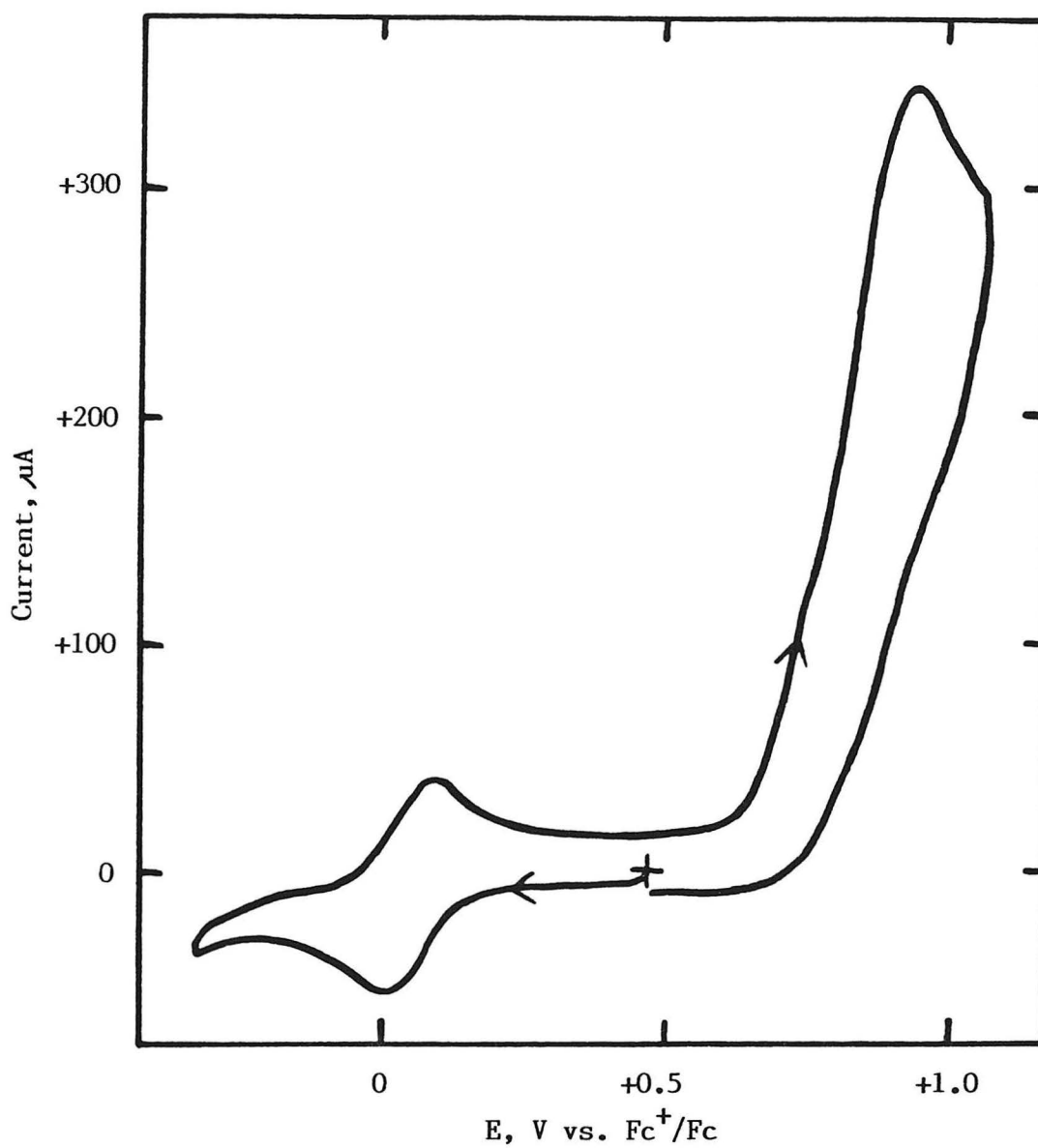


Figure 3.5. Cyclic voltammogram of 1 mM $\text{H}_2\text{-11}^{2+}$ + 0.5 M *n*-butanol in CH_2Cl_2 , 0.1 M TBAP at 0.17 cm^2 BPG electrode. Scan rate = 200 mV/sec.

concentrations of benzyl alcohol revealed that the anodic currents seen with the triphenylphosphine oxide containing catalysts, trans-11' and 15 (a dimer, vide infra) tended to increase slowly if at all above about 200–500 mM benzyl alcohol, while with the cis-alpha bis-pyridine catalysts the anodic response increased almost linearly up to 1 M benzyl alcohol.

Table 3.1 lists the different catalysts studied and Table 3.2 summarizes the electrochemical data for each.

Table 3.1. Catalysts for the electrochemical oxidation of alcohols.

Compound Number ^a	Formula ^b
<u>11</u>	<u>cis-alpha</u> -Os(CHBA) ₂ (Py) ₂
<u>11</u> -(<u>t</u> -Bupy)	<u>cis-alpha</u> -Os(CHBA) ₂ (<u>t</u> -Bupy) ₂
<u>11'</u> -(<u>t</u> -Bupy)	<u>trans</u> -Os(CHBA) ₂ (<u>t</u> -Bupy) ₂
<u>13</u>	<u>trans</u> -Os(CHBA) ₂ (<u>t</u> -Bupy)(Ph ₃ P=O)
<u>14</u>	<u>cis</u> -Os(CHBA) ₂ (<u>t</u> -Bupy)(Ph ₃ P=O) ^c
<u>15</u>	Os ₂ (CHBA) ₄ (<u>t</u> -Bupy) ₄

^aCompounds are numbered so as to correspond to numbering in the literature. ^bIn all cases the CHBA ligand is coordinated as a bidentate dianion as depicted in Figure 3.1. ^cWhether 14 is cis-alpha or cis-beta is unknown.

One catalyst species which gave surprising CV results was 15. Initial indications were that it was the cis-beta isomer of Os(CHBA)₂(t-Bupy)₂. However, when a 1 mM solution was prepared and examined by CV, it displayed two reversible reductions at -0.64 and -1.05 V, each with peak currents of about 30 μ A. All of the other catalyst compounds displayed CV peak currents at 1 mM of about 60 μ A. Also, the -0.64 V couple is normal for an Os(IV/III) couple, but the -1.05 V couple

Table 3.2. Electrochemical data for catalyst compounds.

Compound	Os(III/II)	Formal Potential, V ^a Os(IV/III)	Os(V/IV) ^b
<u>11</u>	-1.90	-0.67	(+0.71)
<u>11</u> -(<u>t</u> -Bupy)	-1.99	-0.70	(+0.72)
<u>11'</u> -(<u>t</u> -Bupy)	-1.97	-0.70	(+0.63)
<u>13</u>	c	-0.91	(+0.54)
<u>14</u>	c	-0.95	(+0.52)
<u>15</u>	c	-1.05, -0.64 ^d	(+0.78) ^d

^aMeasured in CH₂Cl₂/0.1 M TBAP and referenced to Fc⁺/Fc internal standard.
^bPeak potentials for irreversible oxidation to Os(V). ^cNot measured. ^d15 is a dimer and so displays two Os(IV/III) couples. Only one oxidation to Os(V) could be clearly seen.

is much too high for the Os(III/II) couple in this type of compound.

These observations led to the proposal that 15 is actually a dimer and both of the reductions observed are Os(IV/III) couples. The proposal of a dimeric structure is also supported by NMR evidence of hindered rotation of one of the pyridine rings [2]. The proposed structure of 15 is shown in Figure 3.6.

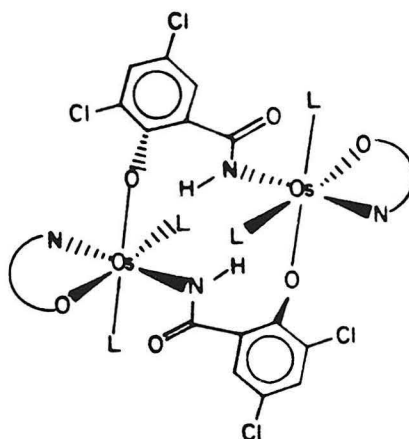


Figure 3.6. A possible dimeric structure for 15.

Controlled potential oxidations of alcohols in the presence of catalysts

In order to verify that the anodic activity observed with the catalyst compounds in the presence of alcohols arose from oxidation of the alcohols to aldehydes and ketones, controlled potential electrolyses were performed. A solution containing the catalyst compound, about 50 μ M, and the alcohol, usually 0.5 M, was oxidized at a basal plane pyrolytic graphite (BPG) working electrode at a potential where anodic activity was observed, usually +0.97 V. The carbonyl products were determined by HPLC analysis after derivatizing them with benzoyl hydrazine. Blank experiments were performed with the alcohols in the absence of catalyst to verify that no significant amount of uncatalyzed oxidation took place and to provide blank charge and carbonyl product concentration data for use in calculating the current efficiency of the catalytic oxidations [9]. The charge consumed in catalyst decomposition, about 3 F/mol of Os, was not corrected for in the current efficiency calculations, so the observed current efficiencies are not expected to reach 100%.

Initial electrolysis experiments clearly indicated that alcohol oxidation was taking place, but the catalyst had a limited lifetime. During the electrolyses the current steadily decreased as the blue color of the catalyst faded. The current eventually reached a steady low value and the color of the solution faded to clear or very light yellow. Figure 3.7 shows a series of UV-visible spectra taken during an electrolysis of $\text{H}_2\text{-11}^{2+}$ and benzyl alcohol. After a short induction period during which the position of the visible band of $\text{H}_2\text{-11}^{2+}$ shifted to higher wavelengths, the absorbance of this band decreased in a regular manner. In fact, as demonstrated in Figure 3.8, a plot of absorbance of the visible band as a function of charge passed during the electrolysis is quite linear. This

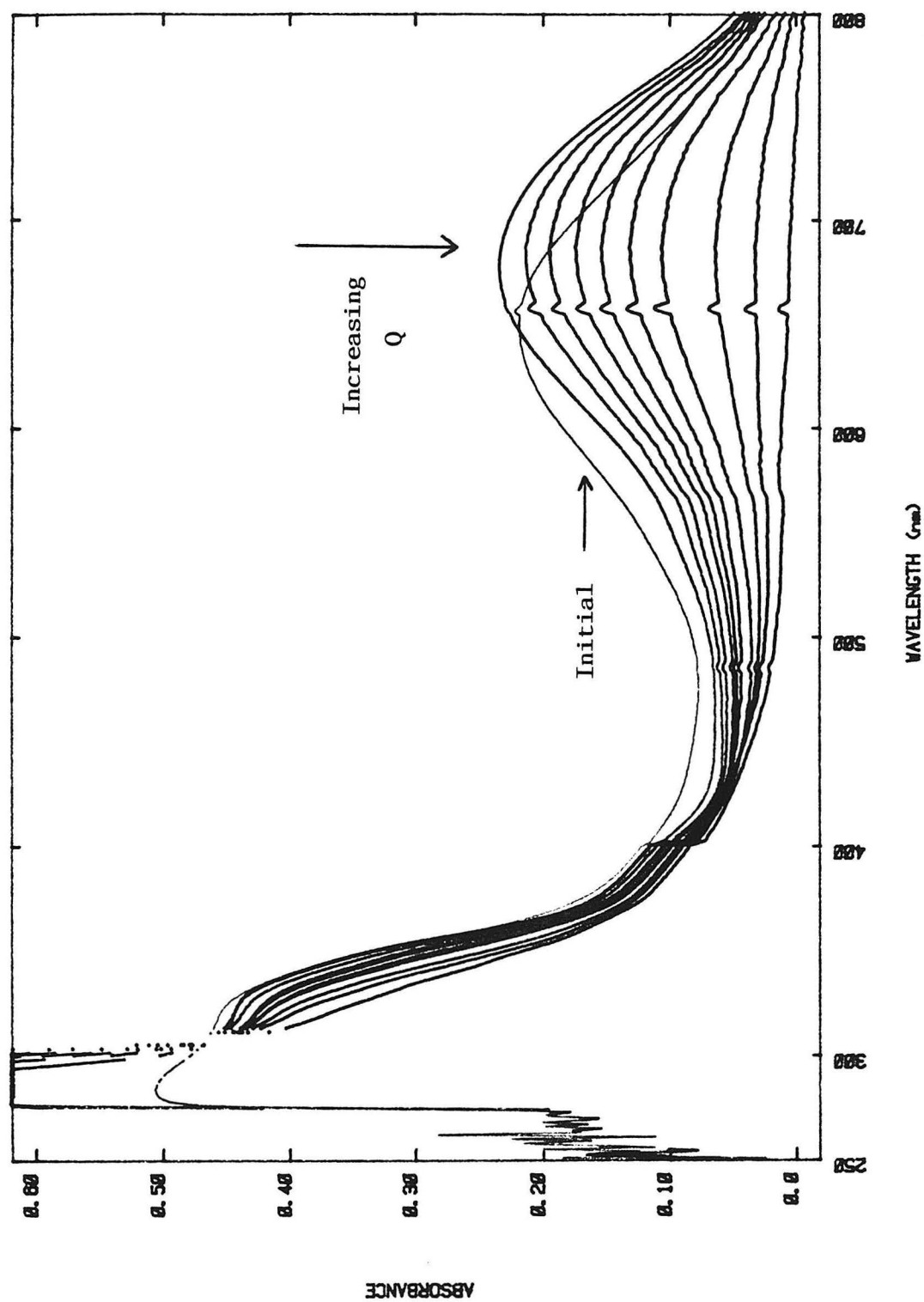


Figure 3.7. UV-visible spectra taken during controlled potential electrolysis of $60 \mu\text{M H}_2^{-11}2^+$ + 0.5 M benzyl alcohol in CH_2Cl_2 , 0.1 M TBAP at +0.97 V.

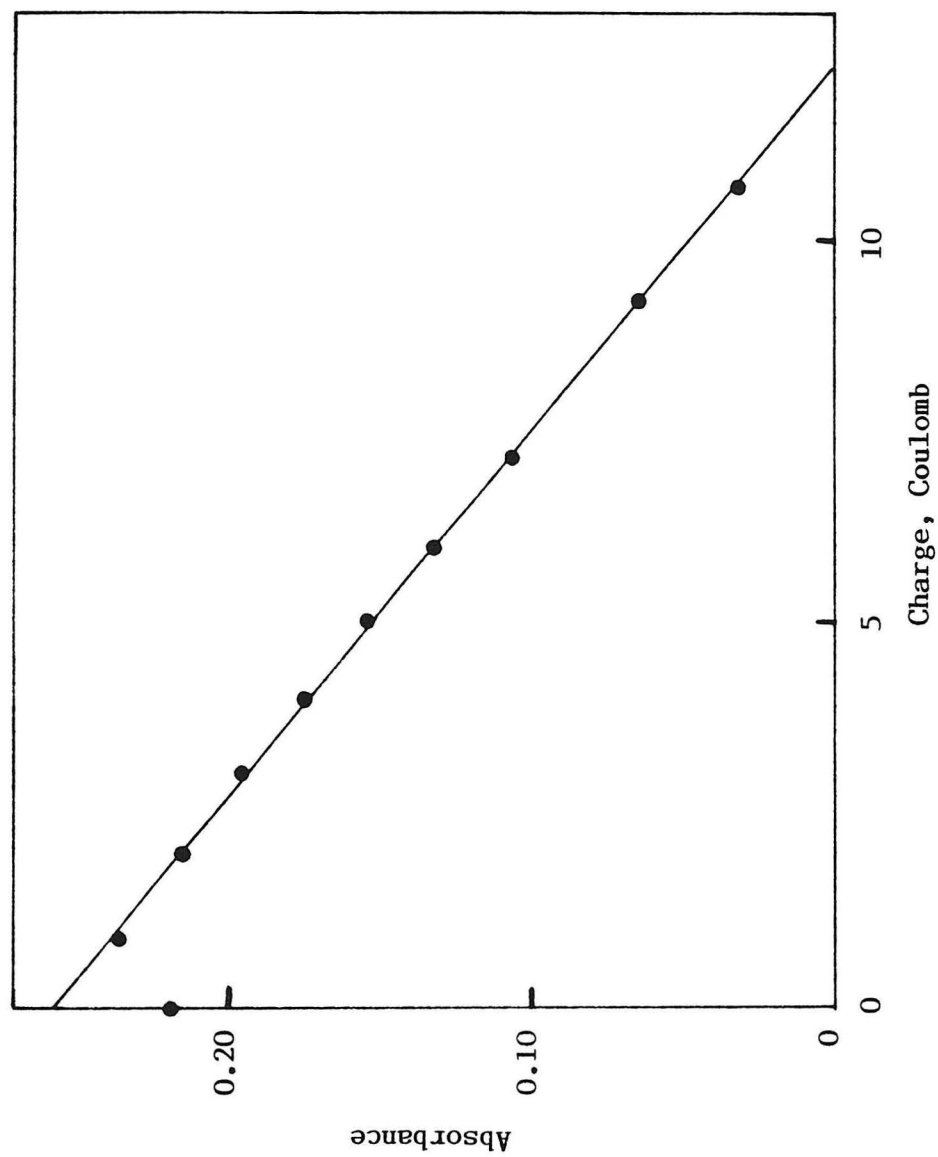


Figure 3.8. Plot of Absorbance vs. Charge with data taken from Figure 3.7 for electrolysis of $60 \text{ } \mu\text{M H}_2\text{-11}^{2+}$ + $0.5 \text{ M benzyl alcohol}$.

plot also shows an induction period, during which the absorbance increases slightly before the linear decrease begins. The same types of plots were obtained with the other catalysts studied except that only the cis-alpha compounds, 11 and 11-(t-Bupy), displayed the induction period.

These linear plots of absorbance versus charge turned out to be very useful. It was desirable to determine the effect of various reaction conditions on the lifetime, or maximum turnover number, of the catalysts. It was very difficult to estimate the point at which all of the catalyst had been decomposed because the current during the electrolyses decreased very slowly near the end and never seemed to reach a true background level. However, using plots of absorbance of the catalyst visible band versus charge consumed in the electrolyses, it was possible to estimate the maximum charge which would have been consumed by simply extrapolating the line to zero absorbance. At that point all of the catalyst would be decomposed and the charge represents the maximum attainable under the reaction conditions. This extrapolation saved time and was more accurate than actually waiting for the catalyst decomposition to go to completion. The charge determined by extrapolation and the known amount of catalyst added to the solution were then used to calculate the maximum turnover number of the catalyst for that experiment, expressed as one-electron turnovers.

The effect of reaction conditions on the lifetime of the catalyst was investigated for the the oxidation of benzyl alcohol with 11. The results of this series of experiments are presented in Table 3.3.

Under all conditions the benzyl alcohol was oxidized to benzaldehyde with high current efficiency. However, the lifetime of 11, the maximum

Table 3.3. Effects of reaction conditions on the oxidation of benzyl alcohol with 11.^a

[<u>11</u>], μM	[BzOH], M	E, V ^b	Base	C.E., % ^c	Max. T.N. ^d
48	0.5	+0.97	None	98	247
37	"	"	Py	—	224
55 ^e	"	"	Na ₂ CO ₃	93	205
23	"	"	"	97	254
224	"	"	"	96	91
64	"	+1.07	"	High	159
56	"	+0.87	"	High	136
56	0.1	+0.97	"	High	40
52	1.0	"	"	High	297

^aElectrolyses in CH₂Cl₂/0.1 M TBAP at BPG anode. ^bPotential referenced to Fc⁺/Fc. ^cCurrent efficiency for production of benzaldehyde determined by HPLC analysis and corrected for blank experiment in absence of catalyst. High C.E. indicates no blank was run. ^dMaximum turnover number determined by extrapolation of absorbance vs. charge plots to zero absorbance. ^eAverage of six separate experiments.

turnover number, was dramatically affected by the reaction conditions.

The first factor to be investigated was the effect of the acid produced

during the electrolysis. Since the deprotonated form of 11 was most

easily isolated and purified, it was used for these experiments. But, as

indicated by the CV experiments, as soon as any alcohol oxidation took

place the 11 was converted to H₂-11²⁺. CV results indicated that the

addition of excess trifluoromethanesulfonic acid caused a decrease in the

currents for benzyl alcohol oxidation. Electrolysis experiments also

showed decreased currents as the concentration of acid increased. One way

to prevent build-up of acid during the electrolyses was to add pyridine

periodically to neutralize the acid being formed. This experiment had to be performed very carefully since oxidized 11 reacted in an unknown manner with excess pyridine. So, several times during one electrolysis, pyridine was added in an amount slightly less than the amount of acid formed as calculated from the charge consumed. Very little effect was observed on the lifetime of 11, but the reaction did not slow down so badly during the latter stages of the electrolysis and considerable time was saved. A more convenient method of neutralizing excess acid was found to be the addition of an excess of solid sodium carbonate. The sodium carbonate had the advantages of being very pure, reacting only with excess acid, and being easily removed at the end of the experiment by filtration and so not interfering with the analysis for products. A small decrease in lifetime was observed with sodium carbonate, but current efficiencies were still high and reaction times were lowered as with pyridine, so it was used in all further experiments.

The third entry in Table 3.3 represents an average of six experiments. Among those experiments was one in which the solution was purged with argon during the electrolysis and one in which tetrabutylammonium tetrafluoroborate was substituted for TBAP as the supporting electrolyte. Neither change had any significant effect on the results of the electrolyses. This series of experiments allowed an estimate to be made of the reproducibility of the electrolysis experiments. For these six experiments under identical conditions the average maximum turnover number was 205 with a standard deviation of 37 or 18%. The average current efficiency was 93% with a standard deviation of 3.6%. One experiment not included in this group was conducted with 100 mM water added. The water seemed to collect in the sodium carbonate and had

no effect on the maximum turnover number. This suggests that the catalyst decomposition is not caused by water.

The next factor to be investigated was the concentration of 11. Concentrations around 50 μM were generally used because this was the smallest amount which could be accurately and conveniently weighed out (about 1 mg). A similar lifetime was observed at half this concentration, but on going to much higher concentration, 224 μM , the lifetime dropped by more than half.

The most convenient potential for conducting the electrolyses was +0.97 V, corresponding to +1.5 V versus the Ag/AgCl reference electrode used to control the potential. At this potential significant catalytic activity was observed but no uncatalyzed alcohol oxidation was occurring. This also appears to be the preferred operating potential for 11 since at both higher and lower potentials the lifetime dropped significantly. The lifetime increased at higher benzyl alcohol concentrations and decreased at lower concentrations. This is believed to imply that the alcohol oxidation and catalyst decomposition reactions are in competition, with alcohol oxidation competing more effectively at higher alcohol concentrations.

In all the oxidations of benzyl alcohol with 11 the current efficiency for production of benzaldehyde was essentially quantitative. This implies a high selectivity for the production of aldehydes from primary alcohols. Of course, because of the short catalyst lifetime and the large concentrations of alcohol necessary for observation of the catalysis, only a very small fraction of the alcohol (about 1%) was converted to aldehyde in these experiments. This may in part explain the high selectivity, but CV's and one electrolysis with benzaldehyde

indicated no reactivity of $\text{H}_2\text{-}\underline{11}^{2+}$ with the aldehyde. Several attempts were made to detect benzyl benzoate in product solutions after oxidations of benzyl alcohol, but as would be expected from the high current efficiencies, none could be detected.

From the results in Table 3.3 a standard set of conditions was chosen for further work with other catalyst compounds and other alcohols. These conditions were 50–60 μM catalyst, 0.5 M alcohol, +0.97 V and sodium carbonate present to remove excess acid. The oxidation of benzyl alcohol under these conditions was used to compare the current efficiencies and lifetimes of the different catalyst compounds. The results of this series of experiments are listed in Table 3.4.

Table 3.4. Oxidation of benzyl alcohol with different catalyst compounds.^a

Catalyst	[Catalyst], μM	C.E., % ^b	Max. T.N. ^c
<u>11</u>	55	93	205
<u>11</u> -(<u>t</u> -Bupy)	56	99	216
<u>11'</u> -(<u>t</u> -Bupy)	52	93	36
<u>13</u>	48	98	147
<u>14</u>	52	98	132
<u>15</u> ^d	62	86	9

^aElectrolyses conducted in CH_2Cl_2 /0.1 M TBAP at BPG anode at +0.97 V with excess Na_2CO_3 present. $[\text{BzOH}] = 0.5 \text{ M}$. ^bCurrent efficiency for production of benzaldehyde determined by HPLC analysis and corrected for blank experiment run in absence of catalyst. ^cMaximum turnover number determined by ^dextrapolation of absorbance vs. charge plots to zero absorbance. 15 is a dimer and the concentration listed is the total Os concentration.

The first thing to note from these results is the fact that replacement of pyridine with 4-t-butylpyridine had no significant effect on the catalyst lifetime. However, on going from the cis- α isomer, 11-(t-Bupy), to the trans isomer, 11'-(t-Bupy), the maximum turnover number dropped from 216 to only 36. This change was accompanied by a loss of the induction period in the plots of absorbance versus charge. Compounds 13 and 14 contain one triphenylphosphine oxide and one t-butylpyridine ligand and displayed intermediate lifetimes which were nearly the same within experimental error. It is certain that 13 is the trans isomer, but it is not known whether 14 is cis- α or cis- β . Compound 15 displayed a very low maximum turnover number. This probably arises from steric complications associated with the dimeric structure of 15 [2].

One final set of experiments was performed with 11 under the standard set of conditions but with alcohols other than benzyl alcohol. These results are presented in Table 3.5. As can be seen, benzyl alcohol is by far the best substrate for 11. Cyclohexanone was produced from cyclohexanol and heptanal was produced from n-heptanol, but the maximum turnover number of 11 dropped precipitously with these alcohols. This is not too unreasonable since saturated alcohols have much stronger α C-H bonds than benzyl alcohol [10] and so should be more difficult to oxidize. If, as is proposed, the decomposition of the catalyst competes with alcohol oxidation, then the oxidation of saturated alcohols should be slower and compete less effectively with catalyst decomposition and so result in lower catalyst turnover numbers. The observed current efficiencies for the oxidation of the saturated alcohols were also lower than for benzyl alcohol, but this is also not unexpected. As shown in the

Table 3.5. Oxidation of other alcohols with 11.^a

Alcohol	[<u>11</u>], μ M	C.E., % ^b	Max. T.N. ^c
Benzyl	55	93	205
Cyclohexyl	56	68	10
<u>n</u> -Heptyl	56	70	14
<u>t</u> -2-Hexenyl	56	d	8
Allyl	56	d	6
None	60	—	3

^aElectrolyses conducted in $\text{CH}_2\text{Cl}_2/0.1 \text{ M TBAP}$ at BPG anode at +0.97 V with excess Na_2CO_3 present. [Alcohol] = 0.5 M. ^bCurrent efficiency for production of aldehyde or ketone determined by HPLC analysis and corrected for blank experiment run in absence of catalyst. ^cMaximum turnover number determined by extrapolation of absorbance vs. charge plots to zero absorbance. ^dNot determined.

table, the decomposition of 11 in the absence of alcohols consumes about 3 F/mol of Os and this charge is not corrected for in the calculated current efficiencies. Therefore, for a maximum turnover number of 10, the observed current efficiency should be about 70% if selective oxidation to the aldehyde or ketone is occurring.

The even lower turnover numbers of the allylic alcohols is quite surprising. The bond strength of the alpha C-H bonds in allylic alcohols should be just as low as in benzyl alcohol [10] and so they should be as easy to oxidize. Even if coordination of the benzyl alcohol through the aromatic ring is important, allylic alcohols should be able to coordinate in a similar manner through their double bonds. So this effect is not understood. It should be noted that the HPLC analysis for products was not applicable to the allylic alcohols because of large blank values.

These large blanks may have arisen from carbonyl impurities in the alcohols or from oxidation of the alcohols by the benzoyl hydrazine. Dinitrophenylhydrazine is known to oxidize some allylic alcohols [11].

Mechanistic considerations

For a number of reasons it is very difficult to investigate the mechanistic details of the oxidation of alcohols by the catalyst compounds. Except possibly for reactions with high concentrations of benzyl alcohol, any activity observed arises from both alcohol oxidation and catalyst decomposition occurring simultaneously. The high concentrations of alcohols necessary for the observation of catalytic activity surely introduce significant amounts of impurities, the effects of which are difficult to account for. Finally, control of acidity in CH_2Cl_2 is almost impossible. The oxidation of alcohols produces two protons per mole of alcohol oxidized, so acid quickly builds up during these experiments. Furthermore, the catalyst species all have one nonprotonated and two protonated forms. Without proper control of solution acidity it cannot be said with certainty which species are present or which are carrying out the oxidation.

With these limitations in mind, information about the catalysis can be inferred from the experimental data at hand. First, the catalyst lifetime increases with increasing alcohol concentration. It is believed that this observation implies that the oxidation of alcohols competes with the catalyst decomposition reaction. If the Os(V) form of the catalyst can undergo a first-order decomposition reaction or a second-order reaction with an alcohol, then the alcohol oxidation will compete more effectively and result in higher catalyst lifetimes at higher alcohol concentrations. If this is the case then catalyst lifetime should decrease at higher

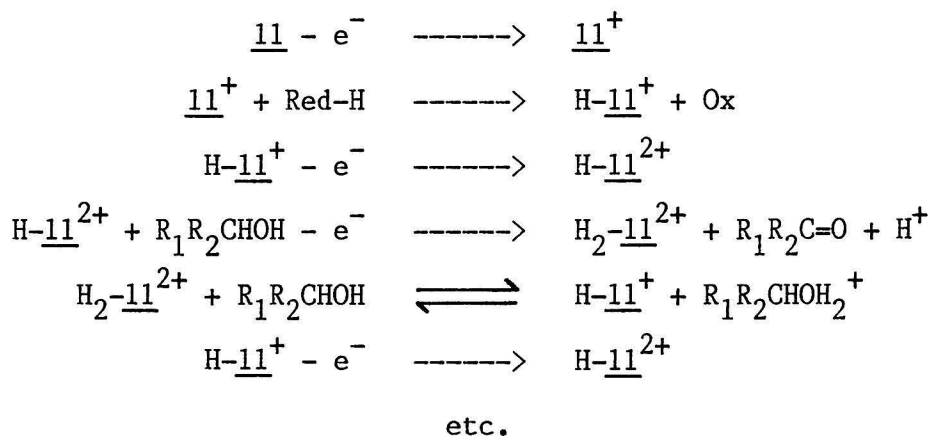
catalyst concentrations and increase at lower concentrations for the same alcohol concentration. This is observed (see Table 3.3) but the increase in lifetime at the lower catalyst concentration is rather small.

Alternatively, if alcohol coordination is necessary for oxidation, higher concentrations of alcohol will result in a larger fraction of the catalyst's being coordinated to the alcohol and thus more alcohol oxidation relative to catalyst decomposition. In this case, the decreased lifetime of the catalyst at the higher concentration might be due to an autocatalysis of the decomposition reaction, with the products of the decomposition hastening the decomposition of the remaining catalyst. However, since the rate of catalyst decomposition would not be constant, the linear plots of absorbance versus charge would not be expected.

An important question is which form of the catalyst compounds is responsible for the alcohol oxidation. It seems unlikely that the nonprotonated form is the active catalyst. As seen in Figure 3.4, the oxidation of the nonprotonated form of 11 is seen before the alcohol oxidation. The triphenylphosphine oxide containing catalysts, 13 and 14, are oxidized to Os(V) at lower potentials and for them the oxidation of the nonprotonated form is even more clearly separated from the alcohol oxidation. The alcohol oxidation is probably not performed by the diprotonated form either, since in the absence of alcohols these species display no anodic activity within the range of potentials accessible in CH_2Cl_2 . It therefore seems reasonable to propose that the active form of the catalysts is the monoprotinated monocationic species. Mixtures containing these species can be produced by adding one equivalent of acid to the nonprotonated form (see Chapter II) and in those experiments an oxidation taken to correspond to the monoprotinated form is observed at a

potential about 200 mV higher than that of the nonprotonated form. During the electrolyses the monoprotinated species could be formed from the diprotonated form by deprotonation by the alcohol. Since the diprotonated species are very strong acids, large concentrations of weakly basic alcohols should deprotonate a significant fraction of the catalyst. This may be why the addition of t-butanol gives rise to anodic activity in CV's of $\text{H}_2\text{-}\underline{11}^{2+}$ even though it is unlikely to be oxidized. Starting with the nonprotonated form, the monoprotinated species may result from reaction of the Os(V) form with a protonic impurity (Red-H in Scheme 3.1), such as water. The oxidation of the nonprotonated forms is quite irreversible, but the compound is clearly not destroyed since CV's in the presence of alcohol indicate that it is all converted to the diprotonated form (see Figure 3.4). The CV of 11 in the absence of alcohol, shown in Figure 3.9, is not as clean, but two broad reductions are seen on the cathodic scan following the irreversible oxidation, one corresponding to the nonprotonated form and one which is at the correct potential for the monoprotinated form. This reasoning is summarized in Scheme 3.1 using 11 as an example.

Scheme 3.1. Electrochemical oxidation of alcohols by 11.



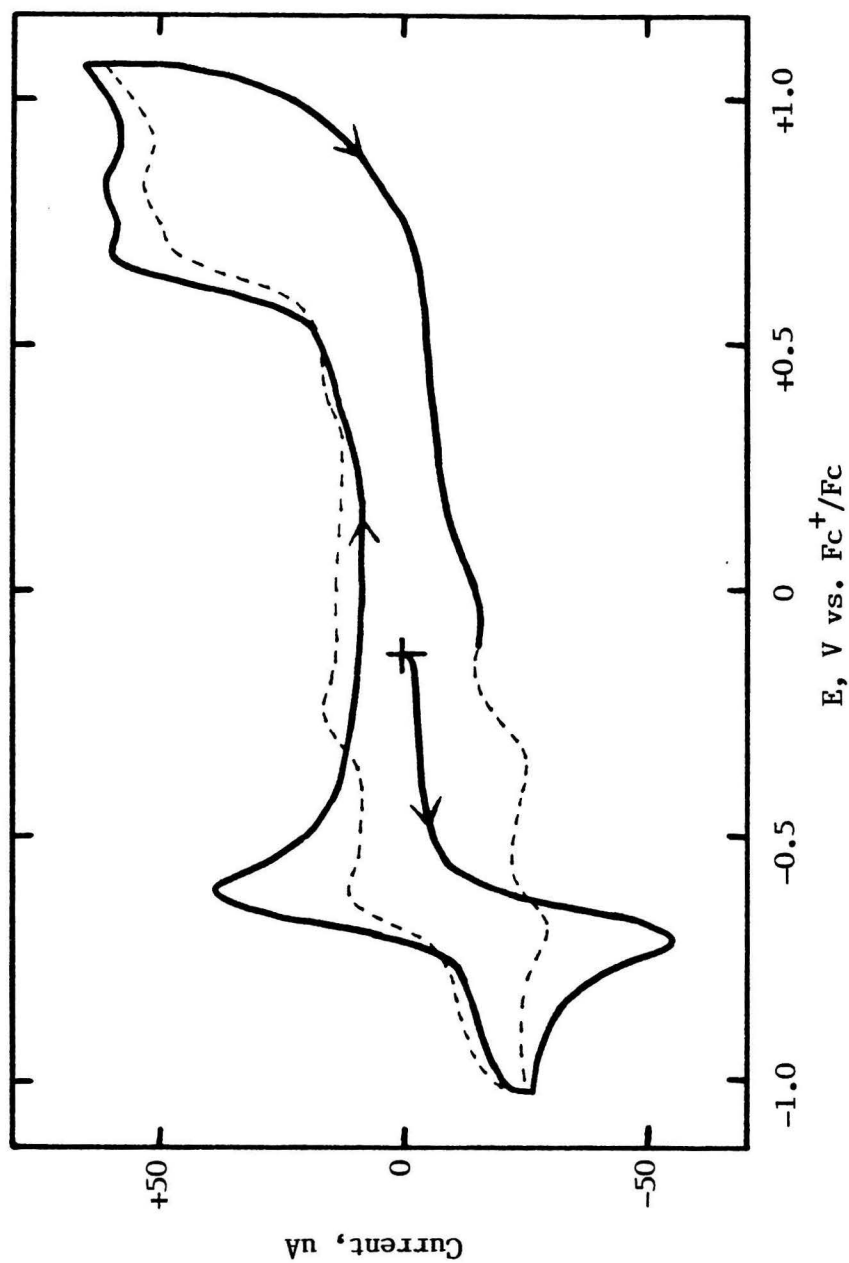


Figure 3.9. Cyclic voltammogram of 1 mM 11 in CH_2Cl_2 , 0.1 M TBAP at 0.17 cm^2 BPG electrode. Scan rate = 200 mV/sec. Dotted line represents second scan.

The mechanism of the oxidation of alcohols by the oxidized monoprotonated catalysts is unknown. It may involve a two-electron oxidation producing the aldehyde or ketone in one step and resulting in reduction of the catalyst to Os(III), or it may be a two-step process, possibly with radical intermediates involved. The acid/base properties of the catalysts must somehow be involved in the alcohol oxidation, since none of the other osmium compounds investigated display the same kind of discrete protonations or the alcohol oxidation. The nature of the effect may simply be a higher affinity of the cationic protonated species for alcohol. Or, the basic sites of the catalysts may be more directly involved in alcohol oxidation by providing a repository for the protons which must be lost from the alcohol upon oxidation. If the function of protonation of the catalysts is simply to provide a cationic species with a higher alcohol affinity, then other methods of producing a positive charge should have the same effect. Specifically, catalyst analogs with alkylated carbonyl groups or pyridine ligands substituted with cationic groups should function as catalysts but not be so sensitive to the concentration of acid in solution. If the alkylated analogs which would presumably lose their acid/base properties showed no catalytic activity, then the more direct involvement of the basic sites would be implicated.

Even less is known about the catalyst decomposition than about the alcohol oxidation. No identifiable products result from the decomposition of the catalysts. The decomposition product is probably not osmium tetroxide, since decomposed catalyst solutions do not display a reversible couple at about -0.5 V which is characteristic of osmium tetroxide in CH_2Cl_2 [12]. The loss of the blue color of the catalyst upon decomposition probably implies disruption of the coordination sphere of

the osmium since the deep blue color is very characteristic of these types of Os(IV) compounds. One possible initial reaction in the decomposition is loss or oxidation of a CHBA or pyridine ligand. If catalyst decomposition is simply caused by dissociation of the ligands, then decomposition may be slowed and the catalyst lifetime increased by using multidentate ligands. The two monodentate ligands could be replaced by a bidentate one such as 2,2'-bipyridine or diphos. The two CHBA ligands could be joined back into a tetradentate ligand at the phenyl rings rather than at the amide nitrogens and so preserve the catalytic activity which seems to depend upon the primary amide groups. Other changes to make the ligands more oxidation-resistant may also be necessary.

The rate of decomposition of the catalysts is clearly affected by the contents and geometry of their coordination spheres. Trans-11'-(t-Bupy) decomposes much more quickly than cis-alpha-11-(t-Bupy). Also, trans-11'-(t-Bupy) decomposes significantly faster than 13, trans-Os(CHBA)₂(t-Bupy)(Ph₃P=O). The reasons for these differences are not understood. More work with new catalyst analogs will have to be done in order to understand the variables which affect catalyst lifetime and so enable synthesis of longer-lived catalysts.

Conclusions

The oxidative degradation of trans-Os(CHBA-Et)(Py)₂, 5, results in the production of cis-alpha-Os(CHBA)₂(Py)₂, 11, and/or trans-Os(CHBA)₂(Py)₂, 11', containing two bidentate dianionic CHBA ligands in place of the tetradentate tetraanionic CHBA-Et ligand. Chemical syntheses starting with the CHBA ligand can produce 11' and several other compounds containing CHBA ligands. All of these compounds share two common features not possessed by any other of the Os(IV) compounds studied. First, the compounds containing two CHBA ligands can all be protonated in two steps. These protonations are believed to occur at the carbonyl oxygens of the CHBA ligands. Why other compounds containing tetradentate tetraanionic ligands with the same types of carbonyl groups are not protonated is unknown. The second common feature of these compounds is their ability to catalyze the electrochemical oxidation of alcohols to aldehydes and ketones.

There are a number of compounds which are capable of catalyzing the electrochemical oxidation of alcohols [4-6], but they usually display poor selectivity for the oxidation of primary alcohols to aldehydes. Other catalysts which can oxidize primary alcohols usually oxidize the aldehydes so formed even faster and so produce carboxylic acids and/or esters. Our osmium catalysts do not appear to react with aldehydes. No activity is observed by CV or electrolysis with benzaldehyde. The oxidation of benzyl alcohol produces benzaldehyde with essentially quantitative current efficiency with no production of benzyl benzoate. 1-Heptanol is oxidized to heptaldehyde with what appears to be quantitative current efficiency.

Unfortunately, all of the catalysts have very limited lifetimes. The decomposition of the catalysts could be followed by monitoring their

UV-visible spectra during the electrolyses. For each catalyst a linear decrease of the absorbance of its visible band near 600 nm with respect to charge passed during the electrolysis could be observed. Extrapolation of this line to zero absorbance provided an estimate of the maximum charge which could have been passed before the catalyst was completely destroyed. The maximum observed lifetime for any of the catalysts was a turnover number of 297 for 52 μM 11 in the presence of 1 M benzyl alcohol. Lower alcohol concentrations or higher catalyst concentrations led to lower lifetimes. Alcohols other than benzyl alcohol gave much lower catalyst lifetimes. This was not unexpected for saturated alcohols, but for some reason even allylic alcohols give very low lifetimes. Changes in the coordination sphere of the catalysts also had large effects on the lifetimes of the catalysts.

Very little is known about the mechanism of the alcohol oxidation. It seems likely that alcohol oxidation competes with catalyst decomposition. At higher alcohol concentrations the alcohol oxidation competes more effectively and so a longer catalyst lifetime is observed. It also seems likely that the species responsible for the catalysis are the monoprotonated forms of the catalysts. For some of the catalysts the oxidation of the nonprotonated form is well separated from the alcohol oxidation indicating that it is not responsible for the catalysis. For all of the catalysts the doubly protonated forms cannot be oxidized at potentials accessible in CH_2Cl_2 and so they are probably not responsible for the catalysis. This leaves the monoprotonated forms as the only reasonable candidates for the active species. They are oxidized about 200 mV positive of the nonprotonated forms, right around the potentials where alcohol oxidation is observed.

The decomposition of the catalysts is even less well understood. Since the characteristic blue color of the Os(IV) complexes is lost, the decomposition probably results from or in loss of one or more ligands. It is expected that changes in the catalyst ligands, such as substitution of a bidentate ligand for the two monodentate ligands or replacement of the two CHBA ligands with a new tetradentate ligand, may lead to longer lifetimes. The information gathered from observing the activity and lifetime of new catalyst species will provide insight into the alcohol oxidation and catalyst decomposition mechanisms.

Once longer-lived catalysts have been developed, a number of important experiments can be attempted. The true selectivity of the alcohol oxidation can be investigated by exhaustively oxidizing alcohols and observing the products. If aldehydes are still produced at high conversions, then these catalysts could be very useful. Modification of the coordination sphere with chiral ligands could lead to even more important uses. A chiral catalyst might oxidize one isomer of a racemic mixture, for example 2-butanol, and so result in the production of pure solutions of the other isomer.

Experimental

Materials

Reagent grade methylene chloride (MCB or Mallinckrodt) was further purified by passing it over a short column of activated alumina (Woelm N. Akt. I). All other solvents were reagent grade (Aldrich, Baker, Mallinckrodt, MCB or USI) and were used as received.

Tetra-n-butylammonium perchlorate supporting electrolyte (Southwestern Analytical Chemicals) was dried, recrystallized twice from acetone/ether, and then dried under vacuum. Alcohols were reagent or spectrophotometric grade and were used as received, except for t-butanol (MCB) which was distilled once. Trifluoromethanesulfonic acid (3M) was distilled and stored at -10 °C. Ferrocene (Aldrich), trifluoroacetic acid (MCB) and benzoyl hydrazine (Aldrich) were used as received.

Compounds 11, 11', 11-(t-Bupy) and 11'-(t-Bupy) were prepared as described in Chapter II starting with 5 or 5-(t-Bupy) supplied by Terry Krafft. The synthesis of compounds 13, 14 and 15 and all compound characterizations were performed by Terry Krafft and details can be found in the appropriate references [2,3].

Apparatus and Procedures

Cyclic voltammetry was performed with a Princeton Applied Research (PAR) Model 173 potentiostat driven by a PAR Model 175 universal programmer using positive feedback IR-compensation. Current-voltage curves were recorded on a Houston Instruments Model 2000 X-Y recorder. Standard two-compartment electrochemical cells were used. When necessary, solutions were purged with argon to remove oxygen. The working electrode was a 0.17 cm² basal plane pyrolytic graphite (BPG, Union Carbide Co.) disc mounted in a glass tube with heat-shrinkable tubing. The counter

electrode was a platinum wire. Various reference electrodes were used, including SCE, SSCE, Ag/AgCl and a silver wire quasi-reference electrode. For each compound studied at least one experiment was performed in the presence of ferrocene as an internal potential standard. The formal potentials of all of the couples of the osmium compounds were then referenced to that of the ferrocene, which was consistently measured as +0.48 V vs. aqueous SCE. Formal potentials of reversible couples were taken as the average of the anodic and cathodic peak potentials. The supporting electrolyte was 0.1 M TBAP.

Controlled potential electrolysis experiments were performed with the PAR Model 173 potentiostat equipped with a Model 179 digital coulometer using positive feedback IR-compensation. Electrolyses in CH_2Cl_2 were performed in a standard three-compartment H-cell with a platinum gauze counter electrode in one compartment and the reference electrode and a 1.7 x 4.5 x 0.07 cm BPG working electrode in the third compartment. The reference electrode used for controlled potential oxidations with the catalyst compounds was a Corning Ag/AgCl double junction reference electrode. The product solution containing decomposed catalyst was found to cause the potential of the usual single junction Ag/AgCl reference electrode to drift by as much as 500 mV. Therefore, the double junction reference electrode was used to maintain proximity of the reference electrode to the working electrode and minimize IR-compensation but at the same time isolate the reference electrode from the catalyst solution. The inner compartment of the double junction reference electrode contained an aqueous solution of saturated KCl and AgCl. The outer compartment contained this solution layered over CH_2Cl_2 containing 0.5 M TBAP. This arrangement gave potentials almost identical to the single compartment

electrode but was not susceptible to drift during the electrolyses. Most electrolyses were performed in the presence of 0.5 g Na_2CO_3 added to neutralize the acid formed by alcohol oxidation. All experiments were performed at room temperature, $22 \pm 2^\circ\text{C}$.

HPLC analyses for aldehydes and ketones were performed on an IBM LC 9533 Ternary Gradient LC equipped with an octadecyl column, an LC 9522 254 nm UV detector and a Hewlett Packard 3390A Integrator. The eluting solvent was 60% methanol + 40% water. All analyses were performed immediately after the electrolyses to minimize the effects of air oxidation of the alcohols. The following procedure was used to prepare all samples. All of the anolyte solution was collected and filtered into a 100 ml flask. 50 mg of benzoyl hydrazine and two drops of trifluoroacetic acid were added and the solution was refluxed for one hour. The CH_2Cl_2 was then removed on a rotovap at 50°C . The resulting oil was dissolved in methanol and diluted to 100 ml. The concentration of product in the sample was determined by comparison of its HPLC peak area with that of a standard solution of the corresponding hydrazone of similar concentration. The hydrazone samples used for preparing the standard solutions were synthesized by reaction of benzoyl hydrazine with the desired aldehyde or ketone in boiling ethyl acetate. The products were recrystallized several times from methanol and thoroughly dried. TLC indicated that they contained little or no unreacted benzoyl hydrazine. The analysis was tested on a sample of benzaldehyde (<100% pure) and returned 93% of the expected concentration of benzaldehyde. Three standard solutions of benzaldehyde benzoyl hydrazone spanning the concentration range obtained from the electrolyses gave a very linear plot of HPLC peak area versus concentration with a zero intercept.

The current efficiency for production of the aldehyde or ketone product was calculated on the basis of a two-electron oxidation of the alcohol. The charge consumed during the electrolysis and the amount of carbonyl product formed were both corrected for values obtained in blank experiments performed with the alcohols in the absence of catalyst. The corrected values were then used to calculate the apparent current efficiency of the oxidation using the formula in footnote 9. The charge consumed in the electrolysis was not corrected for the decomposition of the catalyst which is about a three-electron process, so the observed current efficiency is expected to be less than 100%.

The maximum turnover numbers of the catalysts were determined from UV-visible data taken during the electrolyses. The electrolyses were stopped periodically, usually 4-7 times, to take spectra. If Na_2CO_3 was present the solution was allowed to stand unstirred for several minutes to let the Na_2CO_3 settle. A sample was then taken and its spectrum measured with a Hewlett Packard 8450A Diode Array Spectrophotometer. The sample was then returned to the electrolysis cell and the experiment resumed. The electrolyses were generally ended when the absorbance of the catalyst visible band decreased to about 0.1 since accurate measurements could not be made at lower absorbances, especially in the presence of Na_2CO_3 . The absorbance of the visible band of the catalyst at about 600 nm was then plotted as a function of the total charge consumed at the time of the measurement. If Na_2CO_3 was present the measured absorbance had to be corrected for scattering due to solid which did not completely settle. This was done by subtracting the absorbance measured at 800 nm where the catalysts did not absorb from the absorbance of the catalyst visible band. These plots gave linear sections which were extrapolated to zero

absorbance to determine the maximum charge which could have been passed under the conditions of the experiment. This charge was then divided by the charge corresponding to a one-electron oxidation of the catalyst present to arrive at the reported maximum turnover number.

References and Notes

1. Ligand names are: 1,2-bis(3,5-dichloro-2-hydroxybenzamido)ethane, H₄CHBA-Et; 3,5-dichloro-2-hydroxybenzamide, CHBA.
2. T.E. Krafft, Ph.D. Thesis, California Institute of Technology, February, 1985.
3. F.C. Anson, T.J. Collins, R.J. Coots, S.L. Gipson, J.T. Keech, T.E. Krafft, B.D. Santarsiero and G.H. Spies, manuscript in preparation.
4. B.A. Moyer, M.S. Thompson and T.J. Meyer, J. Am. Chem. Soc., **102**, 2310-2312 (1980).
5. T. Shono, Y. Matsumura, J. Hayashi and M. Mizoguchi, Tet. Lett., **1979**, 165-167.
6. M.F. Semmelhack, C.S. Chou and D.A. Cortes, J. Am. Chem. Soc., **105**, 4492-4494 (1983).
7. For examples see: (a) P.C. Scholl, S.E. Lentsch and M.R. Van De Mark, Tetrahedron, **32**, 303-307 (1976); (b) D.R. Brown, S. Chandra and J.A. Harrison, J. Electroanal. Chem., **38**, 185-190 (1972); (c) E.A. Mayeda, L.L. Miller and J.F. Wolf, J. Am. Chem. Soc., **94**, 6812-6816 (1972).
8. Formal potentials are calculated as the average of the anodic and cathodic peak potentials determined by cyclic voltammetry. All potentials are referenced to the formal potential of a ferrocene internal standard, the potential of which in CH₂Cl₂/0.1 M TBAP has been consistently measured as +0.48 V vs aqueous SCE .
9.
$$C.E. = \frac{(N - N') \times 2 \times F}{Q - Q'} \times 100\%$$

Where N = number of moles of product from electrolysis with catalyst;
 N' = number of moles of product from blank electrolysis; F = 96485 C/mol;
 Q = charge passed during electrolysis with catalyst; Q' = charge passed during blank electrolysis.
10. R.T. Morrison and R.N. Boyd, Organic Chemistry, Third Ed., Allyn and Bacon, Inc.: Boston, 1973, p. 387.
11. R.L. Shriner, R.C. Fuson, D.Y. Curtin and T.C. Morrill, The Systematic Identification of Organic Compounds, 6th Ed., John Wiley and Sons: New York, 1980, p. 162.
12. S.L. Gipson, unpublished results.

CHAPTER IV

The Electrochemical Production of Stable Os(V) Compounds and
the Interconversion of their Stereoisomers Induced by
Modification of Electron Density at the Metal Center

Introduction

In Chapter II of this thesis the oxidative degradation of the CHBA-Et ligand of $\text{Os}(\text{CHBA-Et})(\text{Py})_2$ was discussed. A great deal was learned about the ligand degradation and a catalyst for the electrochemical oxidation of alcohols was discovered, but one of the major goals of this project, the production of stable high oxidation state transition metal complexes, was not realized. The results of the ligand degradation clearly demonstrated that the ethane bridge of the CHBA-Et ligand, and its derivatives, were not suitable components of a ligand coordinated to high-valent, highly-oxidizing metal centers. John Keech of the Collins group therefore set about synthesizing complexes of a new ligand which was expected to be more inert to oxidation [1-3].

The new ligand was CHBA-DCB [4], in which the ethane bridge of CHBA-Et was replaced by a dichlorobenzene bridge. Cyclic voltammetry indicated that $\text{Os}(\text{IV})$ complexes containing the CHBA-DCB ligand, coordinated as a tetradentate tetraanion, and two monodentate ligands, such as pyridine or triphenylphosphine, displayed reductions to $\text{Os}(\text{III})$ and $\text{Os}(\text{II})$ at potentials similar to $\text{Os}(\text{CHBA-Et})(\text{Py})_2$, but also showed completely reversible oxidations to $\text{Os}(\text{V})$. Thus the intentional modification of the tetradentate tetraanionic ligand had the desired effect of eliminating the oxidative ligand degradation and allowing the formation of stable $\text{Os}(\text{V})$ complexes. Unfortunately, these new complexes did not possess the catalytic activity of the compounds discussed in Chapter III.

There are very few examples of stable osmium(V) compounds [5]. We are able to observe this oxidation state because of the oxidative stability of the CHBA-DCB ligand and because of its powerful electron

donating ability. A comparison of the Os(V/IV) formal potentials of our complexes with those of related compounds containing more common ligands (chloride and triphenylphosphine) reveals the profound stabilization of the higher oxidation state by the multianionic chelating ligands. For example, the Os(V/IV) formal potential of trans-Os(CHBA-DCB)(Ph₃P)₂ is at least 750 mV lower than that of trans-OsCl₄(Ph₃P)₂ [6].

Os(IV) complexes of the nonchlorinated analog of CHBA-DCB, HBA-B [4], were prepared by Geoffrey Peake [2,7]. The absence of the chlorine substituents from the aromatic rings of the ligand sacrificed some of its inertness, but replacing the strongly electronegative chlorine atoms with hydrogens made the ligand a better electron donor. As a result, the formal potentials of the osmium couples decreased by over 300 mV on replacing the CHBA-DCB ligand with HBA-B.

For all of the compounds containing the CHBA-DCB and HBA-B ligands, it should be noted that there are electronic structures of the tetradentate tetraanions which may contribute to the structure of the complex and alter the formal oxidation state assignment of the metal center. Contributions of benzoquinonediimine or quinonoid forms of the ligands decrease the formal oxidation state of the osmium. Electrochemical and structural evidence suggests that these structures contribute little in complexes containing the CHBA-DCB ligand, but may be significant in complexes containing HBA-B and osmium in the higher oxidation states.

The stability of the Os(V) complexes was tested by performing controlled potential electrolysis experiments. Stable Os(V) species were formed, but oxidation to Os(V) triggered a partial isomerization of several of the trans compounds to the cis- α isomers. The equilibrium

constant for this isomerization at Os(V) was fortuitously close to unity and the formal potentials of the two isomers were well separated, so both isomers could be observed by cyclic and normal pulse voltammetry, and the equilibrium constants for each of the oxidation states could be calculated. Numerous examples of redox-induced isomerizations of organic and inorganic compounds have been reported [8]. The factors which govern the isomerization reactions are generally steric and/or electronic. If these two factors are in competition, then their relative importance can change upon oxidation or reduction. Such a competition exists for osmium compounds containing the CHBA-DCB and HBA-B ligands. When the electron density on the metal center is decreased, either by oxidation to Os(V) or by coordination of an electron-withdrawing ligand, the tetradentate tetraanionic ligand can respond by adopting a nonplanar conformation where, because of restriction of the amide delocalization, it is a better electron donor. The amide delocalization causes the planar form of the ligand to be energetically favored, but the added stabilization of the metal center in the nonplanar isomer must offset its loss. The importance of electronic factors in this reaction has been demonstrated by the discovery of an approximate correlation of the equilibrium constants with electron-donating ability of the axial ligands for a series of osmium complexes containing the CHBA-DCB ligand and various 4-substituted pyridines. This potential for isomerization introduces another factor to be considered in the design of new ligand systems.

Results and Discussion

Cyclic Voltammetric Results

In Chapter II it was reported that the complex $\text{Os}(\text{CHBA-Et})(\text{Py})_2$ underwent decomposition of the CHBA-Et ligand upon oxidation to Os(V). Since one of the major goals of this project was the production of new stable high oxidation state complexes, it was desirable to eliminate this oxidative degradation. Therefore, John Keech of the Collins group synthesized the potentially tetradentate tetraanionic ligand $\text{H}_4\text{CHBA-DCB}$ [1], shown in Figure 4.1. In this ligand the oxidatively-sensitive ethane bridge of CHBA-Et has been replaced by a dichlorobenzene group which was expected to be much more inert to oxidation.

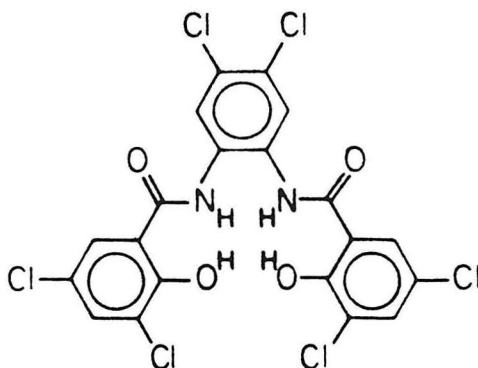


Figure 4.1. Structure of $\text{H}_4\text{CHBA-DCB}$.

Osmium (IV) complexes of CHBA-DCB [9] with a variety of monodentate ligands were synthesized by John Keech [1-3]. The electrochemistry of these complexes was examined and as expected they displayed reversible oxidations to Os(V). The cyclic voltammogram (CV) of trans- $\text{Os}(\text{CHBA-DCB})(\text{t-Bupy})_2$ in CH_2Cl_2 is shown in Figure 4.2. Thus the intentional modification of the tetradentate tetraanionic ligand eliminated the undesirable oxidative degradation reactions. The

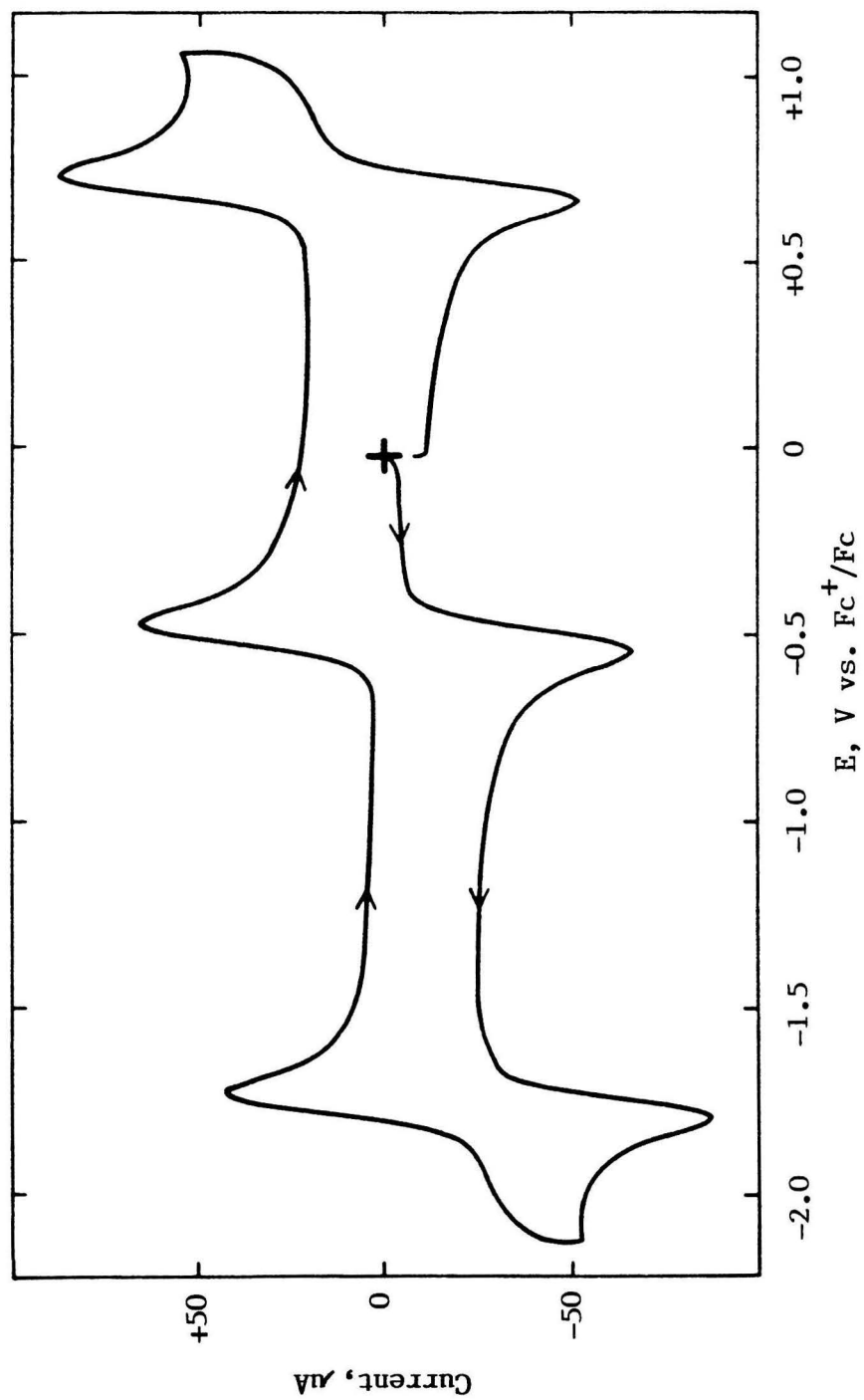


Figure 4.2. Cyclic voltammogram of 1 mM Os(CHBA-DCB)(t-Bupy)₂ in CH₂Cl₂, 0.1 M TBAP at 0.17 cm² BPG electrode. Scan rate = 200 mV/sec.

electrochemical data for some of the various Os(IV) compounds studied containing the CHBA-DCB ligand are summarized in Table 4.1.

Table 4.1. Formal potentials of some osmium complexes containing the CHBA-DCB ligand.

Os(CHBA-DCB)L ₂ L ₂ =	Os(III/II)	Formal Potential, V ^a	
		Os(IV/III)	Os(V/IV)
(Py) ₂ ^b	-1.68	-0.44	+0.72
(<u>t</u> -Bupy) ₂ ^b	-1.77	-0.51	+0.70
(Ph ₃ P) ₂ ^b	(-1.72) ^c	-0.46	+0.59
(Ph ₃ P=O) ₂ ^b	d	-1.05	+0.47
(Ph ₃ P)(<u>t</u> -BuNC) ^e	-1.25	-0.64	+0.74
(<u>t</u> -BuNC) ₂ ^e	-1.05	-0.57	+0.92
(diphos) ^f	-1.22	-0.37	+0.55

^aMeasured in CH₂Cl₂/0.1 M TBAP and referenced to Fc⁺/Fc internal standard.
^bTrans isomer. ^cPeak potential of irreversible reduction to Os(II). ^dNot observed at E > -2.3 V. ^eCis-alpha isomer. ^fCis-beta isomer.

Note that coordination of one or two electron-withdrawing t-butylisocyanide ligands produces complexes with the cis-alpha geometry, while the electron-donating ligands form trans complexes. The reasons for this effect will be discussed in more detail later. Complexes containing the CHBA-DCB ligand and two identical monodentate ligands can form three diastereomeric octahedral complexes with the structures shown in Figure 4.3. The designations trans, cis-beta and cis-alpha have been defined previously for diastereomeric octahedral complexes of tetradentate ligands [10]. For complexes containing different monodentate ligands, such as Os(CHBA-DCB)(Ph₃P)(t-BuNC), there are two different cis-beta isomers.

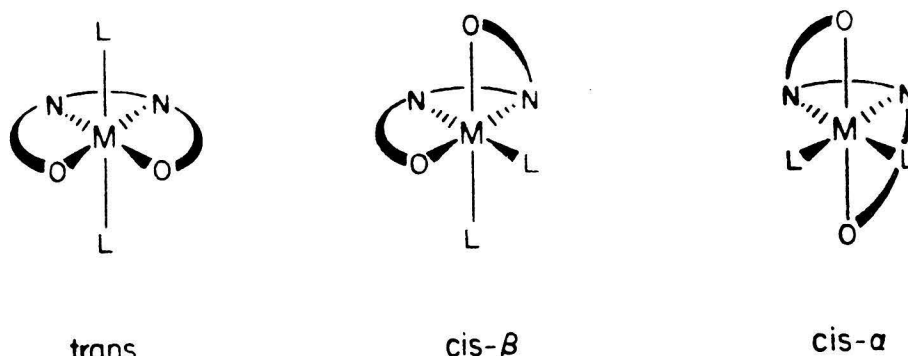


Figure 4.3. Isomer nomenclature for octahedral complexes of tetradentate ligands.

The formal potential of the Os(V/IV) couple varies substantially depending upon the monodentate ligands, ranging from +0.47 V vs. Fc^+/Fc [11] for the bis-(triphenylphosphine oxide) complex to +0.92 V for the bis-(t-butylisocyanide) complex. This variation suggests that the oxidation occurs at the metal rather than at the CHBA-DCB ligand and thus represents a true Os(V/IV) couple. The profound stabilization of the higher oxidation states by the CHBA-DCB ligand is demonstrated by the comparison of formal potentials shown in Table 4.2.

Table 4.2. Comparison of formal potentials of $\text{Os}(\text{CHBA-DCB})(\text{Ph}_3\text{P})_2$ with complexes containing more common ligands.

Compound	Formal Potential, V ^a	
	Os(IV/III)	Os(V/IV)
<u>trans</u> -Os(CHBA-DCB)(Ph ₃ P) ₂	-0.46	+0.59
<u>trans</u> -OsCl ₄ (Ph ₃ P) ₂	-0.12	(+1.34) ^b
[OsCl ₆] ²⁻	-1.19	+0.74

^a Measured in $\text{CH}_2\text{Cl}_2/0.1$ M TBAP and referenced to Fc^+/Fc internal standard.

^b Peak potential of irreversible oxidation to Os(V).

The oxidation of trans-OsCl₄(Ph₃P)₂ [6] not only occurs at a potential 750 mV higher than that of the corresponding CHBA-DCB complex, but its Os(V) form is not stable, as evidenced by the irreversibility of the oxidation. Since the oxidation of OsCl₄(Ph₃P)₂ is irreversible its formal potential cannot be measured, but the following chemical reaction which is probably responsible for the irreversibility shifts the anodic peak potential negative [12], so a 750 mV difference in the formal potentials is a conservative estimate. Thus the CHBA-DCB ligand is both inert to oxidative degradation reactions and capable of stabilizing high oxidation state metal centers, the stabilization being reflected in lower formal potentials. This stabilization arises in part from the well-documented [13-16] powerful donor ability of the N-coordinated organic amido groups. The Os(V/IV) formal potential of the neutral CHBA-DCB complex is even lower than that of the dianionic hexachloroosmate. The Os(IV/III) formal potential of the CHBA-DCB complex is also substantially lower than that of the tetrachloro complex.

Still lower formal potentials were observed with complexes of the ligand HBA-B [4] prepared by Geoffrey Peake [2,7]. The HBA-B ligand is simply the non-chlorinated analog of the CHBA-DCB ligand. Replacement of the highly electronegative chlorines of CHBA-DCB with hydrogens would be expected to increase the donor ability of the ligand and thus stabilize high oxidation states even more. However, the disadvantage of this change is an increased sensitivity of the aromatic rings of the HBA-B ligand to oxidative degradation reactions. A summary of the electrochemical data for the HBA-B complexes examined is presented in Table 4.3 and the CV of Os(HBA-B)(Ph₃P)₂ is shown in Figure 4.4.

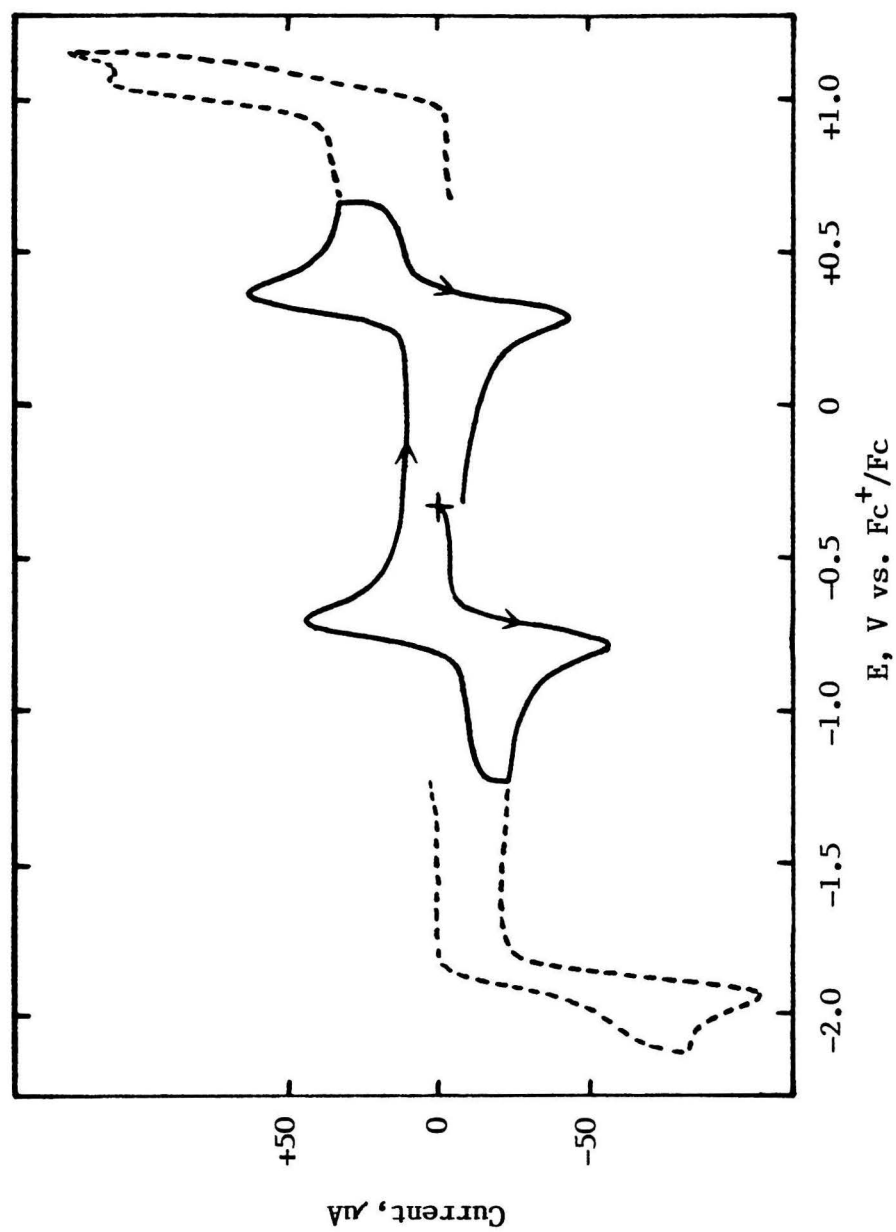


Figure 4.4. Cyclic voltammogram of 1.2 mM Os(HBA-B)(Ph₃P)(t-Bupy) in CH₂Cl₂, 0.1 M TBAP at 0.17 cm² BPG electrode. Scan rate = 200 mV/sec.

Table 4.3. Formal potentials of osmium complexes containing the HBA-B ligand.

$\text{Os}(\text{HBA-B})\text{L}_2$ $\text{L}_2 =$	Os(III/II)	Formal Potential, V ^a	
		Os(IV/III)	Os(V/IV)
$(\text{Ph}_3\text{P})_2^{\text{b}}$	$(-1.73)^{\text{c}}$	-0.79	+0.21
$(\text{Ph}_3\text{P})(\text{Py})^{\text{b}}$	$(-1.94)^{\text{c}}$	-0.73	+0.34 ^d
$(\text{Ph}_3\text{P})(\underline{\text{t}}\text{-Bupy})^{\text{b}}$	$(-1.93)^{\text{c}}$	-0.73	+0.33 ^e
$(\text{Ph}_3\text{P})(\underline{\text{t}}\text{-BuNC})^{\text{f}}$	-1.46	-0.91	+0.46
$(\text{Ph}_3\text{P})(\text{CO})^{\text{f}}$	-1.17	-0.63	+0.90
Diphos ^g	-1.46	-0.67	+0.25
$(\text{Ph}_3\text{P})(\text{bipy})^{\text{h}}$	-1.09	-0.29	+0.70
$(\text{Ph}_3\text{P})(\text{phen})^{\text{h}}$	-1.07	-0.28	+0.70

^aMeasured in $\text{CH}_2\text{Cl}_2/0.1 \text{ M TBAP}$ and referenced to Fc^+/Fc internal standard.

^bTrans isomer. ^cPeak potential for irreversible reduction to Os(II). ^dAn irreversible oxidation at +1.07 V was also observed. ^eAn irreversible oxidation at +1.08 V was also observed. ^fCis-alpha isomer. ^gCis-beta isomer. ^hHBA-B coordinated as a tridentate trianion, see text.

Comparison of the formal potentials of the bis-(triphenylphosphine) complexes shows that those of the HBA-B complex are over 300 mV lower than those of the CHBA-DCB complex. Osmium(IV) coordinated to the HBA-B ligand is even sufficiently basic to coordinate a carbonyl ligand. As with the CHBA-DCB complexes, coordination of an electron-withdrawing monodentate ligand produces the cis-alpha isomer. Interestingly, the diphos (1,2-bis-(diphenylphosphino)-ethane) compound is isolated as the cis-beta isomer. Another interesting aspect of the coordination chemistry of the Os(IV) complexes of HBA-B is the reaction which occurs between the bis-(triphenylphosphine) complex and the bidentate ligands 2,2'-bipyridine, bipy, and 1,10-phenanthroline, phen. Both nitrogens of

the bipy or phen ligand coordinate to the osmium and displace one of the phenoxide oxygens of the HBA-B ligand, which is then protonated. The resulting complex contains the HBA-B ligand coordinated as a tridentate trianion, as shown in Figure 4.5. An x-ray crystal structure has been performed on the Os(III) phen complex.

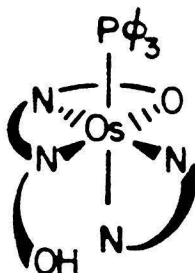


Figure 4.5. Structure of Os(H-HBA-B)(phen).

When considering the formal potentials quoted in this work, one should be cognizant of the fact that there are electronic structures of the tetradentate tetraanions which may contribute to the structure of a metal complex and so alter the formal oxidation state assignment of the metal center. These structures include the benzoquinonediimine (or related semibenzoquinonemonoimine), A, and quinonoid, C, structures shown in Figure 4.6.

Contributions from A or C would not violate the eighteen electron rule in the Os(IV) complexes and so these structures are feasible. However, crystal structure data from a number of compounds containing the CHBA-DCB ligand do not show the shortening of the amide C-N or phenoxide C-O bonds which would be expected if A or C contributed significantly to the structures [3,7]. These alternate structures are less likely

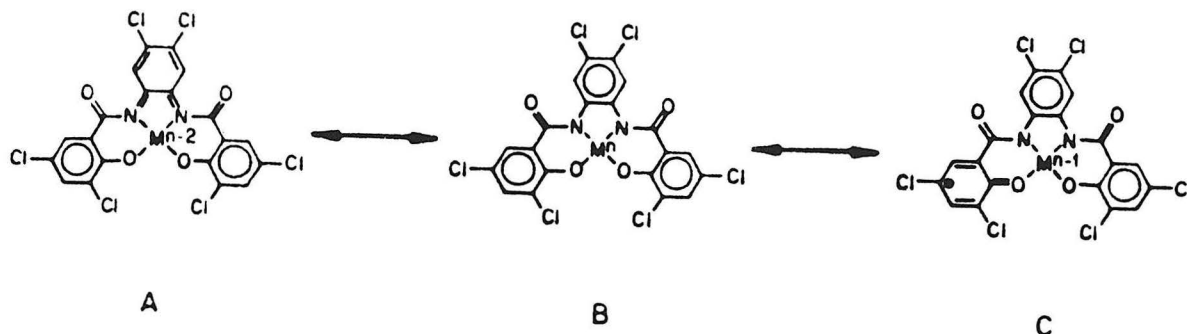


Figure 4.6. Alternate electronic structures of the CHBA-DCB ligand.

to contribute in Os(III) or Os(II) compounds since they would then violate the eighteen-electron rule. No structural data are yet available on the Os(V) complexes, but other data suggest that A and C do not contribute significantly to them. The large changes in the formal potential for the oxidation of the Os(IV) compounds resulting from changes in the monodentate ligands strongly suggest that the oxidation is metal-centered. The isomerization observed upon oxidation of a number of the CHBA-DCB complexes is almost certainly driven by changes in the electron density at the metal center (vide infra) which also argues for the importance of the metal in the oxidation reaction. Finally, in work to be reported in Chapter V, the formal potential for oxidation in liquid SO_2 of $\text{Os}(\text{CHBA-Et})(\text{Py})_2$ is only very slightly higher than that of $\text{Os}(\text{CHBA-DCB})(\text{Py})_2$ (0.86 V vs. 0.82 V). Since structure A, and the semibenzoquinonemonoimine, do not exist for the CHBA-Et ligand, a larger difference would be anticipated if they contributed to the structure of the CHBA-DCB complex.

The absence of the chlorine substituents from the HBA-B ligand makes its complexes more likely to contain contributions from structures A and C since these structures are oxidized forms of the tetradentate tetraanionic

ligand and oxidation should be easier for the more electron-rich HBA-B ligand. There is some structural evidence which suggests that these structures may contribute significantly to HBA-B complexes [7].

Isomerization of trans CHBA-DCB complexes upon oxidation

It was desired to demonstrate the stability of the Os(V) complexes observed by cyclic voltammetry by conducting controlled potential electrolysis experiments. It was expected that, if the Os(V) form were stable, an electrolysis would consume exactly one Faraday per mole of osmium and produce a solution displaying the same CV as the Os(IV) form but with an open circuit potential positive of the Os(V/IV) couple. The results of such an experiment with Os(CHBA-DCB)(t-Bupy)₂ are presented in Figure 4.7.

The CV of trans-Os(CHBA-DCB)(t-Bupy)₂ before the electrolysis is shown in Figure 4.7A. Controlled potential oxidation at approximately +0.75 V consumed 1.0 F/mol of Os as expected. However, the CV after the electrolysis, shown in Figure 4.7B, unexpectedly displayed six reversible reductions instead of three. Three of these reductions corresponded to the original couples, but had lower peak currents after the electrolysis. This decrease in peak currents was approximately accounted for by the appearance of the three new couples at potentials a few hundred millivolts less positive than the original couples. When the oxidized solution displaying the six reductions was reduced at +0.60 V, between the Os(CHBA-DCB)(t-Bupy)₂ Os(V/IV) couple at +0.70 V and the new couple at +0.50 V, the original Os(CHBA-DCB)(t-Bupy)₂ couples were observed to steadily increase in size at the expense of the new couples as the electrolysis progressed. At the conclusion of the electrolysis, after passage of 1.0 F/mol of Os, the original CV of Figure 4.7A was restored.

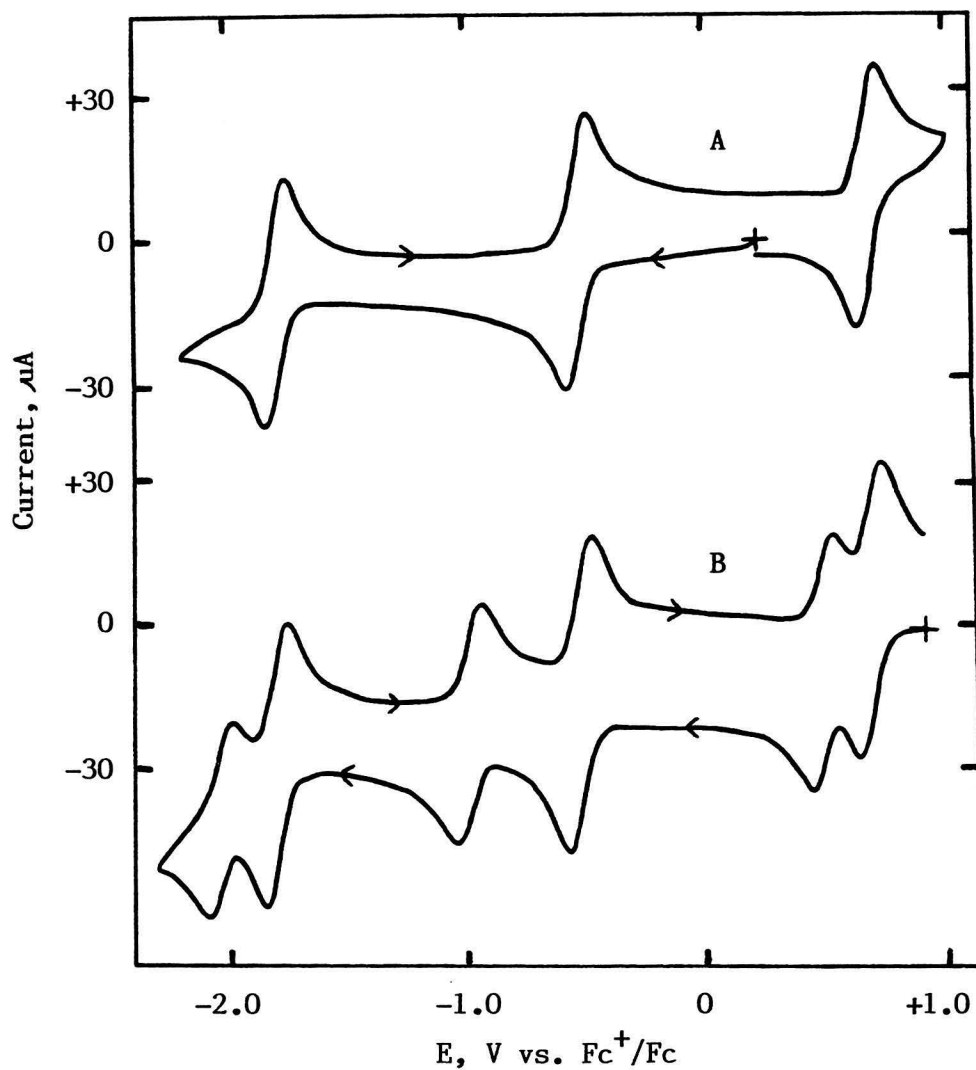


Figure 4.7. Cyclic voltammograms of 4.1 mM $\text{Os}(\text{CHBA-DCB})(t\text{-Bupy})_2$ in CH_2Cl_2 , 0.1 M TBAP at 0.03 cm^2 Pt electrode. Scan rate = 200 mV/sec. A = Os(IV) B = Os(V)

A similar electrolysis experiment was conducted with $\text{Os}(\text{CHBA-DCB})(\text{Ph}_3\text{P})_2$. It also consumed 1.0 F/mol of Os but showed no new couples after the electrolysis. However, CV's of $\text{Os}(\text{CHBA-DCB})(\text{Ph}_3\text{P=O})_2$ displayed new couples like those observed with the bis-(t-butylpyridine) compound simply by scanning over the Os(V/IV) couple. Pausing the scan at potentials positive of the Os(V/IV) couple increased the size of these new peaks.

It was postulated that the new couples observed with the bis-(t-butylpyridine) and bis-(triphenylphosphine oxide) complexes arose from a partial isomerization at Os(V), possibly to the cis-alpha or cis-beta isomers discussed previously and already observed with other ligands. The identity of the compound responsible for the new couples could be established only by isolating it from the electrolysis mixture. This was done by first conducting a controlled potential oxidation of a solution of $\text{Os}(\text{CHBA-DCB})(\text{t-Bupy})_2$ at room temperature to obtain a solution of the Os(V) forms of the two isomers. This solution was then cooled to $-78\text{ }^\circ\text{C}$ and ferrocene was added to reduce the Os(V) compounds to Os(IV). At $-78\text{ }^\circ\text{C}$ the new isomer did not convert back to trans. The resulting solution was syringed onto a jacketed silica gel column cooled to -65 to $-70\text{ }^\circ\text{C}$. The mixture was eluted with precooled solvent (1% THF in CH_2Cl_2). The first band off the column was excess ferrocene. Then followed a reddish-brown band for the new osmium compound and finally a gray-black band for the trans osmium compound. The solvent was removed from the new osmium compound under vacuum. The solid material was quite stable at room temperature. IR and NMR spectra established that the new Os compound was the cis-alpha isomer of $\text{Os}(\text{CHBA-DCB})(\text{t-Bupy})_2$. Cyclic voltammetry at low

temperature demonstrated that it was the compound responsible for the new couples observed after the electrolysis experiment.

It was further postulated that the mixture of isomers obtained upon oxidation of solutions of the bis-(t-butylpyridine) complex was at equilibrium, implying that the equilibrium constant for the isomerization reaction at Os(V) was about unity. This postulate was supported by the fact that the same ratio of isomers, about 60:40 trans to cis- α determined from the ratio of CV peak currents, was obtained when the experiment was repeated several times, and the fact that after the electrolyses this ratio did not change with time. In order to verify that a system is at equilibrium, it is necessary to be able to establish the same composition starting from both sides of the equilibrium. For the bis-(t-butylpyridine) system this was done by reoxidizing the NMR sample of cis- α -Os(CHBA-DCB)(t-Bupy)₂ at low temperature, and then allowing the resulting cis- α -Os(V) solution to warm to room temperature. Upon warming, exactly the same distribution of isomers, as judged by CV peak currents, was obtained as by starting with the trans isomer and oxidizing at room temperature. Thus, the mixture obtained at Os(V) is at equilibrium.

The equilibrium constant for the isomerization of Os(CHBA-DCB)(t-Bupy)₂ at Os(V) is simply the ratio of the concentrations of the two isomers. This ratio is in turn equal to the ratio of the cyclic voltammetric peak currents of the isomers, assuming similar diffusion coefficients. However, CV peak currents are difficult to measure accurately, especially for two or more closely-spaced peaks. Therefore, it was decided to use normal pulse voltammetry (NPV) to measure the relative concentrations of the isomers [17]. A normal pulse

voltammogram of a solution of $\text{Os}^{\text{V}}(\text{CHBA-DCB})(\text{t-Bupy})_2^+$ is shown in Figure 4.8. Instead of peaks, NPV gives waves for the various reductions, the height of which are proportional to the concentrations of the species. The ratio of concentrations of the two isomers was taken to be equal to the ratio of the NPV wave heights, again assuming similar diffusion coefficients for the isomers. Since the $\text{Os}(\text{IV/III})$ reductions are the most widely spaced, they were used to determine the ratio of isomers. The isomerization reaction is slow enough that the same ratio is obtained independent of the couples used or the scan rate, as determined by both cyclic voltammetry and NPV. The limiting currents are determined as shown in Figure 4.9. For the bis-(t-butylpyridine) compound the value determined for the equilibrium constant (trans/cis- α) was 1.3.

Using this one experimentally determined equilibrium constant and the experimentally measured formal potentials, it is possible to calculate the equilibrium constants at the other observable oxidation states. The thermodynamic ladder used for these calculations is shown in Scheme 4.1. The cis- α and trans isomers are related by equilibrium constants, while the different oxidation states are related by formal potentials. Both of these physical constants can be converted to free energy changes using the appropriate thermodynamic relationships. The sum of the free energy changes around a particular cycle was then used to calculate the equilibrium constants at oxidation states IV through II. As can be seen, the trans isomer goes from being slightly favored at $\text{Os}(\text{V})$ to being heavily favored at $\text{Os}(\text{IV})$ through $\text{Os}(\text{II})$. The derived equilibrium constant of 3400 at $\text{Os}(\text{IV})$ is consistent with the fact that the synthesis of $\text{Os}(\text{CHBA-DCB})(\text{t-Bupy})_2$ produces only the trans isomer.

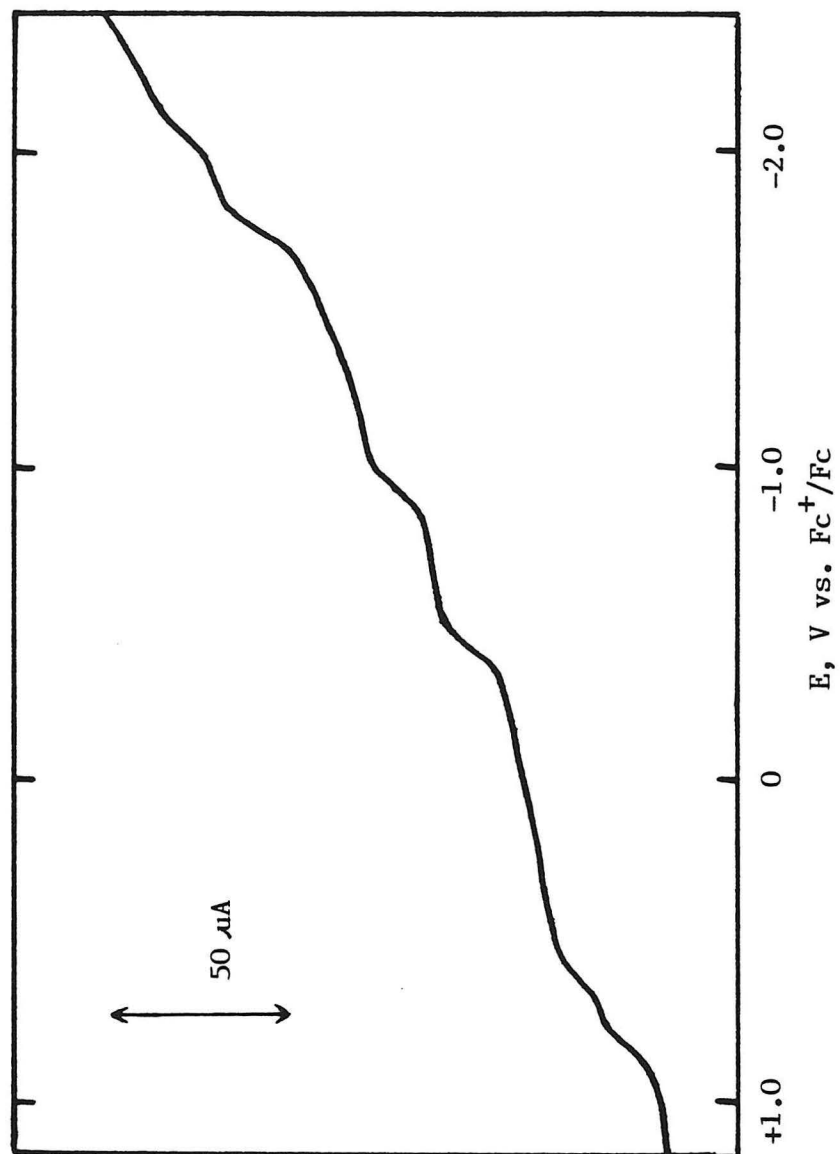


Figure 4.8. Normal pulse voltammogram of 1 mM $\text{Os}^{\text{V}}(\text{CHBA-DCB})(\text{t-Bupy})_2^+$ in CH_2Cl_2 , 0.1 M TBAP at 0.03 cm^2 Pt electrode.

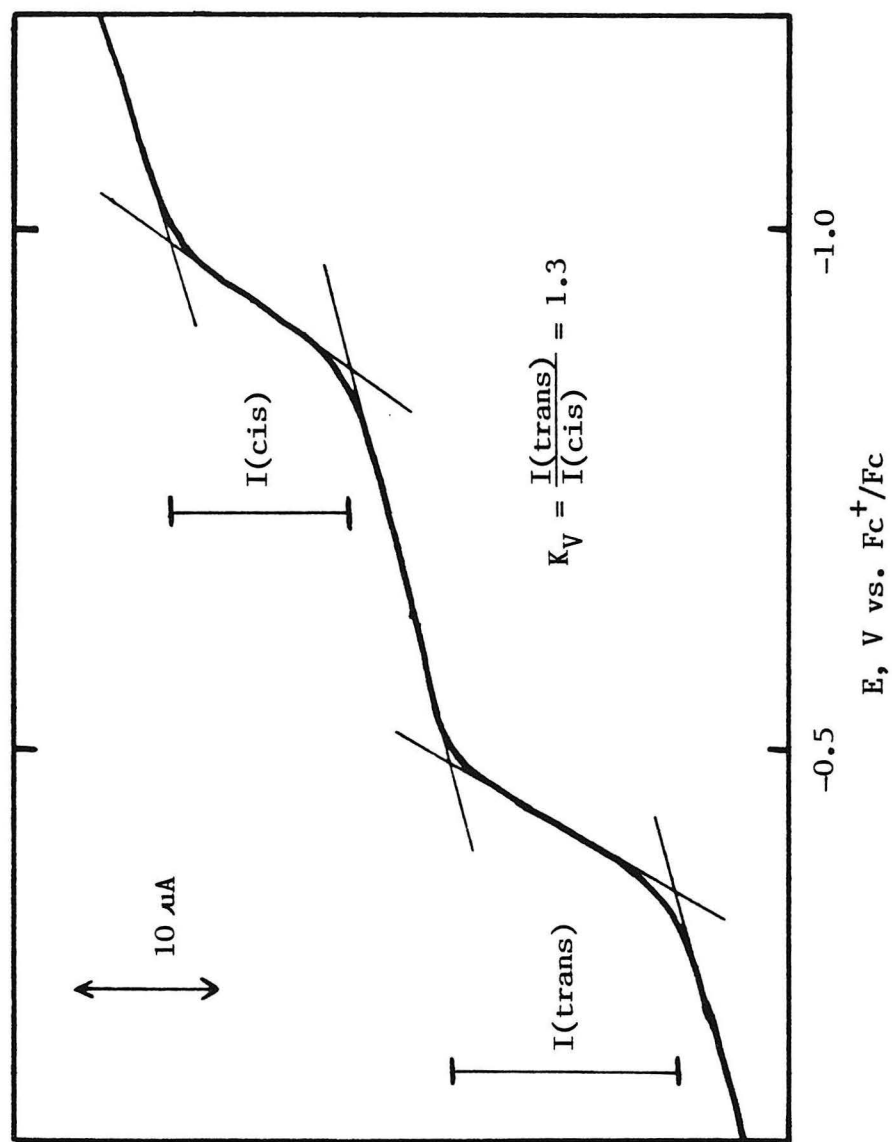
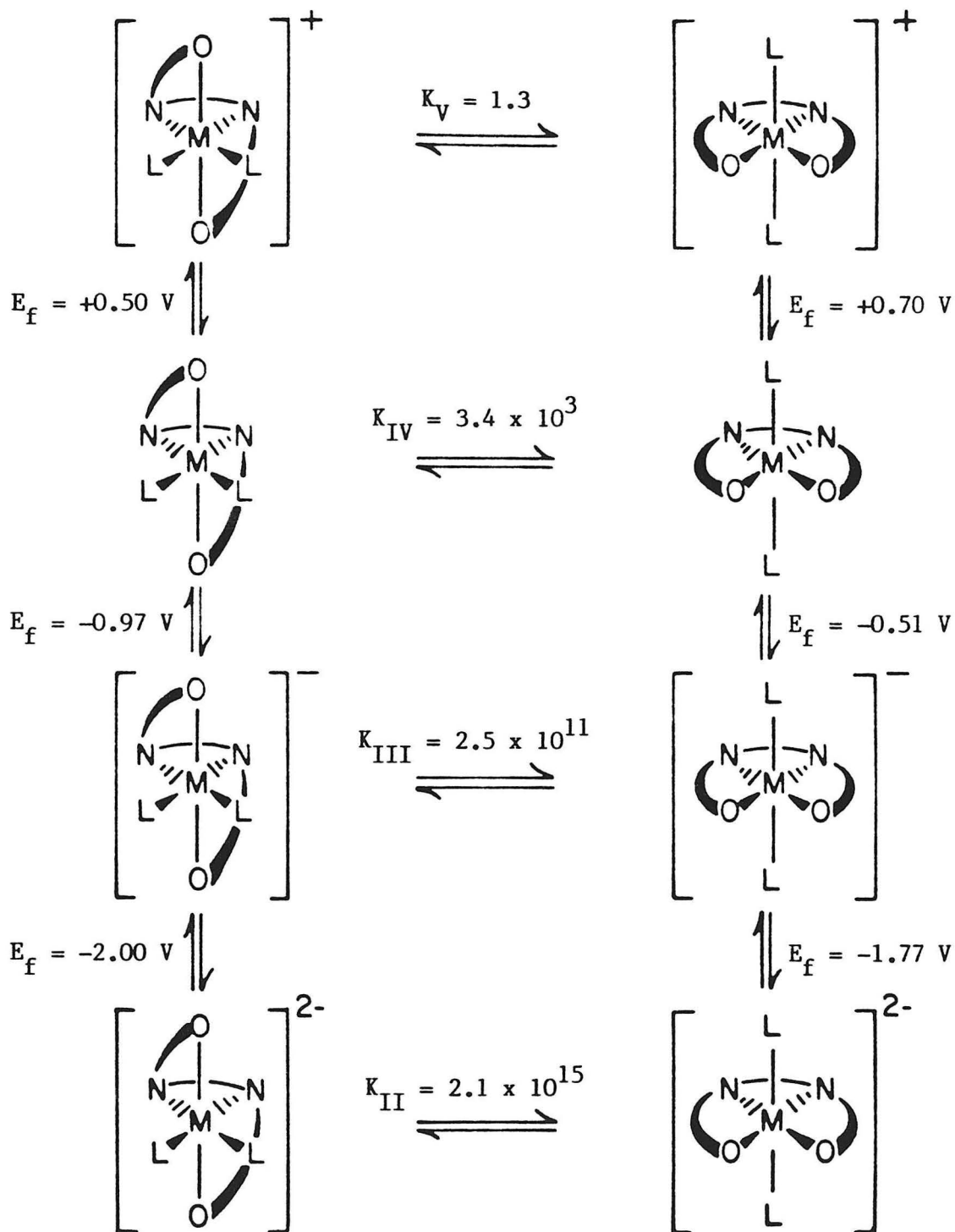
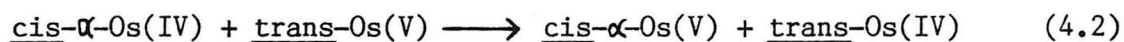
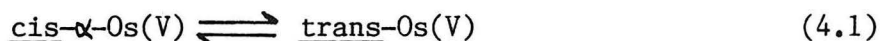


Figure 4.9. Measurement of K_V from NPV of 1 mM $Os^V(\text{CHBA-DCB})(t\text{-Bupy})_2^+$ in CH_2Cl_2 , 0.1 M TBAP at 0.03 cm^2 Pt electrode.

Scheme 4.1. Thermodynamic ladder used to calculate equilibrium constants for trans/cis alpha isomerization of $\text{Os}(\text{CHBA-DCB})(\text{t-Bupy})_2$ at Os(IV), Os(III) and Os(II).



The isolation and characterization of the cis-alpha isomer was done at low temperature because electrochemical reduction of the isomer mixture at room temperature had indicated that the cis-alpha Os(IV) species reverted to trans as quickly as it was formed. After the low temperature work had been done, it was discovered that the isomerization at Os(IV) is actually quite slow. When a solution containing a mixture of Os(V) isomers was reduced electrochemically or chemically with ferrocene at -50 °C and then warmed to room temperature, it was found that the resulting solution of cis-alpha and trans Os(IV) complexes was stable for many days, as long as no Os(V) was present. The total absence of Os(V) was assured by reducing the solution electrochemically by slightly more than one F/mol of Os, or by adding a small excess of ferrocene. Electrochemical generation of as little as 10% Os(V) resulted in rapid reversion of the Os(IV) cis-alpha complex to trans. Thus it appears that the interconversion between trans and cis-alpha isomers is rapid only at the Os(V) oxidation state. Reversion of cis-alpha Os(IV) complexes to trans can occur only through catalysis by Os(V) complexes as illustrated by equations 4.1 and 4.2.



The equilibrium in equation 4.1 has been shown to have an equilibrium constant of nearly one and is known to be established fairly rapidly. Because the Os(V/IV) formal potential of the cis-alpha isomer is always lower than that of the trans isomer, the reaction in equation 4.2 will proceed as shown. Through these reactions a small amount of cis-alpha Os(V) can convert all of the cis-alpha Os(IV) in a solution to the trans isomer. The discovery of the slowness of the isomerization at lower

oxidation states also explains why the cis- α Os(IV/III) and Os(III/II) couples can be observed electrochemically even though the trans isomer is heavily favored at these oxidation states.

It is believed that the isomerizations at Os(V) are triggered by the decrease in electron density at the metal center upon oxidation. The tetradentate tetraanionic ligand responds to this decrease in electron density by adopting a nonplanar conformation where it is a better electron donor. The enhanced electron donation by the ligand in the cis- α isomer is evidenced by the lower formal potentials of the cis- α compounds compared to the trans compounds. If the isomerization is primarily under electronic control, then it would be expected that variations in the electron donating ability of the ligands would alter the equilibrium constant in a predictable manner. This hypothesis was examined by determining the equilibrium constants for a number of osmium CHBA-DCB complexes containing 4-substituted pyridines. The formal potentials of these compounds are listed in Table 4.4 and the corresponding equilibrium constants are presented in Table 4.5.

The formal potentials in Table 4.4 follow exactly the trends expected. Compared to the Os(CHBA-DCB)(Py)₂ formal potentials, complexes with electron-withdrawing groups on the pyridines have higher formal potentials and complexes with electron-donating substituents have lower formal potentials. The equilibrium constant data are also in qualitative agreement with expectations. The agreement seems to be best at Os(V) and Os(IV) where the electronic effects should be most important and where the numbers are least subject to error. The complex containing the electron-withdrawing acetyl group displays the lowest equilibrium constants, indicating the formation of more cis- α at Os(V) as

Table 4.4. Formal potentials of Os(CHBA-DCB)(X-Py)₂ compounds.

Os(CHBA-DCB)(X-Py) ₂ X=	Os(III/II)		Formal Potential, V ^a Os(IV/III)		Os(V/IV)	
	cis-alpha	trans	cis-alpha	trans	cis-alpha	trans
4-Acetyl	-1.46	-1.30	-0.83	-0.32	+0.58	+0.75
4-Chloro	-1.81	-1.59	-0.89	-0.39	+0.58	+0.74
4-Bromo	b	-1.56	-0.89	-0.38	+0.58	+0.75
Unsubstituted	-1.89	-1.68	-0.92	-0.44	+0.54	+0.72
4-Methyl	-1.99	-1.78	-0.97	-0.50	+0.49	+0.70
4-Ethyl	-2.00	-1.78	-0.98	-0.52	+0.49	+0.69
4- <u>t</u> -Butyl	-2.00	-1.77	-0.97	-0.51	+0.50	+0.70
3,4-Dimethyl	-2.05	-1.82	-0.99	-0.54	+0.47	+0.68
4-Methoxy	b	-1.85	-1.00	-0.55	+0.45	+0.67

^aMeasured in CH₂Cl₂/0.1 M TBAP and referenced to Fc⁺/Fc internal standard.

^bIrreversible.

Table 4.5. Equilibrium constants for Os(CHBA-DCB)(X-Py)₂ compounds.

Os(CHBA-DCB)(X-Py) ₂ X=	Equilibrium Constant (Trans/Cis-alpha) ^a			
	K _{II}	K _{III}	K _{IV}	K _V
4-Acetyl	8.4 x 10 ¹³	1.5 x 10 ¹¹	3.0 x 10 ²	0.37
4-Chloro	9.1 x 10 ¹⁴	1.6 x 10 ¹¹	4.5 x 10 ²	0.83
4-Bromo	b	3.8 x 10 ¹¹	7.2 x 10 ²	0.90
Unsubstituted	4.5 x 10 ¹⁴	1.2 x 10 ¹¹	7.3 x 10 ²	0.61
4-Methyl	1.0 x 10 ¹⁵	2.7 x 10 ¹¹	2.5 x 10 ³	0.64
4-Ethyl	1.3 x 10 ¹⁵	2.3 x 10 ¹¹	3.1 x 10 ³	1.2
4- <u>t</u> -Butyl	2.1 x 10 ¹⁵	2.5 x 10 ¹¹	3.4 x 10 ³	1.3
3,4-Dimethyl	8.8 x 10 ¹⁴	1.0 x 10 ¹¹	2.1 x 10 ³	0.54
4-Methoxy	b	3.8 x 10 ¹²	7.7 x 10 ⁴	0.85

^aK_V measured by NPV. Others calculated from K_V and formal potentials in Table 4.4. ^bCannot be calculated because of irreversible cis-alpha Os(III/II) couple.

expected. The equilibrium constants of the unsubstituted and halogenated complexes have intermediate values, and the complexes containing electron-donating alkyl groups have higher equilibrium constants.

Even examining the raw data makes it evident that there are some inconsistencies. These inconsistencies were made clearer by an attempt to quantitatively correlate the equilibrium constants with electron-donating ability of the pyridine ligands. This was done by applying the Hammett equation to the data [18]:

$$\log K = \rho \sigma + \log K_0 .$$

K is the equilibrium constant for the substituted compound, K_0 is the equilibrium constant for the unsubstituted compound, σ is the Hammett parameter for a particular substituent and ρ is a proportionality constant measuring the susceptibility of the reaction to electronic effects. A negative ρ indicates that the reaction is assisted by electron-donating substituents.

For a reaction under simple electronic control a plot of $\log K$ vs. σ would be expected to be linear. Such a plot of $\log K_v$ vs. σ^+ is shown in Figure 4.10. The σ^+ parameter is used for reactions involving an electron-donating group interacting with a developing positive charge in the transition state and so would seem to be appropriate for this equilibrium. As can be seen, there is considerable scatter in the K_v plot. This scatter does not stem from random deviation of the K_v measurements since all of the points represent the average of at least two measurements conducted on the same solution, and several measurements were repeated on different solutions with good reproducibility. A generally correct trend is evident, with decreasing electron donation from the

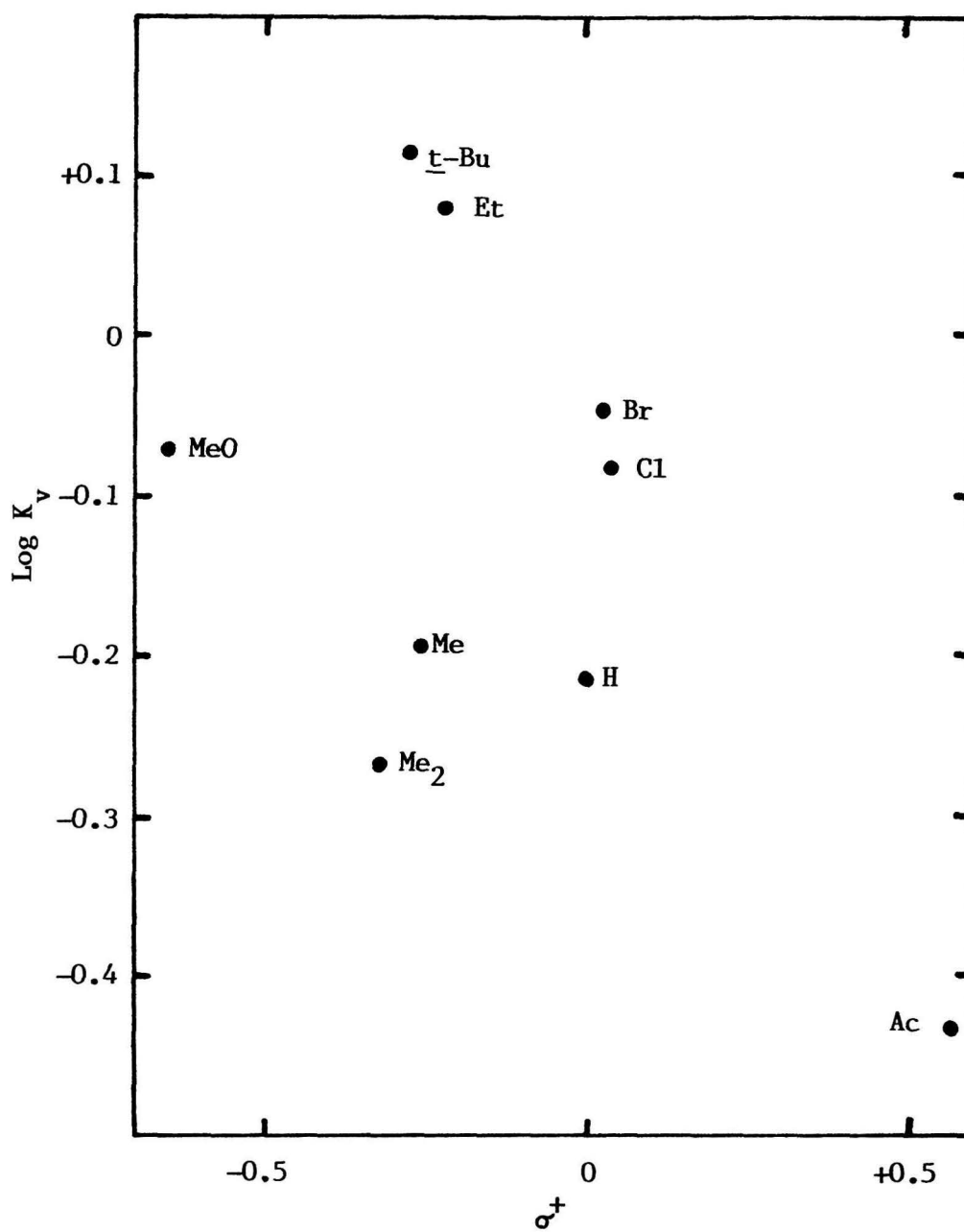


Figure 4.10. Hammett plot of K_v data for $\text{Os}(\text{CHBA-DCB})(\text{X-Py})_2$ complexes.

pyridine ligand (higher σ^+) leading to lower K_v values (more cis-alpha at equilibrium). However, the scatter in the plot indicates that there are other factors involved in determining the value of K_v . One likely factor is solvation. If the difference in solvation of the trans and cis-alpha isomers is not constant for the different complexes, then a linear Hammett plot would not be expected. Therefore, while these results demonstrate the importance of electronic effects in the observed isomerizations at Os(V), there are other factors which obviously influence the equilibrium constants.

The question arises as to the origin of the added electron donation in the cis-alpha compounds. The effect appears to arise from a change in the properties of the CHBA-DCB ligand, rather than a change in the way the ligand interacts with the metal caused by a redistribution of the ligand donor groups in the coordination sphere. This claim is supported by the data in Table 4.6.

Complexes analogous to the CHBA-DCB compounds but lacking the bridging group do not display the large positive shifts in formal potentials upon isomerization as do the CHBA-DCB complexes. Some changes do occur with the bidentate ligands but they are far smaller and less consistent than for the CHBA-DCB containing compounds. The difference between the two types of complexes appears to be the fact that isomerization of the CHBA-DCB complexes is achieved principally by rotation about the amide C-N bonds whereas no such rotation is necessary in the absence of a bridge. The bond rotation in CHBA-DCB restricts the amide delocalization, depicted in Figure 4.11. The x-ray crystal structure of cis-alpha-Os(CHBA-DCB)(Ph₃P)(t-BuNC), shown in Figure 4.12, clearly illustrates the rotation of the amide C-N bond which rotates

Table 4.6. Changes in formal potential upon isomerization from trans to cis-alpha.

Compound	$E_f(\text{trans}) - E_f(\text{cis-alpha}), \text{mV}$		
	Os(III/II)	Os(IV/III)	Os(V/IV)
Os(CHBA-DCB)(<u>t</u> -Bupy) ₂	+230	+460	+200
Os(CHBA-DCB)(Ac-Py) ₂	+160	+510	+170
Os(CHBA-DCB)(Ph ₃ P=O) ₂	a	+300	+280
Os(Fo-CHBA) ₂ (Py) ₂ ^b	0	+70	a
Os(CHBA) ₂ (<u>t</u> -Bupy) ₂ ^b	+20	0	-90
Os(CHBA) ₂ (<u>t</u> -Bupy)(Ph ₃ P=O) ^{b,c}	a	+40	+20

^aData not available. ^bSee Chapter II. ^cCis isomer is either cis-alpha or cis-beta.

the amide carbonyl bond 50-60 degrees out of the C-N-Os plane. This rotation thus restricts the contribution of resonance forms A and C in Figure 4.11.

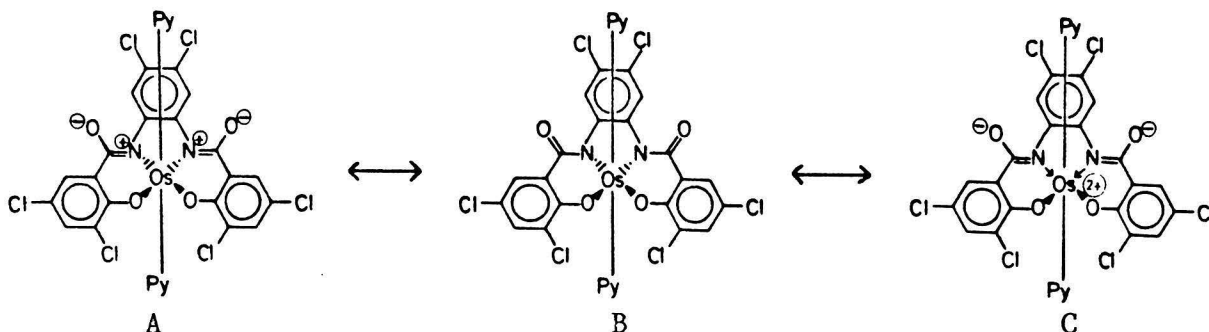


Figure 4.11. Amide delocalization in CHBA-DCB complexes.

In Figure 4.12 the two angles, 51° and 62°, represent the angles between the CHBA planes containing the carbonyl oxygens, and the DCB plane. The angles in brackets, 52° and 61°, represent the torsional angles along the carbonyl oxygen-amide nitrogen-bridge carbon bonds. The equality of these

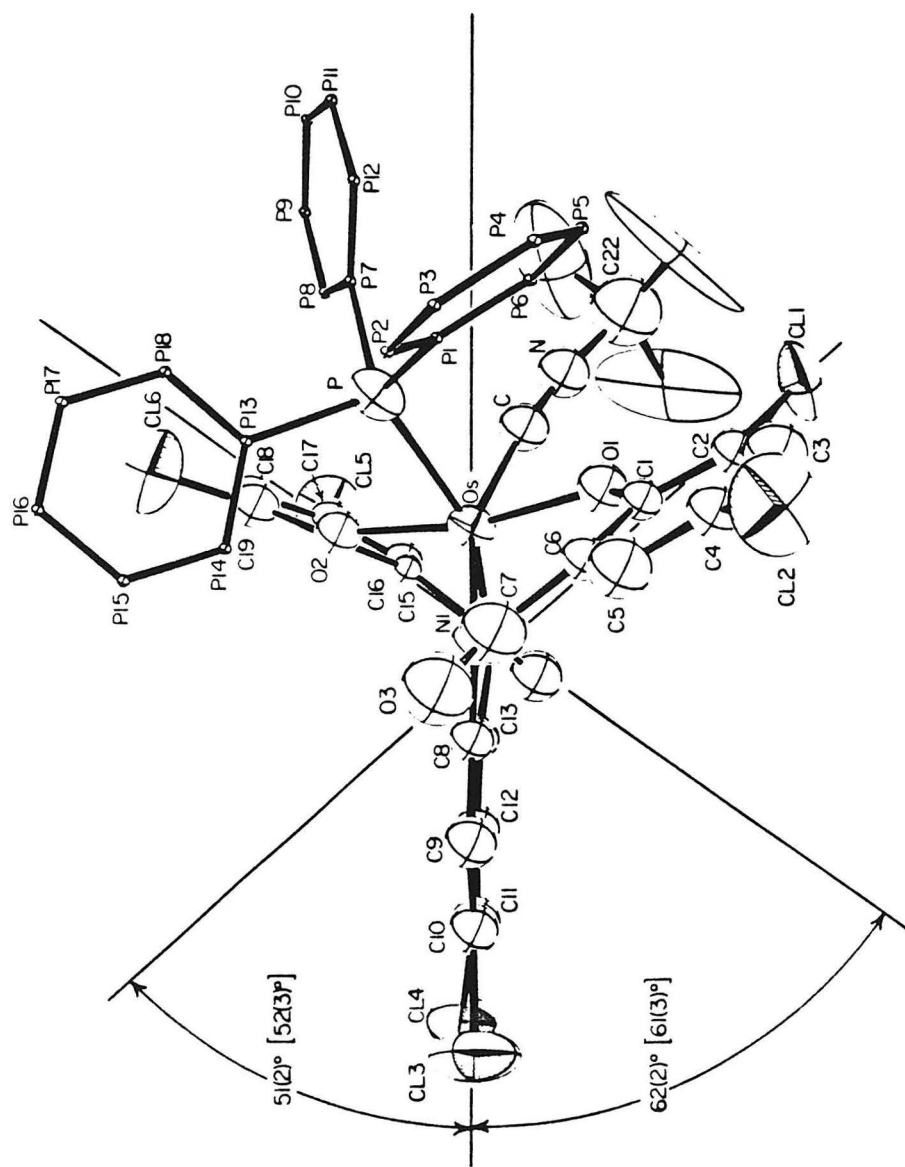


Figure 4.12. X-ray crystal structure of $\text{Os}(\text{CHBA-DCB})(\text{Ph}_3\text{P})(t\text{-BuNC})$.

two measurements indicates that the isomerization is achieved principally by rotation about the amide C-N bond.

This lessened contribution of the amide resonance forms A and C enhances sigma bonding and makes the amide nitrogen lone pair fully available for pi-donation to the metal center in the cis-alpha isomer. The loss of the amide delocalization is energetically unfavorable, but the added stabilization of the metal center apparently compensates for this. The observed shift in the amide C=O stretching frequency to higher energy upon isomerization from trans to cis-alpha is consistent with the loss of amide resonance [3]. Since the amide groups of the complexes containing bidentate ligands are not constrained by a bridge, no lessening of amide delocalization would be expected upon isomerization. This expectation is supported by the lack of significant differences in the formal potentials of the different isomers of these compounds. Neither isomer seems to be particularly favored in the absence of a bridge either since no interconversion of the isomeric pairs has ever been observed for the complexes of bidentate ligands.

No isomerization was observed upon oxidation of $\text{Os}(\text{CHBA-DCB})(\text{Ph}_3\text{P})_2$. This may be an electronic effect, but this seems unlikely since all of the compounds containing substituted pyridines and the bis-(triphenylphosphine oxide) compound isomerized at Os(V). More likely, the isomerization of the bis-(triphenylphosphine) complex is prevented by the steric bulk of the phosphine ligands. None of the trans HBA-B complexes isomerized upon oxidation either. They all contain at least one triphenylphosphine ligand, but since the formal potentials of these complexes are so much lower than any of the CHBA-DCB complexes, the lack of isomerization at Os(V) could also be due to a lack of electronic driving force. The HBA-B

ligand is so electron-donating in the trans isomer that the added electron donation of the cis-alpha isomer may not be needed at Os(V).

Isomerization of cis-alpha CHBA-DCB complexes upon reduction

All of the Os(IV) complexes containing CHBA-DCB or HBA-B and one or two electron-withdrawing monodentate ligands so far encountered have been isolated as the cis-alpha isomer. This observation supports the contention that the isomerization of trans CHBA-DCB complexes upon oxidation to Os(V) is induced by the decrease in electron density at the metal center. A similar decrease in electron density occurs upon coordination of electron-withdrawing ligands such as t-butylisocyanide or CO, and produces the cis-alpha isomer at Os(IV) rather than at Os(V). The isocyanide and carbonyl bands in the IR spectra of these complexes indicate that pi-backbonding is taking place [3,7].

If the above argument is correct, then it would be expected that reduction of a cis-alpha Os(IV) compound containing an electron-withdrawing ligand to Os(III) or Os(II) would lead to an isomerization of the tetradentate tetraanionic ligand to a more planar, less electron-donating, conformation. The results of the reduction of Os(CHBA-DCB)(t-BuNC)₂ to Os(II) are shown in Figure 4.13. The initial CV, seen in Figure 4.13A, displayed the expected two reversible reductions and one reversible oxidation. Note that even on the CV time scale, scanning to the Os(II) oxidation state caused new peaks to appear near the cis-alpha Os(III/II) and Os(IV/III) couples. No change was observed in the CV upon reduction to Os(III), but after reduction to Os(II) the CV in Figure 4.13B was obtained. The Os(III/II) and Os(IV/III) couples had shifted substantially positive, the Os(V/IV) couple had shifted slightly negative and the cis-alpha couples were no longer visible. Surprisingly,

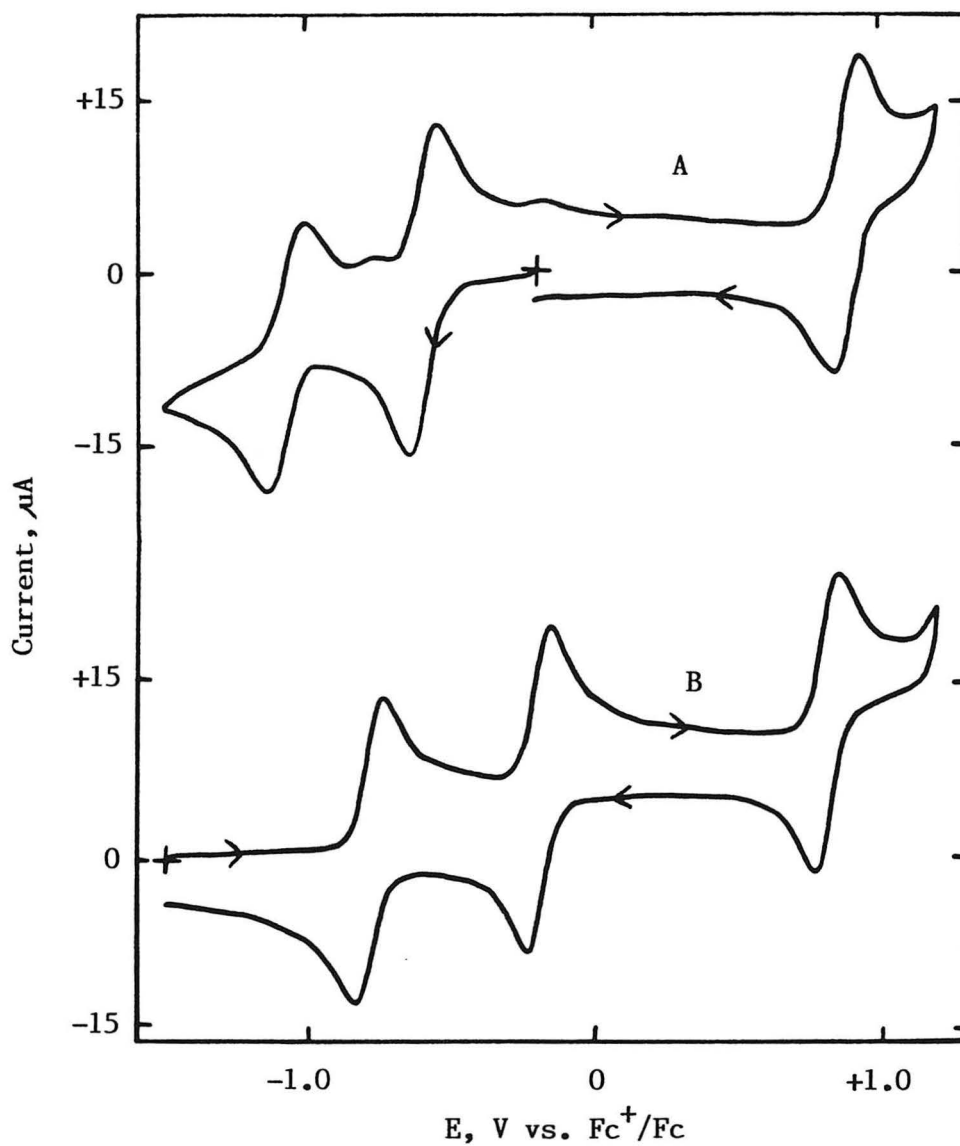


Figure 4.13. Cyclic voltammograms of 1.2 mM $\text{Os}(\text{CHBA-DCB})(\text{t-BuNC})_2$ in CH_2Cl_2 , 0.1 M TBAP at 0.03 cm^2 Pt electrode, before and after reduction to Os(II). Scan rate = 200 mV/sec. A = Os(IV) B = Os(II)

reoxidation of this solution to Os(IV) did not restore the cis-alpha CV. The solution obtained by reoxidation was green, whereas the cis-alpha Os(IV) compound was purple, and the same couples seen at Os(II) were still present in the CV. Isolation of the new Os(IV) compound was easily accomplished by recrystallization. NMR and IR spectra showed it to be the cis-beta isomer of $\text{Os}(\text{CHBA-DCB})(\text{t-BuNC})_2$ (see Figure 4.3). The cis-beta compound did revert with some decomposition to cis-alpha in refluxing xylene, indicating that the cis-beta isomer is kinetically but not thermodynamically stable at Os(IV) [3].

The isomerization of $\text{Os}(\text{CHBA-DCB})(\text{t-BuNC})_2$ from cis-alpha to cis-beta upon reduction to Os(II) is in agreement with the proposal that more electron-rich metal centers favor more planar coordination of the tetradentate tetraanionic ligands. In this case, the isomerization probably did not proceed completely to the trans isomer because this would place the two electron-withdrawing t-butylisocyanide ligands trans to each other. Therefore the complex isomerized to the cis-beta isomer where one of the amide groups is planar and so is less electron-donating, but the isocyanides are still cis.

Neither $\text{Os}(\text{HBA-B})(\text{Ph}_3\text{P})(\text{t-BuNC})$ nor $\text{Os}(\text{HBA-B})(\text{Ph}_3\text{P})(\text{CO})$ isomerized on reduction to Os(III) and both decomposed on reduction to Os(II). $\text{Os}(\text{CHBA-DCB})(\text{Ph}_3\text{P})(\text{t-BuNC})$ also decomposed on reduction to Os(II), but it very slowly isomerized at Os(III). Over a period of three or four hours after the electrolysis was completed, the cis-alpha Os(III/II) and Os(IV/III) couples in the CV were seen to decrease as new couples grew in a few hundred millivolts positive of them. Little change was seen in the Os(V/IV) couple, presumably because both isomers had very similar formal potentials. After the isomerization had proceeded to completion or nearly

so, the solution was reoxidized to Os(IV). During the electrolysis (about 40 minutes) about 40% of the material in solution reisolomerized to the cis-alpha isomer as judged by the CV of the solution. However, no further isomerization took place after the electrolysis over a period of up to two weeks. Thin layer chromatography confirmed the CV results, showing a purple spot for the cis-alpha isomer and a green spot for the new isomer. The green color and the similarity of the shifts in the formal potentials to those of Os(CHBA-DCB)(t-BuNC)₂ strongly suggest that the new isomer is cis-beta-Os(CHBA-DCB)(Ph₃P)(t-BuNC). The reason for the partial isomerization back to cis-alpha on reoxidation to Os(IV) is not fully understood, but may involve a redox-catalyzed isomerization similar to that observed with the bis-(pyridine) compounds (vide supra).

An interesting pattern was observed in the formal potentials of the cis-beta compounds formed by reduction of the cis-alpha compounds. The formal potentials of the Os(III/II) and Os(IV/III) couples shifted positive on isomerization from cis-alpha to cis-beta, as would be expected. However, the Os(V/IV) couple of Os(CHBA-DCB)(Ph₃P)(t-BuNC) shifted only very slightly positive, about 10 mV, and the Os(V/IV) couple of Os(CHBA-DCB)(t-BuNC)₂ actually shifted 90 mV negative. The formal potentials for these compounds and two others displaying cis-beta and cis-alpha and/or trans isomers are listed in Table 4.7. Table 4.8 presents the potential differences between the different isomers of the CHBA-DCB compounds so far studied.

The differences in formal potentials between the trans and cis-alpha isomers are very consistent. The Os(V/IV) and Os(III/II) couples differ by about 200 mV and the Os(IV/III) couples differ by 400-500 mV. The cis-beta structure is intermediate between the trans and cis-alpha

Table 4.7. Formal potentials of CHBA-DCB complexes displaying cis-beta isomers.

Compound	Formal Potential, V ^a		
	Os(III/II)	Os(IV/III)	Os(V/IV)
Os(CHBA-DCB)(Cl-Py) ₂			
trans	-1.59	-0.39	+0.74
cis-beta	^b	-0.48	+0.60
cis-alpha	-1.81	-0.89	+0.58
Os(CHBA-DCB)(bipy)			
cis-beta	-1.37	-0.49	+0.50
cis-alpha	-1.45	-0.86	+0.49
Os(CHBA-DCB)(Ph ₃ P)(<u>t</u> -BuNC)			
cis-beta	-1.08	-0.30	+0.75
cis-alpha	-1.25	-0.64	+0.74
Os(CHBA-DCB)(<u>t</u> -BuNC) ₂			
cis-beta	-0.77	-0.18	+0.83
cis-alpha	-1.05	-0.57	+0.92

^a Measured in CH₂Cl₂/0.1 M TBAP and referenced to Fc⁺/Fc internal standard.

^b Not observed.

Table 4.8. Formal potential differences between isomeric osmium complexes containing the CHBA-DCB ligand.

Isomers of Os(CHBA-DCB)(L) ₂ L ₂ =	Potential Difference, mV ^a		
	Os(III/II)	Os(IV/III)	Os(V/IV)
E _f (trans) - E _f (cis-alpha)			
(4-Acetylpyridine) ₂	+160	+510	+170
(4-Chloropyridine) ₂	+220	+500	+160
(4-Bromopyridine) ₂	b	+510	+170
(Pyridine) ₂	+210	+480	+180
(4-Methylpyridine) ₂	+210	+470	+210
(4-Ethylpyridine) ₂	+220	+460	+200
(4- <i>t</i> -Butylpyridine) ₂	+230	+460	+200
(3,4-Dimethylpyridine) ₂	+230	+450	+210
(Ph ₃ P=O) ₂	b	+300	+280
Average	+211	+460	+198
E _f (cis-beta) - E _f (cis-alpha)			
(4-Chloropyridine) ₂	b	+410	+20
(bipy)	+80	+370	+10
(Ph ₃ P)(<i>t</i> -BuNC)	+170	+340	+10
(<i>t</i> -BuNC) ₂	+280	+390	-90
Average	+177	+378	-12
E _f (trans) - E _f (cis-beta)			
(4-Chloropyridine) ₂	b	+90	+140

^aDifferences in formal potentials calculated from data in Tables 4.4, 4.6 and 4.7. ^bData not available.

structures in that the cis-beta compounds have one phenoxide arm of the CHBA-DCB ligand out of the plane of the osmium and amide nitrogens while the trans and cis-alpha isomers have no, and two, phenoxide arms out of the plane, respectively. This does not imply that isomerization from trans to cis-alpha must pass through the cis-beta isomer. However, because of the expected intermediate donor properties of the ligand in cis-beta isomers, one might expect the potential changes between cis-alpha and cis-beta isomers to be intermediate between those of cis-alpha and trans isomers. This is not the case. The average potential difference between the cis-alpha and cis-beta isomers is nearly the same for the Os(IV/III) and Os(III/II) couples (280 and 390 mV, respectively) as between the cis-alpha and trans isomers. The average potential difference for the Os(V/IV) couple, however, is negligible (-12 mV) between cis-alpha and cis-beta isomers. For the only compound displaying all three isomers, Os(CHBA-DCB)(Cl-Py)₂, these trends are in agreement with the observed formal potentials. The Os(III/II) formal potentials cannot be compared because the cis-beta couple could not be observed, but for the Os(IV/III) couple the largest change, 410 mV, occurs between the cis-alpha and cis-beta isomers, while between cis-beta and trans only a 90 mV difference is observed. For the Os(V/IV) couple the largest potential difference, 140 mV, occurs between the cis-beta and trans isomers, and only a 20 mV change is observed between the cis-alpha and cis-beta isomers.

A possible explanation for the observed formal potential differences between the trans, cis-alpha and cis-beta isomers can be found in the proposed molecular orbital diagrams shown in Figure 4.14. The diagram for the trans isomer was constructed by assigning the x- and y-axes to the two amide nitrogen-osmium-phenoxide oxygen axes, so that the z-axis contains

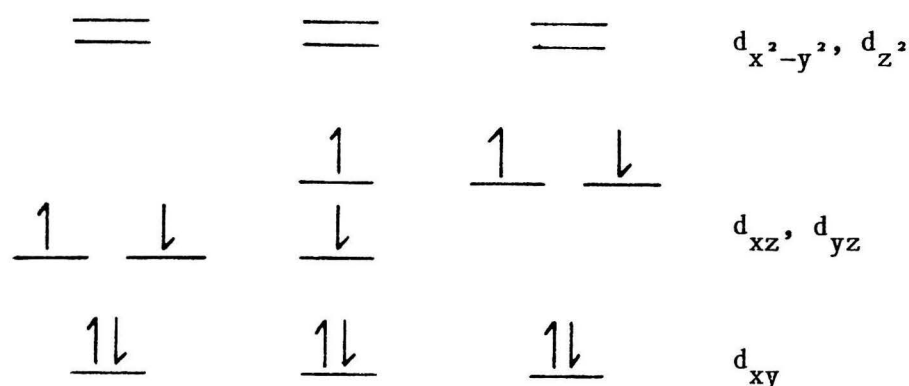


Figure 4.14. Proposed molecular orbital diagrams for $\text{Os}(\text{CHBA-DCB})(\text{Py})_2$

the trans axial ligands. For pyridine-type axial ligands the ordering will be as shown, with the d_{xy} orbital lowest, followed by the degenerate pi-bonding d_{xz} and d_{yz} orbitals, and the d_{z^2} and $d_{x^2-y^2}$ orbitals at high energy. The principal change occurring upon isomerization to the cis-beta isomer is an increase in the interaction of one of the amide nitrogen lone pairs with one of the pi-bonding d-orbitals, splitting their degeneracy and pushing one of them to higher energy. Upon isomerization to the cis-alpha isomer the other pi-bonding d-orbital is also raised in energy and so the two orbitals are once again degenerate.

The orbitals in Figure 4.14 are drawn for the d^4 Os(IV) oxidation state. Based on the approximate ordering indicated and assuming the intermediate spin state with two unpaired electrons, it is reasonable that oxidation of the cis-beta isomer should be easier than the trans isomer and about as easy as the cis-alpha isomer, since oxidation involves removal of an electron from the HOMO. Likewise, reduction of the trans isomer should be about as easy as the cis-beta isomer, and reduction of the cis-beta isomer should be easier than the cis-alpha isomer, since

reduction involves adding an electron to the lowest available orbital.

This explanation is in no way quantitative and makes no effort to explain any differences in the Os(III/II) formal potentials, but it does provide a reasonable explanation for much of the observed behavior. A more detailed explanation is beyond the scope of this project.

Conclusions

The intentional replacement of the oxidatively sensitive ethane bridge of the CHBA-Et ligand with a dichlorobenzene bridge in CHBA-DCB or a benzene bridge in HBA-B eliminated the oxidative ligand degradation reactions previously observed with $\text{Os}(\text{CHBA-Et})(\text{Py})_2$. Complexes containing osmium, CHBA-DCB or HBA-B and a variety of monodentate ligands have been synthesized and shown to form stable Os(V) species. Not only are these new ligands stable when coordinated to highly oxidizing metal centers, but they are also capable of substantially decreasing the formal potentials of their osmium complexes, indicating a stabilization of the higher oxidation state. For example, the formal potential of trans- $\text{Os}(\text{CHBA-DCB})(\text{Ph}_3\text{P})_2$ is at least 750 mV lower than that of trans- $\text{OsCl}_4(\text{Ph}_3\text{P})_2$.

The controlled potential oxidation of complexes containing the CHBA-DCB ligand produces stable Os(V) compounds, but a number of the complexes undergo a reversible isomerization from the trans to the cis- α isomer upon oxidation. For a series of bis-(4-substituted-pyridine) complexes, the equilibrium constant for isomerization at Os(V) correlates qualitatively with the electron-donating ability of the pyridine ligands. This result points to electronic control of the isomerization. It is believed that the decrease in electron density at the metal center upon oxidation causes the tetradentate tetraanionic ligand to adopt a nonplanar conformation where it is more electron-donating. The increase in electron donation by the CHBA-DCB ligand is effected by reducing the amide delocalization upon isomerization, thus making the amide nitrogen lone pair more fully available for donation to the metal center.

Cis- α isomers of CHBA-DCB and HBA-B complexes can also be formed by coordination of electron-withdrawing ligands to Os(IV) complexes. The electron-withdrawing t-butylisocyanide and CO ligands decrease the electron density on the metal center just as oxidation to Os(V) does. The ligand then adopts the cis- α conformation in which it can donate more electron density to the electron-deficient metal center. Increasing the electron density on the metal center by reduction of the complexes to Os(III) or Os(II) triggers an isomerization to the more planar cis- β isomer, in agreement with the proposal that more electron-rich metal centers should favor more planar coordination of the tetradentate tetraanionic ligands.

The work with complexes of the CHBA-DCB and HBA-B ligands has provided more valuable information about the design of new ligands for coordination to high oxidation state metal centers. The aromatic bridges are inert to oxidative degradation reactions, but do make available alternate electronic structures which can affect the formal oxidation state assignment of the metal. Therefore, it seems desirable to eliminate in the future the aromatic groups responsible for this uncertainty. The discovery of the isomerization reactions revealed an unexpected design feature. Ligands of this type for which stabilization of a high oxidation state metal center is the main objective should incorporate the flexibility to assume the most stable isomer. However, if the objective is highly oxidizing complexes, the ligand should be designed so as to lock in the desired geometry and maintain high oxidation potentials.

Experimental

Materials

Reagent grade methylene chloride (MCB or Mallinckrodt) was further purified by passing it over a short column of activated alumina (Woelm N. Akt. I). For controlled potential electrolysis experiments the CH_2Cl_2 was dried over CaH_2 , degassed and vacuum transferred into the cell. All other solvents were reagent grade (Aldrich, Baker, Mallinckrodt, MCB or USI) and were used as received. Tetra-n-butylammonium perchlorate supporting electrolyte (Southwestern Analytical Chemicals) was dried, recrystallized twice from acetone/ether, and then dried under vacuum. Ferrocene (Aldrich) was used as received. Tetrabutylammonium hexachloroosmate was prepared by reaction of ammonium hexachloroosmate (Aesar) and tetrabutylammonium bromide (Eastman Kodak) in water followed by recrystallization from acetone/water. Trans- $\text{OsCl}_4(\text{Ph}_3\text{P})_2$ was supplied by Brian Treco.

All osmium compounds containing the CHBA-DCB and HBA-B ligands were prepared by John Keech and Geoffrey Peake, respectively. Details of their synthesis and characterization can be found in the appropriate references [1-3,7].

Apparatus and Procedures

Cyclic voltammetry was performed with a Princeton Applied Research (PAR) Model 173 potentiostat driven by a PAR Model 175 universal programmer using positive feedback IR-compensation. Current-voltage curves were recorded on a Houston Instruments Model 2000 X-Y recorder. Standard two-compartment electrochemical cells were used. When necessary, solutions were purged with argon to remove oxygen. The working electrode was a 0.17 cm^2 basal plane pyrolytic graphite (BPG, Union Carbide Co.)

disc mounted in a glass tube with heat-shrinkable tubing or a 0.03 cm^2 platinum disc sealed in glass. The behavior and formal potentials of the osmium compounds were not dependent upon the electrode used. The counter electrode was a platinum wire. Various reference electrodes were used, including SSCE, Ag/AgCl and a silver wire quasi-reference electrode. For each compound studied at least one experiment was performed in the presence of ferrocene as an internal potential standard. The formal potentials of all of the couples of the osmium compounds were then referenced to that of the ferrocene, which was consistently measured as +0.48 V vs. aqueous SCE. Formal potentials of reversible couples were taken as the average of the anodic and cathodic peak potentials. The supporting electrolyte was 0.1 M TBAP.

Controlled potential electrolysis experiments were performed with the PAR Model 173 potentiostat equipped with a Model 179 digital coulometer using positive feedback IR-compensation. The electrolyses were performed in a three-compartment cell to be described in Chapter V. Before each electrolysis the cell was loaded with supporting electrolyte and the osmium compound and placed on a vacuum line to dry overnight. The cell was then cooled to $-78\text{ }^{\circ}\text{C}$ in a dry ice/isopropanol bath and the dried, degassed CH_2Cl_2 was vacuum transferred in to a predetermined level known to correspond to 15 ml in the working compartment. The working and counter electrodes were platinum gauzes, the CV electrode was a 0.03 cm^2 platinum disc and the reference electrode was a silver wire located in a separate compartment and separated from the working solution by a glass frit. The solution was stirred magnetically with a teflon-coated stirring bar. All experiments were performed at room temperature, $22 \pm 2^{\circ}\text{C}$.

Normal pulse voltammetry was performed on the oxidized solutions using a Bioanalytical Systems, Inc., BAS-100 Electrochemical Analyzer. The parameters used were a pulse period of 400 ms, a pulse width of 50 ms, a sample width of 17 ms and a scan rate of 20 mV/sec. Changing the parameters to a pulse period of 5000 ms and a scan rate of 4 mV/sec had no effect on the measured equilibrium constant, which was taken to be equal to the ratio of wave heights of the two Os(IV/III) reductions.

Column chromatography at low temperature was performed on a 25 cm jacketed column packed with 32-63 micron silica gel (Woelm). The coolant was methanol, cooled first in a Neslab RTE-4 cooling bath/circulator to about -35 °C. The methanol was then circulated through copper cooling coils immersed in a dry ice/isopropanol bath and from there to the column. The temperature measured inside the column was about -65 °C. The solution containing the two isomers was loaded onto the column with a precooled syringe and the isomers were eluted with precooled solvent (1% THF in CH₂Cl₂) and collected in flasks immersed in dry ice/isopropanol baths. The solvents were removed under vacuum.

References and Notes

1. F.C. Anson, J.A. Christie, T.J. Collins, R.J. Coots, T.T. Furutani, S.L. Gipson, J.T. Keech, T.E. Krafft, B.D. Santarsiero and G.H. Spies J. Am. Chem. Soc., **106**, 4460-4472 (1984).
2. F.C. Anson, T.J. Collins, R.J. Coots, T.T. Furutani, S.L. Gipson, J.T. Keech, T. Lai, S.C. Lee, G.T. Peake and T.G. Richmond, manuscript in preparation.
3. John T. Keech, unpublished results. All syntheses and characterizations of compounds containing the CHBA-DCB ligand were performed by John Keech.
4. Ligand names are: 1,2-bis(3,5-dichloro-2-hydroxybenzamido)ethane, $H_4CHBA-Et$; 1,2-bis(3,5-dichloro-2-hydroxybenzamido)-4,5-dichlorobenzene, $H_4CHBA-DCB$; 1,2-bis(2-hydroxybenzamido)benzene, H_4HBA-B .
5. For leading references see: K. Dehnicke, U. Muller and R. Weber, Inorg. Chem., **23**, 2563-2564 (1984).
6. $OsCl_4(Ph_3P)_2$ supplied by Brian Treco.
7. Geoffrey T. Peake, unpublished results. All syntheses and characterizations of compounds containing the HBA-B ligand were performed by Geoffrey Peake.
8. For leading references see: J.G. Gaudiello, T.C. Wright, R.A. Jones and A.J. Bard, J. Am. Chem. Soc., **107**, 888-897 (1985).
9. Except where noted, in all compounds reported in this work the potentially tetradentate tetraanionic ligands CHBA-DCB and HBA-B are coordinated as such.
10. A.M. Sargeson and G.H. Searle, Inorg. Chem., **4**, 45-52 (1965).
11. Formal potentials are calculated as the average of the anodic and cathodic peak potentials determined by cyclic voltammetry. All potentials are referenced to the formal potential of a ferrocene internal standard, the potential of which in $CH_2Cl_2/0.1$ M TBAP has been consistently measured as +0.48 V vs aqueous SCE.
12. A.J. Bard and Faulkner, Electrochemical Methods, Fundamentals and Applications, John Wiley and Sons: New York, 1980, pp. 452-453.
13. H. Sigel and R.B. Martin, Chem. Rev., **82**, 385-426 (1982).
14. (a) D.W. Margerum, Pure Appl. Chem., **55**, 23-34 (1983). (b) L.L. Diaddario, W.R. Robinson and D.W. Margerum, Inorg. Chem., **22**, 1021-1025.
15. E. Kimura, A. Sakonaka, R. Machila and M. Kodama, J. Am. Chem. Soc., **104**, 4255-4257 (1982).

16. (a) A. Buttafava, L. Fabbrizzi, A. Perotti and B. Seghi, J. Chem. Soc., Chem. Commun., 1982, 1166-1167. (b) L. Fabbrizzi, A. Perotti and A. Poggi, Inorg. Chem., 22, 1411-1412 (1983).
17. Bard and Faulkner, pp. 186-199.
18. J. March, Advanced Organic Chemistry, McGraw-Hill: New York, 1977, pp. 251-254.

CHAPTER V

Investigation of the Electrochemistry of Osmium Complexes Containing
Multianionic Chelating Ligands in Liquid Sulfur Dioxide

Introduction

It was reported in Chapter IV that osmium complexes containing the CHBA-DCB ligand [1] could be oxidized to stable Os(V) species. That work demonstrated the ligand's oxidative stability and powerful stabilization of high oxidation state metal centers. The question naturally arose as to whether even higher oxidation states were accessible with these complexes. However, within the range of potentials easily accessible in methylene chloride, to about +1.4 V vs. Fc^+/Fc , no anodic activity past the Os(V/IV) couple could be observed for complexes such as $\text{Os}(\text{CHBA-DCB})(\text{Py})_2$ or $\text{Os}(\text{CHBA-DCB})(\text{Ph}_3\text{P})_2$. Recent reports in the literature from the group of Allen Bard [2-7] have detailed the large anodic range available for electrochemistry in liquid sulfur dioxide. It was therefore decided to examine the electrochemistry of our osmium compounds in this novel solvent in search of very highly oxidized species.

Liquid sulfur dioxide has some very desirable properties as a solvent for electrochemistry. It is an aprotic, dipolar solvent (dielectric constant of 24.6 at -69°C) with a wide liquid range of -75 to -10°C [8]. Sulfur dioxide can be obtained in very high purity and is easy to further purify by vacuum line techniques. Many organic compounds, especially those containing aromatic groups, are soluble in SO_2 , but saturated aliphatics are generally not soluble. Ionic compounds, except alkali salts of iodide or thiocyanate, have poor solubility in SO_2 , but tetraalkylammonium salts are soluble enough for use as supporting electrolytes. The low temperature, high purity and low nucleophilicity of SO_2 make it very suitable for studying potentially reactive highly oxidized species.

Very little electrochemistry was done in liquid SO_2 until the 1970's. Early work was hampered by the lack of a good supporting electrolyte and a stable reference electrode [9]. In 1970, Miller and Mayeda [10] reported that the use of tetraalkylammonium salts as supporting electrolytes in SO_2 gave reasonable conductivities and that 9,10-diphenylanthracene could be oxidized reversibly in SO_2 to a stable cation radical. Launay and Castellonese [11,12] have performed anodic halogenations with trityl and tetraalkylammonium halides in SO_2 . Lacaze et. al have used AlCl_3 as both a drying agent and supporting electrolyte in SO_2 and have studied the oxidation of aromatics [13-15]. The oxidation of mercury in SO_2 to produce Hg_3AsF_6 and Hg_3SbF_6 has also been studied [16].

The pioneering work in the use of liquid SO_2 as an electrochemical solvent for working at very highly oxidizing potentials has been done by Professor Allen Bard and his coworkers. In 1979 this group first reported the oxidation of thianthrene, phenothiazine and 9,10-diphenylanthracene in SO_2 [2]. With tetrabutylammonium perchlorate as supporting electrolyte they observed an anodic limit in SO_2 of about +3.4 V vs. SCE, and within this limit each compound studied could be reversibly oxidized to its radical cation and dication. The oxidation of thianthrene in the presence of water and anisole was also studied [3]. Bard et al. then began reporting work in SO_2 with inorganic complexes. The complexes $\text{Ru}(\text{bipy})_3^{2+}$ and $\text{Fe}(\text{bipy})_3^{2+}$ were studied in SO_2 with tetrabutylammonium BF_4^- and PF_6^- as supporting electrolytes [4]. The use of the BF_4^- and PF_6^- anions extended the anodic range to +4 V vs. SCE or about +3.5 V vs. Fc^+/Fc . Highly oxidized forms of ferrocene, decamethylferrocene, iron bis-(tris-(1-pyrazolyl)borate) [5], bipyridine and phenanthroline

complexes of osmium, ruthenium and iron [6], and copper tetrakis-(pyridine-N-oxide) [7] have all been produced in SO_2 .

The reported successes of the Bard group with highly oxidized transition metal complexes in liquid SO_2 led us to investigate the electrochemistry of the osmium CHBA-DCB complexes in SO_2 . Additional oxidations were found just beyond the range of potentials accessible in CH_2Cl_2 . $\text{Os}(\text{CHBA-DCB})(\text{Py})_2$ and $\text{Os}(\text{CHBA-DCB})(\text{Ph}_3\text{P})_2$ both displayed two reversible oxidations in addition to their $\text{Os}(\text{V/IV})$ couples. However, these oxidations produce compounds of only marginal stability and their potentials are identical for the two compounds investigated. These observations led to the suspicion that these oxidations are ligand-localized and do not represent true $\text{Os}(\text{VI/V})$ and $\text{Os}(\text{VII/VI})$ couples. If these oxidations are ligand-localized, then new ligands will have to be designed in order to enable the production of even higher oxidation state and/or more highly oxidizing complexes.

Liquid SO_2 is also a very useful solvent for investigating the electrochemistry of reactive compounds. The oxidation of $\text{Os}(\text{CHBA-Et})(\text{Py})_2$ is irreversible in CH_2Cl_2 because of oxidative degradation of the CHBA-Et ligand. However, in SO_2 this complex displays two reversible oxidations on the CV time scale. Likewise, the other complexes encountered in the oxidative degradation of $\text{Os}(\text{CHBA-Et})(\text{Py})_2$ display additional reversible electrochemistry in SO_2 .

Results and Discussion

Electrochemistry of osmium CHBA-DCB complexes in SO₂

Osmium(IV) complexes containing the CHBA-DCB ligand [1,17] and two monodentate ligands such as pyridine or triphenylphosphine displayed two reversible reductions and one reversible oxidation in CH₂Cl₂ (see Chapter IV). The low Os(V/IV) formal potentials and the stability of the Os(V) forms of these complexes demonstrated the powerful stabilizing ability and inertness to oxidative degradation reactions of the CHBA-DCB ligand. It was desirable to probe the limits of the oxidative stability of the CHBA-DCB ligand by producing even more highly oxidizing complexes. However, within the range of potentials easily accessible in CH₂Cl₂, to about +1.4 V vs. Fc⁺/Fc, no anodic activity past the Os(V/IV) couples could be observed. Therefore, it was decided to examine the electrochemistry of the CHBA-DCB complexes in liquid SO₂ which has an anodic range to about +3.5 V vs. Fc⁺/Fc.

Before electrochemical studies were attempted, the solubility of the CHBA-DCB complexes in SO₂ was examined. It was found that Os(CHBA-DCB)(Py)₂ and Os(CHBA-DCB)(Ph₃P)₂ were reasonably soluble, but that Os(CHBA-DCB)(t-Bupy)₂ was quite insoluble. These solubilities agree with reports that aromatic compounds are soluble in SO₂ but saturated aliphatics are not. During later work some problems did develop. Occasionally an Os(IV) compound would dissolve, but later would suddenly precipitate and could not be redissolved by stirring, warming or cooling. These incidents were unpredictable and it is not known what factors caused the precipitation.

Figure 5.1 shows the cyclic voltammogram, CV, of Os(CHBA-DCB)(Ph₃P)₂ in SO₂. The Os(IV/III) couple is seen at E_f = -0.14 V vs. Fc⁺/Fc [18] and

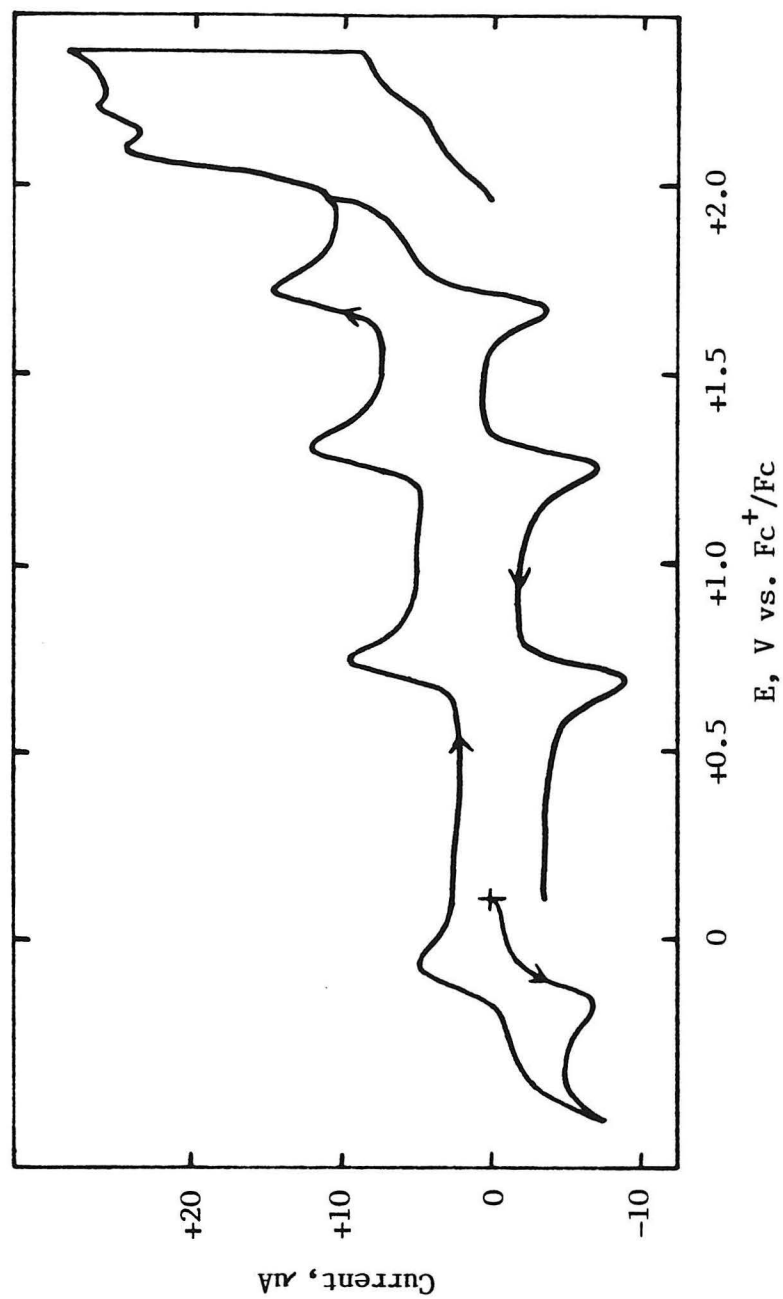


Figure 5.1. Cyclic voltammogram of 1 mM $\text{Os}(\text{CHBA-DCB})(\text{Ph}_3\text{P})_2$ in SO_2 , 0.1 M TBABF_4 at -60°C at 0.03 cm^2 Pt electrode. Scan rate = 200 mV/sec .

three reversible oxidations are seen at +0.72, +1.29 and +1.71 V. Following the third reversible oxidation, irreversible anodic activity begins. An almost identical CV was obtained with $\text{Os}(\text{CHBA-DCB})(\text{Py})_2$. The only other osmium CHBA-DCB complex examined in SO_2 was $\text{Os}(\text{CHBA-DCB})(\text{t-BuNC})_2$. The second and third oxidations of this complex were not completely reversible. The formal potentials of the CHBA-DCB complexes examined in SO_2 are summarized in Table 5.1.

Table 5.1. Formal potentials of osmium CHBA-DCB complexes in SO_2 .

$\text{Os}(\text{CHBA-DCB})\text{L}_2$ L=	Formal Potential, V ^a				
	Os(IV/III)	Os(V/IV)	2+/1+	3+/2+	4+/3+ ^b
Py^c	-0.15	+0.82	+1.29	+1.69	(+2.12)
Ph_3P^c	-0.14	+0.72	+1.29	+1.71	(+2.16)
t-BuNC^d	-0.30	+0.98	+1.48 ^e	+1.70 ^e	(+2.20)

^aFormal potential measured in $\text{SO}_2/0.1 \text{ M TBABF}_4$ and referenced to Fc^+/Fc internal standard. ^bPeak potential of irreversible oxidation. ^cTrans isomer. ^dCis-alpha isomer. ^eOxidations not completely reversible.

It is interesting to compare the formal potentials measured in SO_2 with those in CH_2Cl_2 (see Table 4.1). All of the Os(IV/III) couples are shifted about 300 mV positive, while the Os(V/IV) couples are shifted about 100 mV positive. The large positive shifts of the Os(IV/III) couples may arise from a strong solvation of the anionic Os(III) species by SO_2 . It has been reported that SO_2 does not solvate cations but interacts strongly with nucleophiles and donor molecules [3]. The reason for the shift of the Os(V/IV) formal potentials is not known.

The large variation in formal potential for the oxidation of the osmium CHBA-DCB complexes in CH_2Cl_2 with changes in the monodentate

ligands was cited as evidence for involvement of the metal in the oxidation. A more limited variety of compounds was examined in SO_2 , but some tentative conclusions can be drawn from the available data. The Os(V/IV) formal potentials vary with monodentate ligands in the same way and with the same magnitude as in CH_2Cl_2 . However, the other oxidations show very little variation with monodentate ligand. Note in particular that the second, third and fourth oxidations of $\text{Os}(\text{CHBA-DCB})(\text{Py})_2$ and $\text{Os}(\text{CHBA-DCB})(\text{Ph}_3\text{P})_2$, which are both trans isomers, occur at essentially identical potentials. The potentials for $\text{Os}(\text{CHBA-DCB})(\text{t-BuNC})_2$, a cis-alpha isomer, are less certain due to the second and third oxidations being less than reversible, but the potentials for its third and fourth oxidations are almost identical to those of the other two CHBA-DCB complexes. This independence of the potentials for the second, third and fourth oxidations of the CHBA-DCB complexes with varying monodentate ligands strongly suggests that these oxidations are ligand-localized and do not represent Os(VI/V), Os(VII/VI) and Os(VIII/VII) couples.

The observation of ligand-localized oxidations with CHBA-DCB complexes will have an impact on future ligand designs. If the oxidations are ligand-localized, then it seems likely that they occur at one or more of the aromatic rings. Therefore, future ligands for use with extremely oxidizing complexes may need to be totally aliphatic in nature. Since it has already been shown that methylene groups on such ligands are oxidatively sensitive, the new ligands may have to be fluorinated, methylated or in some other way protected. Work is currently under way to produce new ligands and complexes without aromatic groups [19].

The stability of the second and third oxidation products of the CHBA-DCB complexes was investigated by controlled potential electrolysis

experiments. As would be expected, the first oxidation products of both $\text{Os}(\text{CHBA-DCB})(\text{Py})_2$ and $\text{Os}(\text{CHBA-DCB})(\text{Ph}_3\text{P})_2$ were quite stable, although occasionally some minor impurity peaks could be seen in the CV's after the electrolyses. For $\text{Os}(\text{CHBA-DCB})(\text{Py})_2$ the second oxidation product was stable in solution or as a solid under vacuum at -40°C , but on warming the solid to room temperature it quickly decomposed to a brown product with no reversible electrochemistry. The third oxidation product decomposed slowly in solution at -40°C . The second and third oxidation products of $\text{Os}(\text{CHBA-DCB})(\text{Ph}_3\text{P})_2$ were significantly less stable than those of the bis(pyridine) complex. Several attempts were made to isolate $\text{Os}^{\text{V}}(\text{CHBA-DCB})(\text{Py})_2^+$ produced in SO_2 by precipitating it with benzene or chlorobenzene. None of the attempts were successful, although one experiment with chlorobenzene did lead to the isolation of a tiny amount of a solid which produced a purple CH_2Cl_2 solution and so was probably the desired compound.

It was reported in Chapter IV that oxidation of $\text{Os}(\text{CHBA-DCB})(\text{Py})_2$ caused a reversible isomerization from the trans to the cis-alpha isomer, with the cis-alpha isomer displaying formal potentials several hundred millivolts negative of the trans isomer. This type of isomerization was never observed in SO_2 , presumably because of the low temperature. In order to see if any isomerization could be observed on cycling to the more highly oxidized species, CV's of $\text{Os}(\text{CHBA-DCB})(\text{Py})_2$ were examined in SO_2 at room temperature. The vapor pressure of SO_2 at 20°C is 3.23 atm [8] so it was felt that the experiment could be done in the smaller of the cells used if all of the joints were secured. This procedure worked reasonably well and the resulting CV's are shown in Figure 5.2. At 500 mV/sec scan rate the first two oxidations appeared normal, except that a small new

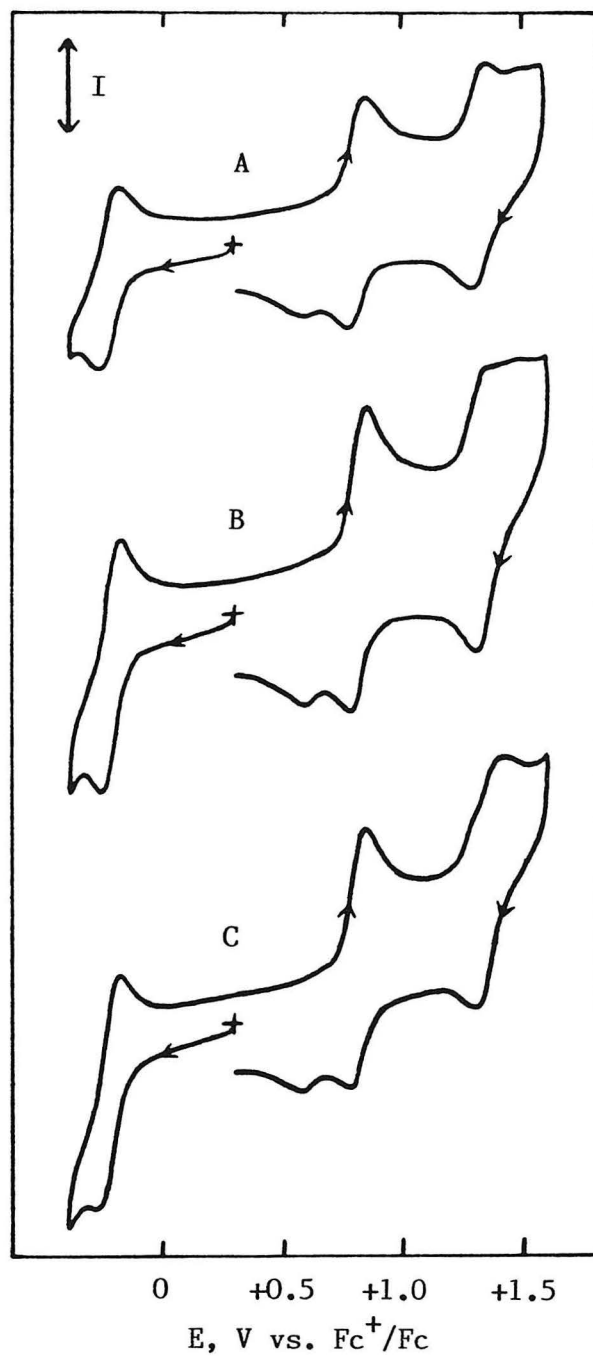


Figure 5.2. Cyclic voltammograms of 2 mM $\text{Os}(\text{CHBA-DCB})(\text{Py})_2$ in SO_2 , 0.1 M TBABF_4 at +22 °C at 0.32 cm^2 glassy carbon electrode. Scan rate, I: A = 500 mV/sec, 100 μA ; B = 200 mV/sec, 40 μA ; C = 50 mV/sec, 10 μA .

peak could be seen about 200 mV negative of the Os(V/IV) cathodic peak. This new peak is probably the Os(V/IV) reduction of the cis- α isomer. It does not appear in SO₂ or CH₂Cl₂ after scanning only over the first oxidation. As the scan rate was slowed, the second oxidation's anodic peak began to flatten. Then at very slow scan rates a new anodic peak for the second oxidation appeared about 50 mV positive of the original peak. The other features of the CV did not appear to change at the lower scan rates. These results indicate that isomerization at the second oxidation product is much faster than at Os(V), but the potential shift with decreasing scan rate is not explainable.

Electrochemistry of Os(HBA-B)(Ph₃P)(CO) in SO₂

The only osmium complex containing the HBA-B ligand to be examined in SO₂ was Os(HBA-B)(Ph₃P)(CO) [1]. This complex displayed a reversible oxidation in CH₂Cl₂ at +0.90 V. It was decided to examine the complex's electrochemistry in SO₂ to see if further reversible oxidations could be observed and to see if the one-electron oxidized product, formally an osmium(V) carbonyl, were stable. The CV in SO₂ showed the expected Os(IV/III) and Os(V/IV) couples, but all other anodic electrochemistry was irreversible. In addition, after several scans to high potentials the peak currents of the Os(V/IV) couple were observed to increase substantially, suggesting that the electrode might have been covered with an electroactive polymer. When the electrode was removed from the SO₂ cell and examined in acetonitrile it displayed a reversible reduction and a reversible oxidation at about the same potentials as Os(HBA-B)(Ph₃P)(CO). It appears that the complex polymerized on the electrode surface, a reaction made possible by the lack of chlorine substituents on the HBA-B ligand's aromatic rings. Subsequent oxidation

of the $\text{Os}(\text{HBA-B})(\text{Ph}_3\text{P})(\text{CO})$ solution in SO_2 consumed at least 1.2 F/mol of Os and the current never reached a background value, indicating that the Os(V) form of the complex is not stable even in SO_2 at -40°C .

Electrochemistry of $\text{Os}(\text{CHBA-Et})(\text{Py})_2$ and its derivatives in SO_2

In addition to providing a large anodic range for the examination of highly oxidizing species, SO_2 is an excellent solvent for examining the electrochemistry of reactive species formed at more moderate potentials because of its low temperature, high purity and low nucleophilicity. For example, the oxidation of $\text{Os}(\text{CHBA-Et})(\text{Py})_2$, 5, [1] in CH_2Cl_2 is totally irreversible because of oxidative degradation reactions which occur at the ethane bridge of the CHBA-Et ligand. In SO_2 the CV shown in Figure 5.3 was obtained. Not only was the first oxidation reversible, but a second reversible oxidation could be seen on the CV time scale. A third oxidation was only partially reversible and further anodic activity was irreversible. None of the oxidized forms was stable on the controlled potential electrolysis time scale. The formal potentials for the three oxidations are +0.86, +1.37 and +2.01 V. Note that the formal potential of the first oxidation, the Os(V/IV) couple, is only 40 mV higher than that of the Os(V/IV) couple of $\text{Os}(\text{CHBA-DCB})(\text{Py})_2$. This similarity of potentials suggests that alternate electronic structures of the CHBA-DCB ligand, which do not exist for the CHBA-Et ligand, do not contribute to the structure of $\text{Os}(\text{CHBA-DCB})(\text{Py})_2^+$, so the oxidation is a true Os(V/IV) couple (see Chapter IV).

The first oxidative derivative of $\text{Os}(\text{CHBA-Et})(\text{Py})_2$ is $\text{Os}(\text{CHBA-Ethylene})(\text{Py})_2$, 7 [1]. Its CV in SO_2 is shown in Figure 5.4. In CH_2Cl_2 this complex displayed one reversible oxidation at +0.37 V and one irreversible oxidation at +0.92 V. In SO_2 it showed three reversible

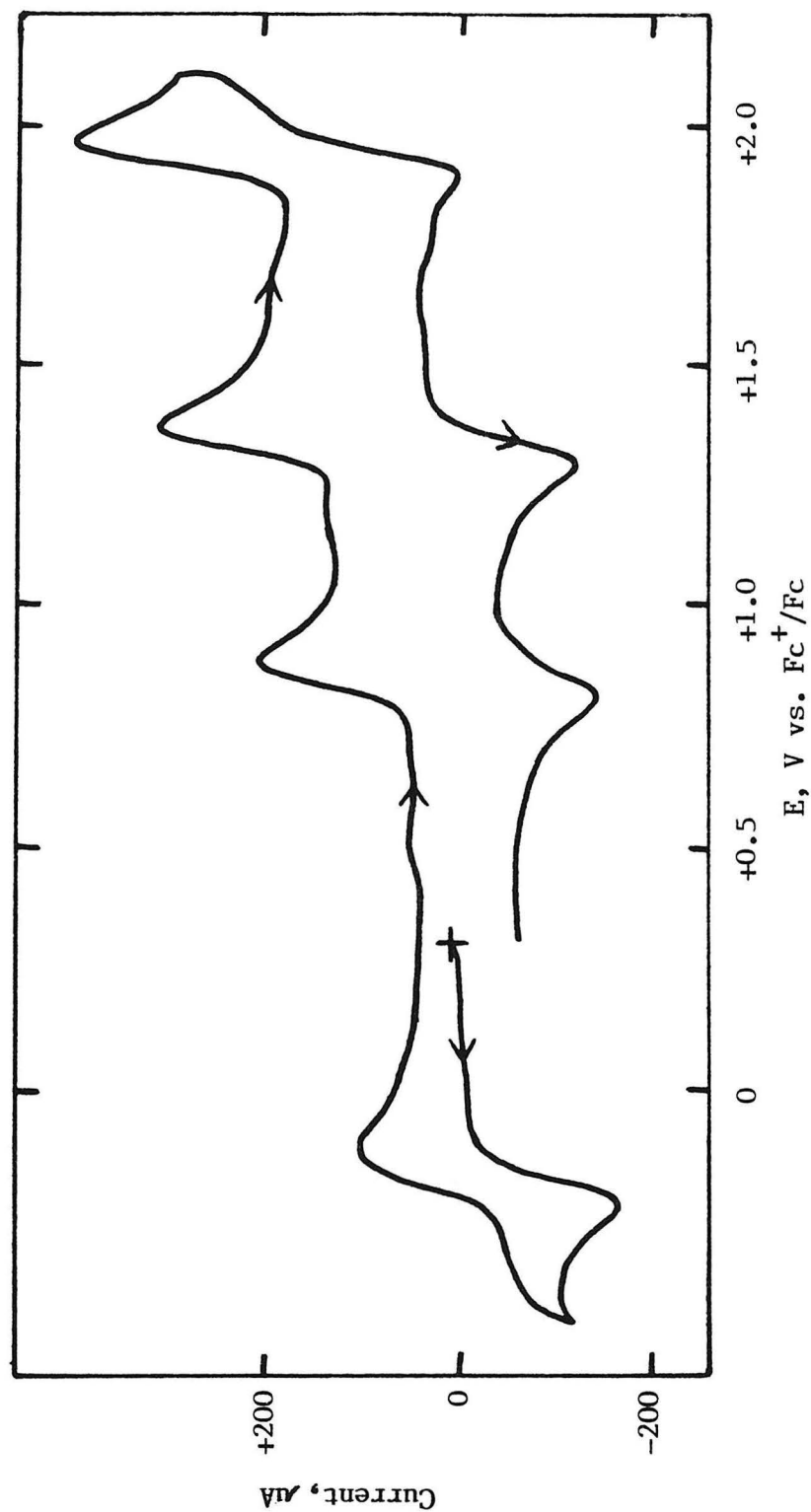


Figure 5.3. Cyclic voltammogram of 3 mM $\text{Os}(\text{CHBA-Et})(\text{Py})_2$ in SO_2 , 0.1 M TBABF_4 at -60°C at 0.32 cm^2 glassy carbon electrode. Scan rate = 200 mV/sec .

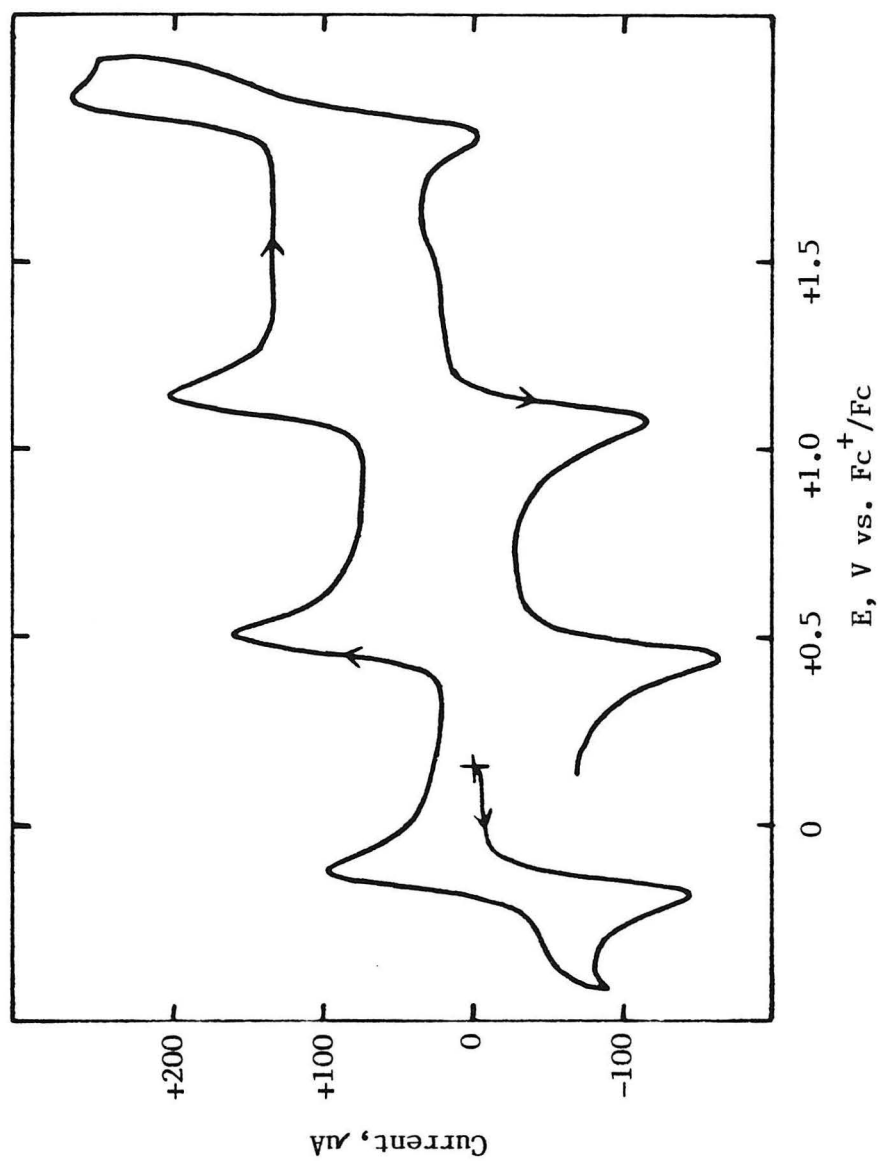


Figure 5.4. Cyclic voltammogram of 2.4 mM Os(CHBA-Ethylene)(Py)₂, 7, in SO₂, 0.1 M TBABF₄ at -40 °C at 0.32 cm² glassy carbon electrode. Scan rate = 200 mV/sec.

oxidations at +0.48, +1.11 and +1.89 V and irreversible anodic activity starting at +2.17 V.

The next derivative in the oxidative degradation pathway is $\text{Os}(\text{CHBA-}\underline{\text{t}}\text{-1,2-diRO-Et})(\text{Py})_2$, 8 [1]. In CH_2Cl_2 it displayed one partially reversible oxidation at about +0.90 V. In SO_2 two reversible oxidations at +1.00 and +1.47 V were seen.

The final products of the oxidative degradation of $\text{Os}(\text{CHBA-Et})(\text{Py})_2$ are the cis-alpha and trans isomers of $\text{Os}(\text{Fo-CHBA})_2(\text{Py})_2$, 9 and 9' [1]. Neither of the complexes displayed any anodic activity in CH_2Cl_2 . The CV of 9 in SO_2 , shown in Figure 5.5, displayed one reversible oxidation at +1.28 V and one partially reversible oxidation at +1.79 V. Note that replacement of the amido groups of CHBA-Et with the imido groups of the Fo-CHBA ligands increased the formal potential of the Os(V/IV) couple over 400 mV.

The complexes 9 and 9' undergo acid catalyzed hydrolyses of the Fo-CHBA ligands to give complexes containing CHBA ligands [1]. One analog of these complexes, trans- $\text{Os}(\text{CHBA})_2(\underline{\text{t}}\text{-Bupy})(\text{Ph}_3\text{P=O})$, 13, was examined in SO_2 . Unfortunately, even at -78 °C its oxidation was completely irreversible and led to numerous products.

The formal potentials for these complexes are summarized in Table 5.2.

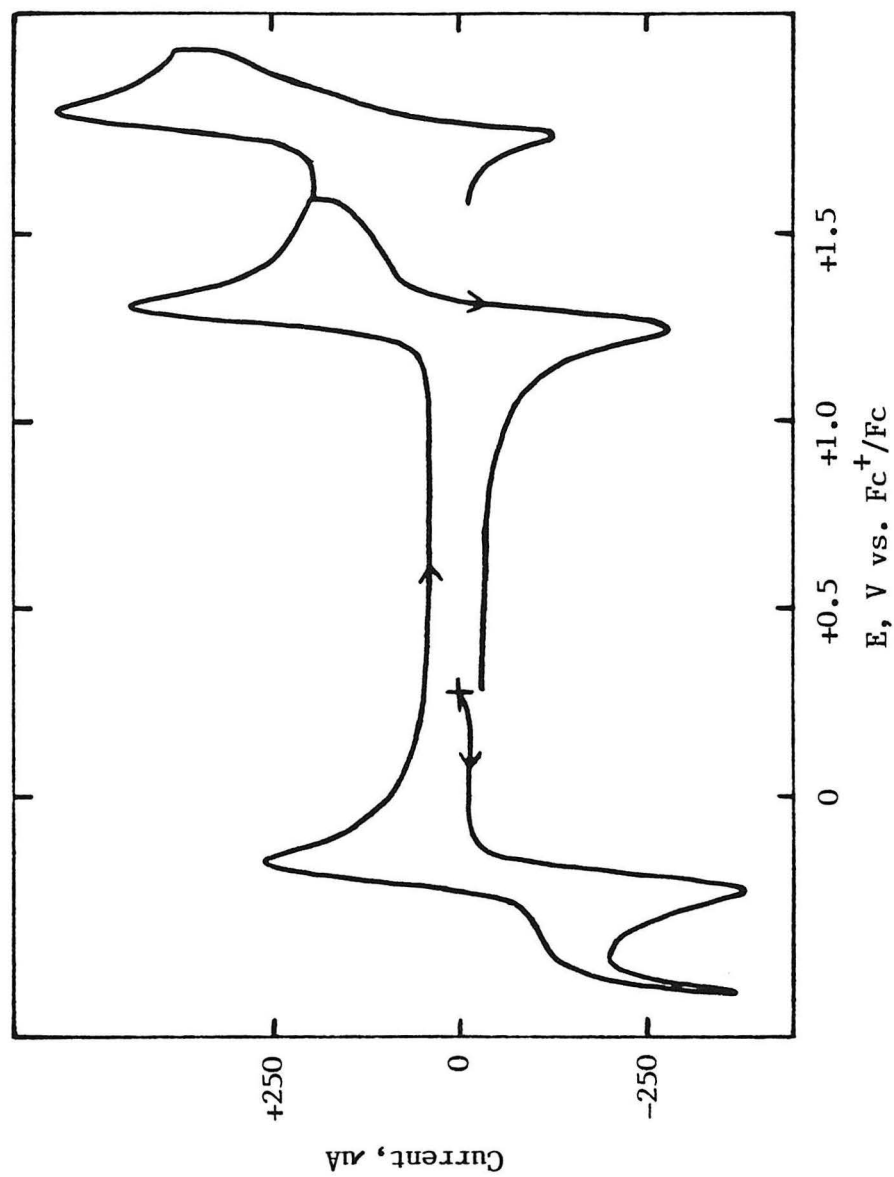


Figure 5.5. Cyclic voltammogram of 4.4 mM cis- α -Os(Fo-CHBA) $_2$ (Py) $_2$, 9, in SO $_2$, 0.1 M TBABF $_4$ at -40 °C at 0.32 cm 2 glassy carbon electrode. Scan rate = 200 mV/sec.

Table 5.2. Formal potentials of Os(CHBA-Et)(Py)₂ and its derivatives in SO₂.

Compound ^a	Formal Potential, V ^b			
	Os(IV/III)	Os(V/IV)	2+/1+	3+/2+
<u>5</u>	-0.19	+0.86	+1.37	+2.01
<u>7</u>	-0.13	+0.48	+1.11	+1.89
<u>8</u>	-0.20	+1.03	+1.46	
<u>9</u>	-0.22	+1.28	+1.79	

^aFor numbering see text and Chapter II. ^bFormal potential measured in SO₂/0.1 M TBABF₄ and referenced to Fc⁺/Fc internal standard.

Conclusions

Liquid sulfur dioxide has been found to be a very useful solvent for probing the electrochemistry of very highly oxidizing and/or reactive species. The anodic range of SO_2 extends to about +3.5 V vs. Fc^+/Fc , compared to about +1.4 V under normal conditions in CH_2Cl_2 . The low temperature, high purity and low nucleophilicity of SO_2 allow the observation of oxidized species which would otherwise be very unstable. Since many of the osmium compounds studied in this work were soluble in SO_2 , their electrochemistry was examined with the goal of finding additional anodic activity of the compounds and of testing the ultimate stability of the multianionic chelating ligands.

The osmium(IV) complexes of the CHBA-DCB ligand containing pyridine, triphenylphosphine and *t*-butylisocyanide monodentate ligands were examined in SO_2 . They all exhibited additional anodic activity not observed in CH_2Cl_2 . However, the wide range of formal potentials observed with the different ligands at the Os(V/IV) and lower oxidation state couples was not observed for the new oxidations. It is especially interesting that the CV's of $\text{Os}(\text{CHBA-DCB})(\text{Py})_2$ and $\text{Os}(\text{CHBA-DCB})(\text{Ph}_3\text{P})_2$, both trans isomers, were essentially identical. This lack of variation of the formal potentials of the more highly oxidized forms suggests that these oxidations are ligand-localized and so do not represent higher oxidation states of the osmium. The more highly oxidized forms were only marginally stable in solution at low temperatures. These observations have prompted an effort to synthesize new ligand systems with totally aliphatic, but protected, structures which may be more stable to very highly oxidizing conditions.

The electrochemistry of $\text{Os}(\text{HBA-B})(\text{Ph}_3\text{P})(\text{CO})$ was examined in SO_2 . No reversible anodic activity other than the $\text{Os}(\text{V}/\text{IV})$ couple was observed, and scanning over the high-potential irreversible oxidations caused polymerization of the compound on the electrode surface. This polymerization demonstrates the susceptibility of the unprotected HBA-B ligand to degradation reactions. Controlled potential oxidation did not produce a stable $\text{Os}(\text{V})$ carbonyl complex.

In CH_2Cl_2 $\text{Os}(\text{CHBA-Et})(\text{Py})_2$ undergoes a series of oxidative degradation reactions of the CHBA-Et ligand upon oxidation to $\text{Os}(\text{V})$. In SO_2 it displayed two completely reversible oxidations on the CV time scale. This allowed measurement of the formal potential of the $\text{Os}(\text{V}/\text{IV})$ couple which could not be done in CH_2Cl_2 . The other complexes encountered in the oxidative degradation of $\text{Os}(\text{CHBA-Et})(\text{Py})_2$, and described in Chapter II, all displayed new reversible electrochemistry in SO_2 . However, the one catalyst compound (see Chapter III) examined did not display a reversible $\text{Os}(\text{V}/\text{IV})$ couple even at -78°C . These experiments demonstrated the usefulness of SO_2 as a solvent for examining the electrochemistry of very reactive species formed at more moderate potentials.

Experimental

Materials

Sulfur dioxide (Matheson) was anhydrous grade and was further purified by passing it through concentrated sulfuric acid to remove SO_3 and some water and then passing it over P_2O_5 on glass wool for final drying. Tetra-n-butylammonium tetrafluoroborate supporting electrolyte (Southwestern Analytical Chemicals) was recrystallized three times from ethyl acetate/ether, and then dried under vacuum. Ferrocene (Aldrich) was used as received.

All osmium compounds containing the CHBA-DCB and HBA-B ligands were prepared by John Keech and Geoffrey Peake, respectively. $\text{Os}(\text{CHBA-Et})(\text{Py})_2$ and its derivative complexes were prepared by Terry Krafft. Details of the synthesis and characterization of the osmium complexes can be found in the appropriate references [20-24].

Apparatus and Procedures

Cyclic voltammetry was performed with a Princeton Applied Research (PAR) Model 173 potentiostat driven by a PAR Model 175 universal programmer using positive feedback IR-compensation. Current-voltage curves were recorded on a Houston Instruments Model 2000 X-Y recorder. The working electrode was a 0.32 cm^2 glassy carbon (Tokai) disc mounted in a metal support and sealed with heat-shrinkable tubing or a 0.03 cm^2 platinum disc sealed in glass. Both working electrodes were prepared by polishing with 0.3 micron alumina polishing powder (Linde), sonicating and rinsing with water, acetone and methylene chloride. The behavior and formal potentials of the osmium compounds was not dependent upon the electrode used. The counter electrode was a platinum wire. The reference electrode was a silver wire polished with 0.3 micron alumina polishing

powder (Linde) and placed in a separate compartment containing only supporting electrolyte and solvent. For each compound studied at least one experiment was performed in the presence of ferrocene as an internal potential standard. Formal potentials of reversible couples were taken as the average of the anodic and cathodic peak potentials. The supporting electrolyte was 0.1 M TBABF₄. The cell used for experiments involving only cyclic voltammetry was a conventional two-compartment H-cell modified for use on a vacuum line. The ground glass joints and the connections to the vacuum line are similar to those described below for the larger cell and loading of the SO₂ was accomplished by the same procedure. For experiments conducted at room temperature the two ground glass joints and the septum were securely wired down.

Controlled potential electrolysis experiments were performed with the PAR Model 173 potentiostat equipped with a Model 179 digital coulometer using positive feedback IR-compensation. The cell used for these experiments is shown in Figure 5.6. The cell is a three-compartment electrochemical cell designed for use on a vacuum line. All electrical connections are made through ground glass joints. The working, counter and reference electrodes are connected to the electrical leads in the joints by brass clips and so can be removed and cleaned between experiments. The counter and working electrodes are platinum gauzes. The CV electrode is a 0.03 cm² platinum disc sealed in glass or a 0.32 cm² glassy carbon disc. The reference electrode is a silver wire located in a separate compartment containing only solvent and supporting electrolyte and with a fine frit at the bottom. A small hole in the reference electrode compartment allows it to fill with SO₂. Care had to be taken during electrolysis experiments since oxidized species migrating into the

Figure 5.6. Three-compartment electrochemical cell for work in SO_2 .

1. Platinum gauze counter electrode.
2. Extra fine frit.
3. Brace.
4. Silver wire quasi-reference electrode.
5. Platinum disc CV electrode.
6. Platinum gauze working electrode.
7. Solid addition port.

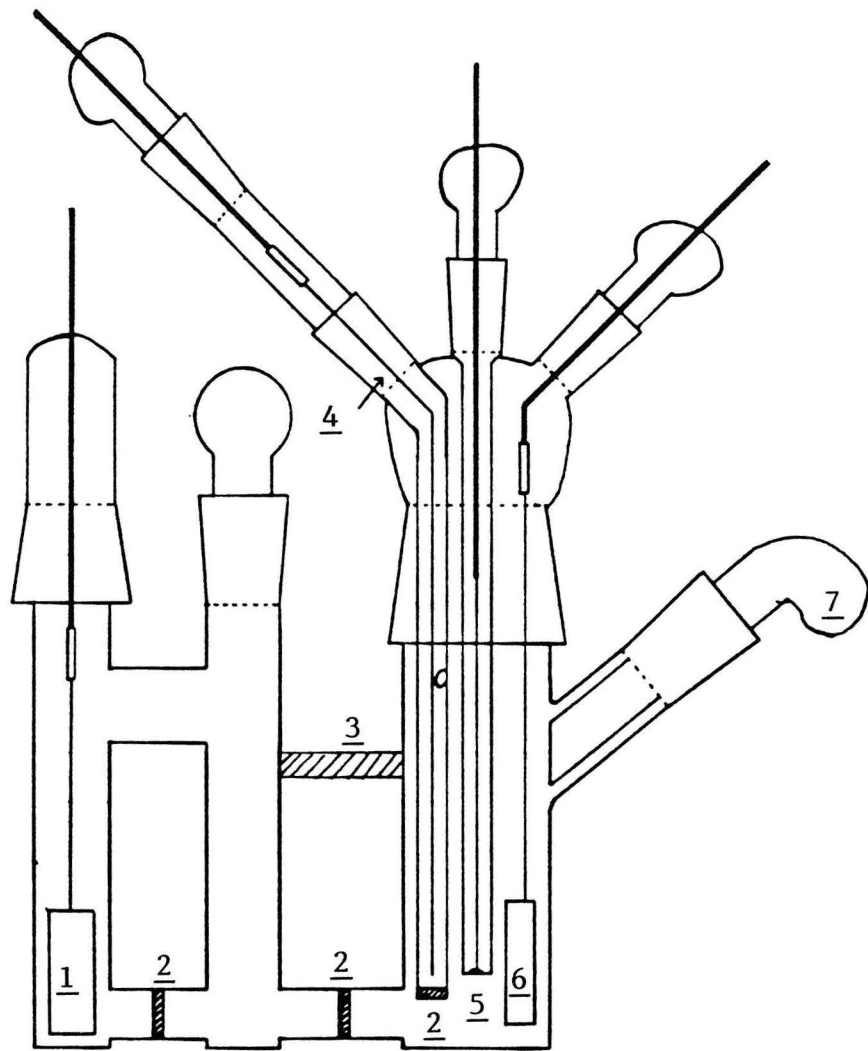


Figure 5.6

reference electrode compartment caused the potential of the reference electrode to drift substantially. Not shown in the figure is a septum port at the front of the cell through which solutions, such as that of the ferrocene internal standard, could be introduced. The cell is equipped with a solid addition port, but because of difficulty in quantitatively transferring the solid it was not used. Instead, before each experiment the cell was loaded with supporting electrolyte in all compartments and the osmium compound in the working compartment. The cell was then placed on the vacuum line and dried overnight. Initially the cell was heated to 100 °C during drying, but some compounds decomposed at this temperature, so most samples were dried without heating. The electrodes were prepared as described above. All ground glass joints were greased with silicone high vacuum grease (Dow Corning) since SO_2 reacted with other types of grease.

Not shown in the figure are the connections to the vacuum line at the back of the counter and working compartments. At the back of these two compartments a glass tube was connected and these two tubes met at a teflon valve. At the other side of the valve was an o-ring joint for connection to the vacuum line shown in Figure 5.7. The vacuum line consists of mechanical and oil diffusion pumps connected to the right side of the line and the SO_2 inlet at the left side. The line is also equipped with an argon Schlenk line and a mercury manometer. A 5 lb cylinder of SO_2 is connected through rubber vacuum tubing to a gas washing bottle containing concentrated sulfuric acid. The gas washing bottle is equipped with a pressure equalizing valve to prevent backing up of sulfuric acid into the SO_2 tank. The gas washing bottle is connected by glass tubing to two 50 cm columns containing P_2O_5 on glass wool, and these are connected to the vacuum line. All valves in the system are teflon valves.

Figure 5.7. Vacuum line for SO₂ electrochemistry.

1. 5 lb SO₂ tank.
2. H₂SO₄ gas washing bottle.
3. 2 x 50 cm P₂O₅ on glass wool drying columns.
4. Vacuum line.
5. Argon Schlenk line.
6. Mercury manometer.
7. Liquid nitrogen trap.
8. High vacuum from oil diffusion pump.
9. Diffusion pump inlet.
10. Rough pump.

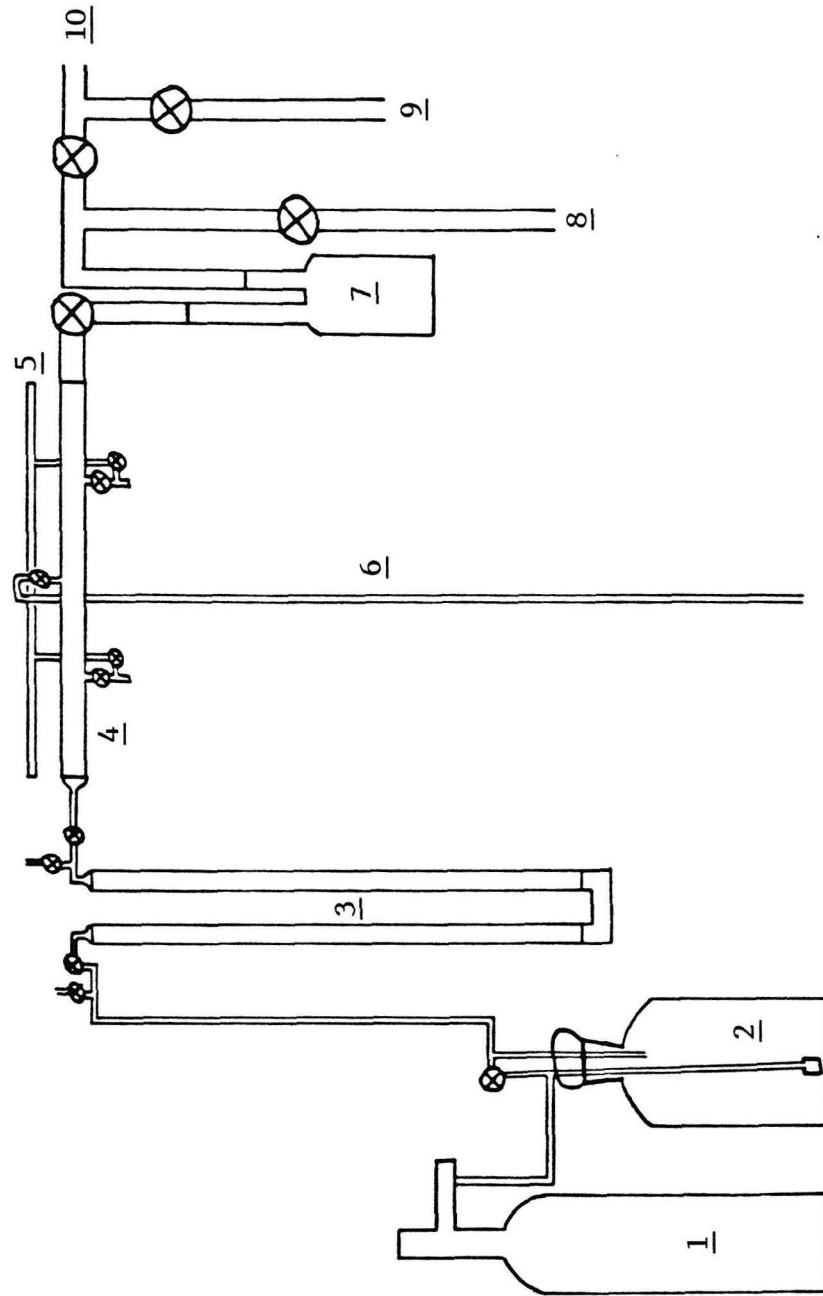


Figure 5.7

In order to fill the cell it was first cooled to $-78\text{ }^{\circ}\text{C}$ in a dry ice/isopropanol bath. The vacuum line from the P_2O_5 columns onward was evacuated and the manometer opened. After the gas washing bottle and its lines had been purged for several minutes open to the atmosphere, its purge valve was closed, the flow rate of the SO_2 was reduced and the SO_2 was admitted to the vacuum line and the cell. The open manometer prevented any dangerous buildup of pressure. The cell was filled to a predetermined level known to correspond to approximately 15 ml in the working compartment. After the cell was filled its valve was closed, the cell was removed from the vacuum line and the temperature of the bath was adjusted, usually to about $-40\text{ }^{\circ}\text{C}$. The temperature of the bath was maintained to $\pm 5\text{ }^{\circ}\text{C}$ by periodically adding small amounts of dry ice. The solutions were stirred magnetically with a teflon-coated stirring bar.

References and Notes

1. Ligand names are: 1,2-bis(3,5-dichloro-2-hydroxybenzamido)ethane, $H_4CHBA-Et$; 1,2-bis(3,5-dichloro-2-hydroxybenzamido)ethylene, $H_4CHBA-Ethylene$; 1,2-bis(3,5-dichloro-2-hydroxybenzamido)-trans-1,2-dialkoxyethane, $H_4CHBA-t-1,2-diRO-Et$; N-formyl-3,5-dichloro-2-hydroxybenzamide, $H_2Fo-CHBA$; 3,5-dichloro-2-hydroxybenzamide, H_2CHBA ; 1,2-bis(3,5-dichloro-2-hydroxybenzamido)-4,5-dichlorobenzene, $H_4CHBA-DCB$; 1,2-bis(2-hydroxybenzamido)benzene, H_4HBA-B .
2. L.A. Tinker and A.J. Bard, J. Am. Chem. Soc., **101**, 2316-2319 (1979).
3. L.A. Tinker and A.J. Bard, J. Electroanal. Chem., **133**, 275-285 (1982).
4. J.G. Gaudiello, P.R. Sharp and A.J. Bard, J. Am. Chem. Soc., **104**, 6373-6377 (1982).
5. P.R. Sharp and A.J. Bard, Inorg. Chem., **22**, 2689-2693 (1983).
6. J.G. Gaudiello, P.G. Bradley, K.A. Norton, W.H. Woodruff and A.J. Bard, Inorg. Chem., **23**, 3-10 (1984).
7. P.R. Sharp and A.J. Bard, Inorg. Chem., **22**, 3462-3464 (1983).
8. P.J. Elving and J.M. Markowitz, J. Chem. Ed., **37**, 75-81 (1960).
9. (a) P.J. Elving, J.M. Markowitz and I. Rosenthal, J. Phys. Chem., **65**, 680-686 (1961). (b) P.J. Elving, J.M. Markowitz and I. Rosenthal, J. Phys. Chem., **65**, 686-690 (1961). (c) Also see References 2 and 8.
10. L.L. Miller and E.A. Mayeda, J. Am. Chem. Soc., **92**, 5818 (1970).
11. G. Launay and P. Castellonese, Bull. Soc. Chim. Fr., **1978**, I-226-230.
12. P. Castellonese and G. Launay, Bull. Soc. Chim. Fr., **1978**, I-317-322.
13. P.C. Lacaze, J.E. Dubois and M. Delamar, J. Electroanal. Chem., **102**, 135-137 (1979).
14. J.E. Dubois, M. Delamar and P.C. Lacaze, Electrochim. Acta, **25**, 429-433 (1980).
15. M. Delamar, P.C. Lacaze, J.Y. Dumousseau and J.E. Dubois, Electrochim. Acta, **27**, 61-65 (1982).
16. G.E. Whitwell II, D.C. Miller and J.M. Burlitch, Inorg. Chem., **21**, 1692-1693 (1982).
17. In all complexes discussed in this chapter, the potentially tetradentate tetraanionic ligands are coordinated as such.

18. Formal potentials are calculated as the average of the anodic and cathodic peak potentials determined by cyclic voltammetry. All potentials are referenced to the formal potential of a ferrocene internal standard.
19. B.G.R.T. Treco, unpublished results.
20. F.C. Anson, T.J. Collins, R.J. Coots, T.T. Furutani, S.L. Gipson, J.T. Keech, T. Lai, S.C. Lee, G.T. Peake and T.G. Richmond, manuscript in preparation.
21. John T. Keech, unpublished results. All syntheses and characterizations of compounds containing the CHBA-DCB ligand were performed by John Keech.
22. Geoffrey T. Peake, unpublished results. All syntheses and characterizations of compounds containing the HBA-B ligand were performed by Geoffrey Peake.
23. F.C. Anson, J.A. Christie, T.J. Collins, R.J. Coots, T.T. Furutani, S.L. Gipson, J.T. Keech, T.E. Krafft, B.D. Santarsiero and G.H. Spies J. Am. Chem. Soc., **106**, 4460-4472 (1984).
24. T.E. Krafft, Ph.D. Thesis, California Institute of Technology, February, 1985.

CHAPTER VI

The Electrochemistry of Cobalt Complexes Containing
Multianionic Chelating Ligands

Introduction

The work discussed so far in this thesis has dealt only with osmium complexes containing the Collins group's multianionic chelating ligands. The work with the osmium complexes established the synthetic routes and design criteria for the ligand systems under study. Once the osmium chemistry was fairly well understood, it became possible to begin work with other metals. After osmium, the metal which has been most extensively studied synthetically and electrochemically is cobalt. This chapter will describe the electrochemistry of a number of cobalt complexes containing tetradentate tetraanionic ligands which were prepared by Dr. Thomas Richmond of the Collins group [1,2].

Cobalt complexes containing multianionic chelating ligands, for example the CHBA-DCB ligand [3], are synthesized as monoanionic Co(III) salts. The complexes typically contain the tetradentate tetraanionic ligand coordinated in a planar fashion and contain two monodentate ligands, such as pyridine, in the axial positions. The cyclic voltammograms of these complexes in acetonitrile and methylene chloride display two reversible oxidations, but no reversible cathodic activity. The first oxidation produces a stable green complex which can also be produced chemically and which has been shown to be a Co(IV) complex. The second oxidation produces a compound which is stable only on the CV time scale.

The production of a stable Co(IV) complex is a further demonstration of the powerful stabilization of high oxidation state metal centers characteristic of the Collins group's multianionic chelating ligands. Co(IV) is a very unusual oxidation state for cobalt. The only other Co(IV) complexes that have been structurally characterized are several

homoleptic halide and oxide complexes [4]. The complex $\text{Co}(\text{1-norbornyl})_4$ has also been reported and is apparently quite stable. Cobalt(IV) appears to have been generated electrochemically for complexes containing dithiocarbamate [5], dimethylglyoximate and salen [6] ligands. These complexes decompose at room temperature but are stable at low temperatures. The best evidence for the Co(IV) oxidation state exists for the dimethylglyoximate complexes, which are unlikely to involve ligand oxidation and which have been characterized by EPR spectroscopy [7].

Comparison of the structures of Co(III) and Co(IV) complexes containing the CHBA-DCB ligand suggests that an oxidized form of the ligand may contribute significantly to the structure. This contribution would lower the formal oxidation state assignment of the metal. While we believe that the neutral complexes can still legitimately be called Co(IV), the more highly oxidized species, including a 3+ cation observed in liquid SO_2 , are not assigned to higher oxidation state cobalt species.

Results and Discussion

Electrochemistry of cobalt complexes in acetonitrile and CH_2Cl_2

The electrochemistry of osmium complexes containing multianionic chelating ligands such as CHBA-Et, CHBA-DCB and HBA-B [3] has been investigated in CH_2Cl_2 . The electrochemical studies provided input into the design of more stable ligands and demonstrated the stabilization of high oxidation state metal centers by these ligands. Once the usefulness of the ligands had been proven with osmium it became desirable to extend our investigations to other metals. Therefore, Dr. Thomas Richmond of the Collins group began synthesizing cobalt complexes of various tetradentate tetraanionic ligands. One example of these complexes is $\text{Na}[\text{trans-Co}(\text{CHBA-DCB})(\text{t-Bupy})_2] \cdot \text{H}_2\text{O}$, shown in Figure 6.1.

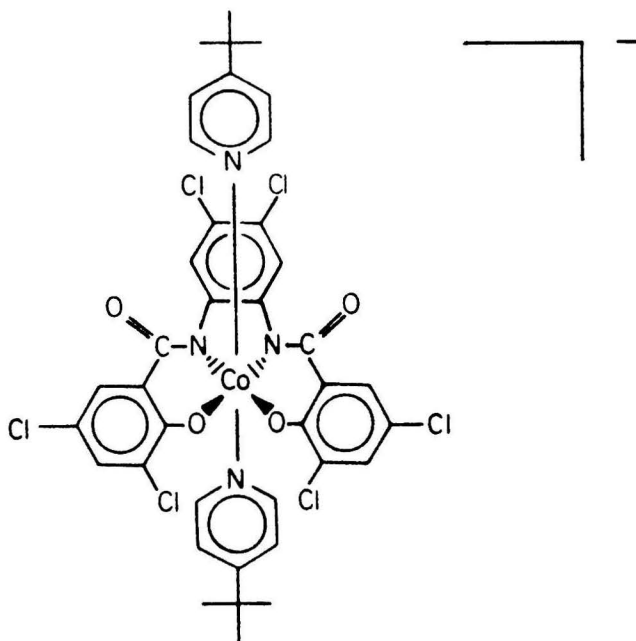


Figure 6.1. Structure of $\text{Na}[\text{trans-Co}(\text{CHBA-DCB})(\text{t-Bupy})_2]$

This complex is soluble in acetonitrile and in CH_2Cl_2 . Its cyclic voltammogram (CV) in acetonitrile is shown in Figure 6.2.

$\text{Na}[\text{Co}(\text{CHBA-DCB})(\text{t-Bupy})_2] \cdot \text{H}_2\text{O}$ displayed no reversible reductions, but two

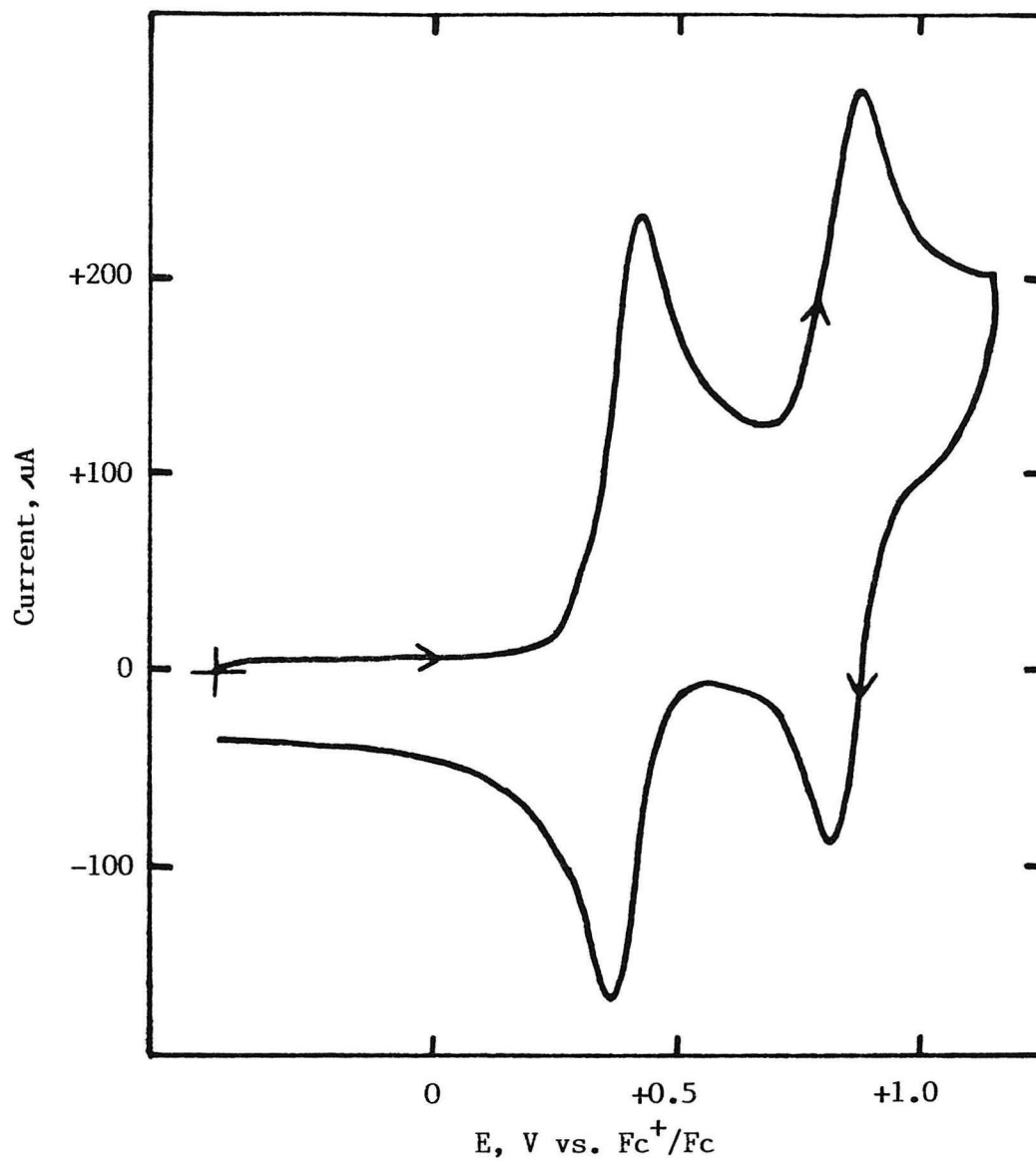


Figure 6.2. Cyclic voltammogram of 3.7 mM Na[trans-Co(CHBA-DCB)(t-Bupy)₂] in acetonitrile, 0.1 M TBAP at 0.17 cm² BPG electrode. Scan rate = 200 mV/sec.

reversible oxidations were seen at $E_f = +0.39$ and $+0.84$ V vs. Fc^+/Fc [8]. Controlled potential oxidation at $+0.62$ V consumed about 1.4 F/mol of Co but the current never decreased to a background value. The solution color changed during the electrolysis from deep orange to green. The CV at the conclusion of the electrolysis showed some broadening of the CV peaks and some loss of peak currents, but both couples were still observable and the rest potential of the electrode was about $+0.6$ V. Further oxidation at $+1.0$ V consumed more than 3.3 F/mol of Co and resulted in a brown solution showing no electrochemical activity.

The behavior of the bis-(t-butylpyridine) complex in CH_2Cl_2 was almost identical to that in acetonitrile. Two reversible oxidations were observed at $+0.24$ and $+0.83$ V. Controlled potential electrolysis at $+0.54$ V consumed 1.1 F/mol of Co but, as in acetonitrile, the current never reached a background level. The poor results of the controlled potential electrolyses in acetonitrile and CH_2Cl_2 were probably not the result of instability of the Co(IV) species. Once the electrolyses were stopped, the green solutions were quite stable and showed the expected CV's. Also, the Co(IV) compound could be synthesized chemically by oxidation with Ce(IV) [2] and the product was quite stable. When the chemically prepared Co(IV) complex was dissolved in CH_2Cl_2 and reduced electrochemically, the reduction consumed 0.9 F/mol of Co.

The two-electron oxidized species is definitely unstable on the controlled potential electrolysis time scale. It seems possible that the extra charge consumed and the partial decomposition observed during electrolyses at the first oxidation of $\text{Na}[\text{Co}(\text{CHBA-DCB})(\text{t-Bupy})_2] \cdot \text{H}_2\text{O}$ could stem from partial oxidation to the two-electron oxidized compound. This partial oxidation probably arises simply from the proximity of the

potential of the second oxidation to that of the first. Alternatively, the two-electron oxidized product could be formed during the electrolysis by disproportionation of the Co(IV) complex. In CH_2Cl_2 the two oxidations are separated by 590 mV. This gives an equilibrium constant for disproportionation of about 1×10^{-10} . In acetonitrile the potential difference decreases to 450 mV and the equilibrium constant is about 2×10^{-8} . This disproportionation does not proceed very far at equilibrium, but at the potentials of the electrolyses, all of the Co(III) formed would rapidly be oxidized to Co(IV) and so drive the equilibrium farther. The decomposition of the two-electron oxidized species would also drive the disproportionation. Support for this argument is found in a report of the two-electron reduction of indenenes [9] which occurs at the potential of the first reduction and involves disproportionation to the two-electron reduced form. For these compounds the equilibrium constants for disproportionation ranged from 10^{-6} to 10^{-10} .

The cause of the instability of the two-electron oxidized product is unknown. It seems unlikely that the instability arises from oxidative degradation of any of the ligands since osmium(V) forms stable compounds with the same ligands but with higher formal potentials. It was felt that the decomposition of the two-electron oxidized product might be caused by ligand dissociation. The *t*-butylpyridine ligands would be most likely to dissociate, so the CV's of the complex were examined in the presence of added pyridine. The pyridine had little effect on the first oxidation, but even one equivalent of pyridine caused the second oxidation to be much less reversible and gave rise to new activity after scanning over the second oxidation. In addition, the two-electron oxidized product of $\text{Na}[\text{Co}(\text{CHBA-DCB})(\text{bipy})]\cdot\text{H}_2\text{O}$ also decomposed in both acetonitrile and

CH_2Cl_2 . Thus, ligand dissociation does not seem to be the cause of the instability.

The electrochemistry of a number of other cobalt complexes containing different tetradentate tetraanionic and monodentate ligands has been examined in acetonitrile by Dr. Thomas Richmond. A summary of the formal potentials of these complexes is presented in Table 6.1.

Table 6.1. Formal potentials of cobalt complexes in acetonitrile.

MAC	$\text{Co}(\text{MAC})\text{L}_2^{\text{a}}$ L	Co(IV/III)	Formal Potential, V^{b} 1+/0
CHBA-DCB	<u>t</u> -Bupy	+0.39	+0.84
CHBA-DCB	DMAP ^c	+0.33	+0.79
CHBA-DCB	$\text{Et}_3\text{P}=\text{O}$	+0.37	+0.67
CHBA-DCB	bipy	+0.31	+0.67
CHBA-B	<u>t</u> -Bupy	+0.23	+0.74
CHBA-B	bipy	+0.14	+0.53
CHBA-DMB	<u>t</u> -Bupy	+0.10	+0.60

^aTrans isomers except for bipy complexes which are cis-beta. ^bFormal potential measured in acetonitrile/0.1 M TBAP and referenced to Fc^+/Fc internal standard. ^cDMAP = N,N'-dimethylaminopyridine.

The potentials of the cobalt complexes varied significantly with changes in tetradentate and monodentate ligands. As would be expected, replacement of the chlorines on the dichlorobenzene bridge of CHBA-DCB with hydrogens in CHBA-B and methyl groups in CHBA-DMB caused substantial decreases in the formal potentials of both oxidations. Changes in the monodentate ligands of the trans- $\text{Co}(\text{CHBA-DCB})\text{L}_2$ complexes caused surprisingly little variation in the formal potential of the first

oxidation. This formal potential decreased only 20 mV on going from the bis-(t-butylpyridine) complex to the bis-(triethylphosphine oxide) complex. This compares to a 540 mV change in the Os(IV/III) formal potential for the osmium complexes containing t-butylpyridine and triphenylphosphine oxide ligands. A large variation was also observed in the Os(V/IV) formal potential with changes in monodentate ligands, and this variation was part of the evidence for that oxidation's being metal-centered. Therefore, it seems possible that alternate electronic structures of the ligands which would decrease the formal oxidation state assignment of the cobalt, shown in Figure 6.3, may participate significantly in the structure of the "Co(IV)" species (see Chapter IV).

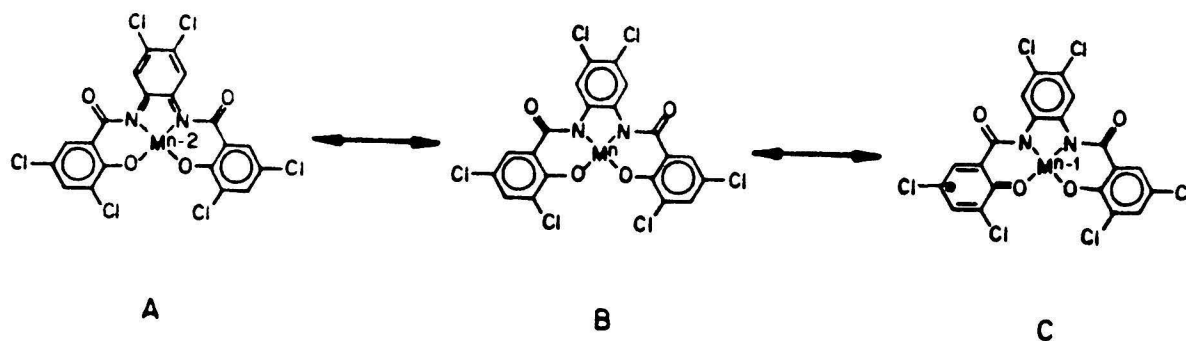


Figure 6.3. Alternate electronic structures of the CHBA-DCB ligand.

Comparison of the x-ray crystal structures of $[\text{Co}(\text{CHBA-DCB})(\text{t-Bupy})_2]^-$ and $\text{Co}(\text{CHBA-DCB})(\text{t-Bupy})_2$ reveals some shortening of the bridge carbon to amide nitrogen and carbon to phenoxide oxygen bonds in the neutral species [2]. These changes are consistent with some contribution from structures A and C. The contributions of A and C to the structure of the neutral species cannot be quantified but based on its EPR spectrum, it seems probable that the cobalt is present as Co(IV) [1,2]. Therefore, the dominant ligand structure is believed to be B.

Electrochemistry of cobalt complexes in liquid SO₂

In Chapter V the electrochemistry of osmium complexes in liquid SO₂ was described. This novel solvent possesses a very large anodic range so that activity not observable in CH₂Cl₂ or acetonitrile may be detected. In addition, because of its high purity, low temperature and low nucleophilicity, SO₂ is an excellent solvent in which to examine the electrochemistry of very reactive oxidized species. Therefore, it was decided to examine the electrochemistry of some of the cobalt complexes in SO₂ in search of more highly oxidized species and with the intent of stabilizing the two-electron oxidized product.

The CV of Na[trans-Co(CHBA-DCB)(t-Bupy)₂]⁺H₂O in SO₂ is shown in Figure 6.4. Four reversible oxidations are seen at E_f = +0.57, +0.90, +1.29 and +1.45 V. Controlled potential oxidation to the Co(IV) species at +0.73 V consumed 0.93 F/mol of Co and produced a stable green solution. Then oxidation at +1.10 V consumed 1.0 F/mol of Co, but the current never decreased to background. Nevertheless, a reasonably stable solution of the two-electron oxidized product was obtained. Some distortion was seen in the CV after the second oxidation but all of the couples were still clearly visible. Further oxidation at +2.2 V led to decomposition of the cobalt complex.

Very similar results were obtained with Na[trans-Co(CHBA-DMB)(t-Bupy)₂]⁺H₂O. The formal potentials of its oxidations were +0.41, +0.70, +1.28 and +1.45 V. Note the similarity of the potentials of the third and fourth oxidations to those of the CHBA-DCB complex. This may imply that these oxidations are localized in the CHBA arms of the tetradentate ligands. The CV of Na[trans-Co(CHBA-Et)(t-Bupy)₂]⁺H₂O showed a completely irreversible

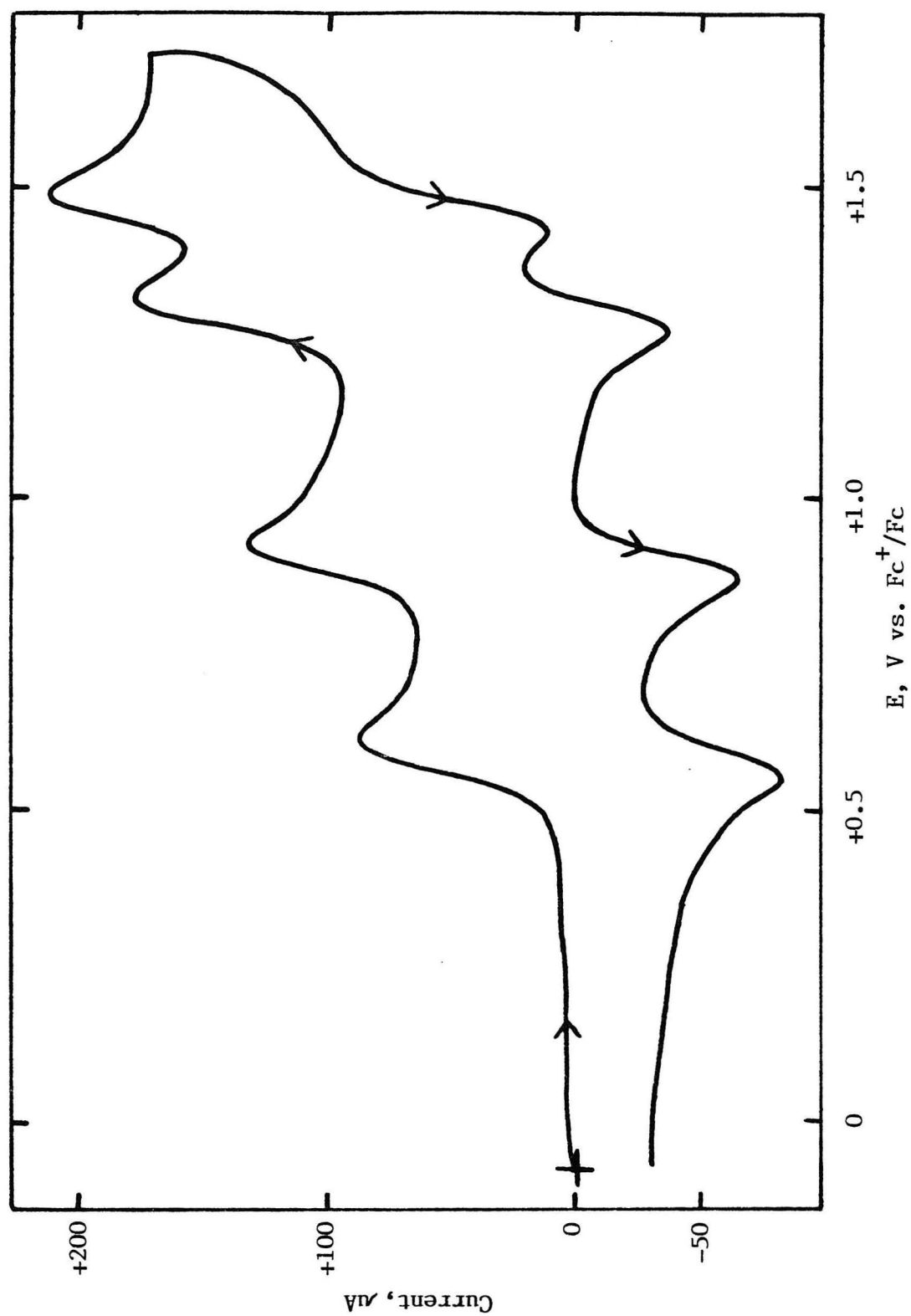


Figure 6.4. Cyclic voltammogram of 1 mM Na[trans-Co(CHBA-DCB)(t-Bupy)₂] in SO₂, 0.1 M TBABF₄ at -40 °C at 0.32 cm² glassy carbon electrode. Scan rate = 200 mV/sec.

oxidation to Co(IV) in acetonitrile. When examined in SO_2 this oxidation remained irreversible even at -65°C . This behavior contrasts with that of the corresponding osmium complex, the first oxidation of which became reversible in SO_2 .

The two-electron oxidized product of $\text{Na}[\text{trans-Co}(\text{CHBA-DCB})(\text{t-Bupy})_2]\cdot\text{H}_2\text{O}$ appeared to be stable in SO_2 . It was felt that if this species were a Co(V) complex it should be NMR-observable. NMR has been performed in liquid SO_2 [10]. One need be concerned only with interference from the supporting electrolyte since the SO_2 is aprotic. Dr. Thomas Richmond and I attempted to observe the NMR spectrum of the two-electron oxidized product generated in SO_2 . We were not successful with NMR studies using tetramethylammonium fluoroborate as supporting electrolyte because of the large tetramethylammonium signal. We therefore decided to try to use an aprotic supporting electrolyte. This proved to be impossible in SO_2 alone, but it was found that NaClO_4 was soluble in a mixture of 20% CD_3CN and 80% SO_2 . We were able to generate the two-electron oxidized product in this solvent system but were still unable to observe an NMR spectrum. However, the discovery of this solvent system may be of some use in the future if a similar need arises.

Conclusions

A number of cobalt complexes containing the Collins group's tetradentate tetraanionic ligands have been synthesized by Dr. Thomas Richmond and their electrochemistry has been examined in acetonitrile, CH_2Cl_2 and SO_2 . The complexes can be chemically and electrochemically oxidized by one electron to stable Co(IV) species. Structural data suggest that these complexes contain some contribution from oxidized ligand resonance forms, but their EPR spectra are consistent with a Co(IV) oxidation state assignment. The production of stable Co(IV) complexes with such low Co(IV/III) formal potentials further demonstrates the powerful stabilization of high oxidation state metal centers by the Collins group's multianionic chelating ligands. A second reversible oxidation was observed in CV's of the cobalt complexes in acetonitrile and CH_2Cl_2 , but the product of this oxidation is not stable on the controlled potential electrolysis time scale.

In liquid SO_2 the CV's of the cobalt complexes displayed four reversible oxidations. The low temperature and high purity of SO_2 allowed production of reasonably stable solutions of the two-electron oxidized product. The more highly oxidized species were completely unstable. An NMR spectrum could not be observed for the two-electron oxidized product. The lack of an NMR spectrum for this compound may have arisen from paramagnetic impurities in the solution or it may indicate that the second oxidation is ligand-localized and does not lead to a Co(V) complex.

Experimental

Materials

Acetonitrile was Burdick and Jackson distilled in glass grade and was used as received. Reagent grade methylene chloride (MCB or Mallinckrodt) was further purified by passing it over a short column of activated alumina (Woelm N. Akt. I). SO_2 (Matheson) was purified as explained in Chapter V. All other solvents were reagent grade (Aldrich, Baker, Mallinckrodt, MCB or USI) and were used as received.

Tetra-n-butylammonium perchlorate (Southwestern Analytical Chemicals) was dried, recrystallized twice from acetone/ether, and then dried under vacuum. Tetrabutylammonium tetrafluoroborate (Southwestern Analytical Chemicals) was recrystallized three times from ethyl acetate/ether and dried under vacuum. Anhydrous sodium perchlorate (99+%, Aldrich) and ferrocene (Aldrich) were used as received.

All cobalt complexes were synthesized and characterized by Dr. Thomas Richmond [1,2].

Apparatus and Procedures

Cyclic voltammetry was performed with a Princeton Applied Research (PAR) Model 173 potentiostat driven by a PAR Model 175 universal programmer using positive feedback IR-compensation. Current-voltage curves were recorded on a Houston Instruments Model 2000 X-Y recorder. Standard two-compartment electrochemical cells were used. When necessary, solutions were purged with argon to remove oxygen. The working electrode was a 0.17 cm^2 basal plane pyrolytic graphite (BPG, Union Carbide Co.) disc mounted in a glass tube with heat-shrinkable tubing, a 0.03 cm^2 Pt disc sealed in glass or a 0.32 cm^2 glassy carbon disc (Tokai) mounted in a metal support and sealed with heat-shrinkable tubing. The counter

electrode was a platinum wire. Various reference electrodes were used, including SCE, SSCE, Ag/AgCl and a silver wire quasi-reference electrode. For each compound studied at least one experiment was performed in the presence of ferrocene as an internal potential standard. The formal potentials of all of the couples of the cobalt compounds were then referenced to that of the ferrocene, which was consistently measured as +0.39 V vs. aqueous SCE in acetonitrile and +0.48 V vs. SCE in CH_2Cl_2 . Formal potentials of reversible couples were taken as the average of the anodic and cathodic peak potentials. Supporting electrolytes were 0.1M NaClO_4 or TBAP in acetonitrile, TBAP in CH_2Cl_2 and TBABF_4 in SO_2 .

Controlled potential electrolysis experiments were performed with the PAR Model 173 potentiostat equipped with a Model 179 digital coulometer using positive feedback IR-compensation. Electrolyses in acetonitrile and CH_2Cl_2 were performed in standard three-compartment H-cells. The working and counter electrodes were platinum gauzes. When working in acetonitrile the reference electrode was located in a separate compartment, but in CH_2Cl_2 the reference electrode was placed in the working compartment close to the working electrode to minimize the amount of IR-compensation needed. All experiments were performed at room temperature, $22 \pm 2^\circ\text{C}$.

Cyclic voltammetry and controlled potential electrolyses in SO_2 were performed as described in Chapter V. It was important not to heat the cell when drying on the vacuum line since the cobalt complexes were particularly sensitive to heat.

References and Notes

1. F.C. Anson, T.J. Collins, R.J. Coots, S.L. Gipson and T.G. Richmond, J. Am. Chem. Soc., **106**, 5037-5038 (1984).
2. T.G. Richmond, unpublished results. All syntheses and characterizations of Co complexes were performed by T.G. Richmond.
3. Ligand names are: 1,2-bis(3,5-dichloro-2-hydroxybenzamido)ethane, H₄CHBA-Et; 1,2-bis(3,5-dichloro-2-hydroxybenzamido)-4,5-dichlorobenzene, H₄CHBA-DCB; 1,2-bis(3,5-dichloro-2-hydroxybenzamido)benzene, H₄CHBA-B; 1,2-bis(3,5-dichloro-2-hydroxybenzamido)-4,5-dimethylbenzene, H₄CHBA-DMB.
4. (a) W. Klemm, W. Brandt and R. Hoppe, Z. Anorg. Allg. Chem., **308**, 179-189 (1961). (b) J.W. Quail and G. Rivett, Can. J. Chem., **50**, 2447-2450 (1972). (c) V.M. Jansen and R. Hoppe, Z. Anorg. Allg. Chem., **398**, 54-62 (1973). (d) V.M. Jansen, Z. Anorg. Allg. Chem., **417**, 35-40 (1975).
5. A.M. Bond, A.R. Hendrickson, R.L. Martin, J.E. Moir and D.R. Page, Inorg. Chem., **22**, 3440-3446 (1983).
6. (a) I. Levitin, A.L. Sigan and M.E. Vol'pin, J. Chem. Soc., Chem. Commun., **1975**, 469-470. (b) R.H. Magnuson, J. Halpern, I. Levitan and M.E. Vol'pin, J. Chem. Soc., Chem. Commun., **1978**, 44-46. (c) J. Halpern, M.S. Chan, T.S. Roche and G.M. Tom, Acta Chem. Scand. Sect. A., **A33**, 141-148 (1979).
7. (a) J. Topich and J. Halpern, Inorg. Chem., **18**, 1339-1343 (1979). (b) J. Halpern, J. Topich and K.I. Zamaraev, Inorg. Chim. Acta, **20**, L21-L24 (1976). (c) J. Halpern, M.S. Chan, J. Hanson, T.S. Roche and J.A. Topich, J. Am. Chem. Soc., **97**, 1606-1608 (1975).
8. Formal potentials are calculated as the average of the anodic and cathodic peak potentials determined by cyclic voltammetry. All potentials are referenced to the formal potential of a ferrocene internal standard.
9. G. Farnia, F. Marcuzzi, G. Melloni and G. Sandona, J. Am. Chem. Soc., **106**, 6503-6512 (1984).
10. J.G. Gaudiello, P.G. Bradley, K.A. Norton, W.H. Woodruff and A.J. Bard, Inorg. Chem., **23**, 3-10 (1984).

CHAPTER VII

Chemical Modification of Electrodes with Osmium Complexes
of Multianionic Chelating Ligands

Introduction

One of the major goals of this project was the development of catalysts for the selective electrochemical oxidation of organic substrates. It was anticipated that once any catalysts had been studied in homogeneous solution, it would then be attempted to attach them to electrode surfaces. Chemical modification of electrodes offers a number of advantages, such as the absence of the catalyst from the bulk solution and the small amount of catalyst necessary compared to homogeneous systems.

The field of chemically modified electrodes has grown rapidly since its inception in 1975. The many different methods of localizing electroactive species on electrode surfaces have been reviewed in a number of papers [1-4]. The simplest method is adsorption of the electroactive species directly onto the electrode surface. The electroactive species may also be chemically linked to the electrode surface using reactions such as silylation. Electroactive species may be indirectly linked to the electrode surface through adsorbed polymers. The electroactive component may be chemically attached to the polymer or it may be electrostatically bound within an oppositely charged polymer.

The complexes synthesized by the Collins group are hydrophobic enough to be adsorbed onto graphite electrodes and display electroactivity in aqueous solution. A more interesting method of attaching one of these complexes to electrodes was reductive electropolymerization of a 4-vinylpyridine-containing complex. The groups of T.J. Meyer and R.W. Murray have reported numerous examples of the reductive electropolymerization of complexes containing 4-vinylpyridine (vpy), vinyl-2,2'-bipyridine and similar polymerizable ligands [5]. These

complexes were reduced first at a bipyridine ligand and then underwent intramolecular electron transfer to the vinyl-containing ligand. Polymerization was believed to occur through hydrodimerization and/or conventional anionic or radical polymerization.

Since the complex $\text{Os}(\text{CHBA-Et})(\text{Py})_2$ [6] is reduced to Os(II) at potentials similar to those of the bipyridine reductions of Meyer and Murray's complexes, it was felt that the 4-vinylpyridine analog might reductively electropolymerize. Therefore, the complex $\text{K}[\text{Os}(\text{CHBA-Et})(\text{vpy})_2]$ was synthesized from the Os(VI) bis-oxo complex and 4-vinylpyridine. It was found to very slowly reductively electropolymerize onto graphite and platinum electrodes from acetonitrile solution. The modified electrodes could then be transferred to acetonitrile, CH_2Cl_2 or water and showed reversible Os(IV/III) and Os(III/II) couples. The electrodes were quite stable. They could be cycled for hours with only small losses of activity. However, the polymer coating was rapidly lost in nonaqueous solutions in the presence of acid. This prevented conversion of the polymer-bound CHBA-Et complex into the CHBA-containing catalysts described in Chapter III, since the oxidative ligand degradation which produces the CHBA complexes also produces acid.

Results and Discussion

Adsorption of osmium complexes on graphite electrodes

The complex with which this project began was $\text{Os}(\text{CHBA-Et})(\text{Py})_2$ [6]. This complex was soluble in CH_2Cl_2 but only very slightly soluble in acetonitrile and totally insoluble in water. In an attempt to examine its electroactivity in water, an acetone solution of the complex was evaporated onto a graphite electrode and the response of the electrode was examined in 0.1 M aqueous HClO_4 by cyclic voltammetry. A broad reversible couple was observed at +0.10 V vs. SCE. This compares to an $\text{Os}(\text{IV/III})$ formal potential of -0.65 V vs. Fc^+/Fc , or about -0.1 V vs. SCE, in CH_2Cl_2 . Acid is known to shift the formal potential of this couple positive in CH_2Cl_2 and so the acidic conditions of the aqueous solution are probably responsible for the observed difference in formal potential. The peak currents of the couple in aqueous solution decreased about 50% after cycling for 5 minutes over the $\text{Os}(\text{IV/III})$ couple. Integration of the cyclic voltammetric peaks gave only 25% of the expected charge even on the first scan. Most of the material applied to the electrode must have been either lost immediately or electroinactive. The modified electrode also displayed two irreversible oxidations at +1.0 and +1.3 V vs. SCE which appeared only on the first scan and which caused loss of all electroactivity.

The complexes containing the CHBA-DCB ligand displayed reversible oxidations to $\text{Os}(\text{V})$ in CH_2Cl_2 (see Chapter IV). Some activity for the catalytic oxidation of chloride in CH_2Cl_2 was observed with $\text{Os}(\text{CHBA-DCB})(\text{Ph}_3\text{P})_2$ and $\text{Os}(\text{CHBA-DCB})(\text{t-Bupy})_2$ [7]. It was desired to see if this activity could also be observed in aqueous solution where it would be more useful. Therefore, solutions of these two complexes were

evaporated onto graphite electrodes and their activity in aqueous solution containing 0.1 M HClO_4 and 0.1 M NaCl was observed by cyclic voltammetry. For both complexes reversible Os(V/IV) couples could be observed at around +1.0 V vs. SCE, but no catalytic oxidation of the chloride was detected. The response of these electrodes also rapidly decreased on repeated cycling.

Reductive electropolymerization of $\text{K}[\text{Os}(\text{CHBA-Et})(\text{vpy})_2]$

Since our osmium complexes are reduced to Os(II) at potentials similar to those of the bipyridine reductions of Meyer and Murray's compounds, it was felt that it might be possible to reductively electropolymerize a 4-vinylpyridine-containing osmium complex. The goal of our electrode modification work was attachment of some type of catalyst to the electrode surface, so a logical complex to attempt to electropolymerize was $\text{Os}(\text{CHBA-Et})(\text{vpy})_2$. Once polymerized, this complex might then be oxidatively converted to CHBA complexes which are catalysts for the electrochemical oxidation of alcohols to aldehydes and ketones (see Chapter II).

The complex $\text{Os}(\text{CHBA-Et})(\text{Py})_2$ is prepared by reduction of $\text{K}_2[\text{Os}(\text{CHBA-Et})(\text{O})_2]$ with triphenylphosphine in the presence of pyridine, followed by oxidation of the Os(III) product to Os(IV) with H_2O_2 [8]. It seemed reasonable that if 4-vinylpyridine were substituted for pyridine the desired complex could be synthesized. The reaction proceeded cleanly and the product was isolated as the potassium salt of the Os(III) complex. The reaction was not heated and the product was not oxidized to Os(IV) in order to minimize chances of reactions occurring at the sensitive vinyl groups. The product showed a cyclic voltammogram (CV) in acetonitrile almost identical to that of $\text{Os}(\text{CHBA-Et})(\text{Py})_2$ in CH_2Cl_2 .

Figure 7.1 shows the results of cycling at 200 mV/sec for three hours over the Os(IV/III) and Os(III/II) couples of $\text{K}[\text{Os}(\text{CHBA-Et})(\text{vpy})_2]$ in acetonitrile. The peaks of the two couples very slowly increased in size and broadened, indicating the formation of an electroactive polymer on the electrode surface. The same results were obtained on both graphite and platinum electrodes. The polymerization shown in Figure 7.1 was performed by scanning continuously between -0.19 and -2.49 V vs. Fc^+/Fc . When the experiment was repeated with a fresh graphite electrode and the scan was extended to -2.69 V, the peak currents of the polymer film grew about three times faster than on scanning to -2.49 V. When the scan was shortened to -1.99 V the peak currents grew about three times slower. Holding the potential at -2.49 V also caused polymerization, but the rate was slower than with potential cycling.

When the polymer modified electrodes were removed from the solution in which they were prepared and rinsed with acetonitrile, a blue color could be seen clearly on the electrode surfaces. When the electrodes were placed in fresh acetonitrile containing only TBAP or NaClO_4 supporting electrolyte, both the Os(IV/III) and Os(III/II) couples could be seen, as shown in Figure 7.2. The CV's were somewhat distorted, with pre-peaks before the Os(III/II) reduction and the Os(III/IV) oxidation and with an apparent doubling of the Os(III/II) couple's peaks. Similar results were also obtained in CH_2Cl_2 , but the peaks were even broader. In CH_2Cl_2 it was also observed that ferrocene could penetrate the polymer film with no change in formal potential or peak currents compared to those at a bare electrode, but with broadening of the peaks. The CV of a polymer-modified electrode in neutral aqueous solution containing 0.1 M NaClO_4 is shown in Figure 7.3. The peaks are broad but both the Os(IV/III) and Os(III/II)

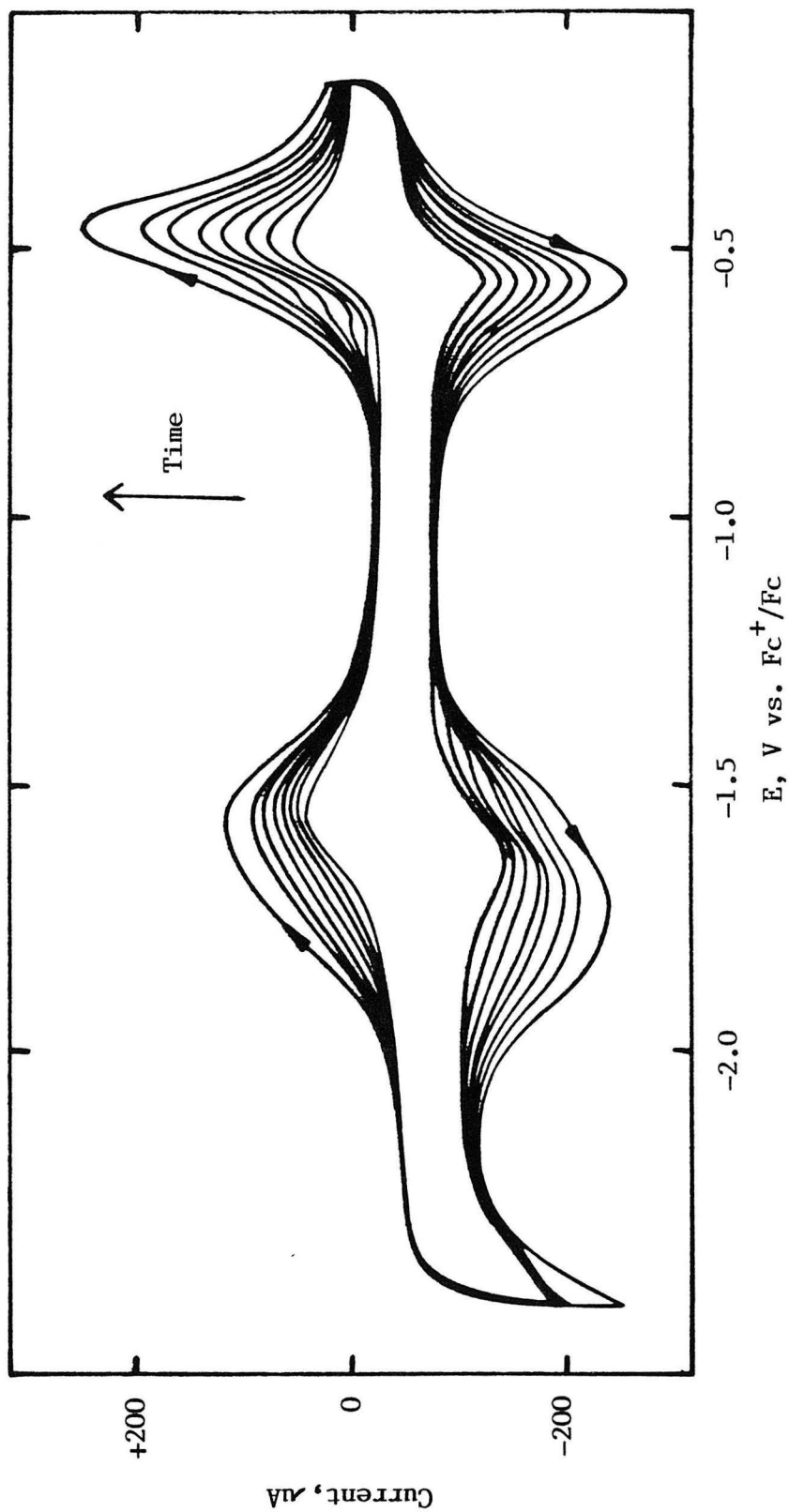


Figure 7.1. Cyclic voltammograms of 1.1 mM K[Os(CHBA-Et)(vpy)₂] in acetonitrile, 0.1 M TBAP at 0.17 cm² BPG electrode after 0, 7, 20, 40, 60, 90, 120 and 180 minutes of continuous cycling.
Scan rate = 200 mV/sec.

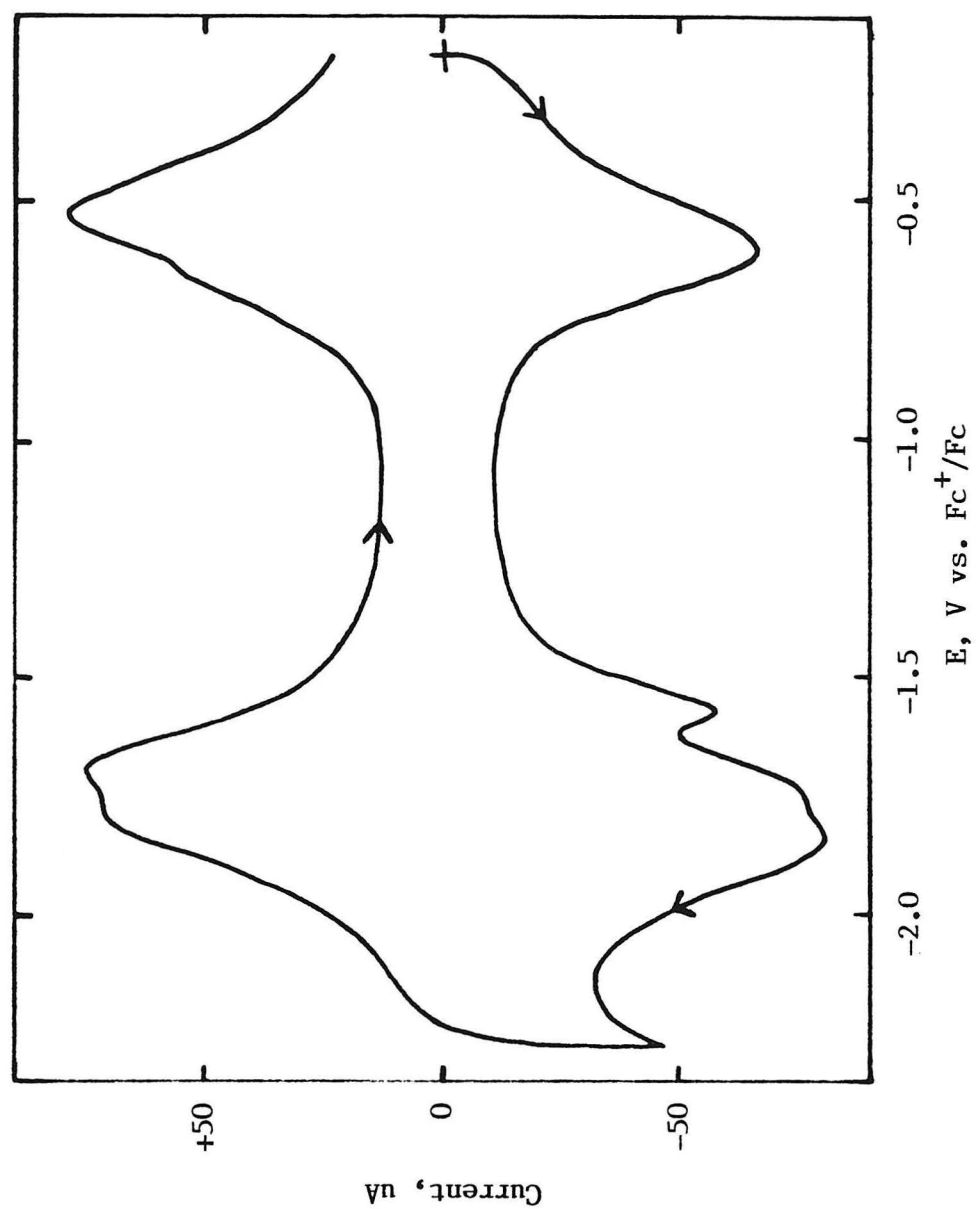


Figure 7.2. Cyclic voltammogram of $\text{Os}(\text{CHBA-Et})(\text{vpy})_2$ polymer modified electrode in acetonitrile, 0.1 M TBAP. Scan rate = 200 mV/sec.

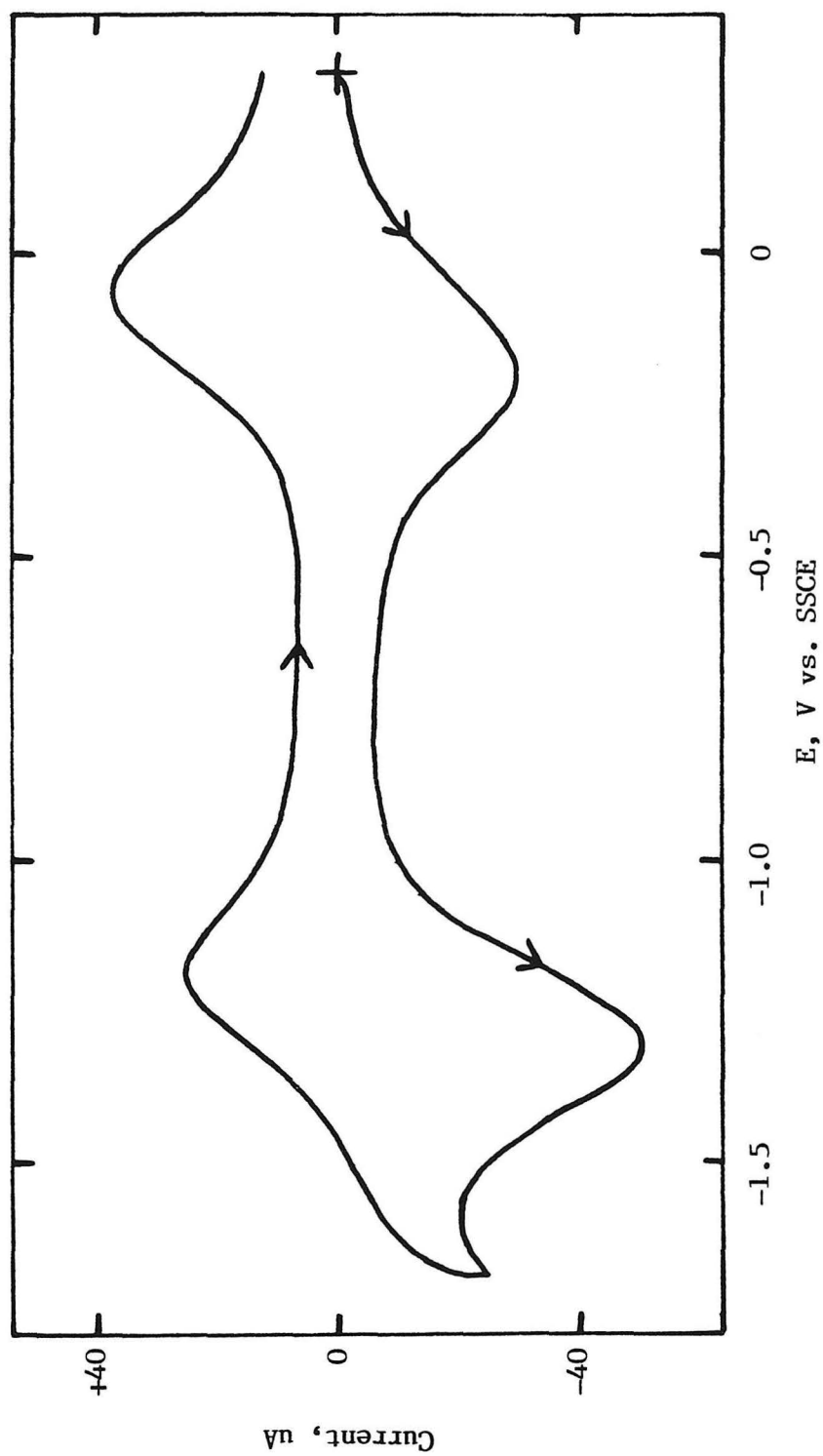


Figure 7.3. Cyclic voltammogram of $\text{Os}(\text{CHBA-Et})(\text{vpy})_2$ polymer modified electrode in 0.1 M aqueous NaClO_4 . Scan rate = 200 mV/sec.

couples are clearly visible. In 0.1 M aqueous HClO_4 the Os(IV/III) couple sharpened, as shown in Figure 7.4. Figure 7.4 also shows the behavior of this couple as a function of scan rate. Here, as in all other solvents, the peak currents of the couple varied directly with scan rate as they should for a surface-bound species, not with the square root of scan rate as is observed for solution species.

The polymer modified electrodes were quite stable to extended cycling. In one experiment in 0.1 M aqueous HClO_4 , an electrode was cycled over the Os(IV/III) couple for a total of 210 minutes. During the first 40 minutes the peak currents decreased about 10%, and then over the next 170 minutes they decreased another 10%. However, cycling over the irreversible oxidation to Os(V) caused total loss of electroactivity in all solvents. Even in the presence of alcohols, oxidation of the polymer modified electrodes did not produce the catalyst species as described in Chapters II and III. The reason for this failure is believed to be the sensitivity of the polymer film to acid. It was found that exposure of a polymer modified electrode to 20 mM trifluoromethanesulfonic acid in acetonitrile caused rapid loss of the polymer as indicated by loss of the blue color and electrochemical response of the electrode. Since acid is formed during the oxidative conversion of the CHBA-Et complex to the catalyst species, there seems to be no way to convert the polymer modified electrodes to the catalysts. If at some future date a long-lived catalyst is developed, then it may be worthwhile to synthesize it with vinyl-substituted ligands and prepare polymer modified electrodes from it. Since the present catalysts have such short lifetimes, no further attempts were made to prepare polymer modified electrodes from them.

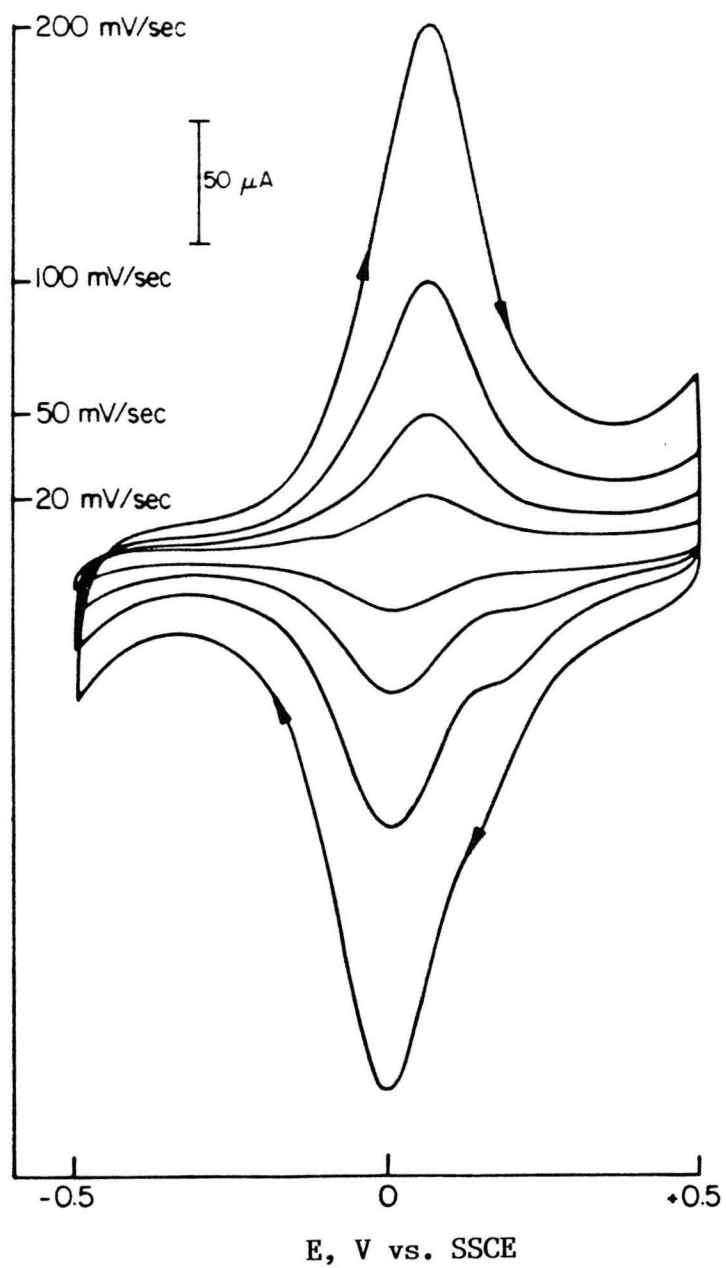


Figure 7.4. Cyclic voltammograms of Os(CHBA-Et)(vpy)₂ polymer modified electrode in 0.1 M aqueous HClO₄.

Conclusions

At the beginning of this project it was anticipated that when catalysts for electrochemical oxidations had been found and studied, they would be used to prepare chemically modified electrodes. The modified electrodes would have advantages such as requiring only small amounts of catalyst and excluding catalyst from the bulk solution. Although no truly useful catalysts have yet been developed, it has been shown that there are ways of localizing the Collins group's compounds on electrode surfaces. This was most simply done by adsorbing them directly onto the electrode. Since the compounds were not soluble in water, the electrodes could be used in aqueous solution. Responses could be observed with these electrodes, but the compounds were lost fairly rapidly from the electrode surface.

A far superior method of derivatizing electrodes was reductive electropolymerization of a complex containing 4-vinylpyridine. The complex $K[Os(CHBA-Et)(vpy)_2]$ was prepared and found to electropolymerize reductively from acetonitrile solution during scanning over its $Os(III/II)$ couple. The polymer-modified electrodes so obtained showed reversible $Os(IV/III)$ and $Os(III/II)$ couples in acetonitrile, CH_2Cl_2 and water. The electrodes were very stable unless cycled over the irreversible oxidation to $Os(V)$ or exposed to acid in nonaqueous solution. Because of the sensitivity to acid, the polymer-modified electrodes could not be converted to catalysts for alcohol oxidation. If in the future a long-lived alcohol oxidation catalyst or some other catalyst is developed, then this method could allow the convenient synthesis of catalytic polymer-modified electrodes for use in aqueous media.

Experimental

Materials

Acetonitrile was Burdick and Jackson distilled in glass grade and was used as received. Reagent grade methylene chloride (MCB or Mallinckrodt) was further purified by passing it over a short column of activated alumina (Woelm N. Akt. I). Aqueous solutions were prepared from deionized water which had been passed through a purification train (Barnstead Nanopure). All other solvents were reagent grade (Aldrich, Baker, Mallinckrodt, MCB or USI) and were used as received. Trifluormethanesulfonic acid (3M) was distilled and stored at -10°C . Tetra-n-butylammonium perchlorate (Southwestern Analytical Chemicals) was dried, recrystallized twice from acetone/ether, and then dried under vacuum. Anhydrous sodium perchlorate (99+%, Aldrich), perchloric acid (Baker Analyzed), 4-vinylpyridine (98%, Aldrich), triphenylphosphine (MCB) and ferrocene (Aldrich) were used as received.

The complexes $\text{Os}(\text{CHBA-Et})(\text{Py})_2$ and $\text{Os}(\text{CHBA-Et})(\text{O})_2$ were prepared by Terry Krafft and $\text{Os}(\text{CHBA-DCB})(\text{t-Bupy})_2$ was prepared by John Keech [8]. $\text{K}[\text{Os}(\text{CHBA-Et})(\text{vpy})_2]$ was prepared by reaction of 45.6 mg $\text{K}_2[\text{Os}(\text{CHBA-Et})(\text{O})_2] \cdot 4\text{H}_2\text{O}$ and 0.16 g triphenylphosphine in 10 ml 4-vinylpyridine. After stirring overnight at room temperature the orange solution was loaded onto a 4 cm diameter, 2 cm tall silica gel column and washed with 150 ml of acetone. The orange $\text{Os}(\text{III})$ complex was then eluted with methanol and recrystallized from acetone/cyclohexane. Since the complex showed the expected cyclic voltammogram, no further characterization was performed. Yield of dried solid was 35 mg (70%).

Apparatus and Procedures

Cyclic voltammetry was performed with a Princeton Applied Research (PAR) Model 173 potentiostat driven by a PAR Model 175 universal programmer using positive feedback IR-compensation. Current-voltage curves were recorded on a Houston Instruments Model 2000 X-Y recorder. Standard two-compartment electrochemical cells were used. When necessary, solutions were purged with argon to remove oxygen. The working electrode was a 0.17 cm^2 basal plane pyrolytic graphite (BPG, Union Carbide Co.) disc mounted in a glass tube with heat-shrinkable tubing or a 0.03 cm^2 Pt disc sealed in glass. The counter electrode was a platinum wire. Various reference electrodes were used, including SCE, SSCE, Ag/AgCl and a silver wire quasi-reference electrode. In nonaqueous solvents potentials were referenced to the formal potential of ferrocene as an internal potential standard. The potential of the ferrocene couple was measured as +0.39 V vs. SCE in acetonitrile and +0.48 V vs. SCE in CH_2Cl_2 . Formal potentials of reversible couples were taken as the average of the anodic and cathodic peak potentials. Supporting electrolytes were 0.1 M NaClO_4 or TBAP in acetonitrile, TBAP in CH_2Cl_2 , and NaClO_4 or HClO_4 in water. All experiments were performed at room temperature, $22 \pm 2^\circ\text{C}$.

Polymer-modified electrodes were prepared by continuously cycling the potential of the electrodes between -0.19 and -2.49 V vs. Fc^+/Fc in an argon-purged acetonitrile solution containing 1.1 mM $\text{K}[\text{Os}(\text{CHBA-Et})(\text{vpy})_2]$ and 0.1 M TBAP. The potential was generally cycled for about one hour. The electrodes could be removed from the solution, rinsed with acetonitrile and stored for future use.

References and Notes

1. R.W. Murray, Electroanal. Chem., **13**, 191-369 (1984).
2. R.W. Murray, Accts. Chem. Res., **13**, 135-141 (1980).
3. W.J. Albery and A.R. Hillman, Annual Report, C., R. Soc. Chem. London, **1981**, 377-437.
4. L.R. Faulkner, Chem. Eng. News, **62**, No. 9, 28-45 (1984).
5. For leading references see: J.M. Calvert, R.H. Schmehl, B.P. Sullivan, J.S. Facci, T.J. Meyer and R.W. Murray, Inorg. Chem., **22**, 2151-2162 (1983).
6. Ligand names are: 1,2-bis(3,5-dichloro-2-hydroxybenzamido)ethane, $H_4CHBA-Et$; 1,2-bis(3,5-dichloro-2-hydroxybenzamido)-4,5-dichlorobenzene, $H_4CHBA-DCB$; 3,5-dichloro-2-hydroxybenzamide, H_2CHBA .
7. S.L. Gipson, unpublished results.
8. F.C. Anson, J.A. Christie, T.J. Collins, R.J. Coots, T.T. Furutani, S.L. Gipson, J.T. Keech, T.E. Krafft, B.D. Santarsiero and G.H. Spies, J. Am. Chem. Soc., **106**, 4460-4472 (1984).